N° : 40869

Thèse de doctorat de l'Université Lille 1 Sciences et Technologie

Ecole doctorale	Sciences de la Matière, du Rayonnement et de l'Environnement
Spécialité	Molécules et Matière Condensée

Maryska MULLER

Ingénieur ENSCL

Systemic Approach of the Synergism in Flame Retarded Intumescent Polyurethanes

Soutenue le 27 Septembre 2012

Thèse dirigée par : **Mme DUQUESNE Sophie**, Professeur à l'ENSCL
Mr BOURBIGOT Serge, Professeur à l'ENSCL

Composition du jury :

Dr.	**LEFEBVRE Jean-Marc**	Université Lille 1	**Président**
Prof.	**CAMINO Giovanni**	Politecnico di Torino	**Rapporteur**
Prof.	**MAROSI György**	Budapest University	**Rapporteur**
Dr.	**EHRHARDT Dorothee**	Huntsman Polyurethane	**Examinateur**
Dr.	**KLEIN Rene**	Huntsman Polyurethane	**Examinateur**
Prof.	**DUQUESNE Sophie**	ENSCL	**Directrice de thèse**
Prof.	**BOURBIGOT Serge**	ENSCL	**Co-directeur de thèse**

ACKNOWLEDGEMENTS

This Ph.D work has been carried out within the UMET laboratory (CNRS UMR 8207), led by *Pr. Alexandre Legris*, and more precisely within the ISP team led by *Pr. Jean-Marc Lefebvre*. I would like to thank them for giving me the opportunity to join their laboratory. I would also like to thank *Mr Bernard Fontaine*, head of the Ecole Nationale Supérieure de Chimie de Lille (ENSCL), where the laboratory is located.

Once again I would like to thank *Pr. Jean-Marc Lefebvre*, who agreed to be the chairman of this jury. I am very grateful to *Pr. Giovanni Camino* and *Pr. György Marosi*, who accepted to evaluate this Ph.D thesis and to bring in their knowledge. I also acknowledge *Dr. René Klein* and *Dr. Dorothee Ehrhardt* who agreed to be part of this jury.

I especially thank *Pr. Sophie Duquesne* and *Pr. Serge Bourbigot*, my supervisors, for helping me during my Ph.D. You were very good supervisors to me: available, always listening and open to my suggestions.

I am now going to tell you the story of Maryska and her Ph.D …

Once upon a time, a young ENSCL student met Sophie and decided to do a training period within the PERF laboratory (currently named UMET-ISP). The work atmosphere was very nice and motivating. She discovered that burning items could be real fun and wanted to learn more about it. A few years and events later, after a few discussions with Serge, a Ph.D program was offered to her. The Huntsman team wanted to pursue its collaboration with ENSCL to understand the synergy mechanisms leading to fireproofed polyurethanes. This project represented the perfect professional opportunity for Maryska and she accepted. Through this collaboration, she met *Giacomo Giannini*, *René Klein*, *Chris Lindsay*, *Dorothee Ehrhardt* and *Mathilde Teboul* who work at the Huntsman Polyurethane research center. The exchanges were always rewarding and nice; the Huntsman team was also very supportive toward Maryska and the project. As working with polyurethanes is not always easy, Maryska could count on the precious help, tips and kindness of *Fabienne Samyn-Solarski* who would always to pass on her knowledge in the field. After 4 months working in the lab synthesizing polyurethanes, a terrible incident happened: Maryska was found to be allergic to isocyanates (the monomer used to prepare polyurethane). At that moment, *Christine Rodzinka*, the health and safety agent, led her to the appropriate medical staff. That was terrible for the project and a solution had to be found as soon as possible! *Catherine Candelier*, technician at the ENSCL, was the right person to prepare the polyurethanes. She was careful, hardworking, serious and reliable while making the samples for Maryska. The timetables were not always easy to synchronize but the good atmosphere between both colleagues helped to find solutions. Finally, the cooperation has been a success for 3 years and everyone in the project was happy about it. The formulations prepared worked very well against fire; it was thus decided at first to fill a patent and secondly to guide the project to the understanding of physical and chemical aspects leading to performing materials. That was the occasion to meet very interesting people who helped Maryska achieving these Ph.D's objectives. The "NMR team" (*Bertrand Revel, Bertrand Doumert, Gregory Tricot, Julien Trebosc, Laurent Delevoye, Marc Bria, Pierre Watkin*) was incredibly available to teach Maryska all she had to know about NMR. She often came with new questions and problems and a solution was always given to her. This effective collaboration with the NMR department is partly responsible for the success of this Ph.D. The meetings with *Jelle Vlassenbroeck* were also very interesting and rewarding since a new technique, the tomography was found interesting in characterizing intumescence. XRD analyses were provided by *Maxence Vandewalle*. A training in SEM was organized by *Ahmed Addad* and allowed Maryska to capture nice pictures of her materials. *Séverine Bellayer* performed the EPMA experiments. At the laboratory, a perfect handyman, *Pierre Bachelet*, was always ready to help Maryska for professional or non-professional problems; his qualities and jokes made the problems disappear. *Brigitte Versmessen* did a really good job taking care of the non-scientific topics and her "craziness" is always appreciated. At the ENSCL, technical and administrative departments were really helpful. The kindness of some (*Patrick Duplouy, Ali Gamgani, Philippe Lambourg, Pascal Vasseur, Liliane Verheyde, Carole Warembourg*) was sometimes a real asset.

One part of Maryska's job as Ph.D student, because she decided so, was to teach. Thanks to *Jean Marko*, she was affected to the practical work of organic chemistry with first year students at the ENSCL. The team and teachers (*Aurélie, Cédric, Céline, Christophe, Elina, Michel, Patrick, Valérie, Vangelis*) passed on their knowledge of organic chemistry and most importantly their "on the job experience" about what one should do or should not do with the students. In particular, *Gaëlle Fontaine* took this role very seriously and helped Maryska a lot and always in a good mood.

In her daily laboratory life, Maryska could always rely on her colleagues to help her, answer her questions and chat. Those moments were shared with the current members of the UMET-ISP team: *Aurore, Bastien, Charaf, Fouad, Franck-Estime, Ghassan, Gwenaëlle, Hassan, Marianne, Marion, Mathilde, Maude, Mert, Michel, Nicolas, Sofian, Thi* and also the former ones: *Antoine, Caroline, Christelle, Fatima, Hélène, Jérémy, Louis, Mohammad Ali, Nadine, Oriane, René*. During those 3 years, Maryska also met a lot of students during their training period and enjoyed discussing and learning new things from them.

Some members of the laboratory have not been named yet because they have become more than colleagues to Maryska eyes; they are now real friends with whom sharing time after work is precious. *Clémence* managed to work in front of Maryska every day and this was a real challenge, so she has earned by far the "friend status". *Mathilde* is always ready to help anyone and to do many activities; this is why it is nice to be friend with her (by the way, do not forget

that I still have your furniture in my cellar). *Jérémie* is appreciated for his “Jérémie behavior” like an electric guitar in a world of acoustic guitar. It is such a pleasure to be invited to discuss and have a drink or eat with *Mathieu*, especially in his new apartment. *Pauline* arrived just a few months before the end of the contract of Maryska but it was enough to spend good times and to become friends. Finally a German girl named *Carmen* changed part of Maryska’s life because they have spent much time together since the first time they have met. One week in Bavaria to discover Carmen habits was organized and a week of holiday in Brittany is already planned. A beautiful partnership has developed between the girls and it's not going to change!

During trainings taken in the “Ecole Doctorale”, exchanges between Ph.D students were important and connections were created. Maryska is now in good contact with *Emma, Nizar* and particularly *Adeline*. They like to share moments at a bar or test new restaurants.

Last but not least, I would like to thank specially all the people who have been listening to me talking about my Ph.D (sometimes a lot) without knowing exactly what I was doing (of course, it was highly confidential)!! Thanks to all in my family and especially *Mum (14), Dad (Grand Maître), Roman (Ni) and my grandparents*. Thanks to my friends: *Alexandra, Ana, Andrea, Audrey, Baptiste, Bryce, Camille, Catherine, Chloé, Chloé, Claire, Claire, Elise, Florian, Gaëlle, Guillaume, Hélène, Julie, Laetitia, Lolita, Lucile, Marie, Matthieu, Maxime, Mickaël, Ophélia, Pierre, Pierre-Antoine, Stéphane, Stéphanie*. And a final special thank to the one who have been supporting me during my writing: *Laurent*.

For the great moments we have already had together and hopefully the ones to come, I will always be grateful …

CONTENTS

LIST OF FIGURES

LIST OF TABLES

ABBREVIATIONS

APP	Ammonium polyphosphate
ATH	Aluminium tri-hydroxide
BSE	Back scattering electron spectroscopy
CCD	Charge-Coupled Device
CNT	Carbon nanotube
CP	Crossed polarization
CT	Computed tomography
DD	Dipolar decoupling
DSC	Differential Scanning Calorimetry
EDS	Energy-dispersive X-ray spectroscopy
EG	Expandable graphite
EO	Oxyethylene
EPMA	Electron probe microanalysis
EVA	Ethyl vinyl acetate
Figra	Fire growth rate index
FP	Fire performance
FR	Fire retardant
FTT	Fire testing technology
HRR	Heat release rate (or RHR for rate of heat release)
IR	Infrared
JWL440	Jeffox WL440 = polyol
LOI	Limiting oxygen index
MAS	Magic angle spinning
MDI	Diphenylmethane diisocyanate
Mel	Melamine
MLC	Mass loss cone calorimeter
MMT	Montmorillonite
Mw	Molecular weight
NMR	Nuclear magnetic resonance
NP	Nanoparticle
OHv	Hydroxyl value
OMMT	Organomodified montmorillonite
OMPOSS	OctaMethyl Polyhedral Oligomeric Silsesquioxanes
PA	Polyamide
PER	Pentaerythritol
PET	Polyethylene terephtalate

pHRR	Peak of heat release rate
PLA	Polylactic acid
PMMA	Polymethyl methacrylate
POSS	Polyhedral oligomeric silsesquioxanes
PP	Polypropylene
PPA	Polyphosphoric acid
PU	Polyurethane
RF	Rheometer furnace
RPUF	Rigid polyurethane foam
S2020	Suprasec 2020 = isocyanate
SEM	Scanning electron microscopy
TGA	Thermogravimetric analysis
TGA-FTIR	Thermogravimetric analysis – Fourier transformation infrared
THR	Total heat release
TO	Tubular oven
TPU	Thermoplastic polyurethane
WDS	Wavelength-Dispersive X-Ray Spectroscopy
Wt	Weight

RESUME (FRANÇAIS)

L'utilisation des polymères a subit un grand essor il y a environ 60 ans et depuis les polymères sont incontournables dans notre vie quotidienne. Cela est dû à leurs propriétés variées qui leur permettent d'être utilisés dans de nombreux domaines d'application. Parmi ces matériaux, les polyuréthanes (PUs), apparus en 1937, répondent à de nombreuses demandes du marché. En effet, selon la composition chimique des monomères utilisés, les PUs ont des propriétés qui leur permettent d'être utilisés comme revêtements, mousses, thermoplastiques, adhésifs …

Un des inconvénients majeur des PUs est qu'ils brûlent très facilement. Ce sont en effet des matériaux organiques et de ce fait, ils produisent des composés volatils inflammables lorsqu'ils sont soumis à une source de chaleur. Cette propriété des PUs limitent actuellement leur utilisation dans un certain nombre de domaine où les risques d'incendie ne peuvent être négligés. L'objectif de ce travail de thèse est donc de développer une stratégie pour obtenir des PUs ignifugés.

Afin d'ignifuger les polymères, deux approches peuvent être envisagées : l'approche dite réactive qui consiste à greffer une fonction active sur la chaîne du polymère et l'approche dite additive qui consiste à ajouter des retardateurs de flamme lors de la mise en œuvre des polymères. Cette deuxième approche est la stratégie choisie lors de ce travail car le coût est avantageux et la modification n'affecte pas la synthèse du PU. D'autre part, les additifs intumescents (formant une barrière thermique expansée sous l'effet d'une source de chaleur) ont été choisis car ils permettent une nette amélioration des propriétés feu dans les PUs. L'ajout d'agent de synergie sera également étudié afin d'obtenir de meilleures performances à un taux de charge constant.

Cette thèse a été menée en collaboration avec un partenaire industriel, Huntsman Polyurethanes (Everberg, Belgique), et est la suite d'un projet de six mois dont le sujet était l'ignifugation des PUs. Lors de cette pré-étude, un effet de synergie entre le polyphosphate d'ammonium (APP) et des nanoparticules (NPs) a été mis en évidence dans le PU. Le but de la thèse est donc double : comprendre les mécanismes d'action gouvernant la synergie entre l'APP et les NPs puis définir les paramètres influents permettant d'obtenir des formulations optimisées.

Les travaux de thèse ont été réalisés sur un PU modèle dont la formule chimique est détaillée dans la **Figure 1**. L'idée est de travailler sur ce matériau modèle afin de faciliter le travail de compréhension des mécanismes. Dans un second temps, les concepts obtenus pourront être élargis et transposés à tous types de PU tels que les mousses, les thermoplastiques …

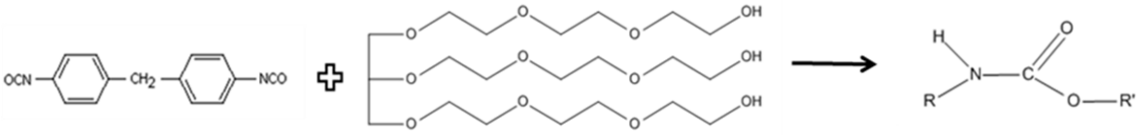

Figure 1 : Réaction entre le polyol (Jeffox WL440) et l'isocyanate (Suprasec 2020) utilisés dans cette étude

Les additifs sélectionnés lors de l'étude sont l'APP et quatre différentes nanoparticules : nano MgO, nano SiO_2, nano or et octamethyl polyhedral oligomeric silsesquioxanes (OMPOSS) dont la structure chimique est présentée sur la **Figure 2**.

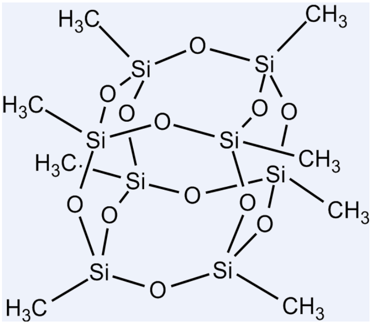

Figure 2 : Structure chimique de l'OMPOSS

Le **Tableau 1** récapitule les différentes formulations de PUs étudiées dans cette thèse. La quantité d'additifs est fixée à 30% sauf lorsque les NPs sont incorporées seules dans la matrice polymère (dans ce cas 5%). Une petite quantité d'APP est substituée par les NPs dans les formulations PU/APP/NP.

Tableau 1 : Différentes formulations de PUs étudiées (en % massique)

Nom	PU (%)	APP (%)	NP (%)
PU	100	0	0
PU 30%APP	70	30	0
PU 5%nano MgO	95	0	5
PU 29%APP 1%nano MgO	70	29	1
PU 28%APP 2%nano MgO	70	28	2
PU 25%APP 5%nano MgO	70	25	5
PU 5%nano SiO_2	95	0	5
PU 28%APP 2%nano SiO_2	70	28	2
PU 28%APP 2%OMPOSS	70	28	2
PU 29.5%APP 0.5%nano gold	70	29.5	0.5
PU 29%APP 1%nano gold	70	29	1
PU 28%APP 2%nano gold	70	28	2

Une caractérisation chimique par RMN du solide (^{13}C et ^{31}P) a dans un premier temps été réalisée sur les formulations de PUs et il a été démontré qu'il n'y a pas d'interaction chimique entre le PU et les additifs lors de la synthèse. De plus, la dispersion des additifs a été caractérisée par microscopie électronique à balayage (MEB) et analyse dispersive en énergie (EDS). Une dispersion homogène a été mise en évidence même si les nanoparticules ne sont pas dispersées de manière individuelle (nanodispersion) mais sous forme d'agglomérats. Enfin, il a été montré que la température de transition vitreuse du PU est affectée par l'incorporation d'additifs. Notamment, l'APP utilisé seul ou en combinaison avec le nano MgO a un effet plastifiant alors que l'effet inverse est observé en combinant l'APP au nano SiO_2.

Les propriétés feu des formulations à base de PUs ont été étudiées à l'aide de deux tests normalisés : le cône calorimètre à perte de masse (MLC : ISO 5660-1 et 2) et l'indice limite d'oxygène (LOI : ISO 4589-1 et 2). La **Figure 3** présente l'évolution du débit calorifique en fonction du temps obtenu lors d'un test au MLC pour toutes les formulations étudiées. Les valeurs de LOI obtenues suivent la même tendance que les résultats obtenus au MLC. Le PU brûle très facilement comme prévu avec un pic de débit calorifique d'environ 450 kW/m^2. L'ajout de 5% de NPs n'améliore pas les propriétés feu du PU, en revanche l'ajout de 30% d'APP permet une réduction du pic de débit calorifique d'environ 50%. Dès qu'une NP est utilisée en combinaison avec l'APP, quelque soient la nature de la NP et le ratio APP/NP, un effet de synergie est observé puisque les propriétés feu sont meilleures que l'APP seul (les propriétés des NPs seules dans le PU étant très mauvaises). Par contre, l'apport de la combinaison APP/NP est différent selon la nature et la quantité de NPs utilisées. Les formulations présentant les propriétés optimales combinent APP et nano MgO (PU 28%APP 2%nano MgO et PU 29%APP 1%nano MgO).

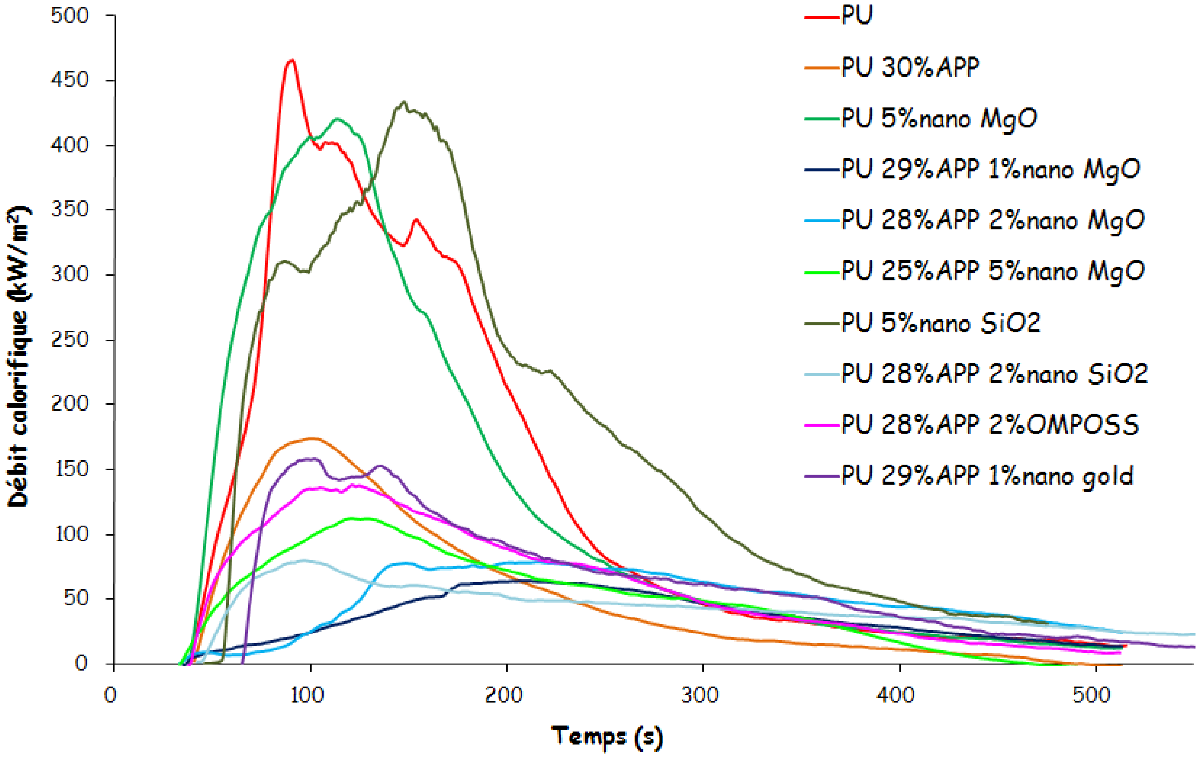

Figure 3 : Evolution du débit calorifique en fonction du temps pour les formulations de PU, PU/APP, PU/NP, PU/APP/NP

Lors du test au MLC, il a été remarqué que les résidus n'ont pas le même aspect et les mêmes propriétés en termes d'expansion et de masse résiduelle. L'objectif de la seconde partie du travail de thèse a donc consisté à déterminer quels sont les paramètres qui permettent d'obtenir les meilleures propriétés feu dans le PU et surtout à déterminer les mécanismes d'action ayant lieu dans ces matériaux lors de leur dégradation.

Dans ce cadre, une première étape a eu pour objectif d'étudier la dégradation thermique des matériaux lors d'une analyse thermogravimétrique (ATG). L'évolution de la masse résiduelle en fonction de la température lors d'une rampe de température de 10°C/min a été mesurée pour le PU, le PU 30%APP et le PU/APP/nano MgO aux ratios 29/1 et 28/2 (**Figure 4**).

La dégradation du PU est largement reportée dans la littérature[1,2]. Elle a lieu en deux étapes sous air, la première commence vers 250°C avec une perte de masse d'environ 50% puis l'oxygène permet de stabiliser le système entre 400 et 500°C où un résidu carboné se forme. Ce dernier est finalement oxydé, ce qui donne un résidu final nul à partir de 675°C. Sous azote, il n'y a qu'une seule étape de dégradation et un résidu final d'environ 14% est obtenu à 800°C.

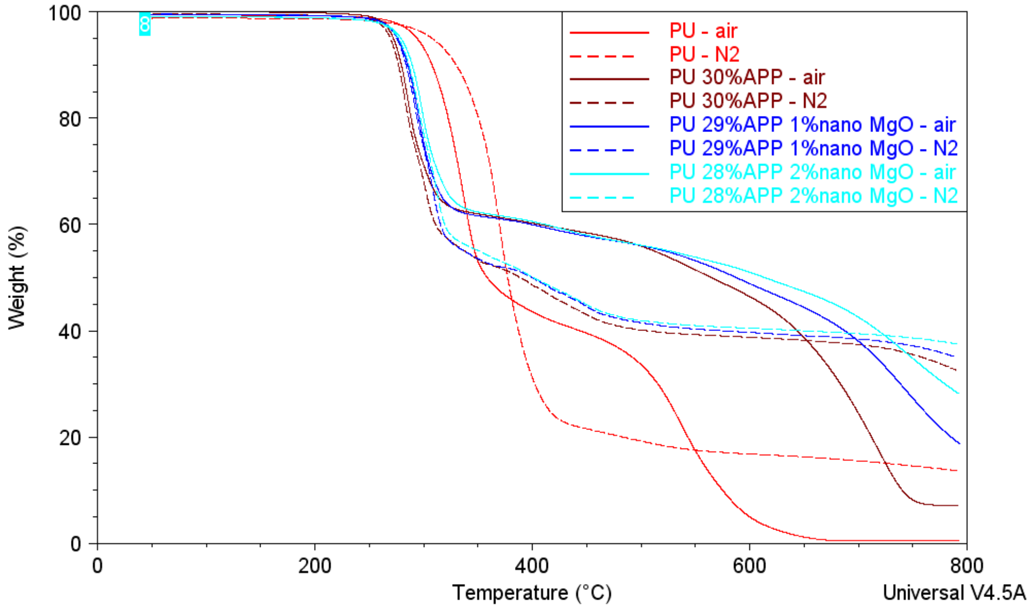

Figure 4 : Evolution de la masse résiduelle en fonction de la température pour les formulations PU, PU 30%APP, PU/APP/nano MgO (29/1 et 28/2) (trait plein : sous air, tiret : sous azote)

Lorsque des additifs sont incorporés dans la matrice PU, les mécanismes de dégradation sont totalement modifiés. Notamment en présence d'APP, la dégradation commence à plus basse température, ce qui prouve que le retardateur de flamme agit sur la dégradation du PU. Cette accélération du processus de dégradation est attribuée à une catalyse acide due à l'APP. Sous air, un

---

[1] S.DUQUESNE, *Etude des procédés d'ignifugation de substrats polymères par revêtements intumescents - Application aux polyuréthanes* 2001, UNIVERSITE DES SCIENCES ET TECHNOLOGIES DE LILLE: Lille.

[2] N.GRASSIE and M.ZULFIQAR, *The effect of the fire retardant ammonium polyphosphate on the thermal degradation of a polyurethane*. DEVELOPMENTS IN POLYMER STABILISATION. Vol. 1. 1979: G Scott Ed.

matériau stable est formé autour de 350°C qui se dégrade d'abord lentement entre 350 et 500°C puis plus rapidement à plus haute température pour former un résidu stable à 800°C. Sous azote, la dégradation est identique jusqu'à 350°C mais après la dégradation est beaucoup plus lente. Une masse résiduelle de 33% environ est obtenue à 800°C.

Les courbes de perte de masse sont modifiées à haute température (T > 550°C) par l'incorporation de NPs dans le système PU/APP. Sous azote la dégradation est identique avec ou sans NPs et permet d'obtenir une masse résiduelle légèrement plus élevée avec 2 puis 1% de nano MgO. Sous air, la différence de mécanisme conduisant à un résidu à haute température est nettement plus importante avec le nano MgO. Un effet de stabilisation des NPs utilisés en combinaison avec l'APP dans le PU est en effet mis en évidence.

Les mécanismes de dégradation ont ensuite été étudiés en caractérisant à l'aide de différentes techniques spectroscopiques les différents composés formés au cours de cette dégradation.

La phase gaz a tout d'abord été étudiée par analyse thermogravimétrique couplée à un infra rouge à transformée de Fourier (ATG-FTIR). Il a été démontré que le mécanisme de synergie entre l'APP et les NPs n'est pas un mécanisme en phase gaz. Les gaz détectés sont identiques pour le PU 30%APP et le PU/APP/nano MgO (ratios 29/1, 28/2 et 25/5). En revanche entre le PU et le PU 30%APP, les produits volatils de dégradation sont différents, notamment des fragments contenant du phosphore et de l'azote sont détectés.

Puisque l'étude porte sur la synergie entre l'APP et les NPs, nous nous sommes intéressés plus particulièrement à l'étude de la phase condensée, c'est-à-dire là où les mécanismes de synergie ont lieu. Afin d'étudier les réactions chimiques ayant lieu en phase condensée, des spectres en RMN du solide ^{31}P ont été acquis sur les résidus des formulations PU 30%APP et PU/APP/NP obtenus après un test au MLC (**Figure 5**).

Sur le spectre du PU/APP, le pic à 0 ppm correspond à de l'acide phosphorique et celui à environ 33 ppm correspond à de l'acide phosphonique. Le premier pic résulte de la dégradation de l'APP qui est bien connue alors que le second était moins attendu. Il est attribué à un produit de réduction qui est rendu possible par la déplétion en oxygène et la structure graphitique du résidu carboné qui peut jouer le rôle d'agent réducteur.

Des espèces chimiques supplémentaires sont mises en évidence sur les spectres des résidus correspondant au PU/APP/NP par rapport au PU/APP. La présence d'un pic à -11,5 ppm révèle une réaction entre le PU et l'APP car ce pic est caractéristique de liaisons P-O-C qui se retrouvent dans les orthophosphates liés à des structures aromatiques. De plus, à -8 ppm des pyrophosphates sont détectés. L'ajout de NPs dans le mélange PU/APP permet donc systématiquement de modifier soit le mécanisme de dégradation de l'APP dans la matrice PU, soit la réactivité entre le PU et l'APP, soit la cinétique de ces processus ou toute combinaison de ces différentes modifications. D'autre part, la formation de phosphates de magnésium dans les formulations PU/APP/nano MgO et de phosphates de silicium dans les formulations PU/APP/nano SiO_2 et le PU/APP/OMPOSS est également mise en évidence. En revanche l'or ne semble pas réagir avec l'APP puisque seuls les pics d'acide phosphorique, ainsi que ceux attribués aux liaisons P-O-C et P-O-P sont détectés.

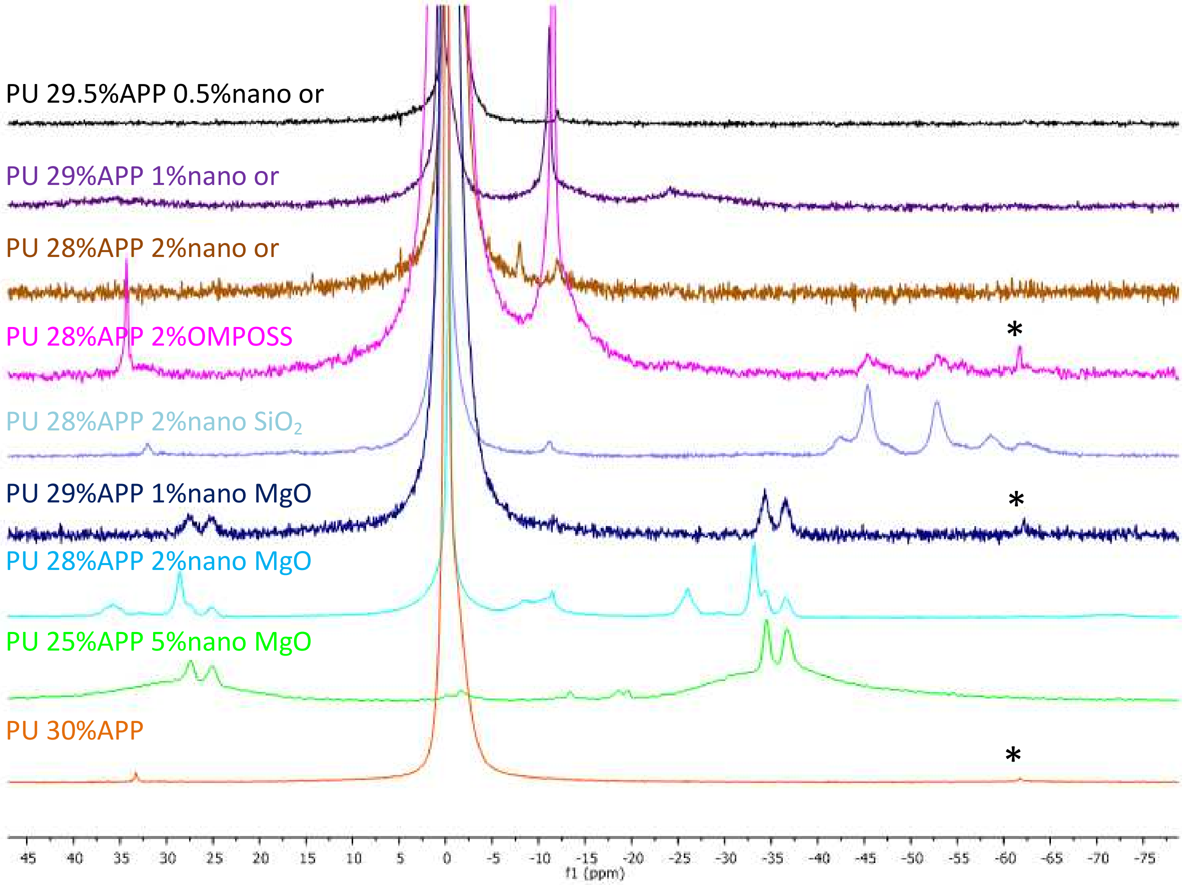

Figure 5 : Spectre DD-MAS RMN ^{31}P des résidus de MLC pour le PU 30%APP et toutes les formulations PU/APP/NP

Toutes les nouvelles espèces créées lors de la dégradation de PU contenant à la fois de l'APP et des NPs jouent un rôle dans le mécanisme de synergie. Ces espèces chimiques vont d'autre part avoir un impact sur les propriétés physiques de la structure carbonée développée lors de la dégradation des matériaux. Ceci fait l'objet de la seconde partie de l'étude dédiée à la compréhension des mécanismes d'action de l'APP et de sa combinaison avec les NPs.

Dans un premier temps, l'effet barrière thermique des formulations PU, PU/APP, PU/APP/nano MgO et PU/nano MgO a été évalué lors d'un test au MLC en mesurant la température au dos de l'échantillon en fonction du temps lors d'un essai (**Figure 6**). Le processus d'intumescence repose en effet sur la formation d'une structure carbonée expansée qui va permettre de limiter les échanges de chaleur et de matière entre la source du feu et le matériau résiduel non dégradé. L'évaluation de l'effet barrière thermique est donc essentielle. Avant ignition, il n'y a pas d'effet des additifs sur la température, ce qui est normal puisque la plaque de polymère n'est pas encore dégradée à ce stade. Ensuite une forte augmentation de la température est mesurée pour le PU vierge et pour la formulation contenant 5% de nano MgO, cela est dû au fait que la plaque est totalement dégradée et que le thermocouple est de ce fait plus ou moins en contact direct avec la flamme. En revanche avec l'APP ou une combinaison d'APP et de nano MgO, la formation d'une structure carbonée est mise en évidence et permet de protéger la plaque plus efficacement, ce qui entraîne un profil de température totalement différent. Etant donné les incertitudes de mesure, il est possible de considérer que toutes les formulations PU/APP/nano MgO ont la même efficacité de protection thermique. Un écart d'environ 400°C à la fin du test entre le PU vierge et les formulations intumescentes est obtenu.

Suite à ces observations d'effet de barrière thermique, il a été décidé d'étudier plus en détails les paramètres permettant cette amélioration des propriétés feu. La conductivité thermique propre du matériau, l'expansion de la structure carbonée et sa morphologie sont les trois principaux paramètres qui vont avoir une influence sur ces propriétés barrière.

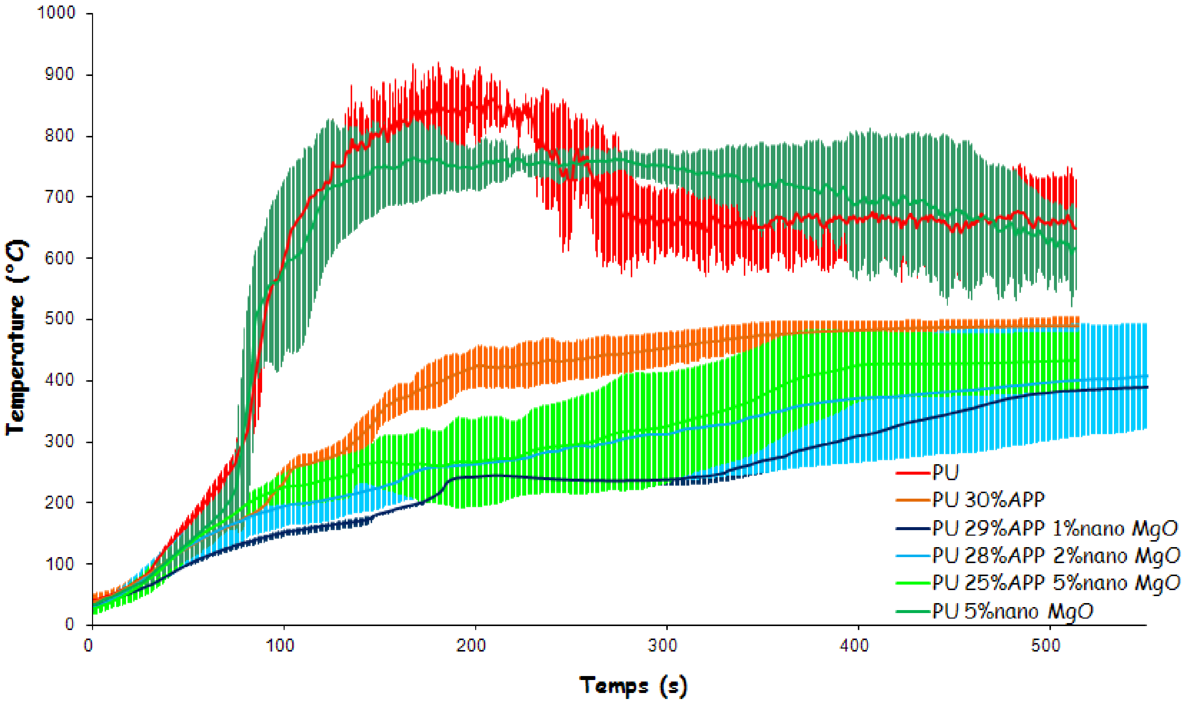

Figure 6 : Suivi de la température au dos d'un échantillon en fonction du temps lors d'un test au MLC pour le PU et les formulations PU 30%APP, PU/APP/nano MgO (29/1, 28/2 et 25/5) et PU 5%nano MgO

La conductivité thermique et en particulier son évolution en fonction de la température pour le PU 30%APP et le PU 28%APP 2%nano MgO est dans un premier temps étudiée. Les résultats sont présentés sur la **Figure 7**.

Tout d'abord, il a été montré que l'incorporation d'additifs dans le PU vierge augmente la conductivité thermique à température ambiante. Lorsque la température augmente, le processus d'intumescence se met en place et mène à la formation d'une couche carbonée expansée qui est caractérisée par sa faible conductivité thermique. Ce phénomène a lieu entre 200 et 400°C comme le montre la **Figure 7**. En effet, avant 200°C, la matrice n'est pas encore dégradée et donc la conductivité thermique est similaire à celle mesurée à température ambiante. L'évolution de la conductivité thermique en fonction de la température est similaire pour le PU/APP avec ou sans nano MgO mais les valeurs relevées sont significativement différentes. En particulier les différences sont mises en évidence à partir de 350°C. Cela signifie que les propriétés intrinsèques des structures intumescentes sont différentes entre le PU 30%APP et le PU 28%APP 2%nano MgO. A plus hautes températures, l'évolution de conductivité thermique est tracée en fonction de la température pour chacun des échantillons. Cette dernière augmente au fur et à mesure que la température augmente sauf entre 450 et 550°C où une diminution apparaît. La différence entre les propriétés de conductivité thermique des deux matériaux est constante entre 400 et 700°C.

La structure carbonée développée par le PU/APP avec ou sans nano MgO est donc différente et cela résulte notamment en différence de conductivité thermique qui peut au moins en partie être liée à la morphologie des structures intumescentes et à leur expansion qui est ensuite étudiée.

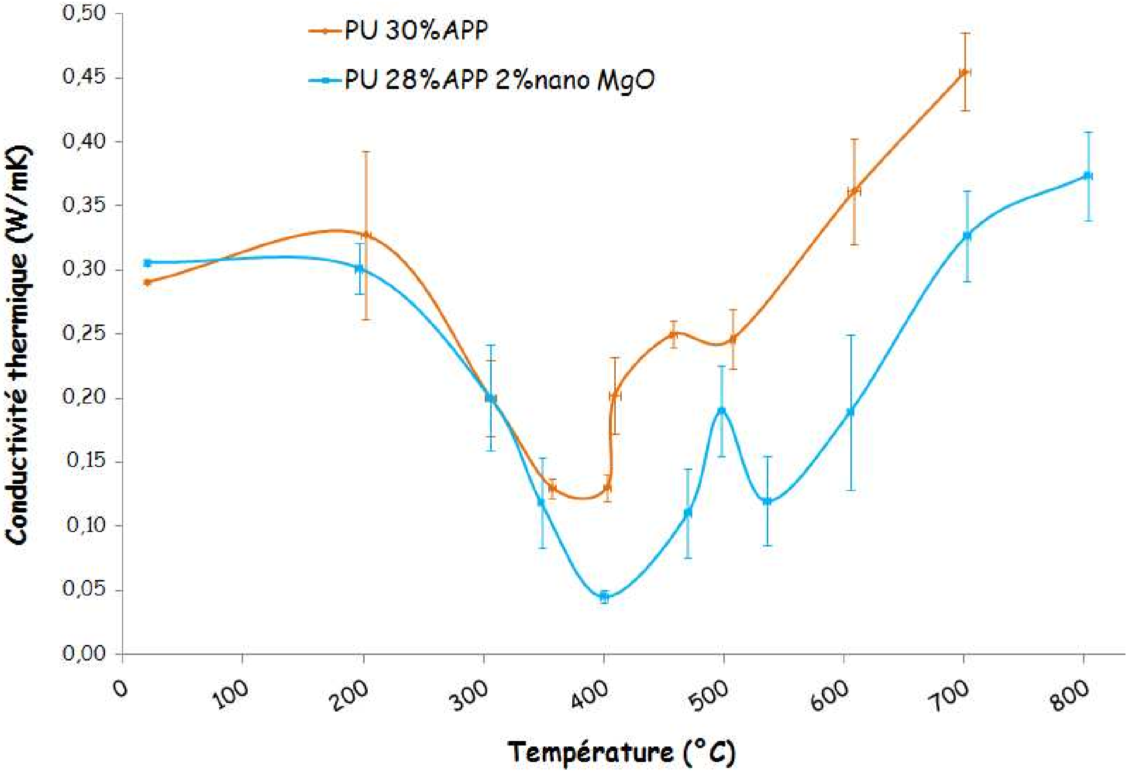

Figure 7 : Comparaison de l'évolution de conductivité thermique en fonction de la température pour le PU 30%APP et le PU 28%APP 2%nano MgO

L'évolution de l'expansion en fonction du temps lors d'un test au MLC a été étudiée sur le PU et les formulations PU 30%APP, PU/APP/nano MgO (29/1, 28/2 et 25/5) et PU 5%nano MgO. Les résultats sont présentés sur la **Figure 8**.

Il n'y a pas d'expansion pour le PU vierge et le PU 5%nano MgO, ce résultat était attendu puisque ces matériaux ne contiennent pas les additifs nécessaires au développement de l'intumescence.

Au contraire, le PU/APP et les PU/APP/nano MgO présentent tous une expansion notable lors d'un test au MLC. Des différences sont cependant mises en évidence entre ces différents matériaux.

Pour le PU 30%APP, une augmentation importante de l'épaisseur de l'échantillon a lieu dès le début du test. La vitesse d'expansion est ensuite réduite jusqu'à atteindre 1100% d'expansion après 3 minutes de test. Cette valeur est la valeur finale d'expansion après 8 minutes et 30 secondes de test.

En présence de nano MgO, l'expansion débute à des temps plus courts comparativement à l'utilisation d'APP seul. Juste après le début de l'expansion, un premier plateau est observé. Cela est sans doute dû à un changement de viscosité du système qui est lui-même sans doute relié à un changement de composition chimique de la structure carbonée, comme mis en évidence précédemment. En effet, cette gamme de temps correspond à celle où les phosphates de magnésium sont obtenus. Après ce plateau, l'expansion augmente de nouveau en fonction du temps. L'augmentation est très rapide de 120 à 180 secondes puis la hauteur maximale est quasiment atteinte pour le PU 25%APP 5%nano MgO et le PU 29%APP 1%nano MgO alors que la structure carbonée du PU 28%APP 2%nano MgO se développe encore après 180 secondes.

A la fin du test, la formulation la plus expansée est celle à base de PU 28%APP 2%nano MgO (2100%) puis les formulations PU/APP/nano MgO aux ratios 29/1 et 25/5 (≈ 1700%) et enfin le matériau PU 30%APP est le moins expansé avec une hauteur de 1200% à 510 secondes.

Ainsi, l'incorporation de nano MgO modifie le processus de formation et d'expansion de la structure carbonée lors d'un test au cône calorimètre. Ces différences conduisent à des différences de morphologie de ces résidus qui sont analysées dans la suite de l'étude.

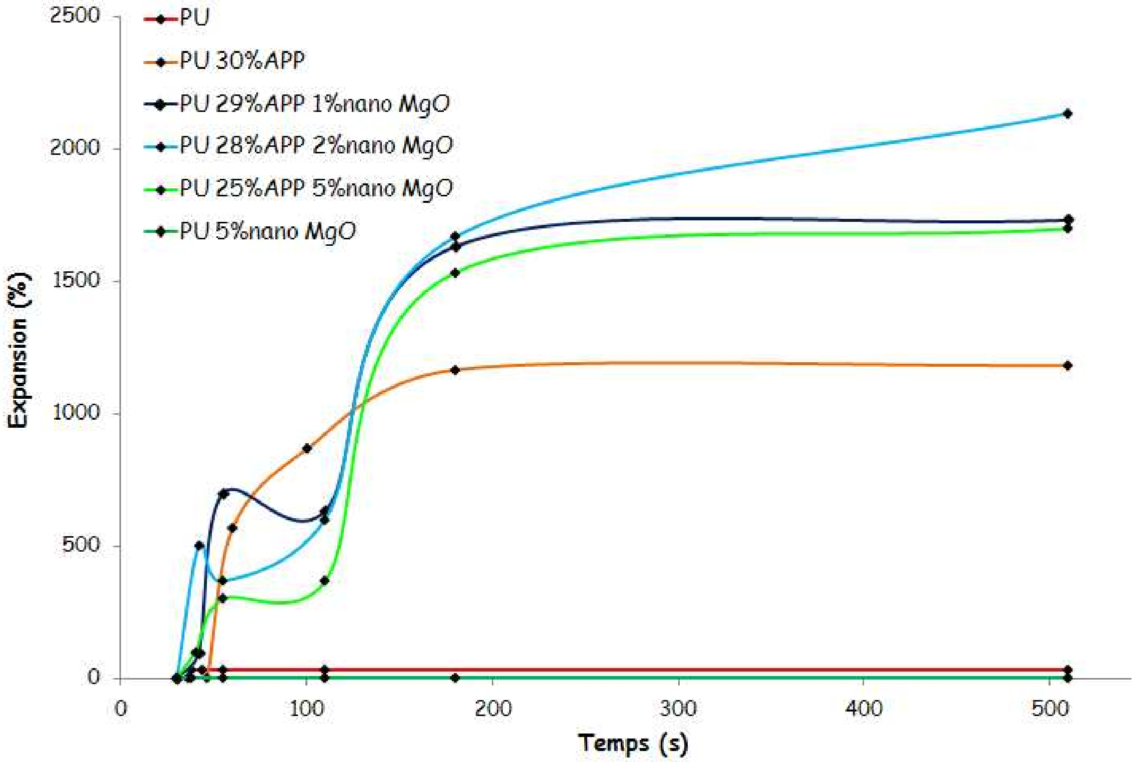

Figure 8 : Suivi de l'expansion en fonction du temps lors d'un test au MLC pour PU, PU/APP, PU/APP/nano MgO et PU/nano MgO

L'étude de la morphologie des structures carbonées développées à la fin d'un test au MLC a été réalisée par tomographie. Cette technique permet d'observer la structure interne d'un échantillon sans préparation initiale. L'utilisation de rayons X permet de voir « à travers » la matière et également de déterminer la répartition des additifs dans le matériau en se basant sur une différence de numéro atomique entre les éléments présents carbone, oxygène par rapport au phosphore, magnésium et or. Cette technique est très innovante dans le domaine de la protection au feu et apparaît très prometteuse car les structures carbonées que l'on cherche à étudier sont souvent très fragiles et ne peuvent être manipulées.

La **Figure 9** présente les photographies des structures carbonées expansées développées à la fin d'un test au MLC pour le PU 30%APP, le PU 28%APP 2%nano MgO, le PU 28%APP 2%nano or et PU 25%APP 5%nano MgO.

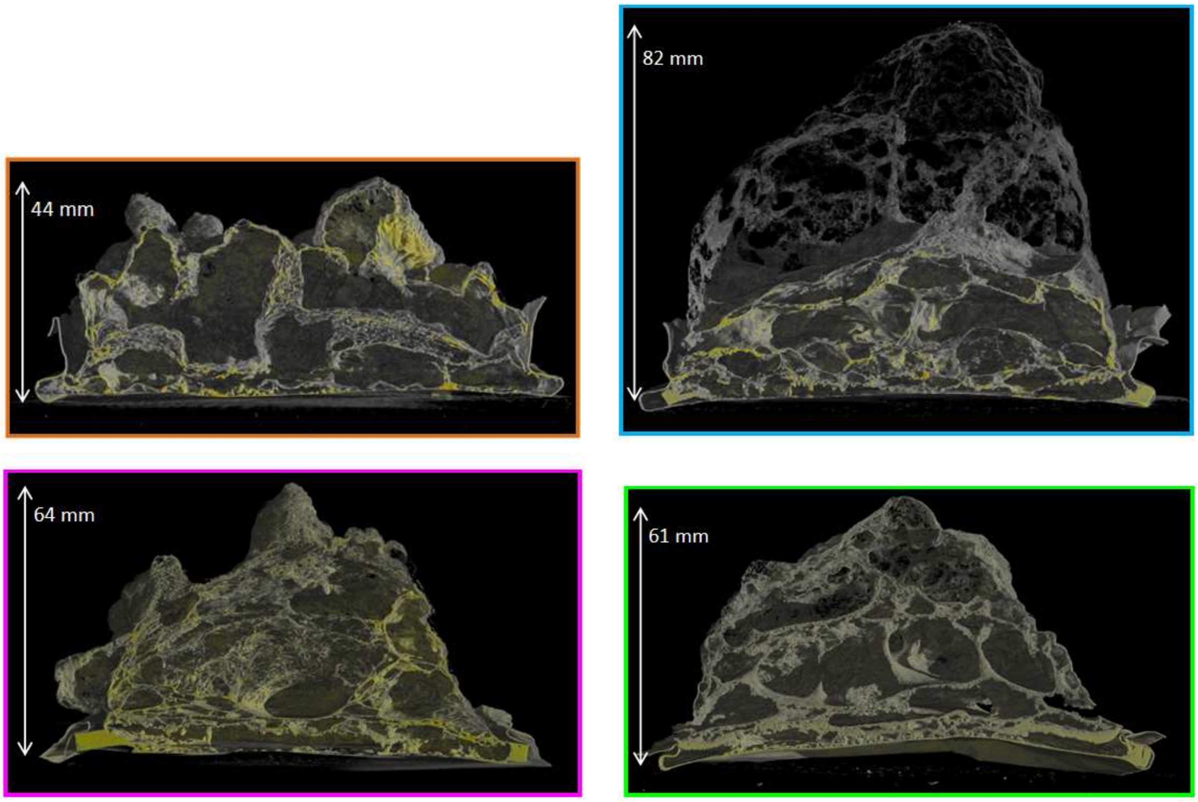

Figure 9 : Photographies de la structure interne du char (environ à la hauteur maximale du char) récupéré à la fin d'un test au MLC obtenues par tomographie (orange : PU 30%APP, bleu : PU 28%APP 2%nano MgO, rose : PU 28%APP 2%nano or, vert : PU 25%APP 5%nano MgO)

Le PU 30%APP est caractérisé par une structure externe très irrégulière alors que l'intérieur du char est beaucoup plus homogène. Ce dernier est composé de grosses bulles séparées par des parois plutôt épaisses.

A l'opposé, le PU 28%APP 2%nano MgO a une surface extérieure très régulière mais l'intérieur est composé de deux parties bien distinctes : en bas, il y a de nombreuses bulles de tailles variables mais globalement petites qui sont séparées par des parois fines ; en haut, seulement une ou deux grosses bulles sont détectées.

Pour la structure carbonée obtenue à partir du PU 28%APP 2%nano or, la surface extérieure ressemble à celle du PU 30%APP. Certaines zones sur les côtés des images montrent qu'il reste encore du polymère non dégradé pour cette formulation, cela correspond au fait que la cinétique de dégradation du polymère est ralentie par l'incorporation de NPs dans la matrice. En bas et sur les côtés de cette structure carbonée, une structure « feuilletée » est observée alors qu'au centre de grosses bulles sont présentes.

Enfin pour le PU 25%APP 5%nano MgO, la couche externe est régulière et semble plus épaisse que dans les cas des autres échantillons. La structure carbonée est constituée en bas d'un feuilleté très compact alors que plus haut, l'échantillon est plus aéré et présente de plus grosses bulles. Pour conclure sur l'étude de la morphologie, on peut voir que, peu importe la nature et la quantité de NPs incorporée dans le PU intumescent, la morphologie de la structure carbonée est affectée par la présence de NPs. Cela se voit sur l'expansion, la taille, le nombre et la répartition des bulles, l'épaisseur des parois entre les bulles et l'aspect de la structure externe.

Tous ces matériaux sont performants en termes de protection au feu par rapport au PU vierge, ce qui prouve bien que le développement d'une structure carbonée expansée par l'intermédiaire du processus d'intumescence est important. Cependant, selon les propriétés de cette couche carbonée, les performances feu seront plus ou moins importantes.

Afin de mieux comprendre l'origine de l'obtention de ces différentes morphologies, une méthode originale a été développée pour étudier le comportement des additifs seuls. En effet, il est connu que le PU est la source de carbone qui va permettre la formation d'un réseau carboné en combinaison avec les additifs mais quelle est la contribution des additifs en dehors de la matrice PU. Pour cela, il a été choisi de suivre l'évolution de la distance (gap) entre les deux plateaux d'un rhéomètre plan/plan en fonction de l'augmentation de température imposée par le four (10°C/min) ; les résultats sont donnés sur la **Figure 10** pour l'APP seul et des mélanges d'APP et de nano MgO à différents ratios : 15/15, 25/5, 28/5, 29/1.

De la température ambiante jusqu'à environ 250°C, chaque additif présente la même augmentation du gap qui correspond à l'expansion du porte échantillon.

Après cela, une forte expansion est observée pour l'APP seul jusqu'à 3000% (courbe limitée à 120% ici). Cette valeur correspond cependant aux limites expérimentales dues à l'équipement utilisé. Cette augmentation est due à la dégradation de l'APP. Ce phénomène est en fait dû à un dégagement de gaz durant la dégradation de l'APP ; ces gaz se dégagent violemment et entraînent le plateau du rhéomètre vers le haut de l'appareil. En effet le gonflement seul du résidu ne permet pas d'enregistrer une aussi grande augmentation de l'écart entre les deux plateaux du rhéomètre. La température à laquelle est relevée ce phénomène correspond de plus au début de la dégradation de l'APP qui a été étudiée en ATG.

Quand du nano MgO est mélangé à l'APP, quel que soit le ratio, la libération de gaz est fortement ralentie. Tout se passe comme si le nano MgO jouait un rôle de régulateur du débit de gaz dégagé par l'APP pendant sa dégradation. Aux ratios 15/15 et 25/5, une diminution du gap est observée entre 300 et 350°C puis il augmente de nouveau. Pour les plus bas ratios, le processus est encore totalement différent puisque le gap stagne pour la formulation 28%APP 2%nano MgO et diminue considérablement pour la formulation 29%APP 1%nano MgO. Cela signifie que le nano MgO joue un rôle sur la structure et la rhéologie du réseau formé par l'APP lors de sa dégradation. A haute température, ce nouveau réseau se dégrade et laisse un résidu vitreux.

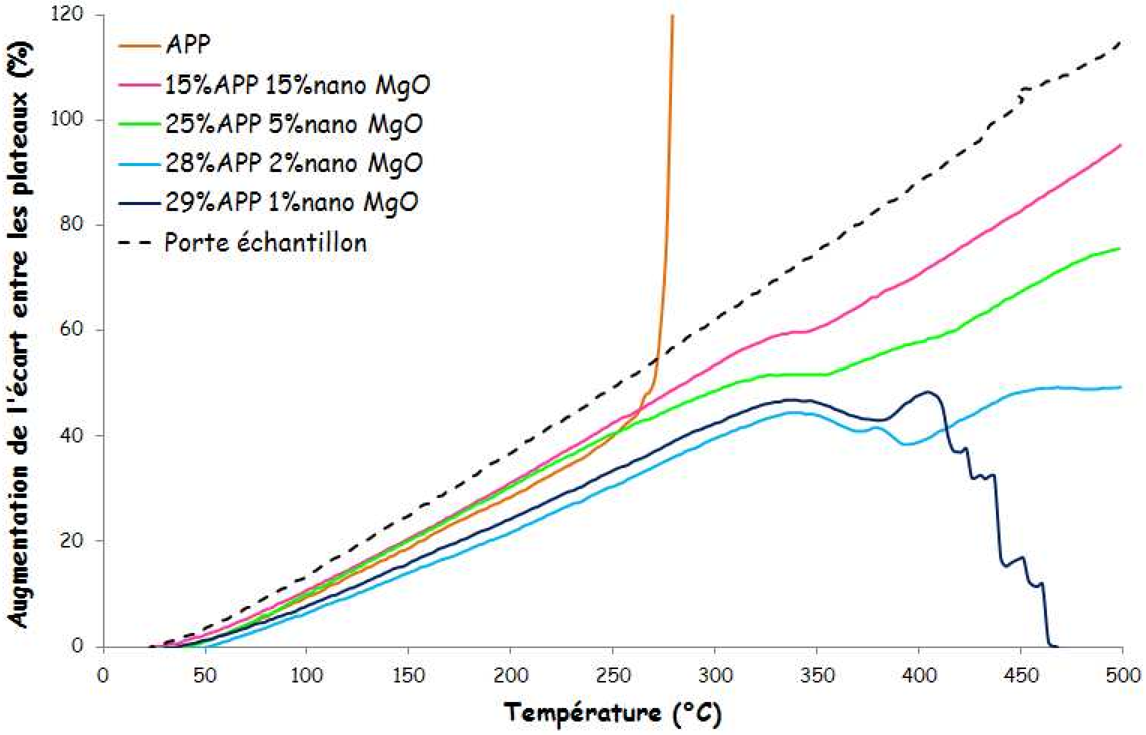

Figure 10 : Evolution de l'augmentation du gap en fonction de la température lors d'une rampe de 10°C/min pour l'APP et un mélange d'APP et de nano MgO en différentes proportions (15/15, 25/5, 28/2, 29/1) lors d'un test au rhéomètre

Afin de mieux comprendre les phénomènes se produisant entre les plateaux du rhéomètre lors de la dégradation de l'APP, la même expérience (chauffage à 10°C/min de la température ambiante jusqu'à 400°C) a été réalisée dans un four et les résidus obtenus par la dégradation d'APP et d'un mélange de 28% d'APP et 2% de nano MgO ont été observés (**Figure 11**). Ces photographies mettent en évidence les processus évoqués précédemment. En effet, l'APP entraîne la formation d'un réseau vitreux mais son aspect et ses propriétés sont affectés par la présence de nano MgO. Dans le cas de l'APP seul, on voit bien des bulles (certaines sont d'ailleurs percées) qui permettent l'évacuation des gaz. Avec le nano MgO, un réseau compact et organisé est formé sous l'effet de la chaleur. Le nano MgO permet de piéger les gaz dégagés lors de la dégradation de l'APP dans le résidu formé entre l'APP et le nano MgO. Il est très probable que la formation de phosphates de magnésium soit responsable de cette différence de comportement sous une source de chaleur.

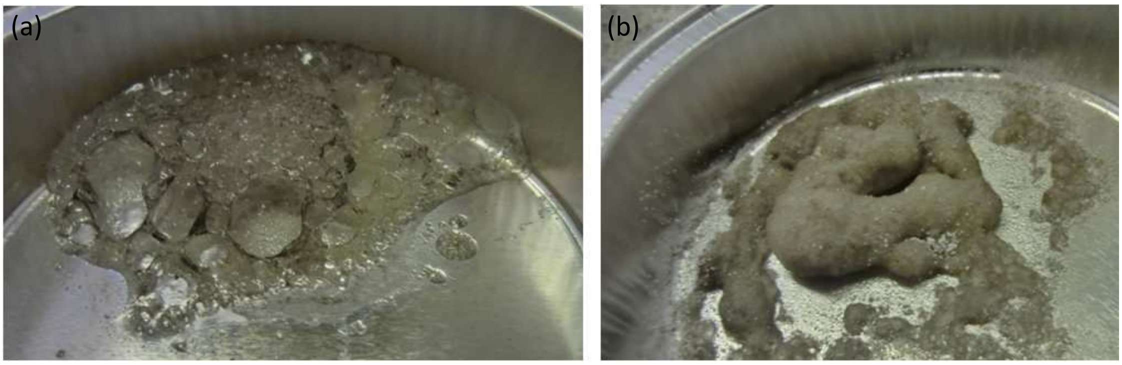

Figure 11 : Photographies des résidus obtenus après traitement thermique à 10°C/min jusqu'à 400°C (APP seul (a) et de 28%APP 2%nano MgO (b))

Enfin, le dernier paramètre clé de l'étude des propriétés physiques de la structure carbonée expansée développé concerne l'étude de ses propriétés mécaniques. En effet, ceci est très important puisque si la structure carbonée possède une conductivité thermique, une morphologie et une expansion lui donnant d'excellentes propriétés de barrière thermique mais qu'elle est détruite par la moindre action mécanique ; elle ne sera plus efficace. Les actions mécaniques envisageables sont multiples car elles peuvent résulter de phénomènes extérieurs (vent, contact …) mais aussi simplement être dues au régime turbulent du processus de combustion.

Une méthode a été développée à l'université de Lille pour déterminer la résistance mécanique de la structure carbonée en fonction de la force appliquée sur celle-ci. Cette méthode consiste à développer la structure carbonée dans le four d'un rhéomètre (10°C/min de la température ambiante jusqu'à 500°C) puis à mesurer sa force de compression lorsque l'échantillon est écrasé par le plateau supérieur à vitesse constante. L'évolution de la force de compression (due à la résistance de l'échantillon) en fonction de l'écart entre les deux plateaux du rhéomètre a été tracée sur la **Figure 12** pour les matériaux suivants : PU, PU 30%APP, PU 29%APP 1%nano MgO et PU 28%APP 2%nano MgO. Les photographies des résidus obtenus après le test de résistance mécanique sont présentées dans la **Figure 13**. Le comportement des formulations est totalement en accord avec les résidus obtenus.

Les propriétés mécaniques de la structure carbonée dépendent des additifs incorporés dans la matrice PU car l'évolution de la force en fonction du gap est très différente selon l'échantillon considéré.

La structure carbonée du PU est très fragile et elle est totalement détruite en imposant une force très faible entre 8 mm et 3 mm. Vers 3 mm, la force augmente énormément et atteint même la force maximale mesurable par le rhéomètre (1600 g). Cela est dû au fait que tous les fragments de la structure carbonée du PU sont tassés dans le fond du porte échantillon après la destruction de l'échantillon. Ce phénomène est observable sur la photo du résidu (**Figure 13**).

Pour les deux échantillons contenant de l'APP et du nano MgO, le comportement est similaire et reflète un matériau relativement fragile. En effet, on observe une destruction des échantillons (**Figure 13**) mais une légère force de résistance est mesurée entre 25 et 5 ou 4 mm.

Cette force évolue d'ailleurs de façon progressive et irrégulière. Ainsi, l'addition d'APP et nano MgO dans le PU permet d'améliorer légèrement les propriétés mécaniques de la structure carbonée.

Enfin, une amélioration notable des propriétés mécaniques est observée pour le PU 30%APP. Il n'y a en effet pas du tout de destruction de la structure carbonée pour cet échantillon, ceci est confirmé par la photo du résidu. Dès que le plateau supérieur est en contact avec l'échantillon, la force mesurée atteint son maximum, ce qui est typique d'un matériau extrêmement résistant. L'aspect de cette structure carbonée est incohérent avec l'aspect observé au cône calorimètre, ce qui nous a amené à étudier ce phénomène plus en détail.

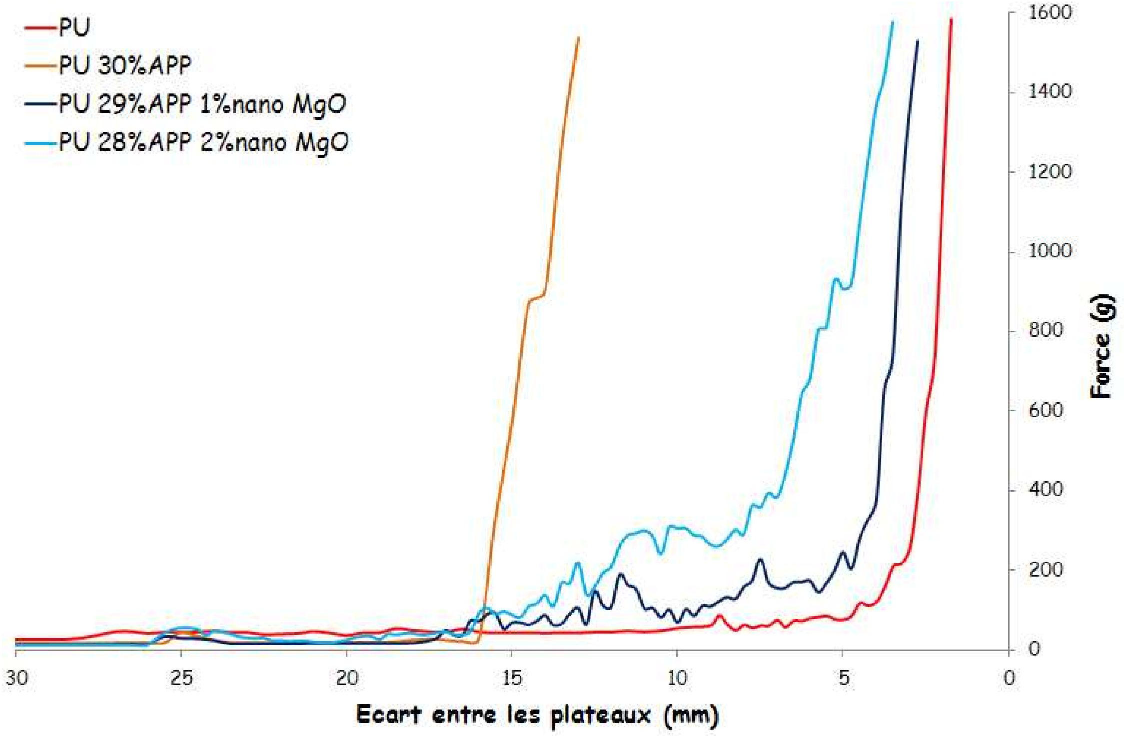

Figure 12 : Suivi de la force de compression en fonction du gap pour le PU et les formulations PU 30%APP, PU 29%APP 1%nano MgO et PU 28%APP 2%nano MgO préparés dans le rhéomètre

Figure 13 : Photographies des résidus obtenus après la mesure de la force pour les échantillons préparés au rhéomètre (rouge : PU, orange : PU 30%APP, bleu foncé : PU 29%APP 1%nano MgO et bleu clair : PU 28%APP 2%nano MgO)

Ainsi, la résistance mécanique des structures carbonées développées lors d'un test standard au MLC a été évaluée par la même méthode que précédemment et les résultats sont présentés sur la **Figure 14**. Il est possible de voir que dans ce cas, la résistance mécanique est similaire, ce qui était prévisible au vu de l'étude de la morphologie des structures.
Une étude détaillée a été menée pour déterminer l'origine de ces différences et il a été montré que la vitesse de chauffe de l'échantillon était un paramètre critique déterminant la résistance de la structure carbonée expansée développée par le PU 30%APP. En particulier, un matériau extrêmement résistant est obtenu à 10°C/min.

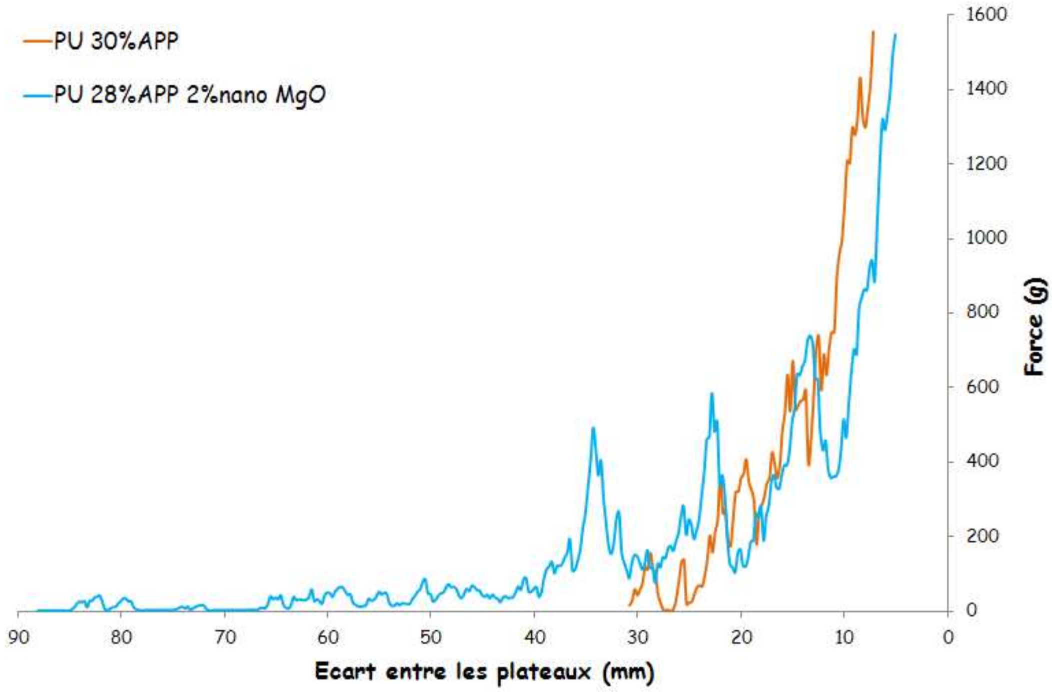

Figure 14 : Suivi de la force en fonction du gap pour le PU 30%APP et le PU 28%APP 2%nano MgO récupérés après un test au cône calorimètre

Pour conclure sur ces travaux de thèse, le mécanisme de synergie gouvernant les excellentes propriétés feu observées dans un système PU/APP/NP a été élucidé. L'incorporation de NPs dans le PU intumescent permet la formation d'espèces chimiques particulières dans la phase condensée qui sont observées également à des temps bien particuliers. Ces espèces chimiques amènent la formation d'une structure intumescente avec des propriétés physiques optimales. La faible conductivité thermique, l'expansion importante et la morphologie multicellulaire que présente la structure carbonée formée à partir du PU 28%APP 2%nano MgO permettent en effet d'apporter une meilleure efficacité d'isolation thermique. D'autres paramètres, tels que la composition chimique de la phase gaz ou encore la résistance mécanique des matériaux, ont été étudiés mais ne permettent pas d'expliquer le phénomène de synergie observé entre l'APP et les NPs.

GENERAL INTRODUCTION

The production of plastics began in the 1840s with the development of an artificial rubber by means of nitrate of cellulose [1], but it is possible to consider that it really starts since approximately 60 years. Since that development, polymeric materials really consist really in an everyday life inescapable material. This massive use of polymer materials is probably driven by their remarkable combination of properties, low weight and ease of processing. Consequently, nowadays plastics or polymers replace advantageously the conventional materials such as wood, metals in diversified domains (**Table 1**).

Table 1: Domains of application of polymers and respective percentages

Domains	Percentages	Domains	Percentages	Domains	Percentages
Packing	40%	**Electricity**	7%	**Medicine**	1%
Building	22%	**Sports**	5%	**Other**	8%
Transport	14%	**Furniture**	3%		

Among the different classes of polymers, the polyurethanes (PUs) represent a large family. The pioneering work on PU was conducted by Otto Bayer and his coworkers in 1937 [2]. 2012 is a special year for PUs: the sector is celebrating the 75th anniversary of this patent giving a detailed description of the basic chemistry behind polyurethane manufacture. PUs are unique polymeric materials with a wide range of physical and chemical properties. With well-designed combinations of monomeric materials, PU can be tailored to meet diversified demands of various applications such as coatings, adhesives, fibers, thermoplastic elastomers, and foams (**Figure 15**) [3].

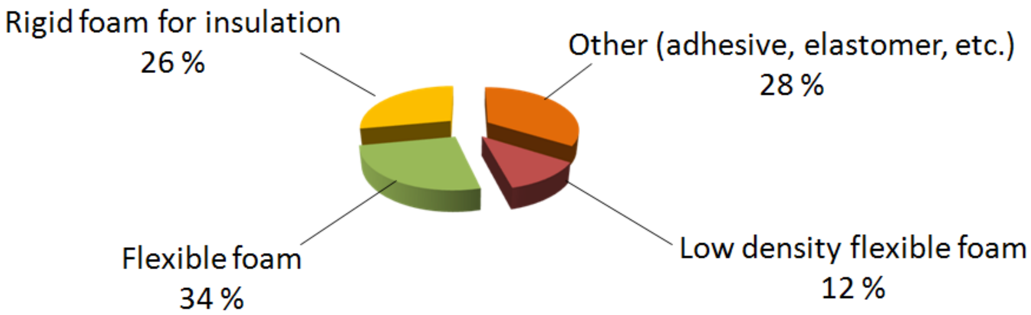

Figure 15: Worldwide market for PUs in 2003 [4]

However, polymers in general and PUs in particular are known for their relatively high flammability; most often accompanied by the production of corrosive or toxic gases and smoke during combustion [5]. Fires cause measurable human casualties, economic damage and environmental pollution, as shown in **Figure 16**.

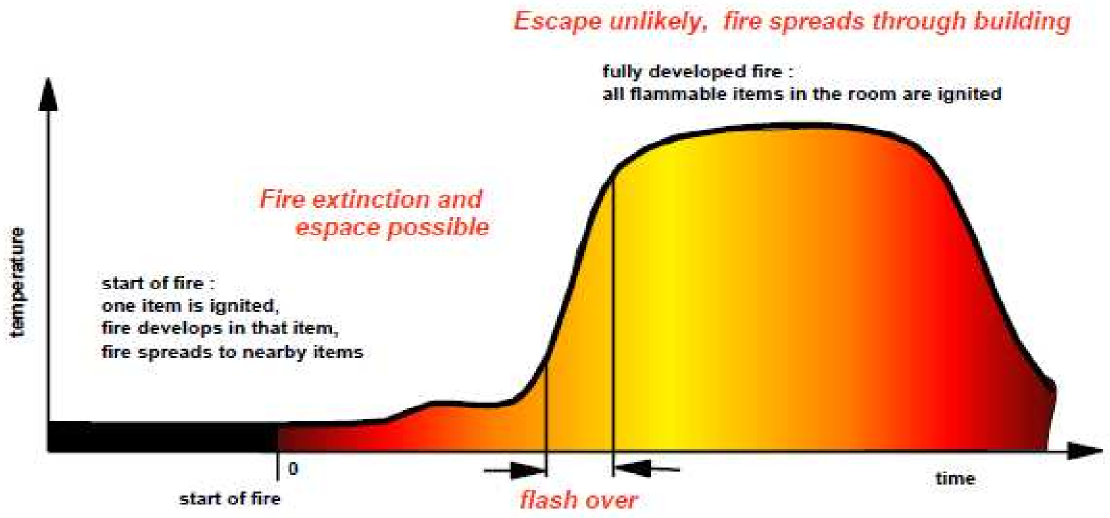

Figure 16: Different phases in the course of a fire (from http://www.flameretardants.eu)

The use of PU, which is combustible, leads to an increase in fire risks (it is also true for polymeric materials in general). For example, a cone calorimeter survey of plastic materials was conducted in the 1990s. In it a plain (non-fire-retarded) flexible polyurethane foam ranked worst (out of 35 materials) in terms of ignitability and ''fire performance index'' (ratio of time to ignition and peak heat release rate) and in the lower third of the pack in terms of heat release [6]. This study highlighted the need to find solutions to fireproof polyurethanes.

Improving the fire retardant behavior of polymers is a major challenge for extending their use to most applications. In response to a wide variety of requirements, manufacturers and specialist formulators offer an immense range of different flame retardant products, based on a number of very different types of chemicals (**Figure 17**). In many cases, several different types of flame retardants are combined to achieve optimal material performance (synergy).

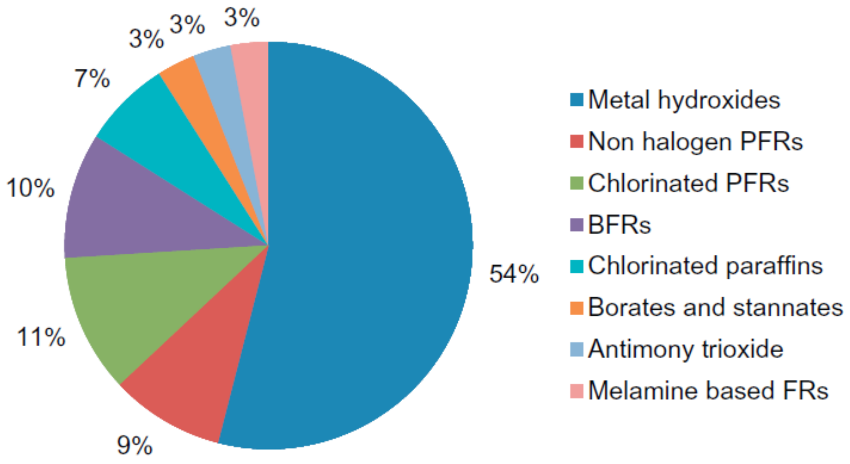

Figure 17: Industry estimate of total consumption of flame retardants in Europe in 2006 (Total = 465000 metric tons) (PFRs = phosphorus flame retardants, BFRs = boron flame retardants, FRs = flame retardants) (from www.cefic-efra.eu)

To enhance flame retardancy of PUs, two ways can be considered [7]: first, it is possible to manufacture new polymers which are already fireproofed by their intrinsically chemical composition. The second strategy consists in incorporating flame retardant additives. The latter route was preferred during this Ph.D work because it is of acceptable cost and easy to realize due to the a posteriori modification of the polymer. Among the various types of additives, the intumescent ones have several advantages in particular it allows both the fire properties and mechanical behavior to be optimized [8]. In addition to the flame retardant, synergistic agents are often used to boost the performances and/or to reduce the total loading of additives [8-10].

This Ph.D work, in collaboration with Huntsman, follows a 6 months postdoctoral position on the flame retardancy of PUs [11]. During this first study, it has been shown that ammonium polyphosphate (APP), used as intumescent flame retardant, and combined with nanoparticles (NPs) gives high fire protection to PUs. This very efficient combination, never studied before, seems very promising to design polymers with improved flame retardancy. The final goal of the project is thus to understand the mechanism of action leading to the synergy between APP and NPs in a PU matrix and to draw general rules associated to well define governing parameters for preparing PUs with enhanced flame retardancy. Phenomena leading to fire retardant performances will thus be widely investigated.

This Ph.D thesis is focused on the understanding of the synergy mechanism obtained by a combination of APP and NPs in a PU matrix. To answer that question, the discussion is divided into five main chapters.

The first chapter reviews the literature concerning the PUs and their flame retardancy. To introduce the subject, a brief presentation of the PUs, their properties, application and thermal stability will be presented. The influence of the PU composition on its fireproofing will be discussed. After a brief review of the basis of flame retardancy and use of flame retardant additives, the state of the art will focus on the intumescent concept and on the synergy in intumescent systems. This corresponds indeed to the kind of system developed during the collaboration between Huntsman and the laboratory. On the basis of the literature, strategies will be developed to understand the flame retardant mechanisms of PU/APP/NP formulations.

The second chapter presents the materials and methods used to understand the flame retardancy of PU formulations. The method of preparation of the PU castings will first be detailed. The methods to characterize the properties of the formulations and their heat treated residues will then be presented. In particular, several innovative techniques in the field of flame retardancy (thermal conductivity, tomography, gas evolution during additives degradation) have been used and will be detailed in this chapter.

The third chapter aims to study the PU/APP/NP systems in terms of physico-chemistry properties, fire performances and thermal degradation. It will first be evaluated if the incorporation of additives in the PU matrix modifies its properties such as its chemistry and its glass transition temperature. Then the fire performances will be investigated thanks to two standard fire tests: mass loss cone calorimeter and limiting oxygen index. Finally the thermal degradation of the PU matrix, of the additives and of the PU formulations will be studied.

The fourth chapter investigates the chemical aspects leading to the synergy between APP and NPs in PUs. The chemical composition of the gases evolved during degradation will first be studied to see if a gas phase mechanism is involved. The condensed phase will then be characterized. The evolution of the condensed degradation products formed during a cone calorimeter test will be followed. Finally, the influence of the heating rate on the thermal degradation and degradation products will be investigated.

The last chapter deals with the physical aspects leading to the synergy between APP and NPs in PUs. The insulation efficiency of the PU formulations will be quantified as well as the thermal conductivity in order to investigate the thermal barrier effect of the chars. The expansion and morphology of the chars will then be characterized. Finally the mechanical resistance of the chars will be evaluated.

A general conclusion is finally drawn from all these results in the last part of this thesis and future works to commercially apply this system and to go further in the understanding of synergy mechanisms will be considered.

Chapter I - State of the art

The pioneering work on polyurethane (PU) was conducted by Otto Bayer and his coworkers in 1937 [2]. PUs are unique polymeric materials with a wide range of physical and chemical properties. With well-designed combinations of monomeric materials, PU can be tailored to meet diversified demands of various applications such as coatings, adhesives, fibers, thermoplastic elastomers and foams [3]. In this state of the art, the discussion will concern all types of PUs. The Ph.D work will then focus on a casting PU model to have a fundamental approach. The results would however be applied in all types of PU systems. The importance of fire issues in most of the PUs application fields has to be considered. Therefore this chapter presents first how polyurethanes are produced, why they are used and how they degrade when undergoing an external heat source. The strategies developed for protecting PUs against fire are then described. A special focus is finally drawn on the use of intumescent systems and on how synergy can be used to enhance the performances of intumescent systems.

1 GENERAL PRESENTATION OF POLYURETHANES

1.1 Description, properties and applications of polyurethanes

PUs are an important and versatile class of polymeric materials whose properties can be easily tailored through changing the molecular structures of the flexible and rigid segments constituting the polymer chain. PU can thus be manufactured in an extremely wide range of grades, in density from 6 kg/m^3 to 1220 kg/m^3 and in polymer stiffness from very flexible elastomers to rigid, hard plastics; as illustrated in **Figure 18**.

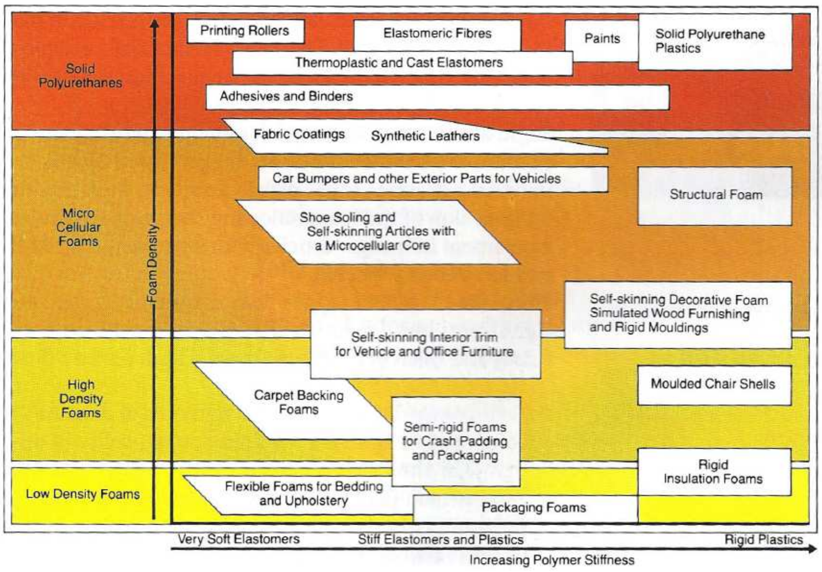

Figure 18: Property of PUs [3]

This chart illustrates the broad range of PUs applications and a classification of materials depending on the density and stiffness is made:

- Low-density flexible foam used in upholstery, bedding, and automotive seating
- Low-density rigid foam used for thermal insulation
- Soft solid elastomers used for gel pads and print rollers
- Low density elastomers used in footwear
- Hard solid plastics used as structural parts.

All the PUs are based on the following exothermic reaction **Figure 19** [12],[13]:

Isocyanate + Polyol --------> Polyurethane

Figure 19: Polyurethane formation reaction

The repeating unit in PU is the urethane linkage obtained from the reaction of an isocyanate with an alcohol **Figure 20** [14]:

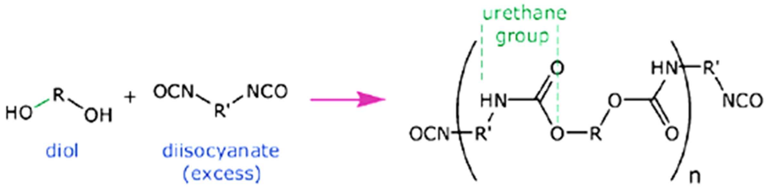

Figure 20: Urethane linkage produced from reaction between a diol and a diisocyanate

Relatively few basic isocyanates and a range of polyols of different molecular weights and functionalities are used to produce the whole spectrum of PU materials [3]. The most commonly used polyols are polyethers or polyester polyols as well as acrylic polyols. On the other hand, methylene diphenyl diisocyanate (MDI), hydrogenated MDI (H_{12}MDI), toluene diisocyanate (TDI), isophorone diisocyanate (IPDI), xylene diisocyanate (XDI) and 1,5-naphthalene diisocyanate (NDI) are widely used diisocyanates in PU formulations [14]. Although PU contains repeating urethane groups, other moieties such as urea, ester, ether and aromatic may also be present in the structure. The molecular structures of PUs vary thus from rigid cross-linked polymers to linear, highly extensible elastomers.

The efficient polymerization reaction may be catalyzed allowing extremely fast cycle times and quantity production [3]. A number of catalysts may be used for this reaction and in particular aliphatic and aromatic tertiary amines or organo-metallic compounds. The rate of polymerization reaction depends anyway upon the structure of both the isocyanate and polyol. For instance aliphatic polyols with primary hydroxyl end groups are the most reactive. After the reaction with polyols, the next most important reaction of isocyanates is that with water [3]. This yields a substituted urea and carbon dioxide (**Figure 21**), causing a source of gas for blowing.

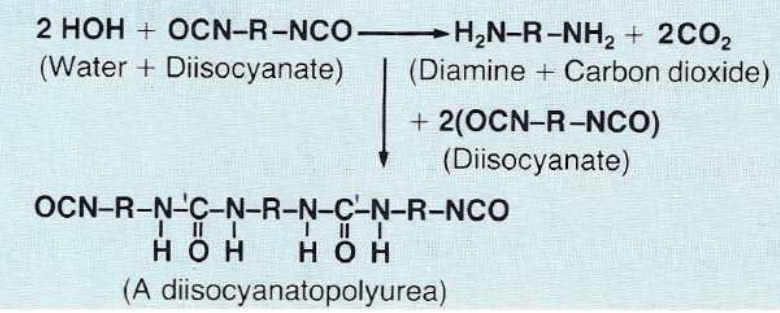

Figure 21: Reaction of isocyanate with water [3]

In addition to isocyanates and polyols, a wide range of auxiliary chemicals may be added to control and to modify both the PU reaction and the properties of the final polymer. These additives include chain extenders, cross-linking agents, surface active materials, coloring agents, fillers and flame retardants.

The aim of this Ph.D is to flame retard PUs and to understand its fire protection mechanisms. Thermal stability and thermal decomposition are the first steps leading to the combustion of PUs and those properties must be examined: that is the reason why it is the purpose of the next section.

1.2 Thermal stability and thermal decomposition of polyurethanes

PUs and as in the case of mainly organic polymeric materials, show significant changes in physical properties with temperature changes. High temperatures may cause irreversible chemical changes and/or degradation of the polymer.

Upon thermal stresses, the covalent bonds in PU chains undergo complex vibration and rotation within their local space. With further excitation, these bonds can break to form a variety of fragment radicals or small molecules, which may further mutually recombine or undergo further fragmentation [14]. Ultimately, the resulting fragments may be vaporized, diffused out, or carbonized. The decomposition process ends with the loss of all volatile material and with the formation of char. In addition to the carbonaceous residue, inorganic residue might also be present and originates from heteroatoms contained in the PU, either within the structure or as a result of additive incorporation.

The thermal decomposition of PU takes place via any of the following routes or more likely through a combination of them [14]: random-chain scission, chain-end scission (unzipping) and crosslinking. However, random chain scission and crosslinking are predominant routes for the decomposition of PUs. Consequently the thermal degradation of PU (**Figure 22**) occurs in a two- to three-step process [15]. The first step is due to degradation of the urethane (depolymerization), which results in the formation of isocyanate and alcohol. The second and third steps correspond to the di- and trimerization; they are much slower than the first step. The thermal stability of PU depends firstly on the polymerization/depolymerization equilibrium of the functional groups in the polymer molecule; indeed all of these units thermally decompose to regenerate their respective precursor groups [16]. The composition of the decomposition products depends also on the structure of the PU material.

The relatively low thermal stability of the isocyanate-derived groups that link the polyether chains and their apparently straightforward decomposition pathway would have been expected to give a simple picture for the decomposition of PU. But thermal stability of PU is affected by the hard segment structure, the soft segment structure and molecular weight, the chain extender structure, the ratio of isocyanate to hydroxyl (NCO/OH), the catalyst and the crosslink density.

During oxidative degradation process [14], free radicals are produced and react rapidly with molecular oxygen to form peroxy radicals, which may further react with the PU chain and form hydroperoxides. In the presence of heat, hydroperoxides decompose and produce more radicals that can reinitiate the decomposition of PU. However, researchers reported that the presence of oxygen does not influence the decomposition rate of PU to diisocyanates and polyols, although it affects the breakage of the polymeric chains [17].

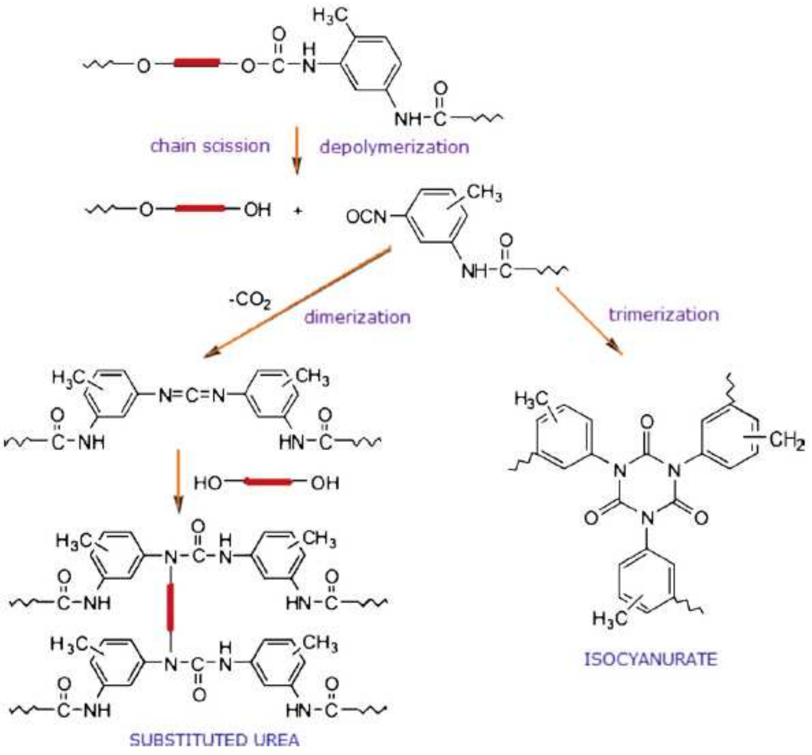

Figure 22: Mechanism of PU thermal degradation under N_2 [14, 16]

The use of PUs, and polymeric materials in general, leads to an increase in fire risks because they do not present a good thermal stability and are thus combustible. Strategies to flame retard these materials are consequently required; the **section** 2 **Flame Retardancy of Polyurethanes p48** will review the different researches and results on the topic. However, PUs exhibit a large range of possible chemical composition, this is a first parameter that can have consequences on its flammability and that will thus be studied next.

1.3 Influence of polyurethane composition on polyurethane fireproofing properties

All different PUs may have a different behavior against fire because they have a proper composition in which each molecule has its fire resistance. The first important parameter is the nature of the polyol and of the isocyanate and more particularly the ethylene oxide content of the polyol, the isocyanate index[3] and their ratio in the final PU formulation. For instance, aromatic polyol based PU present a lower flammability compared to aliphatic polyol based PU foams [14]. Few publications deal with the influence of the PU components in PU castings but in the case of foam, this has been investigated. In foams, many parameters of the foam network as its density, its porosity, its composition, etc., could have a significant effect on the fire properties of the resulting material. The presence of water, catalyst, surfactant or any other additive will indeed largely affect the fire properties.

The influence of the composition of conventional flexible PU foams on their thermal stability and fire behavior has been investigated [18]. The combustion of flexible PU foams under cone calorimeter conditions may be described as a two-step process (**Figure 23**). First the foam degrades and melts to give a carbonaceous part and a tar (first peak of heat release rate (pHRR): pHRR1 and corresponding fire growth rate index (Figra): Figra1). Secondly the tar burns with a relatively high production of heat (second peak: pHRR2 and Figra2).

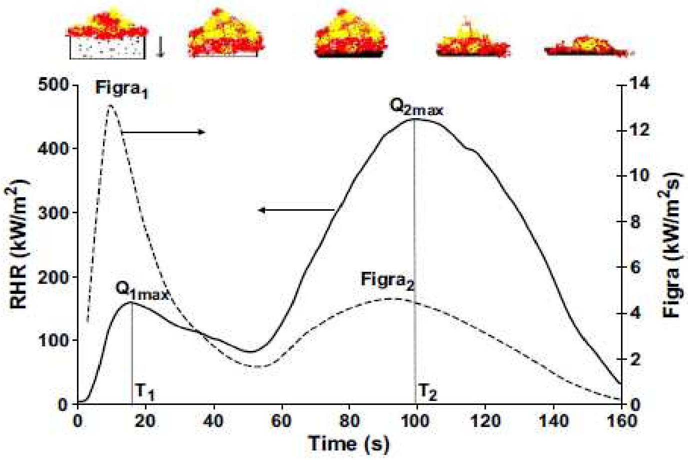

Figure 23: Combustion of a flexible PU foam under cone calorimeter [18]

The flammability of this flexible PU foam depends strongly on the chemical and physical properties of the foams as shown in **Table 2** [18, 19]. The water index is directly linked to the foam properties, an increase in the water index indeed leads to a reduction in the density of the foam [18]. While incorporating water, it reacts with isocyanate and the carbon dioxide created participates to give defined porosity and density to the foam network. This directly affects the fire properties of the resulting material.

---

[3] The isocyanate index is the excess of isocyanate over the theoretical amount for (1:1) reaction with all active H expressed in percentage.

Table 2: Influence of the composition of PU on its fire properties and thermal stability

Factors increased	Effects on fire properties and thermal stability
EO (ethylene oxide) content of the polyol	Time to ignition increases Same intensity of pHRR Quantity of heat released during the combustion increases
Isocyanate index	Reduction in the time to ignition Same intensity of the first pHRR
Concomitant increase of water index and isocyanate index	Reduction in density of foam Do not modify the time to ignition Reduces the time of combustion Increase in the intensity of the first pHRR Produce smoke during the first stage of combustion
Catalyst content	Higher time to ignition Increase the index of porosity of the foam
Surfactant content	Decrease the fire properties

In the case of foams, it was shown that PU fireproofing depends first on PU composition but in any cases by only playing on the composition it is impossible to reach an efficient fireproofed PU. The modification of the material by either reactive or additive FR is thus required to achieve the targeted fire properties.

2 FLAME RETARDANCY OF POLYURETHANES

2.1 Basics of flame retardancy

Due to their chemical structure, made up mainly of carbon and hydrogen, polymers are highly combustible [10], that is why it is necessary to flame retard them in order to decrease the risks in case of fire. The combustion of polymers is a very complex process inducing various steps and which has already been widely studied even if some uncertainties remain.

The combustion reaction involves three components: one or more combustibles (polymers), a combustive (oxidizing agent, generally oxygen from air) and heat. The whole process usually starts with an increase in the temperature of polymeric material due to an external heat source, coming from either an inner (e.g. exothermicity of the combustion reaction) or outer heat source. Polymer bond scissions are then induced and the resulting volatile fractions of polymer fragments diffuses into air and creates a combustible gaseous mixture: the ignition occurs [10]. A fire development depends also on the environment, environmental conditions and heat transfers [20].

The combustion of a polymer is the result of a combination of the effects of heat, symbolized by two mechanisms [10] (**Figure 24**):

- Non oxidizing thermal degradation (pyrolysis): initiated by chain scission under the effect of temperature increase
- Oxidizing thermal degradation: reaction with oxygen to produce a variety of low molecular weight products.

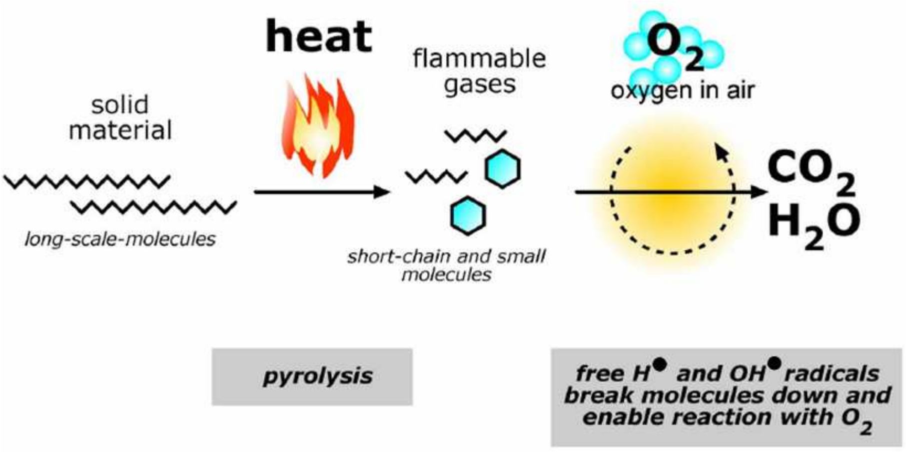

Figure 24: Combustion of a polymer [21]

Flame retardancy intends to inhibit or to stop the polymer combustion process by modifying the ‘actors’ of fire development. Flame retardants are highly efficient at improving the fire safety of plastics; they can increase resistance to ignition, reduce the rate of burning, flame spread, smoke emission and minimize dripping during combustion [22]. But a wrong type of flame retardant can negatively affect material properties, produce unwanted side effects and add unnecessary cost.

To fireproof a polymer, two ways can be considered [7]: first, it is possible to manufacture new polymers which are already fireproofed by their intrinsically chemical composition. The second strategy consists in elaborating new formulations or materials using flame retardants.

The reactive flame retardants are incorporated into the polymer chain during its synthesis (monomers, precursor) or in a post-reaction process (grafting) [13]. These flame retardants are directly integrated in the polymer chains. Reactive flame retardants are often used in polycondensates such as polyesters, polyurethanes and are very efficient.

The flame retardant (FR) additives are added either during the synthesis, the compounding or the shaping of the polymer. This approach is generally preferred because it is of acceptable cost and easy to realize due to the a posteriori modification of the polymer. **Table 3** sums up the different mechanisms of action and gives corresponding FR examples. A FR can act either by a physical or a chemical way or by a combination of both [10]:

- Physical action :
    - Cool the reaction medium: endothermic decomposition of flame retardant
    - Limit the fuels concentration: formation of inert gases instead of combustible gases
    - Limit heat and mass transfers: protective solid or gaseous layer
- Chemical action :
    - Reactions to produce either less reactive or inert molecule (flame retardant releasing specific radicals)
    - Accelerate polymer chain rupture: polymer moves away from the flame action zone
    - Formation of a carbonized or vitreous layer by chemical transformation of the degrading polymer chain (condensed phase action)

Table 3: Modes of action of widely used flame retardant

Mode of action	**Flame retardant**
Condensed phase	
Endothermic decomposition of flame retardant	Metal hydroxide
Dilution (limit the concentration of reagents)	Hydroxide or carbonates
Protective solid or gaseous layer	Intumescent systems
Gas phase	
Radical inhibition	Halogenated flame retardants
Dilution	Products giving water, CO_2 ...

A presentation of the conventional FR and their mechanism of actions will be done in the **section 2.3 p52** by discussing the possibilities to reach fireproofed PUs. But the next section will first be dedicated to the use of reactive flame retardant systems typically used in PUs.

2.2 Use of reactive flame retardant systems

The first widely studied route to achieve flame retarded PUs is the use of flame retardant reactive systems, this mechanism is very efficient and particularly appreciated in PUs.

Chemical modifications of the PU backbone through the introduction of thermally stable heterocyclic structure (isocyanurate, oxazolidone, imide, triazine, phosphazene) are viable methods for improving thermal stability and flammability (**Figure 25**) [14]. It is possible to manufacture poly(urethane isocyanurate), poly(azomethine urethane), poly(urethane oxazolidone), poly(urethane imide), etc. The use of a soft component containing a thermostable heterocyclic ring, of hyperbranched polyol or polyamine as crosslinking agent or high aromatic ring concentrations in the hard or soft segment as well as the incorporation of azomethine linkages in the PU structure is reported.

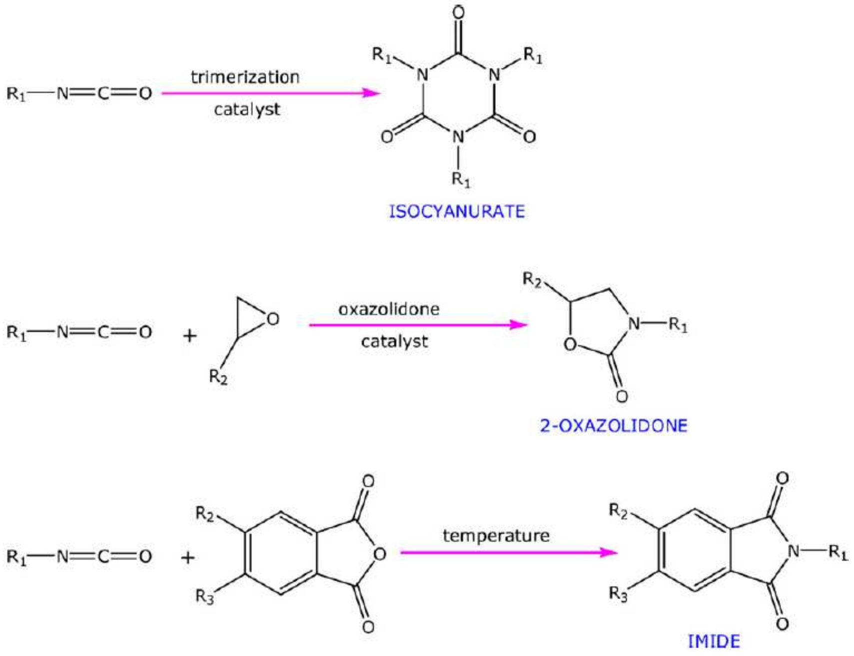

Figure 25: Formation of heat resistant isocyanates [14]

Phosphorus-containing compounds containing reactive functional groups that can be reacted with a suitable functional group in PUs are the most used as reactive type flame retardants [14]. Phosphorus compounds indeed act as char-forming agents reducing the generation of flammable gases. Many researches have been made on the flame retardancy of PU by bonding them chemically with phosphonate-based compounds [23-25]. An example of diphosphonate diol used to prepare PU is given in **Figure 26**. Phosphonates considerably modify the thermal degradation of PU [25]. The PU-phosphonate diols are stable up to 250°C and then exhibit two-step degradation behavior. Fire protection mechanism starts with the breaking of phosphonate, then it volatilizes and starts the fireproofing action before the beginning of combustion of PU (it can be seen by a decrease of combustible products at the beginning of the decomposition and considerable reduction of oxidation reactions with oxygen). The thermal stability decreases as the phosphorus content increases and finally, there is formation of a carbonaceous residue which forms a barrier preventing migration of the volatile products. The residue is higher with higher percentages of phosphorus.

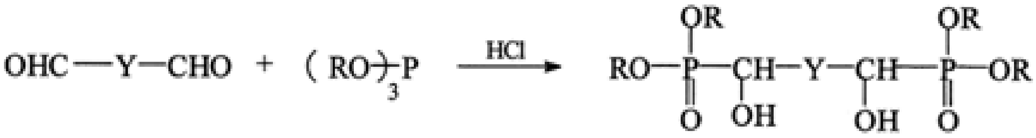

$$\mathrm{OHC{-}Y{-}CHO} + (\mathrm{RO})_3\mathrm{P} \xrightarrow{\mathrm{HCl}} \mathrm{RO}-\overset{\mathrm{OR}}{\underset{\mathrm{O}}{\mathrm{P}}}-\underset{\mathrm{OH}}{\mathrm{CH}}-\mathrm{Y}-\underset{\mathrm{OH}}{\mathrm{CH}}-\overset{\mathrm{OR}}{\underset{\mathrm{O}}{\mathrm{P}}}-\mathrm{OR}$$

Figure 26: Reaction of dialdehyde and trialkylphosphite to prepare a diphosphonate diol [23]

Through all these new linkages in the PU structure which allow the introduction of thermally stable structures, the thermal degradation of the PU is totally modified. An improvement of the fire properties is easily reached with a pertinent selection of the compounds. This method is certainly efficient but has several disadvantages among them its price and its difficulty to process especially at an industrial scale. The next part is thus dedicated to the use of flame retardant as additives in PUs.

2.3 Use of flame retardant additives

The use of flame retardant as additives is the preferred route for its price, availability and easy processing. When incorporating fillers, the thermal stability of PU depends on the size, shape, nature, amount of filler used, dispersion uniformity and degree of interaction between the filler and the PU matrix [14]. The first main challenge is, when adding flame retardants to PU by physical means, to ensure a good compatibility. When this is achieved, depending on the flame retardant type, different modes of actions coexist in the gas phase and/or in the condensed phase as discussed previously. A large variety of flame retardants, such as phosphorus-, boron-and silicon-containing additives, halogenated additives, melamine based systems, nanoclays or mineral fillers [14], can be used in PU formulations. This section surveys the different FRs used to fireproof PUs. A review of the different type of FR additives will indeed first be presented to then further focus on the additives used in the project.

2.3.1 Halogenated flame retardant additives

A wide variety of halogen-containing products have been reported in the literature as fire retardants for polyurethane [26, 27]. The effectiveness of halogenated-based flame retardants increases in the following order: fluorine > chlorine > bromine > iodine. Iodinated compounds however exhibit too weak dissociation energy to be effective, whereas fluorinated compounds, the most thermally stable additive, release effective halogenated species only above the decomposition temperature of PU. Chlorinated and overall brominated compounds are thus suitable to take part in the combustion process. Even if halogenated flame retardants might be effective, they tend to disappear because of environmental restrictions linked to the generation of toxic and corrosive fumes during combustion or recycling (incineration). In particular, PBDE (polybrominated diphenyl ethers) and PBB (polybrominated biphenyls) are banned by the RoHS (restriction of the use of certain hazardous substances) directive in electric and electronic devices. Even if the regulatory aspects are not always very clear concerning the use of halogenated products, they do not have a good image on the actual market. Despite this, the halogenated compounds are still used nowadays to fireproof PUs.

2.3.2 Nitrogenated flame retardant additives

The principal nitrogen-containing compounds of interest as fire retardants for PU foams include melamine, urea and dicyandiamide [28]. Melamine can also be found under derivatives such as melamine cyanurate and melamine phosphate (**Figure 27**). Melam, melem and melon are the products of the high-temperature condensation of melamine.

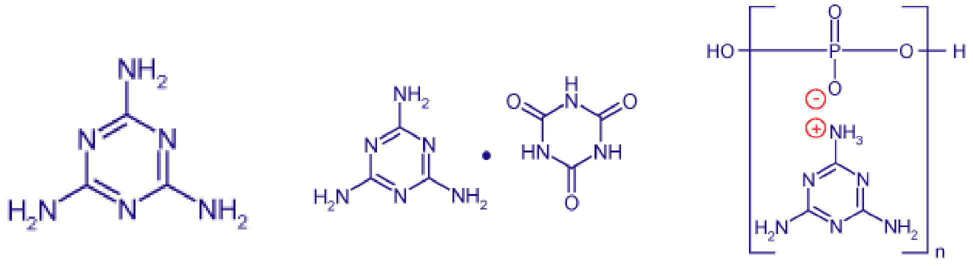

Melamine **Melamine cyanurate** **Melamine phosphates**

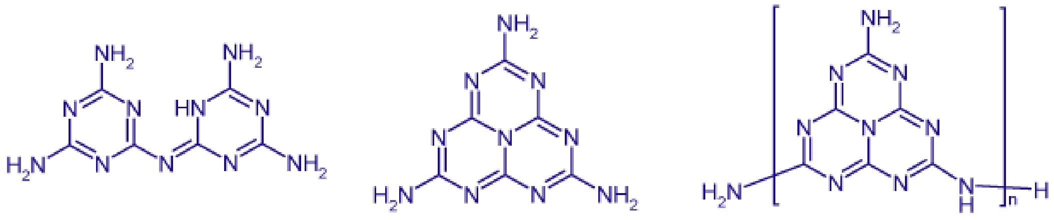

Melam **Melem** **Melon**

Figure 27: Chemical composition of melamine and its derivatives [29]

Melamine was used to prevent the fire propagation in flexible polyurethane foam, which is used in airplane seat cushion [30]. A 30 wt.% concentration of melamine is sufficient to produce a self-extinguishing urethane foam [31]. Urethane foams incorporated with 10, 20, or 30% melamine exhibit a burning rate of respectively 2.1, 1.7, or 1.5 mm/s according to ISO 3582 and an oxygen index of respectively 19.0, 22.0, or 24.0 according to ASTM D 2863. In this case melamine, by acting as a heat sink, increases the heat capacity of the combustion system and lowers the surface temperature of the foam by absorbing the heat. More precisely the mechanism of action consists in the sublimation of melamine that cools down the system because of the endothermic process. The formation of nitrogen (inert gas) or ammoniac during melamine condensation will moreover dilute the gas phase. Another study [32] shows that the weight of residues obtained from thermally degraded foams indicate that melamine did not have a pronounced effect on char formation. This was attributed to the fact that most of it escapes early on because of the relatively slow heating rates employed. However microanalysis revealed a slightly higher percentage of nitrogen remaining in the char of the PU including melamine. In situ ^{1}H NMR has provided definitive evidence that melamine also acts in the condensed phase in terms of promoting the char formation.

The flame retardant properties of rigid PU foam filled with melamine phosphate and melamine cyanurate characterized by cone calorimeter, smoke density measurements, limiting oxygen index (LOI) and also rate of burning and char yield is also reported [33]. The results reveal first that the peak heat release rate (pHRR) of melamine cyanurate and overall melamine phosphate filled PU is lower than that of neat PU. The same trends are observed according to LOI. The virgin PU has a LOI of 22 vol-%, it increases up to 24 vol-% with 10 wt.% of melamine cyanurate and up to 28 vol-% at 25 wt.% of melamine phosphate. This is attributed to a combination of effects. First the endothermic decomposition of melamine compounds releases non-combustible gases. After that in condensed phase, melamine condenses in melam, melem and melon, which may contribute to the formation of a protective layer. Melamine cyanurate and melamine phosphate are moreover very interesting for PUs because they release fumes with low toxicity and low opacity which are poorly corrosive.

2.3.3 Boron-based flame retardants

Boron-based flame retardants can be effective in condensed phase. Zinc borates, borax (sodium tetraborate), orthoboric acid, organic borates, ammonium biborate and ammonium pentaborate are typically used in PUs. They can promote the char formation and enable an intumescent process (the intumescence will be described in detail in **section 2.4 p59**). Polyurethanes are polymers containing oxygen atoms, thus the presence of boric acid causes dehydration, leading to the formation of a carbonized layer [10]. Upon heating, boron-based flame retardants lead to endothermic reactions and water and eventually boric acid and $BO^\bullet$ radicals are released. For instance zinc borate (the most widely used) endothermically decomposes between 290 and 490°C; liberating water, boric acid and boron oxide (B_2O_3). The later softens at 350°C and flows above 500°C leading to the formation of a protective vitreous layer at the polymer surface [10].

2.3.4 Metal hydroxides

Metal hydroxides, and in particular aluminum tri-hydroxide (ATH) and magnesium dihydroxyde (MDH) are widely used inorganic filler to flame retard polymer. They have different actions in polymer and in PU in particular [10, 21] (**Figure 28**):

- it reduces the content of combustible products
- it releases water
- it modifies the thermal conductivity of the resulting material and all its thermophysical properties
- it changes the viscosity of the resulting material
- it can produce a non-flammable and ceramic like layer on the surface of material

Inorganic compounds are however of a relatively low efficiency and are often used in relatively large content (higher than 50 wt.%) and/or usually in combination with other types of flame retardants [21]. These compounds are nevertheless widely used because they are cheap and easy to be incorporated into the polymer.

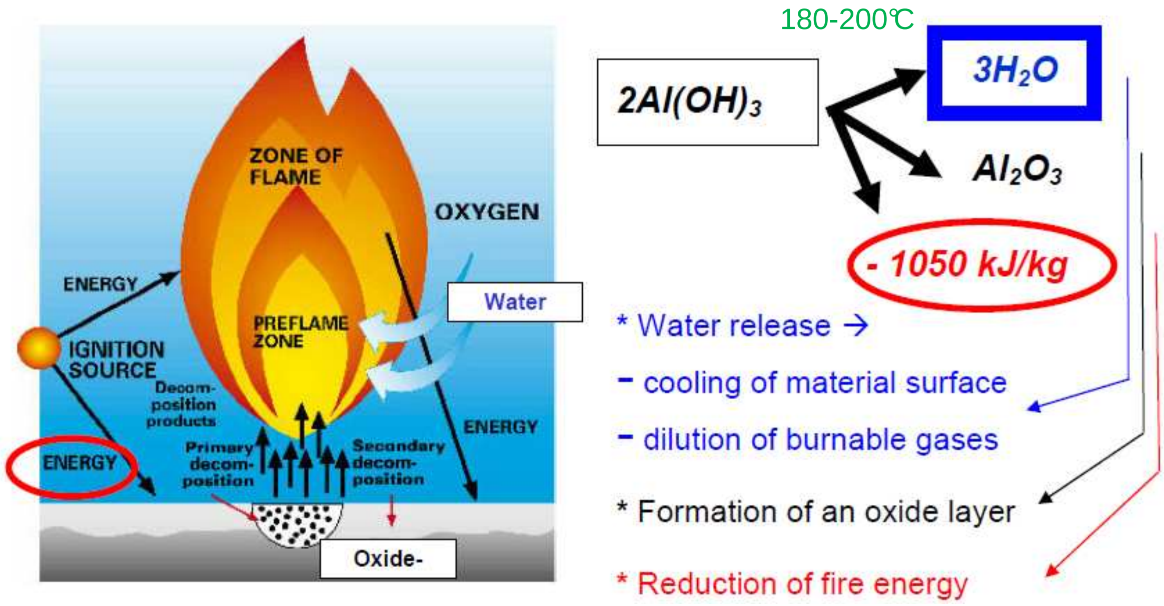

Figure 28: Schematic representation of the mechanism of action of ATH [21]

PU elastomer/ATH composites were obtained with micron-size $Al(OH)_3$ as additive. The oxygen index shows that flame retardancy increases with the increase of $Al(OH)_3$ content in the composites and can reach an interesting level. The use of different types and amounts of ATH and the resulting structure-property relationship in a PU foam is also reported [34]. ATH was also incorporated into TPU composites in combination with mica in order to investigate if the mica play a role in the flame retardancy of PU/ATH formulations [35].

The use of MDH to flame retard PU is also reported in the literature [36]. It acts with the same mechanisms as ATH, the only difference is its higher decomposition temperature (300°C).

On the other hand, the fire-retardant properties of urethane foams are greatly enhanced by the synergistic action of an ATH and MDH combination [31]. Synergism is the result of the difference in the temperatures at which the two metal hydroxides give off their water. ATH loses water at 220-250°C, whereas MDH loses water at 300–340°C.

Calcium carbonate has a small effect on fire performance of PU (the LOI increases from 22.0 to 22.5 vol.-%); however, the smoke obscuration number is lowered from 122 to 57.2 measured by the smoke density chamber test [33]. All carbonates release CO_2 at high temperatures but only magnesium and calcium carbonates release it below 1000°C, (magnesium carbonate : 550°C, calcium carbonate : 800°C) [10].

2.3.5 *Specific fillers*

Decreases in the flammability and increases in the oxygen index of rigid polyurethane foams have been also found with expandable graphite, exfoliated vermiculite, mica, calcium sulfate or arsenic oxide [31].

The thermal stability of TPU/mica composites prepared by melt mixing was first investigated [37]. It has been shown that mica incorporation delays the process of degradation of TPU/mica composites and that the thermal stability of the composites increases incorporating mica. It was also concluded that the use of mica does not modify to the fire retardant properties of PU (V-2 at UL-94).

The effects of five different types of fillers, two types of carbon black, silica, aluminum oxide, and zirconium (III) oxide, on the thermal and mechanical properties of hydroxyl-terminated polybutadiene-based PU elastomers were explored to develop a filled PU elastomeric liner for rocket motors [38]. The studied fillers do not considerably change the thermal degradation temperatures neither the thermal conductivity of the PU elastomers with filler content up to 16 wt.%. Finally, aluminum oxide-filled elastomers seem to be the most suitable composition.

Synthesis and following use of salen copper complexes as flame retardants in TPU has also been performed [39]. 10% loading of additives in TPU decreases significantly the pHRR; this diminution depends on the structure of the salen copper complex. The first investigations of mechanism suggest a condensed phase action.

2.3.6 Silicone based products

Various silicones were found to be efficient fire retardants in TPU, especially in terms of decreasing pHRR [16]. For example, an amine-functionalized siloxane which was incorporated in the TPU chain at 5 wt.% reduced the pHRR by 79%. The non-functionalized siloxane additive at 5wt.% loading showed a 70% reduction in the pHRR.

2.3.7 Nanocomposites

It is generally agreed that ideal performance in flame retardancy of polymers are given by inorganic fillers of nanoscale dimensions uniformly dispersed throughout the matrix and which interact strongly with the organic matrix [14]. By reducing the size and increasing the aspect ratio of the filler, the effectiveness against thermal degradation is indeed enhanced mainly because it increases interfacial interaction [40, 41]. This applies as well in PU and the nano-sized filler widely used in PU are nano-silica, clay particles, Fe_2O_3 and TiO_2.

Organo-modified clay fillers reduce the flammability of PU [42] mainly due to the formation of a multilayered carbonaceous-silicate structure in the condensed phase, through a physical mechanism [43]. This high-performance carbonaceous silicate char builds up on the surface of burning PU insulates the underlying material. However, natural clays are hydrophilic, thus a modification to make them hydrophobic and organically compatible is required (intercalating with amino acids, alkyl ammonium, phosphonium salt, cationic surfactants) [14]. Polyurethane/clay nanocomposite elastomers were synthesized using polyol-clay blends with different levels of dispersion, which affected the final elastomer microstructure [44] and the fire properties of these composites (**Table 4**). The exfoliated clay structure gives stability at high temperatures, suppresses the dripping and char formation is accelerated [45]. However, since dripping cannot occur, flame propagates and thus the material is not classified according to UL94.

Table 4: UL94 test results for PU, PU/clay microcomposite and nanocomposite

UL94 test	PU/clay microcomposite	PU/clay nanocomposite	Unmodified PU
UL94 test comments	Drips heavily Rapid extinction of flame Ignition of underlying cotton wool	No dripping at first Flame propagates up to the top of specimen	Drips heavily Rapid extinction of flame Ignition of underlying cotton wool
UL94 test rank	V-2	unclassified	V-2

In another study [45] the effect of polyol molecular weight and functionality on nanodispersion of clay in PU/clay nanocomposites and the correlated thermal and combustion properties were investigated. It has been first shown that the degree of dispersion is improved with the molecular weight of the polyol and unaffected by increasing functionality. Then the thermal and fire properties were investigated as shown in **Table 5**. The PU/clay nanocomposites volatilization is noticeably delayed in air owing to the barrier effect of the clay platelets. Furthermore, the intimate contact between clay layers and PU matrix seems to favor their interaction leading to thermally stable structures and to a decrease in the peak of HRR. The results of the UL 94 testing demonstrate the potential to use nanocomposite technology to eliminate fire-induced dripping in thermoplastic polymers. It is however pointed out that to achieve real non burning behavior nanocomposites, conventional flame retardant have to be added.

Table 5: Thermal and fire properties of PU/clay nanocomposite compared to virgin PU

Test	PU/clay nanocomposite	Unmodified PU
UL94 test	Nearly no dripping Extensive surface charring Flame propagates up to top of specimen	Drips heavily Rapid extinction of flame Ignition of underlying cotton wool
	unclassified	V-2
Cone calorimeter	After an initial mass loss, form a compact skin	Bubbles, quickly releases combustible degradation products
	Formation of char during combustion: lowers the pHRR for nanocomposite Time to ignition nearly similar	
TGA	Delay of degradation products release in nanocomposite compared to virgin polymer	

PU nanocomposites reinforced with organoclay or nanosilica were also prepared by dispersing the filler during polymerization [40]. The thermal stability of PU was enhanced with the addition of fillers and the effect was more pronounced with organoclay than with nanosilica; which was attributed to the fact that the mobility of PU chain is more restricted by the filler in the case of organoclay.

The effect of several nanofillers on thermal insulating properties of rigid PU foam was also analyzed; the nanofillers used differ for chemical nature and aspect ratio (pristine and organically-modified layered silicates; inorganic spherical nanopowders such as TiO_2 and SiO_2) [46]. The aspect ratio of the fillers was not determining for the enhancement of the analyzed properties. Good results were obtained for both layered silicates and spherical nanoparticles. The functionalization of the filler is the most important parameter because it enables the compatibilization between the polymer and the filler.

PU nanocomposites with inorganic nanofillers, based on montmorillonite (MMT) and Bi_2O_3, for the improvement of thermal stability were prepared [47]. pHRR of PU/MMT and PU/Bi_2O_3 nanocomposites were decreased by 50% compared to the PU matrix and fire retardant properties of PU nanocomposite including both MMT/Bi_2O_3 had the best improvement. The LOI of PU nanocomposites were also improved.

Finally an innovative technique to develop PU foams containing nanoparticles was introduced [48]. Polymethylene polyphenylisocyanate is mixed with nanoparticles such as SiC and TiO_2, and irradiated with a high power ultrasound liquid processor. In the next step, it is mixed with another mixture, containing polyol resin systems, surfactant and an amine catalyst, through a high-speed mechanical stirrer. Thermogravimetric analyses (TGA) analyses indicate that the modified foams are more thermally stable than the neat system.

2.3.8 Phosphorus based additives

The various phosphorus-containing flame retardants present phosphorus at different oxidation levels: red phosphorus, inorganic/organic phosphate, phosphonate or phosphinate [29] (**Figure 29**).

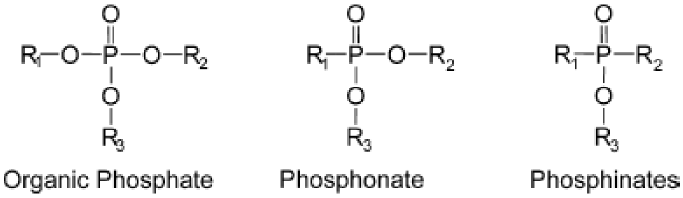

Figure 29: Chemical structures of phosphorus derivatives [10]

Although red phosphorus is used in polyurethane foam formulations, phosphorus compounds in the form of phosphates, phosphites, phosphonates, phosphonitrides, phosphoric acid, phosphonic acid, and halogen-containing phosphorus compounds are more effective [31]. These products are active either in condensed and gas phases depending on their nature (**Figure 30**) [10, 49]. In the gaseous phase, these additives form active radical (for example $PO^{\bullet}$) to react with $H^{\bullet}$ and $OH^{\bullet}$ to perform a radical inhibition process. This effect is significantly increased in oxygen or nitrogen-containing polymers, as PU. In the condensed phase, phosphorus-containing flame retardants are particularly effective with polymers containing oxygen. They produce phosphoric acid and water. The first one catalyzes the dehydration reaction of terminated alcohol and the second one dilutes the oxidizing gas phase. At higher temperature, ortho- and pyrophosphoric acid are transformed into metaphosphoric acid and the corresponding polymer react with these specifies in order to promote char formation.

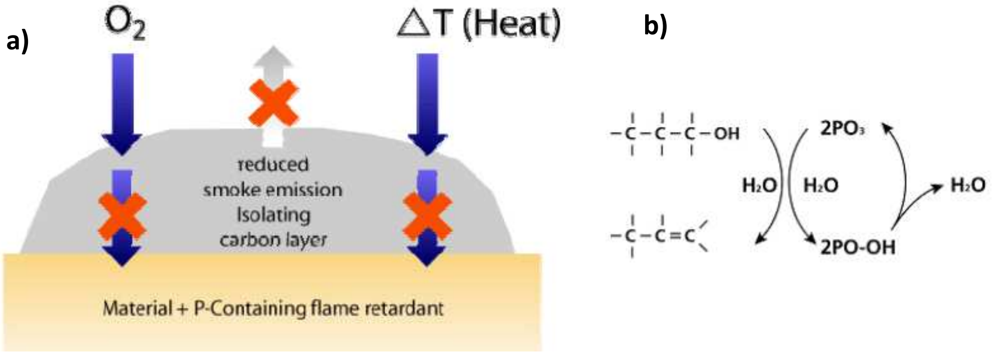

Figure 30: Flame retardancy mechanism of polymer thanks to a phosphorus-based flame retardant (a) condensed phase (b) gas phase (from European Flame Retardants Association, *How do flame retardants work ?* 2006)

Among the various phosphorus-based flame retardant, ammonium polyphosphate (APP) is a common additive and is particularly effective in PU. The addition of APP in urethane foams sharply decreases the emission of CO and HCN, the smoke density and the formation of soot [31].

The condensed phase mechanism leading to a char formation protecting the residual material is the principle of intumescence. The next subsection explains widely this concept and detailed some examples of its use in PUs since the Ph.D work will focus on intumescent PU systems.

2.4 Intumescence concept

2.4.1 General description of intumescent systems

The introduction of intumescent systems in the field of fire protection belongs to H. Tramm and co-workers. While the word intumescence is not mentioned, he first described the intumescence process in the patent literature in 1934 in Germany and 1938 in the USA [50]. On the other hand, the first comprehensive paper was published in the early 70s by H. Vandersall and gives the fundamentals of intumescent [51] but only considered coating. Intumescent coatings are nowadays still used to protect materials such as wood, plastic, steel and other materials from the high temperatures of fires (thus preventing or delaying structural damage during fires) [21]. The first researches to extend intumescent science to polymeric materials belong to G. Montaudo and co-workers [52, 53] and G.Camino and co-workers [54-58]. They indeed widely studied the mechanism of intumescence in fire retardant polymers in 1983-84. This work was useful for the development of products which were launched by different companies in the 90s.

The word “intumescence” comes from Latin “intumescere” which means “to swell up” [59]. The intumescence process [60] basically consists in an increase of volume under a temperature increase. An intumescent material, heated beyond its critical temperature, degrades by swelling. The intumescence process results in the formation of an expanded multicellular barrier (called char) able to protect the residual material or a substrate from the flame (**Figure 31**). In fact, this reaction combines carbonization and swelling as the two principal steps. Flame retarding polymers or textiles by intumescence are essentially a special case of a condensed phase mechanism [59].

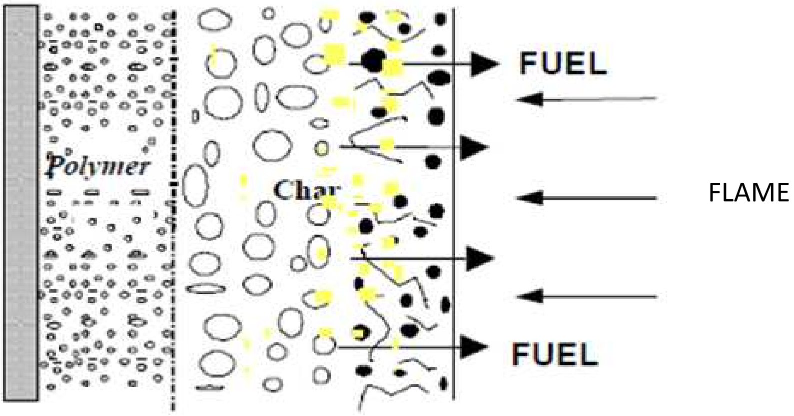

Figure 31: Degradation scheme of an intumescent material [13]

The aim is to develop a carbon structure to trap the gaseous product of the decomposition. This layer acts as insulating and protective barrier reducing heat, fuel and mass transfers between the heat source and the polymer. Depending on the properties of the char (distribution and size of the cells, thickness of the walls, expansion, mechanical resistance, rheology, chemical composition, etc.), the fire protection will be more or less efficient. The mechanical properties of the intumescent shields developed in the case of fire are indeed particularly important since internal pressure (due to degradation products) or external environment can easily destroy it leading to a loss of insulating properties of the protective layer [8].

H.L. Vandersall [51] reviewed for the first time the intumescent chemistry by explaining the role of each component of intumescent systems. He listed ingredients suitable to create intumescence. An intumescent system combines [10, 60] (**Table 6**):

- **An acid source** that promotes the dehydration of carbonizing agent. It is a compound able to release some acidic compound (e.g. phosphoric acid) when there is a rise of temperature. It is released below the decomposition temperature of the carbonizing agent

- **A carbonizing agent** that is dehydrated by the acid source to form a char. The amount of char depends on the number of carbon atoms, on the rate of dehydration and on the number of reactive hydroxyl sites of the carbonizing agent
- **A blowing or swelling agent** that contributes to the expansion of polymer and to the formation of a swollen multicellular layer by releasing gas. Gas must be released during the thermal decomposition of the carbonizing agent in order to allow the expansion of the carbonized layer.

It is also important to notice that a compound can have two actions; for example ammonium polyphosphate (APP) could act at the same time as acid source and blowing agent.

Table 6: Examples of classical molecules used in intumescent systems [29, 59]

Acid source	Carbonizing agent	Blowing agent
Acids : phosphoric, sulfuric, boric	Carbohydrates Starch, dextrin, sorbitol, pentaerythritol, mannitol, methylol melamine	Amines/amides Urea, urea – formaldehyde resins, melamine, dicyandiamide
Ammonium salts : phosphates, polyphosphates, borates, sulfates, halides		
Amines - amides : products of reaction of (guanidyl)urea with phosphoric acids, melamine phosphate		
Organophosphates : Tricresyl phosphate, alkyl phosphate	Others (charring polymers) Polyamide 6, polycarbonate, polyurethane	

We must remember that although flame retardancy could be achieved in several manners, intumescence allows materials to pass many fire specifications keeping the original properties of the polymer at an acceptable level, especially the mechanical properties [61]. Although, intumescence is used for many years on different substrates or for flame retarding polymer, many researches are still going in order to find better intumescent system for polymeric materials.

2.4.2 Use of intumescence in polyurethane

The attractive field of intumescence has been used in a vast range of polymers and for the purpose of this work; the use of intumescence in PUs will be in particular detailed in this section. Only few additives used to flame retard PUs shows a real enhancement of the fire properties due to an intumescent phenomenon; these mechanism of action are detailed in this section.

One advantage of PU compared to other polymeric matrix is that it is naturally a carbonizing polymer which can act as the carbonizing agent in an intumescent formulation. For instance, it has already been used as a char-forming agent in intumescent polypropylene formulations [62]. The intumescent fire retardant/PU system [14] has several advantages such as low smoke production, low toxicity, low corrosion, long life. An organic component which may serve as a binder to hold the material together could act as a char former by thermal degradation at a temperature lower than the temperature at which the PU degrades. In this case, the char formed from the degradation of the organic component is available to protect the PU when the degradation of the PU starts. It has however to be noticed that the physical structure of the char layer plays a very important role in the performance of the flame retardant.

APP, as we have seen in the previous part, is a widely used effective intumescent fire retardant for several kinds of polymer-based materials, and in particular for PU [63]. Expandable graphite (EG) (**Figure 32**) is another typical intumescent flame retardant, which is a graphite intercalation compound [63]. It is a layered crystal consisting of sheets of carbon atoms tightly bound to each other. Chemicals such as sulphuric acid may be inserted between the carbon layers. When exposed to heat, EG expands and generates a voluminous insulative layer thus providing fire-retardant performance to the polymeric matrix. EG is used in a number of fire retardant applications as a blowing agent and as a smoke suppressor and in particular in PUs.

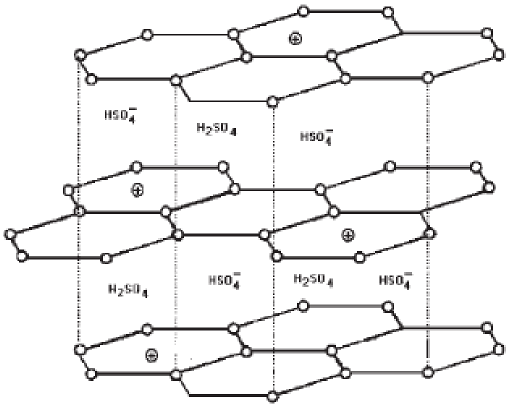

Figure 32: Chemical structure of expandable graphite [64, 65]

The effect of APP and/or EG has been widely studied in the literature. Those additives can thus be used in order to improve the flame retardancy of PUs via an intumescent process [63, 64, 66, 67].

When APP is added to PU, the char formation is favored resulting from interactions between the additive and the polymer; indeed polymer chains are trapped by phosphate links in the carbonaceous shield [67]. The carbonaceous layer, even if it is not expanded, presents a visco-elastic behavior which ensures the fire protection in a large range of temperatures. The efficiency of APP in PU (**Figure 33**) was attributed to its contribution to the char formation through a condensable-phase reaction [63].

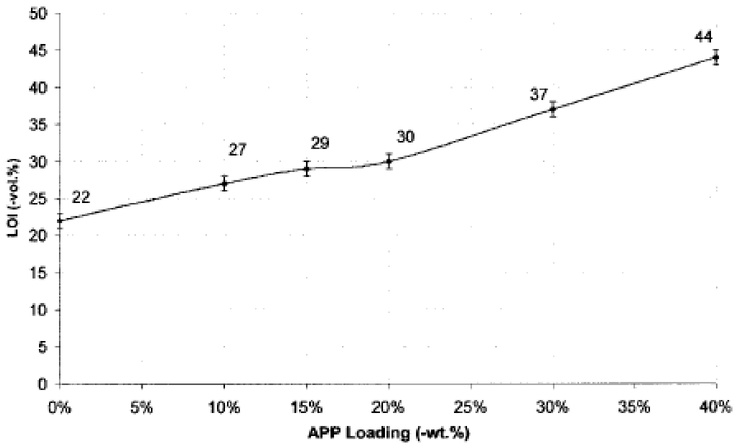

Figure 33: Evolution of LOI values versus APP level in PU [66]

Duquesne et al. [66] studied the mechanism of fire retardancy of PU using APP and the main results are shown in **Table 7**. Under air, PU/APP formulations have a higher thermal stability than the virgin PU for a temperature higher than 320°C. On the other hand, it is also reported that oxygen enhances the thermal stability of both PU and PU/APP at first but then, at higher temperature the rate of weight loss increases which leads to a total degradation for PU and to the formation of a stable residue (10 wt.%) for PU/APP formulations. Similar results were obtained with a combination of phosphorus and brominated flame retardant, which act not only in the gas phase but also in the solid phase [68].

Table 7: Comparison of thermal degradation of PU, APP and PU/APP under air and nitrogen

TGA	APP	PU	PU/APP
Under nitrogen	300°C: elimination of NH_3 + H_2O, formation of PPA (polyphosphoric acid) Above 550°C: PPA dehydration and sublimation of P_4O_{10}	240-400°C: depolycondensation reaction 800°C : **40% wt residue**	Degradation begins at lower temperature: PU + APP react (catalysis by PPA) 240-370°C: major step of degradation 370-500°C: low rate of degradation 800°C: **50% wt residue**
Under air	Similar under air and nitrogen	350-530°C: formation of a carbonaceous material 800°C: **0% wt residue** (oxidation)	290°C: PU + APP react 320-550°C: carbonaceous material formed 600-800°C: rapid degradation, **10% wt residue**

When EG is added to PU [67], there is no chemical reaction between the polymer and the additives and less char is formed than with PU/APP formulations. The mechanism of action is mainly physical. When degrades, the material forms expanded "worms" of graphite embedded in the degraded PU matrix (**Figure 34**). It creates a very thick layer with low density and insulative properties.

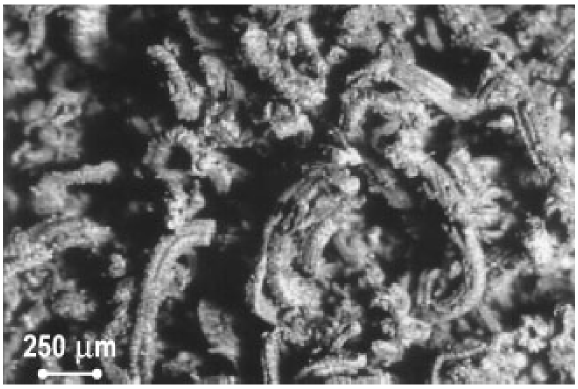

Figure 34: Optical microscopy picture of PU/EG samples showing the expanded worms [64]

Elemental analysis, X-ray diffraction and electron spin resonance investigations [64] are concomitant to conclude that EG and the matrix degrade independently with no interactions. During the blowing measurements, the untreated PU shows no expansion whereas, the PU/EG formulations expand in the temperature range of degradation of EG (210-500°C) creating an insulating layer at the beginning stages of fire. It thus enables the combustion cycle to be stopped early. Otherwise, the high rate of expansion enables EG to smooth the flame. Finally, when characterizing the surface after fire test, observations demonstrate that the untreated PU is flat and present some cracks and holes. On the contrary, the PU/EG surface is thick; it is composed of expanded graphite flakes embedded in degraded PU char. These observations confirm the fact that the layer resulting from the degradation of PU/EG is efficient enough to insulate the substrate from the action of the flame or heat source. In the case of virgin polymer, on the contrary, oxygen diffusion, mass and heat transfer may occur through the cracks present on the surface resulting in a degradation of the underlying material and thus maintaining the combustion cycle. EG has also been used in the same way in water blown polyisocyanurate–polyurethane foams in order to improve their fire behavior [69].

Rigid polyurethane foam (RPUF) filled with various loadings of EG and/or hollow glass microspheres were prepared by cast molding and the flame retardant properties were measured [70]. It has been found that the glass microspheres cannot improve the fire retardancy of RPUF at the contrary to EG.

The effect of the incorporation of APP and/or EG effect on the flame retardant properties of a RPUF was investigated and the main results are presented in **Table 8** [63].

The increase of LOI combining APP and EG is reported to be due to the dispersion of the additives in the RPUF matrix which is improved. EG slices can consequently act as blowing agent for the intumescent structure resulting from PU/APP interaction. Moreover, compact layers may be developed by the worm-like structure of the graphite agglomeration in the high viscosity products of depolycondensation reaction.

Table 8: Comparison of fire properties improvement of RPUF with APP and/or EG

Test	RPUF/APP	RPUF/EG	RPUF/APP/EG
Vertical and horizontal burning tests	- Reduce the burning time - Burning rate reduces gradually with APP content	Reduce the burning time of RPUF	Favorable flame-retardant synergistic effect
LOI	LOI value increases with APP content	LOI value increases with EG content, higher than RPUF/APP	Favorable synergistic effect Optimum : APP/EG = 1/1
TGA	Initial protective layer decomposes to yield a compact char	Formation of a thermally stable material	Favorable and antagonist effect depending on the temperature

TG curves (**Figure 35**) reveal different degradation pathway depending on the filler used.

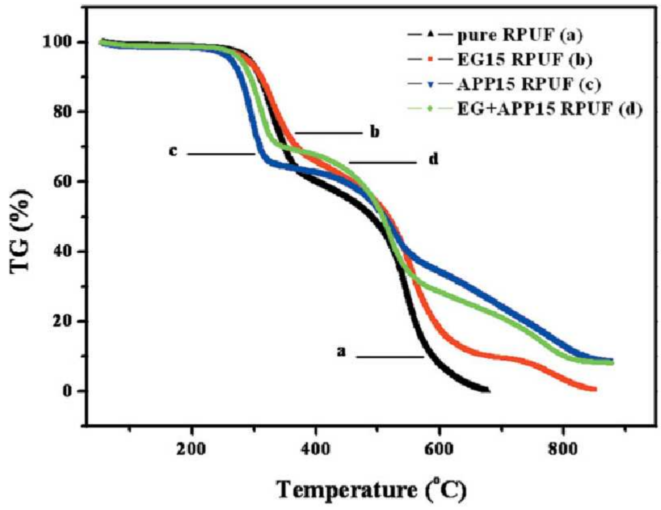

Figure 35: TG curves of pure RPUF and fire retardants filled RPUF (EG, APP or EG + APP) [63]

In regard to pure RPUF [63], the first step of degradation between 250 and 440°C is attributed to the depolycondensation reaction. The second step of degradation between 440 and 676°C leads to no residue. There are two degradation steps for the 15 wt.% RPUF/EG formulation, the first one occurs from about 230 to 450°C with a peak at 331°C corresponding to the expansion of EG. The residual weight of 15 wt.% RPUF/EG is higher than that of pure RPUF from 230 to 850°C. The second step is assigned to the thermooxidative degradation of the transient char that yields high temperature residues; EG leads to the formation of a thermally stable material for RPUF [71]. The degradation of 15 wt.% RPUF/APP is also composed of two steps. RPUF and APP react first; the volatile degradation products of APP at this step are mainly ammonia and water, when crosslinked polyphosphoric acid (PPA) is formed in the condensed phase. Then, acceleration in the depolycondensation reaction takes place due to the acid catalysis by the phosphoric acid. The addition of APP to RPUF decreases the thermal stability of RPUF at the first stage and increases the thermal stability at the second stage. The incorporation of 15 wt.% (APP + EG) in RPUF shows a two-step degradation. The first one occurs with a peak at about 200°C, whereas the second step is observed at a temperature higher than 390°C with a peak at about 526°C. Within the high-temperature range, the amount of residue remains almost constant. From 550 to 850°C, the residual weight is always higher than for 15 wt.% RPUF/EG and lower than for 15 wt.% RPUF/APP. A compact layer may be developed by the worm-like structure of the graphite expansion embedded in the high-viscous products of depolycondensation reaction. This layer can act as a thermal insulative barrier to protect the residual material. This causes the positive interactions of APP and EG and can leads to higher residual weight of material than expected. When the temperature is higher than 550°C, PPA sublimates and/or dehydrates to P_4O_{10}. At the same time, the worm-like structure of EG enlarges the interface between PPA and environment. The degradation is thus accelerated and the antagonistic effect appears [63].

In parallel, an analysis of smoke and gases generated under various thermal decomposition conditions of PU and fire retarded PU coatings is reported [13, 72]. It has been evidenced that the addition of APP in PU sharply decreases at the same time the emission of toxic gases such as CO or HCN, the optical density of smoke, the weight loss and the formation of soot. EG enables a decrease in toxic gases in a lower proportion than APP.

The reaction to fire of TPU containing polyhedral POSS was also investigated [73]. This system does not combine the three components normally required for intumescence as detailed in the previous section. The incorporation of 10 wt.% POSS in TPU decreases however by 80% the pHRR compared to virgin TPU (**Figure 36**). Nevertheless, time to ignition of the composite (60 s) is twice shorter than that of virgin TPU (120 s). We can also note that there is no significant enhancement of LOI (22 vol.% for the virgin TPU vs. 23 vol.% for TPU–POSS) and UL 94 rating (V-2 at 3.2 mm in the two cases) when incorporating POSS in TPU. The protection occurs via an intumescent mechanism even though only POSS was added to TPU. The intumescent material is composed of ceramified char made of silicon network in a polyaromatic structure. This material forms a thermal barrier at the surface of the substrate limiting heat and mass transfer leading to a limited heat release rate (HRR).

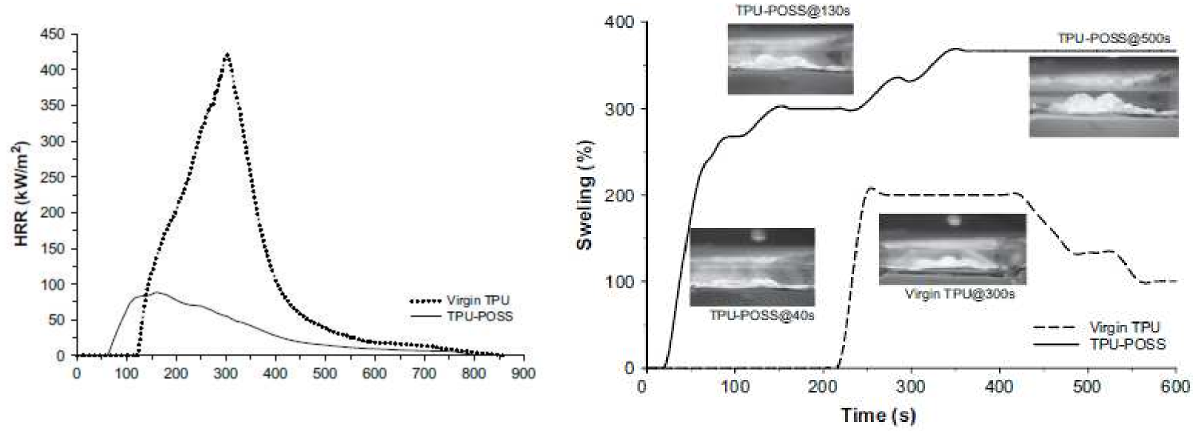

Figure 36: HRR and swelling versus time for virgin TPU and TPU/POSS nanocomposites [73]

The literature concerning the use of intumescent systems in PU clearly shows the efficiency of this approach. Although few additives are significantly used, the gain in fire properties is generally higher than when using flame retardants that do not act as charring promoters. Intumescent PUs are consequently very interesting but the addition of a synergistic agent should allow to manufacture even better systems. To have significant effect in intumescent systems, it is generally required to incorporate a high quantity of additives (around 30 wt.%), thus affecting other properties of the matrix such as mechanical, optical or electric properties. The next part will be dedicated to the study of the synergy in intumescent systems in order to improve the fire performances. The synergy with nanofillers is particularly appreciated because it is well known in many polymers that a combination of intumescent FR and nanoparticles enhances the fire performances and/or allow reducing the additives loading while the performances are maintained.

2.5 Synergy in intumescent systems

2.5.1 The concept of synergy

The concept of synergy in intumescent systems was published first by Scharf and co-workers in 1992 [74]. The effect of two additives (TiO_2 and SnO_2) on an intumescent polypropylene was investigated. The authors found that the TiO_2 gives a synergistic effect whereas the SnO_2 leads to an antagonism in fire properties. Later Levchik and co-workers [75] were also interested in the use of several metal oxides as synergists to increase the carbonization of polyamide/ammonium polyphosphate. In the meantime, the potential synergistic effect of zeolites in an intumescent process was investigated by Bourbigot and co-workers [76, 77]. Regarding the interesting improvement in fire properties reached by adding a small quantity of inorganic particles in an intumescent matrix while reducing the total additive loading, the concept of synergy became an up-to-date topic and is nowadays widely used and studied.

The word "synergy" is derived from the Greek word "synergos", meaning to work together or, literally, to cooperate [8]. The concept of synergism is used to optimize flame retardant formulations and enhance the performance of mixtures of two or more additives [10]. In order to achieve high fire performance levels, it is indeed necessary to develop a flame retardant system based on a combination of different flame retardant agents. The synergism is achieved when the performance obtained for a mixture of additives is greater than that calculated for the linear combination of the single effects of each additive. Incorporation of additional filler in an intumescent formulation can involve some unexpected "catalytic" effects. Performance is enhanced dramatically adding small amount of an additional compound [78]. Synergistic phenomena can be obtained either by a combination of flame retardancy mechanisms, such as char formation by a phosphorus based flame retardant combined with a gas phase action of an halogenated flame retardant, or by a combination of flame retardant agents reinforcing the same mechanism, e.g. nanoclays and phosphorus based flame retardant agents, both acting in the condensed phase. A large range of combinations is conceivable but the main challenge is to find out the governing parameters to finally understand how the synergy works and thus design cleverly new materials.

2.5.2 Understanding of synergy mechanism in intumescent systems

Based on the literature found on the synergy in intumescent systems, whatever the polymeric matrix, this part intends to give clues to answer the question "how does synergy work"? The aim is to identify the characteristics of the synergistic particles and their behavior with the matrix which may be responsible of the enhancement of fire performances. The use of inorganic fillers as synergists has been widely studied and the effects on the flame retardancy depend a lot on the matrix, the intumescent systems and the characteristics of the filler.

In the recent literature, numerous synergists (micro- and nanofillers) have been used in conventional "three-based ingredients" intumescent formulations [78]. It covers the boron compounds (zinc borates, B_2O_3, borophosphate, borosiloxane), phosphorus compounds (phosphazene, $ZrPO_4$), silicon compounds (silica, silicone, silicalite), aluminosilicate (mordenite, zeolite, montmorillonite), rare earth oxides (La_2O_3, Nd_2O_3), metal oxides (MnO_2, ZnO, Ni_2O_3, Bi_2O_3, TiO_2, ZrO_2, Fe_2O_3) and others (carbon nanotubes, silsesquioxanes, layered double hydroxides, Cu, Pt, talc, sepiolite, zinc and nickel salts) [59]. The presence of this additional filler can modify the chemical (reactivity of the filler versus the ingredients of the intumescent system) [79] and physical (expansion, char morphology, char strength and rheology and thermophysical properties) [73] behavior of the intumescent char when undergoing flame or heat flux leading to enhanced performance. This section is devoted to review the literature dealing with the understanding of synergy mechanism in intumescent systems.

The first interesting and widely used class of synergistic agent is the inorganic fillers and in particular the oxide. Their effects depend anyway on the polymeric matrix and intumescent additives, so that a same filler may not always give synergistic effects.

In the work of Scharf and co-workers [74], they found that the TiO_2 gives a synergistic effect whereas the SnO_2 leads to an antagonism in fire properties of an intumescent polypropylene. The outer surface of the unmodified intumescent polypropylene char exhibits a consistently smooth uniform appearance. The TiO_2 modifies the char that is uniform and continuous and has a compact rugged outer surface due to the formation of agglomerates. By contrast, the SnO_2 modified char displays a fine, flaky surface structure with a high degree of porosity and cracks. TiO_2 brings a physical reinforcement of the structure while offering structural support through hydrogen bonding or bridging. SnO_2 is at contrary thought to react with the intumescent system resulting in hydrolytic breakdown of the polyphosphoric acid that serves as char infrastructure. They conclude that TiO_2 that physically interacts with the intumescent matrix appears synergistic to effective flame retardancy whereas SnO_2 that chemically interacts appears antagonistic to effective flame retardancy.

On the other hand, it is also reported that the combination of phosphinate additives with metal oxide nanoparticles such as Al_2O_3 or TiO_2 can enhance the thermal stability and fire behavior of PMMA [80]. All the results suggest that the phosphinate additives act here principally in the condensed phase, the presence of oxides playing a reinforcement role for the carbonaceous layer. However, TiO_2 does not improve the fire behavior of the composites significantly enough whatever the phosphinate additive used; whereas Al_2O_3 give more interesting results.

In another study [81], the degradation process of the intumescent system, PP/APP/PER, with and without SiO_2, Al_2O_3 or blend of SiO_2 and Al_2O_3 was investigated. For PP/APP/PER system with the blend of SiO_2 and Al_2O_3 a maximal synergy was observed at the highest LOI of 35.5 vol.%, 17 units higher than the virgin PP. Its excellent flame retardance was also evidenced by the highest residual char measured from TGA and parameters from cone calorimetry.

Inorganic fillers such as talc, $CaCO_3$, $ZnCO_3$, MnO_2 improve fire retardant action in the system nylon 6/APP [82]. The fillers interact with APP increasing the char yield and improving insulation properties of the char. Phosphate glasses formed on the surface of burning fire retarded polymer protect the char from oxidation and hinder diffusion of combustible gases to the flame.

The use of small amount of talc and manganese dioxide combined with APP in PA-6 promotes charring and enhances insulative properties of the intumescent coating leading to a significant improvement of the flammability performance [83, 84].

The effect of OMPOSS and CNT was investigated in intumescent epoxy/APP formulations [85]. In the presence of APP and OMPOSS, an impressive intumescent structure is created and a synergy is observed in terms of mass loss calorimetry. On the contrary, the incorporation of CNTs together with APP in the epoxy provides a residue that is less structured than that of epoxy/APP. The thermal degradation of the sample containing OMPOSS is slowed down. The better behavior of polymers containing POSS is attributed to the formation of a silica layer in the sample. Silicophosphates can moreover reinforce the char structure but this is not the major reason explaining the synergy. It has been shown that the intumescence occurs earlier with OMPOSS compared to epoxy/APP, therefore offering a protection to the underlying material before further degradation. The development of this intumescent structure before ignition can be attributed to the combination between the release of ammonia by APP and the partial sublimation of OMPOSS. The addition of CNTs to the system on the contrary modifies the otherwise well-organized mechanism of protection of APP in epoxy resin. CNTs do not chemically interact with the other constituents. The swelling begins similarly as with APP alone, but it occurs very briefly. The thermal diffusivity is also significantly reduced. These modifications may explain the antagonism between APP and CNTs.

The formation of a ceramic layer by using borosiloxanes in a combination with an intumescent system is a promising way of forming efficient flame retarded PP [86]. The borosiloxanes react with the polyol component of intumescent systems resulting in increased melt viscosity and thus reduced dripping.

Zinc borates are particularly interesting to offer synergy in intumescent systems because it reacts easily with the other components.

The interaction between zinc borate and APP was also studied [87]; it has been demonstrated that reactions occur between APP and zinc borate leading to the formation of borophosphates and zinc phosphates which stabilize phosphorus species. The borophosphates linked to P-O-C bonds, phosphoric acid and pyrophosphates, coming from the degradation of the polymeric matrix with APP, will give a higher protection [88]. Borophosphates indeed give an interesting mechanical resistance and also a good thermal stability; they indeed sublimate at 1200°C without decomposition.

The flame retardancy of LDPE treated with a flame retardant composed of ultrafine zinc borate and intumescent flame retardant has been investigated and it was proven that a synergy occurs because the residue increases and the quality of the char formed is enhanced [89].

The potential of zeolites as synergists has been investigated in combination with APP and PER.

A 4A type zeolite was added in the intumescent APP/PER system incorporated in polyethylenic-based formulations (ethylenic co/terpolymers) [77]. It has been demonstrated that the polymer-APP/PER-4A improves considerably the fire-proofing properties of the raw materials. The LOI results show that a synergistic effect is obtained at 1.5 wt.% of 4A zeolite; for this level, the LOI values are increased to 39 vol.% in comparison to the classical APP/PER system, which is at 30 vol.%. Nevertheless it is shown that the efficiency of the zeolite depends on the polymer used. Finally, the measurement of the FR performances using cone calorimeter indicates that the zeolite alters the degradation of the intumescent shield to form a more thermally stable material.

The presence of the zeolite leads to an increase in the stability of APP/PER system at high temperature (T > 550 °C). It was attributed to the formation of localized ‘turbostatic carbon’ in the structure [8]. The zeolite permits retention of the comparatively unorganized carbon species in the high-temperature range while ‘‘rigid’’ domains are proposed as initiators for the formation of cracks in the coating without zeolite. The relationship between the formation of a coherent macromolecular network and the improved fire retardant performance of the APP-PER/zeolite system was proposed. The synergistic agent may also have a chemical effect promoting the charring properties and the thermal stability of an intumescent system leading to an increase of its efficiency.

Nanofillers are well known to be particularly efficient when used as synergistic agents.

Polylactic acid (PLA) can be flame retarded using the intumescent combination of APP and melamine (Mel) at total loading of 10 wt.%. This loading is still sufficient to get relatively high LOI (33 vol.-%) and a synergistic effect is observed with an organomodified clay (C30B) (LOI=35 vol.-%). V-0 at UL-94 (3.2 mm) is achieved for the formulations with and without C30B and HRR is decreased by 42% and 33% with and without 30B respectively during a cone calorimetry experiment (external heat flux = 35 kW/m²) [90].

In other polymers, nanoclays are efficient as well. The incorporation of condensed phase flame retardants such as APP or melamine phosphate reduces the pHRR and THR values of a polyester resin. The inclusion of small amount of nanoclay (5 wt.%) in combination with these char-promoting flame retardants causes a total reduction of the pHRR of polyester resin in the range 60–70% [91].

In other work [92], using different clays as synergistic agents, the resulting LOI classification depended on the content of exchangeable cations of the clay (LOI values increase when the number of exchangeable cations per unit cell increases). Kaolinite type minerals do not have such cations while zeolites do. It was thus suggested that the FR performance depends on exchange properties of the aluminosilicates.

In intumescent EVA, the synergistic effect of montmorillonite (MMT) was partially explained by the increase in the mechanical properties of the intumescent shield [93]. This was due to chemical interactions between the particles and the intumescent system leading to the presumed formation of aluminosilicophosphate complexes and/or to the reinforcement due to the presence of a lamellar structure. Moreover, it was also observed that the viscosity of the burning polymer is sharply modified in presence of nanoparticles.

This effect of MMT was observed in other polymeric matrix such as PP [94]. The results show that when the total loading of flame retardants is 30%, the LOI value of the composite reaches 29 vol.%. However when 0.5% OMMT (organomodified MMT) is added into the flame retardant system, the flame retardancy of the materials is improved: LOI value of 31 vol.% and UL-94 V-0 rating.

A physical reinforcement of the intumescent shield can be achieved using particles presenting high aspect ratio [8]. As an example, the addition of a layered inorganic filler (MMT or LDH) in an EVA/APP/PA6 intumescent system leads to classification in the UL94 test (respectively V0 and V2) whereas the formulation without layered filler is unclassified regarding this test. The mode of action of the layered inorganic fillers was attributed to the high aspect ratio of the fillers which is responsible for the increase in the rigidity of the intumescent shield. Higher mechanical stability of the intumescent shield avoids the formation of cracks and so the heat and mass transfer are limited, leading to interruption of the combustion triangle. The formation of rigid crystalline domains in the presence of synergists, for instance, modifies the mechanical properties of the intumescent shield.

It is noteworthy that the synergistic effect is not always observed even if the compounds are supposed to improve the fire properties. As an example, a comparative study on the flammability of polyethylene modified with commercial fire retardants and a zinc aluminum oleate layered double hydroxide has been made, and the combination of these conventional fire retardants with the ZnAl LDH does not offer any advantage in pHRR reductions [95]. Another example concerns the influence of talc on the fire retardant properties of highly filled intumescent polypropylene composites; which decreases slightly the fire performance of the material by affecting the mechanical properties of the intumescent protective char [96].

Those different studies show that a chemical reaction between the fillers and the acid source (mainly phosphate derivatives) often yields phospho-X compounds (e.g. phosphosilicate, zinc phosphate, borophosphate, etc.) reinforcing the structure and/or the action of the fillers (or its reaction products) as nucleating agent an thus permits the formation of an homogeneous foamed structure with appropriate thermophysical properties (lower heat conductivity, lower emissivity at the surface etc.) [78]. Note in the particular case of using phosphinates or phosphonates as intumescent additives, no reaction occurs between the filler and the other ingredients. This has been for instance detailed for the particular case of the addition of OP950 (phosphinate) and OMPOSS in PET [97]. Those fillers offer however the opportunity to enhance the performance of intumescent formulations; the mechanism of action is in this case mainly due to a physical effect.

This overview of synergistic effect in intumescent formulations allows drawing a list of the parameters that potentially explain the synergy:

- chemical reactivity of the system
- dispersion state
- quantity of fillers
- char morphology
- char strength
- rheology
- expansion and expansion rate
- thermal gradient / thermal conductivity
- kinetic
- degradation of the filler
- aspect ratio of the filler
- exchangeable cations if clay

It is anyway important to keep in mind that the synergy process is often so complex that a combination of the listed phenomenon is required to elucidate the entire mechanism. Synergistic agents exhibit indeed not one mode of action but rather a number of concomitant mechanisms of action. This is particularly the case for nanoparticles. Some examples concerning PUs will be detailed and explained by this means in the following section.

2.5.3 Synergy in intumescent polyurethane

The previous section was focused on the general understanding of the synergy mechanism in intumescent systems. Many examples of fillers incorporated in various polymeric matrices were discussed; this section will now focus on the PU.

PU foams containing aluminum phosphinate as flame retardant and both unmodified and organically modified clay were studied in terms of fire performances [43]. Phosphinate is an effective flame retardant for PU foams and it acts in both gas and solid phases. The commercial clays act through a physical rather than a chemical mechanism as they act in condensed phase behaving like inert filler and promoting the formation of a very compact barrier layer. They are therefore effective in delaying the onset of thermo-oxidative degradation and improving thermal stability to some extent, but they show no synergy with flame retardant when dealing with fire behavior. This is in good agreement with the behavior of the system PET/phosphinate/OMPOSS detailed in the previous section [97]. Modesti and co-workers [43] developed and synthesized a suitable layered silicate, modified with phosphonium. It presents both condensed and gas-phase actions, showing, like phosphinate, a radical trapping mechanism. The system phosphinate and phosphonium modified clay shows then a synergy which is very effective in improving fire behavior of polyurethane foams; moreover this system also shows delaying effect on thermo-oxidative degradation of the polymer.

A flame retardant PU/organoclay nanocomposite based on polyether, organoclay (OMT), phenylmethane diisocyanate, diglycol, glycerine and a flame retardant: the melamine polyphosphate (MPP) was synthesized [98]. TGA, cone calorimeter experiments and LOI tests show that a synergistic effect occurs between MPP and OMT added in PU. OMT and MPP when combine enhance the formation of carbonaceous char of PU at high temperature; which delays the heat release (**Figure 37**), the release of smoke and decreases the toxicity of gas released in the combustion process of PU.

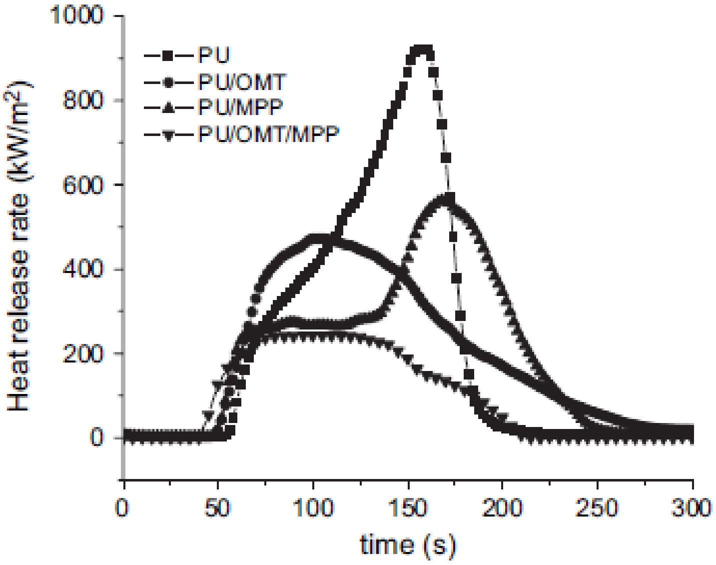

Figure 37: Cone calorimeter curves for PU, PU/OMT, PU/MPP and PU/OMT/MPP [98]

The potential efficiency as synergistic agent of three metal oxides were investigated in an intumescent TPU [99]. MgO, ZnO and Fe_2O_3 were selected to investigate their synergistic effects in a new intumescent TPU composed of APP and a char forming agent which is a triazine polymer. All three metal oxides, especially MgO, remarkably enhanced the LOI values of the TPU composites. The composites containing MgO passed the UL94 V-0 rating (1.6 mm) with a total additive loading (FR + nano MgO) of 30 wt.%. MgO was the most effective inhibitor for the dripping of TPU. MgO and Fe_2O_3 showed efficiency in reducing the pHRR and THR during a MLC experiment. The metal oxides evidently promoted the char residue formation of the intumescent mixture according to TGA experiments; MgO enlarges the most the mass kept. MgO reacts more easily with APP than Fe_2O_3 and ZnO, increasing the degradation temperature of the FR system. MgO is indeed the strongest alkaline metal oxide among the other oxides. It reacts easily with polyphosphoric acid released by the decomposition of APP to produce magnesium phosphate. This results in a decrease in the catalysis of the char formation ability of polyphosphoric acid but the rapid formation of magnesium phosphate in the char residue effectively restricted the dripping of the composites during burning. The char residue surface from the formulation containing MgO almost had no flaws. By a combination of chemical and physical effects, MgO appears at the end as the best synergistic agent in intumescent TPU compared to ZnO and Fe_2O_3.

In another recent paper [100], a new method was used to prepare flame retardant TPU. Nickel phosphate [101] (named NaNiP) layers was prepared by an hydrothermal method and was added to an intumescent TPU formulation, composed of APP and PER. The UL 94 tests showed that TPU containing 20 wt.% FR had no rating, but TPU with 19 wt.% FR and 1 wt.% NaNiP could reach the V-0 rating at 3 mm of thickness. Laser Raman spectroscopy of residual char indicated that the ordered carbon was increased with the addition of 1 wt.% NaNiP and the content ratio of ordered carbon in outer char was larger than that in inner char. The authors detailed a possible mechanism of action. When the TPU/FR/NaNiP system is heated, APP breaks down into pyrophosphoric acid. Acid catalysis accelerates the depolycondensation reaction of TPU. NaNiP and pyrophosphoric acid form a number of bridges. In addition through XPS it has been shown that PER and pyrophosphoric acid esterify, so the system forms a dense char layer. The results of thermogravimetric analysis/infrared spectrometry showed that NaNiP could delay volatilized products in TPU/FR system. The small molecule gases including H_2O, NH_3, and CO_2 make the char layer more effective to improve the flame retardancy. The ammonia from APP decomposition is very active and reacts with carbonaceous species to form stable nitrogenated species. In the TPU/FR/NaNiP matrices, the char layer is composed of condensed aromatic species bridged by P-O-C bonds. Such a structure can retard the formation and propagation of cracks. As a consequence, the stabilization of polymer links that are able to bridge polyaromatic species via the phosphate group may provide the mechanical properties of interest for the carbonaceous shield. If the addition of NaNiP is however too high, there will be too many bridges formed among APP. This structure makes the molecular chain rigid, mobility is reduced greatly, so the flame retardancy is decreased.

This review of papers dealing with significant synergistic effects in intumescent PU reveals that not many works have been carried out in this field. It also shows that it is possible to achieve interesting fire retarded PUs using synergy. The understanding of the mechanism involved in a synergistic intumescent PU formulation is therefore an actual and useful topic to study.

3 CONCLUSION: STRATEGIES TO DEVELOP A NEW FIREPROOFED POLYURETHANE AND TO UNDERSTAND ITS MECHANISM OF ACTION

PU is one of the most effective practical thermal insulation materials, used in applications ranging from buildings to the modest domestic refrigerator [3]. This type of polymer with its properties is consequently in adequacy to the aim of fire protection. To free ourselves from the complexity and heterogeneity of a foam network (which is the most used design), the use of a rigid PU casting was preferred to develop and to understand a new fireproofed PU.

The use of intumescent flame retardant is one of the easiest and most efficient way to protect PUs against fire. An intumescent system leads to the formation of a shield that protects the underlying PU from heat and fire; this lowers the temperature of the material beneath the char and causes a delay in its temperature rise. Additionally the char layer hinders the diffusion of oxygen to the PU, e.g. where the combustion occurs. To that purpose, APP is an interesting compound because in intumescent systems, it can act as acid source and blowing agent.

Considering the possible enhancement of the fire properties by adding a small quantity of a synergist in an intumescent system, this route will be chosen to develop innovative and highly performing materials. The preparation of PU/clay nanocomposite showed that the nanocomposite induces different fire reactions but the fire properties of PU were not enough improved. Nevertheless nanofillers such as oxides or POSS seem to consist in a more promising route to reach high fire performances in PU.

Four nanoparticles (NPs) were therefore selected and studied in this Ph.D work to evaluate their potential synergistic effect when added in a rigid PU/APP casting at 30 wt.% additive loading: nano MgO, nano SiO_2, nano gold and OMPOSS. These combinations seem very promising due partially to previous work in the laboratory [11] and also to the literature described in **section 2.5.3 p72**. When the Ph.D program started, such PU/APP/NP has never been reported in the literature but during the Ph.D other research groups begin to publish on similar topics. For instance, the synergistic effect of MgO, Fe_2O_3 and ZnO was assessed in intumescent TPU [99]. In other polymeric matrix it was very recently evidenced that a little amount of MgO in a polycarbonate/MgO nanocomposite significantly improve the flame retardancy of the material [102]. It appears that MgO, which use was never been reported before as synergist for fire protection, starts to interest for this purpose.

In the previous **section (2.5.2 p68)** a list of parameters which may be responsible for the synergy have been established. The four nanoparticles were judiciously selected to identify the effect of those parameters in our PU/APP casting. First, only spherical particles have been chosen to avoid a potential influence of the shape factor. All the fillers are nanoparticles and their dispersion in the matrix will be characterized. Nano gold is the only NP which will not react with APP according to the literature. Nano MgO and SiO_2 should react with APP and will form different phosphates: magnesium phosphates and silicophosphates are respectively expected. The advantage to use OMPOSS is that it degrades on the contrary of the three other inorganic filler having a good thermal stability. Each NPs incorporated in PU/APP should lead to a char with its own properties (rheology, morphology, strength).

The next chapter is devoted to the presentation of the materials and methods used to prepare novel intumescent PUs and to understand their mechanism of degradation and combustion.

Chapter II - Materials and Methods

According to the state of the art, different parameters that may be responsible for synergistic effects in intumescent PU formulations were listed. It was consequently chosen to build a systemic approach to draw general rules associated to well defined governing parameters for designing PUs with enhanced flame retardancy. The materials and methods developed in this direction are presented in this section which is divided into three parts. The first one describes the preparation of PU samples. The second one details the various techniques and conditions used to characterize PUs and burned residues. Combining the obtained information will allow to evidence which parameter is responsible or not for the synergy in the developed systems. Finally the third section deals with the evaluation of the fire performances by describing the fire tests that have been used and the information collected during them.

1 SAMPLES PREPARATION

This first section, devoted to the samples preparation, presents first the monomers used to prepare the PU casting as well as the additives. The foaming is deliberately avoided by using particular components for the PU matrix and by the drying of all monomers and additives. This is done in order to work on a model system to facilitate the characterizations and the fire tests. The synthesis of PU samples is described and occurs in a two steps protocol; first the preparation of two masterbatches (one with polyol, the other one with isocyanate) and then the casting preparation by mixing the masterbatches. The last part gives a summarized table of the formulations developed in this study.

1.1 Materials

PU is obtained polymerizing a polyol and an isocyanate (**Figure 38**) in presence of a catalyst. All materials were supplied by Huntsman Polyurethane.

The polyol used is *Jeffox WL440* (JWL440), it is a glycerol initiated oxyethylene (EO) polyol with a functionality of 3, a molecular weight (Mw) = 489 g/mol and a hydroxyl value (OHv) = 344. It is dried in a vacuum oven at 105°C for 4 hours.

The isocyanate used is *Suprasec 2020* (S2020) (mixture of pure MDI (diphenylmethane diisocyanate) and uretonimine; functionality: 2.12). A common modification of MDI, especially pure MDI, is the condensation reaction of the isocyanate groups, forming carbodiimide and reversible uretonimine (**Figure 39**). Uretonimine modified MDI is a liquid at room temperature with a viscosity at 25°C of approximately 50 mPa.s. It has been degassed prior to be used in a vacuum oven at room temperature until no more bubbling was observed.

The catalyst is named *Dabco 25S* and is a solution of triethylenediamine in 1,4-butanediol.

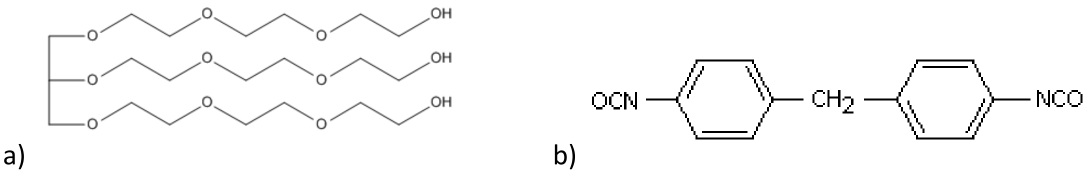

a) b)

Figure 38: Chemical structure of a) polyol JWL440 and b) isocyanate S2020

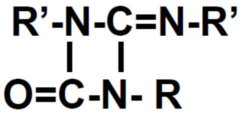

$$\begin{array}{l} R'\text{-}N\text{-}C{=}N\text{-}R' \\ \quad\;\; | \quad\;\; | \\ O{=}C\text{-}N\text{-}R \end{array}$$

Figure 39: Uretonimine structure

Ammonium polyphosphate *Exolit AP422* (APP) from Clariant has been used as flame retardant in the formulations and is dried overnight in an oven at 80°C before use.

Different nanoparticles (NP) have been used and dried in a vacuum oven at 85°C for 4 hours prior to be used in PU formulations:

- nano MgO (d = 21 nm) and nano SiO_2 (d = 53 nm), supplied by Huntsman Polyurethane
- nano gold (d = 36 nm determined by TEM) containing around 60% of organic stabilizer, supplied by Nanocomposix. The quantity incorporated in the formulations corresponds to the pure gold quantity.
- OctaMethyl Polyhedral Oligomeric Silsesquioxanes (OMPOSS) from Hybrid Plastics (**Figure 40**)

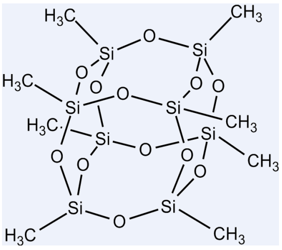

Figure 40: Chemical structure of OMPOSS

1.2 Synthesis of polyurethane formulations

The ISO index of the formulations is defined as $\frac{n(NCO)}{n(OH)}x100$ with n(NCO) corresponding to the number of NCO groups from isocyanate and n(OH) to the number of OH groups from polyol. It has been fixed at 103.6; which give the amount of each component of the neat reference material: 51.8% of JWL440, 47.8% of S2020 and 0.4% of Dabco 25S (in weight %).

1.2.1 Preparation of masterbatches

NPs are dispersed only in the polyol whereas APP is dispersed in both isocyanate and polyol in order to avoid having a too viscous polyol masterbatch. The part of APP added to each monomer is calculated by weighting the total amount of APP by the contents of the monomer. The previously defined amount of APP is first dispersed in the polyol by high shear mixing using a Dispermat for half an hour under nitrogen flow. The NP are then progressively dispersed into the mixture polyol + APP using high shear mixing under nitrogen for one hour followed by sonication (Branson Digital S-450D) for 20 minutes (2sec active-2sec rest) at 40% amplitude. In parallel, the second part of APP is incorporated into the isocyanate by high shear mixing under nitrogen during half an hour. The speed of the Dispermat is fixed between 8000 and 11300 rpm with disks of 30 or 40 mm diameter. This is adjusted depending on experimental conditions to avoid the dispersion to overflow. Finally, the two masterbatches are degassed at room temperature under vacuum until no more bubbling is observed (this takes approximately 1 hour).

1.2.2 Casting preparation

The appropriate amount of the polyol masterbatch (polyol/APP/NP) is weighted in paper cups. The isocyanate masterbatch is added to the polyol in the cup and mixed for a few minutes with a disposable spatula. The catalyst is then quickly added drop by drop. The disposable spatula is used to mix the materials until the mixture starts to heat up. Then, the formulation is quickly poured in a 10x10x0.3 cm^3 Teflon mould. The mould is pre-heated in an oven at 80°C and took out just before the syntesis. The PU is then post-cured at 80°C for 1 hour.

1.3 Polyurethane formulations

A summary of the composition of the studied formulations is presented in **Table 9**.

Table 9: Selected polyurethane formulations

Name	PU (wt.%)	APP (wt.%)	NP (wt.%)
PU	100	0	0
PU 30%APP	70	30	0
PU 5%nano MgO	95	0	5
PU 29%APP 1%nano MgO	70	29	1
PU 28%APP 2%nano MgO	70	28	2
PU 25%APP 5%nano MgO	70	25	5
PU 5%nano SiO_2	95	0	5
PU 28%APP 2%nano SiO_2	70	28	2
PU 28%APP 2%OMPOSS	70	28	2
PU 29.5%APP 0.5%nano gold	70	29.5	0.5
PU 29%APP 1%nano gold	70	29	1
PU 28%APP 2%nano gold	70	28	2

2 METHODS TO CHARACTERIZE THE MATERIALS

Once the materials are prepared, it is important to characterize them. To that aim solid state NMR will be used to check the chemical structure of the PU and to examine if the incorporation of fillers and the temperature modify it. The dispersion of the fillers in the PU matrix will also be evaluated. Thermal analysis will be used to study the degradation of the materials and to identify potential interaction between the components of the formulation. The morphology of chars developed when the intumescent formulations are exposed to heat source will be analyzed by two powerful techniques: electron probe microanalysis and tomography. Finally some rheological experiments will be done to study the degradation of the FR additives, to evaluate the expansion of PU formulations and to measure the char strength.

2.1 Solid state NMR

Solid state NMR is a powerful tool for determining the surrounding of a given nucleus. However, because of the low abundance of some nuclei, the radiofrequency pulse is poorly absorbed in some cases. In order to overcome this limitation, protons of the sample can be excited and a dedicated sequence called crossed polarization (CP) permits to transfer this energy to atoms of lower abundance. On the other hand, the large number of protons in the sample interferes with the decay of the isolated nucleus due to weak interactions of the spins. This results in a broadening of the signal. This drawback can be overcome by the use of a ^{1}H dipolar decoupling (DD): a strong radio frequency signal holds the protons in a highly resonating state so that they are not able to absorb resonance from the nuclei. Finally in solid state, existence of chemical shift anisotropy has a strong effect on the spectra: peaks are broadened. When spinning at the magic angle spinning (MAS), there is minimization of the broadening. All NMR data were collected and analyzed at room temperature with the TopSpin software (Bruker).

^{13}C solid state NMR spectra were obtained at frequency 100.6 MHz (9.4 T) on Bruker Avance II 400 using a 4 mm standard probe. The conditions were a CP ^{1}H-^{13}C (contact time 1 ms) with DD and MAS at R_0 = 10 or 12 kHz. The recycle delay between two pulses was 5 s. The number of scans was fixed between 64 and 1024 depending on the sample.

^{31}P solid state NMR spectra were obtained at frequency 161.9 MHz (9.4 T) on Bruker Avance II 400 using a 4 mm standard probe. The conditions were a DD with MAS at R_0 = 10 or 12.5 kHz. The pulse length is 2.5 µs with a power level for pulse of 7 dB. The recycle delay between two pulses was 120 s to ensure a complete signal relaxation. 8 scans were accumulated and the ^{31}P chemical shifts are referenced to 85% H_3PO_4.

^{29}Si solid state NMR spectra were obtained at a frequency 79.5 MHz (9.4 T) on Bruker Avance II 400 using a 7 mm standard probe with MAS at R_0 = 4 kHz. The pulse length is 2 µs with a power level for pulse of 3 dB. The relaxation delay was 600 s, necessary to have enough time to see the Si-O bonds relaxation. 32 scans were accumulated.

2.2 Microscopies

Electron microscopy permits to observe very small objects thanks to a high energy electron beam. The electrons interact with the atoms that make up the sample and produce signals that contain information about the sample surface topography and composition.

The dispersion of the additives in the PU matrix has thus been examined using scanning electron microscope (SEM) HITACHI S4700. More precise information on the topography and repartition of the chemical elements has been collected thanks to back scattering electron (BSE) pictures and energy dispersive spectroscopy (EDS). The acceleration voltage is fixed at 6 kV and the intensity at 15 µA. The other conditions (magnification, work distance) vary depending on the samples and the information required and they are reported at the bottom of the pictures.

The samples were freeze-fractured and sprayed by a chromium deposit in the case of SEM-BSE analysis and by a carbon deposit for EDS experiments.

2.3 Thermal analysis

2.3.1 Thermogravimetric analysis (TGA)

2.3.1.1 Use of TGA to follow the thermal degradation

Thermogravimetric analyses to follow the thermal degradation of samples have been performed on an apparatus from TA Instrument (Q600). The curves have been recorded with the TA Universal Analysis software. The samples have been prepared by taking sawdust from the middle of a PU sample or using powder of additives ((10.0 ± 0.5) mg except for nanoparticles for which the quantity is adjusted to have a pan correctly filled). An alumina pan is used eventually covered with a gold foil if there is phosphorus in the sample to test (to avoid a reaction between phosphoric structures and the pan). The gas flow (air or nitrogen) is fixed at 100 mL/min. The experiments are carried out from 50 to 800°C using a heating ramp of 10°C/min.

2.3.1.2 Use of TGA to study the degradation kinetic

Thermogravimetric analyses to study the kinetic of degradation of PU formulations have been performed on an apparatus from TA Instrument (Q5000). The curves have been recorded with the TA Universal Analysis software. The samples have been prepared by taking sawdust from the middle of a PU sample with a mass of (3.8 ± 0.2) mg and placed in an alumina pan. After an isotherm of 1 minute to equilibrate the temperature at 50°C, the sample is heated under air from 50 to 1000°C with different heating rates: 0.25, 10, 50, 100, 150 °C/min. At the end, an isotherm of 2 minutes is performed to evacuate all the gases out of the TGA and to avoid the pan to be stuck in the apparatus. The air flow for the TGA is fixed at 25 mL/min while a nitrogen flow of 15 mL/min is also required for the balance chamber. The evacuation line temperature is also heated, so that the gases are not condensed at the TGA exit.

2.3.2 Thermogravimetric analysis coupled with Fourier transformation infrared (TGA-FTIR)

Thermogravimetric analyses coupled with Fourier transformation infrared (TGA-FTIR) have been performed on an apparatus from TA Instruments and Thermo Scientific. The TGA part is the Q5000 (previously described in **section 2.3.1.2 p81**) and the FTIR device is a Nicolet iS10 from Thermo Scientific. The infrared spectra have been recorded with the OMNIC software. The nitrogen flow is fixed at 50 mL/min and a purge of 30 minutes is made before data acquisition. A mass of (3.0 ± 0.5) mg for virgin material and intumescent formulations are put in an alumina pan. After an isotherm of 1 minute to equilibrate the temperature at 50°C, a ramp at 10°C/min is used from 50 to 1000°C. An IR spectrum is collected every minute during all the experiment in the range of wavenumbers: 4000-800 cm^{-1}. The transfer line temperature is fixed at 225°C, to avoid the condensation of gases. The number of scan is fixed at 8 and the resolution at 4, in order to have a good compromise between the accuracy of the IR spectra and the frequency of collection (one per minute).

2.3.3 Differential scanning calorimetry (DSC)

Differential scanning calorimetry is widely used for the characterization of polymers. Different properties such as glass transition, crystallinity or melting temperatures will be measured. Differential Scanning Calorimetry experiments have been performed on a TA Instrument DSC Q100 and monitored with the TA Universal Analysis software in order to investigate the influence of fillers on the glass transition temperature of the PU matrix. The samples have been prepared by taking sawdust from the middle of a PU sample ((4.5 ± 0,5) mg) or using drops of monomers (12.8 mg of polyol and 3.4 mg of isocyanate). The aluminum pan used is sealed and the nitrogen flow is fixed at 50mL/min. Experiments are carried out at 10°C/min. The temperature/time ramp is schematized in **Figure 41**.

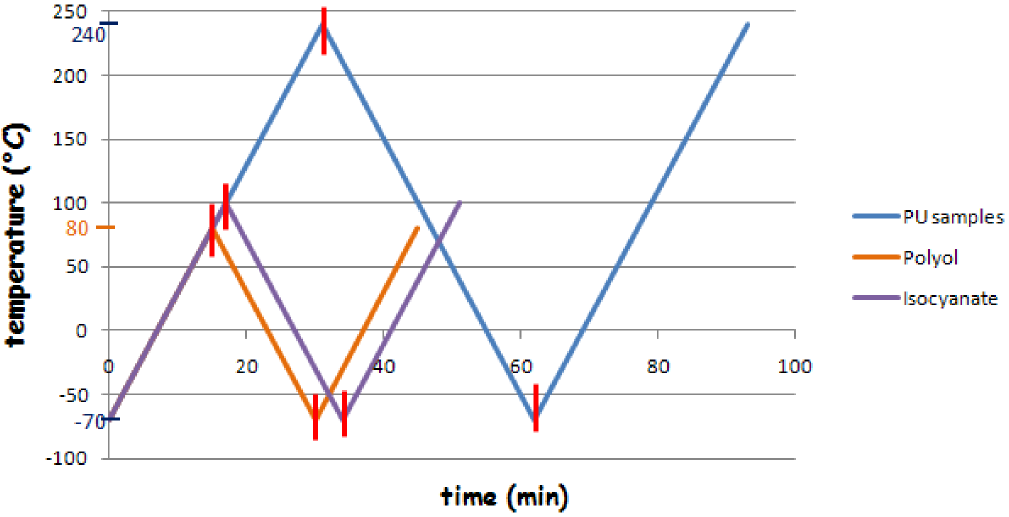

Figure 41: Temperature/time ramp used for DSC experiments

2.3.4 *Thermal conductivity*

The thermal conductivity of PU formulations was measured by a Hot Disk thermal constants analyzer (TPS2500, Sweden) from Thermoconcept (Bordeaux, France), which is based upon the transient plane source method. With the device developed especially for our research area, data could be acquired both at ambient temperature and as a function of temperature while the sample is heated in a furnace controlled by the Hot Disk software (**Figure 42**). The procedure is however different to guarantee a relevant measurement depending on the conditions.

Figure 42: Furnace (left) and sample holder (right) of TPS2500

For the data collected at ambient temperature, the dimension of bulk specimens is 10x10×0.3 cm^3 with the sensor (r = 3.189 mm, Kapton) placed between two similar plates of materials. The sensor supplied a heat pulse between 7 or 10 mW during 20 to 40 s to the sample (depending on the sample). The uncertainties were determined by performing several time the same experiment.

To follow the evolution of the thermal conductivity as a function of temperature a special protocol to prepare the PU formulations has been set up. It is indeed required to place the sensor (in mica to resist at elevated temperature) during the PU synthesis. The two masterbatches (polyol and isocyanate) are mixed without adding the catalyst in order to have enough time before polymerization to place the sensor and overall to split equitably the quantity of polymer on and under the sensor. The size of the PU sample is adjusted to have enough material to give the heat impulsion during the test and to avoid an overflowing of the char from the sample holder. This corresponds at nearly a circle with an average diameter of 25 mm and thickness of 5 mm. Once the PU has polymerized on the sensor, it is placed in the sample holder as shown in **Figure 43** and is ready to be tested. The condition for the heat pulse power and duration is adjusted for each sample and each temperature tested to have optimized response parameters, thus insuring the reliability of measurements. The thermal conductivity has been collected at the following temperatures: ambient temperature, 200, 300, 350, 400, 450, 500, 600, 700, 800°C. The uncertainties were determined by performing the full temperature scheme on two different samples.

Figure 43: PU sample polymerized on the mica sensor and place on the sample holder to measure the thermal conductivity as a function of temperature

At ambient temperature, data were recorded for several formulations whereas to have the trend versus temperature it was only performed on two different PU formulations: PU 30%APP, PU 28%APP 2%nano MgO. This is due firstly to the cost of the experiment (400€ for a sensor which may breaks during or after the experiment or during the cleaning) and secondly to the time required to have a stable temperature (x ± 0.2°C), required to do the measurement.

2.4 Morphology of char

2.4.1 Electron probe microanalysis (EPMA)

Electron probe microanalysis (EPMA) is an analytical particle-beam based technique that is used to establish the composition of small areas on specimens. A beam of accelerated electrons is focused on the surface of a specimen using a series of electromagnetic lenses, and these energetic electrons produce characteristic X-rays within a small volume (typically 1 to 9 cubic microns) of the sample. The characteristic X-rays are detected at particular wavelengths, and their intensities are measured to determine the concentration in different atoms. Elements can be detected because each element emits a specific set of X-rays. Signal cannot however be recorded for H, He and Li because these elements are too light. This analytical technique has a high spatial resolution and sensitivity.

The samples were embedded into an epoxy resin, polished and carbon coated with a Bal-Tec SCD005 sputter coater. A silver cleaning was then required to get rid of the SiC particles. A Cameca SX100 EPMA was used to perform elemental analysis. Back scattered electron images were carried out at 15 kV, 20nA and X-ray mappings were carried out at 15 kV, 40 nA. For mappings, the crystal used to detect the Kα of Mg and P was a TAP crystal.

2.4.2 Tomography

It is one of the first time that tomography is reported in a comprehensive work in the field of fire protection and in particular only few papers report its use for characterizing intumescent char [103-107], that is why a short description on principle of X-ray tomography is given for start. For years X-ray computed tomography (CT) has been widely used as a medical diagnostic tool. This non-destructive technique soon turned out to be very practical in rock material research. In the 1970s CT was just introduced in material research while in the nineties, micro-CT became an important non-destructive research technique. Recently high-resolution is being developed creating even more possibilities for the 3D visualization of small objects [108]. All transmission CT-devices are based on the same principle: the object is positioned in between an X-ray source and an X-ray detector. CT requires a rotational motion of the sample relative to the source-detector system. For non-destructive testing most often the object is placed on a rotation platform. Modern X-ray detector systems are usually 2D-pixel arrays like CCD (charge-coupled device) cameras, flat panel detectors or image intensifiers. They convert X-rays into digital radiographs that are stored on a hard disk. Hundreds to thousands of radiographs are acquired for one CT scan from different rotation angles between 0° and 360°. After the data collection, a computer algorithm (called FDK, Feldkamp and co-workers, 1984 [109]) is used to calculate the slices or cross-sections through the object. The X-ray beam geometry is conical and by moving the object between the source and the detector one can choose an appropriate magnification of the object in the radiography: the closer to the source, the higher the magnification and thus the higher the spatial resolution. The spatial resolution of the images depends not only on the magnification (ratio of the distance between source and detector over the distance between source and sample), but also on the focal spot size of the X-ray tube, the pixel size of the detector and on physical phenomena like X-ray scattering and interaction between the detector pixels. In the ideal case the resolution is determined by the pixel size of the detector divided by the magnification of the system, the best achievable spatial resolution equaling to the X-ray source spot size.

The experimental device is constituted of:

- X-ray source: directional type X-ray tube
- X-ray detector: thin-film-transistor based flat panel, 2048 x 2048 pixels, pixel size 0.2 mm, CsI scintillator material
- Precision air bearing rotation stage to rotate the sample in between projections
- 3 axis sample positioning system

Each sample (char) was positioned on a styrofoam holder and scanned without fixation to preserve the integrity of the sample. A total of 2000 projection images were recorded while the stack of samples rotated over 360°. The series of projection images was reconstructed to obtain a set of cross-sections through the samples. The number of cross-sections varies depending on the sample height. Quantitative analysis is performed by means of the 3D analysis package Morpho+, developed in collaboration between the Centre for X-ray Tomography of the Ghent University (UGCT) and inCT (Zwijnaarde, Belgium).

A voxel size of 75.8 µm, 83.6 µm or 76.3 µm was obtained in the scans (isotropic voxels) depending on the samples. The grayvalue of a voxel in the reconstructed images corresponds to the average attenuation coefficient of the sample material inside the voxel. This is illustrated in **Figure 44**. A voxel containing one (b) or more (c) dense particles will show a higher grayvalue in the reconstructed images than a voxel containing only air (a) (for purposes of illustration, dense particles are indicated in black instead of white, as is the case in the reconstructed images).

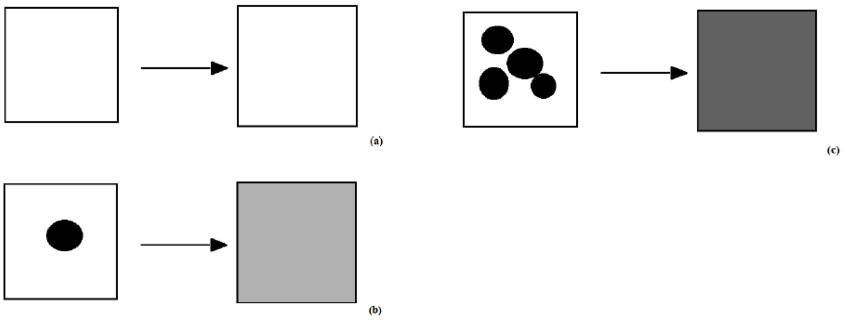

Figure 44: Effect of dense particles on voxel grayvalue

The same principle is applied for a sample composed of multiple materials, such as a PU char containing dense particles. A voxel which only contains PU material will show a relatively low grayvalue, while voxels containing both PU and dense particles (such as APP and NPs) will show a higher grayvalue.

To obtain a qualitative overview of the distribution of the dense particles, a threshold is first used to segment both the PU and particles from the air. Next the average value of the images inside the segmented PU + particle phase is calculated as a function of height. The selection of the threshold to separate the material from the air is not trivial. Since the cell walls are very thin at some locations, the results in grayvalues are very close to the grayvalue of air. Combined with the presence of noise and some artifacts, this has the following result on the analysis:

- a low threshold will include all PU material in the analysis, but will also include some erroneous parts in the analysis, especially in the areas with a high concentration of particles showing streak artifacts
- a high threshold will not include brighter areas caused by streak artifacts, but will omit some of the thinner polyurethane cell walls.

The analysis was consequently performed for multiple threshold values and the average value is finally analyzed.

2.5 Rheological experiments

Intumescence phenomenon exhibits large swelling and blowing which must occur at the right time and temperature to be efficient in case of fire. Gases are released in the medium and an expanded multicellular barrier is created. The study of the rheology of this char is consequently a key parameter to understand the intumescent process.

All rheological measurements have been carried out on a parallel plate high temperature rheometer ARES 20A from Rheometric Scientific (schematized in **Figure 45**).

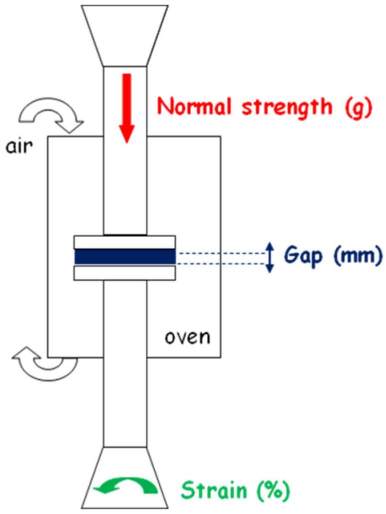

Figure 45: Scheme of the rheometer ARES 20A showing the acquisition parameters

Two types of sample holder for the bottom and the top plates were used on the rheometer (**Figure 46**). The sample holder (a) was specially designed for the project with a diameter close to that of the top plate (the 25 mm top plate will go inside the 27 mm bottom plate). The aim was to prevent the char to get out by the sides. This overflowing phenomenon still occurs with this device but is nevertheless reduced.

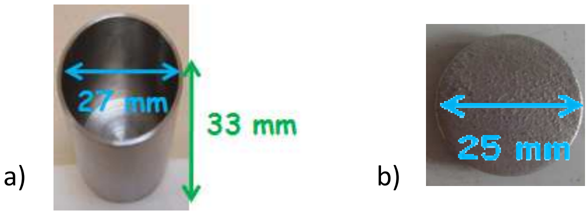

Figure 46: Sample holders used for the bottom (a) and the top (b) plates during rheological measurement

2.5.1 Method to study the additives degradation

The additives have been directly placed in the bottom plate of the rheometer as powders. The test type is a "dynamic temperature ramp test" and the sample is heated from 25 to 500°C (maximum for the apparatus) at 10°C/min. The average thickness for powders is (1.31 ± 0.21) mm. The frequency is fixed at 1 and the strain at 0% to avoid the powder going away by the sides of the sample holder and invalidate measurements. The normal strength is fixed at (10 ± 1) g; a few significant experiments have been made at (50 ± 5) g to see the influence of the normal strength and the same results were obtained in both cases. The gap evolution is recorded during the experiment and the expansion is then calculated with the following formula:

$$\boxed{\text{Expansion}(\%) = \frac{\text{gap}}{e_0} \times 100}$$

The residue is however not swelled when collected after the test and have not swelled during the experiment as well. The recorded gap is then due to gases released during degradation, which push on the upper plate, and not to a real expansion. Through these observations, an innovative method to study the additives degradation by following the gas released pressure was thus put in place.

2.5.2 Expansion measurements on polyurethane formulations

Samples have been tested as thin PU circles of diameter = 25 mm. It is important to have similar thickness between the samples because it will play a role on the expansion; the average thickness for PU formulations is thus (1.7 ± 0.2) mm. The test type is a "dynamic temperature ramp test" and the sample is heated from 25 to 500°C (maximum for the apparatus) at 10°C/min. The frequency is fixed at 1 rad/s, the strain at 1%, the normal strength at (20 ± 2) g. The gap evolution is recorded during the experiment and the expansion is then calculated with the following formula:

$$\boxed{\text{Expansion}(\%) = \frac{\text{gap}}{e_0} \times 100}$$

2.5.3 Mechanical strength of char

The mechanical resistance of the char is a significant factor because in conditions of fire, char destruction may happen by means of external influence such as wind, mechanical action of fire or convective air flows [60].

Berlin et al. used a "Structurometer ST-1", developed at Moscow State Food Academy, to measure the force required to destroy a char [110-112]. The samples were first pyrolyzed and then a destructive force was applied to the sample. It was concluded that one of the main factors influencing the mechanical stability is the char porosity, the smaller the pore size the better the char strength. A similar method was developed in the laboratory at Lille University [67] using the high temperature rheometer ARES 20A from Rheometric Scientific.

Several methods inspired from those previous works were established in this project to measure the mechanical resistance of the chars in order to evaluate the influence of various parameters on the char properties.

Three heating devices were used: the rheometer furnace, the mass loss cone calorimeter and a tubular oven. During the heat treatment, the sample is always let without any strain to freely intumesce. The rheometer furnace was used because it allows an on-line measurement of the mechanical strength at high temperature. The mass loss cone calorimeter (50kW/m^2 for 8'30'' at a distance sample/conical heater = 35 mm) was selected because it is the standard fire test which classifies the materials against their fire performances. It is consequently interesting to measure the mechanical strength on a char having exactly the same properties than the one developed in the case of fire. Finally a tubular oven was also useful because it allows playing on the heating rates and treatment temperatures. The measurement temperature in the rheometer is indeed limited to 500°C and with the cone calorimeter, the standard procedure implies to fix a heat flux but the heating rate is not controlled.

Two different types of sample were also tested. The first one is a thin PU plates (1.7 mm in average) with a diameter of 21 mm. This diameter was chosen after an optimization in a standard furnace to avoid damage to the rheometer furnace. With this size the char do not overflow from the bottom plate of the rheometer. The second type of sample is a standard cone calorimeter sample, i.e. a plate of 10x10x0.3cm^3. Between these two types of sample, the changing parameters are the shape (circle or square), the size, the thickness and the presence or not of “walls” from the sample holder (that limits the expansion within one direction). All these parameters may have an effect on the char development and its consequent mechanical resistance but each parameter have not been tested individually.

After the heat treatment which permits to develop the char, its mechanical resistance was evaluated in every case thanks to the rheometer. The sample which has undergone its defined heat treatment is put in the rheometer furnace at the measurement temperature. The upper plate of the rheometer is brought into contact with the intumesced material and the gap between the bottom and upper plates is reduced linearly by movement of the upper plate (0.02 mm/sec) as schematized in **Figure 47**. The compression force is monitored as a function of the distance between the two plates, corresponding to the gap.

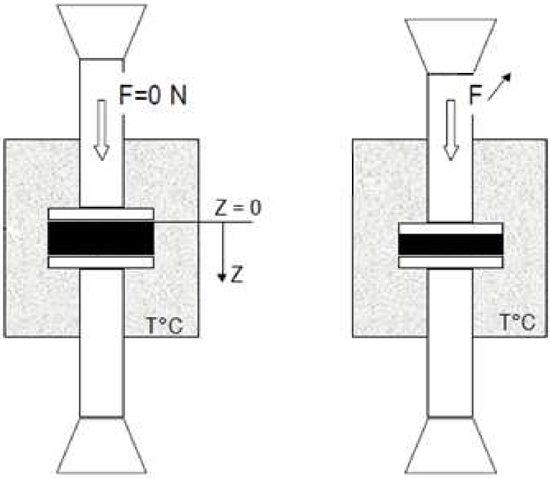

Figure 47: Scheme of char strength measurement procedure

A special device has been set up to test the standard mass loss cone calorimeter sample because due to its size it was not possible to place it on the bottom plate of the rheometer as it has been done for all the other samples. The big char is placed on the rheometer in a parallel plate configuration as shown in **Figure 48**. The upper plate applies its strength in the middle of the char and this is supposed to be representative of the whole char.

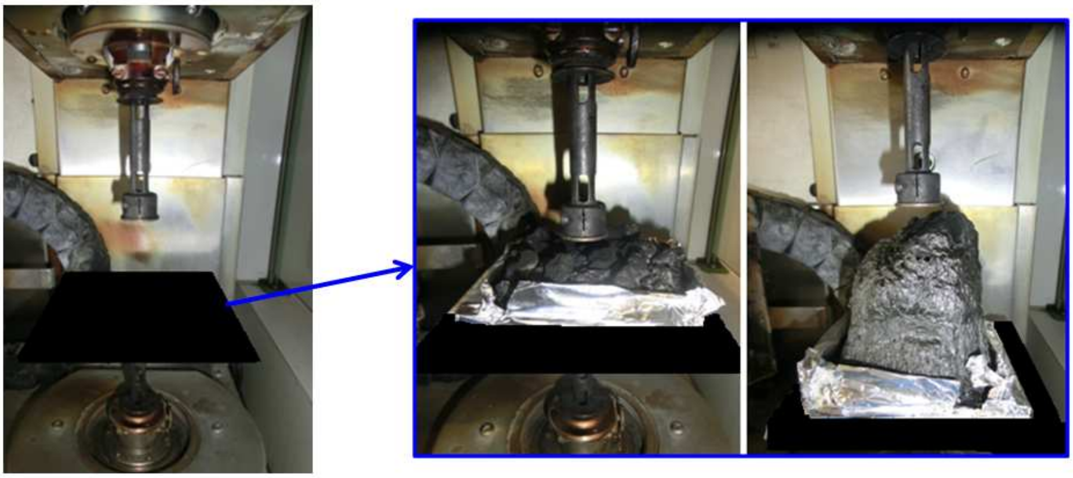

Figure 48: Picture of the device set up to place the mass loss cone calorimeter char on the rheometer in a parallel plate configuration

A total of nine different methods have been tested on PU samples; the conditions and the method code are detailed in **Table 10**.

To ease the reading, a code was given to describe all the methods used for the mechanical characterization of char; its explanation is given below:

- The first capital letters refer to the heating device used: RF = rheometer furnace, MLC = mass loss cone calorimeter (MLCi if the ignition was used and MLCøi if not), TO = tubular oven
- The next code refers to the heating rate: HR stands for the 10°C/min heating ramp and Q corresponds to a quench of the sample by placing it directly at the heat treatment temperature. The number associated with HR is the heat treatment temperature (700 or 500°C)
- The measurement temperature is then precised. For the measurement at ambient temperature (AT), the sample is left 10 minutes at ambient temperature after the treatment and is then analyzed.
- The final character is used to differentiate the thin circled PU samples, marked with **o**, to the big standard MLC sample (☐)

Table 10: Summary table of the different conditions tested to measure the mechanical strength of the char with the corresponding name code

Method name code	Heating type	Heating rate	Heat treatment temperature (°C)	Measurement temperature (°C)	Sample characteristics
RF-HR500-500-o	Rheometer furnace	10°C/min	500	500	Thin PU plates, ø ≈ 21 mm
RF-HR500-AT-o	Rheometer furnace	10°C/min	500	ambient T	Thin PU plates, ø ≈ 21 mm
MLCi-Q-AT-o	MLC (with ignition)	/	/	ambient T	Thin PU plates, ø ≈ 21 mm
MLCØi-Q-AT-o	MLC (without ignition)	/	/	ambient T	Thin PU plates, ø ≈ 21 mm
MLCi-Q-AT-☐	MLC (with ignition)	/	/	ambient T	MLC sample (10x10x0.3cm^3)
TO-HR700-AT-o	Tubular oven	10°C/min	700	ambient T	Thin PU plates, ø ≈ 21 mm
TO-HR500-AT-o	Tubular oven	10°C/min	500	ambient T	Thin PU plates, ø ≈ 21 mm
TO-Q700-AT-o	Tubular oven	/	700	ambient T	Thin PU plates, ø ≈ 21 mm
TO-Q500-AT-o	Tubular oven	/	500	ambient T	Thin PU plates, ø ≈ 21 mm

3 FIRE TESTING METHODS

The principle of mass loss calorimetry and limiting oxygen index is displayed in this section. During a mass loss cone calorimeter experiment, some modifications and/or devices can be added to provide more information such as conversion degree, expansion, temperatures involved. These protocols are also described here.

3.1 Mass loss calorimetry

3.1.1 Principle of measurements with a mass loss cone calorimeter (MLC)

Mass Loss Calorimeter (MLC) was used to carry out measurements on PU samples following the procedure defined in ASTM E 906. Samples (100 x 100 x 3 mm^3) were exposed to a FTT mass loss cone calorimeter (**Figure 49**) under a heat flux of 50kW/m² which corresponds to the heat evolved during a well-developed fire. A spark ignition is used during the experiment. Specimens were wrapped in aluminum foil leaving the upper surface exposed to the heater and placed on a ceramic backing board at a distance of 25 or 35 mm from cone heater. Heat Release Rate (HRR) is measured as a function of time and recorded using a software developed in our laboratory (based on Labview). The experiment is always stopped after 8 minutes 30 seconds; this was decided according to the shape of the first HRR curves performed. By setting a fixed experiment duration, it is possible to ensure that all samples undergo the same thermal treatment. To ensure the repeatability of the experiments (considered reproducible to within ± 10 %), each formulation has been tested at least two times. Additional information can be collected during a mass loss calorimeter experiment such as the expansion, the conversion degree and the specimen temperature.

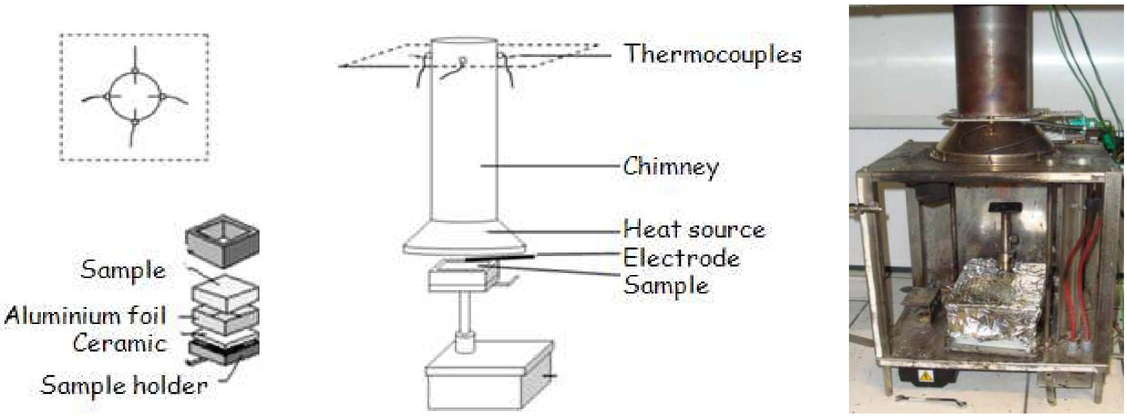

Figure 49: Mass loss calorimeter apparatus

3.1.2 Shutter experiments

The “shutter experiment” consists in a mass loss cone calorimeter experiment stopped at characteristic times. The time chosen for the study are pointed out in the **Figure 50**.

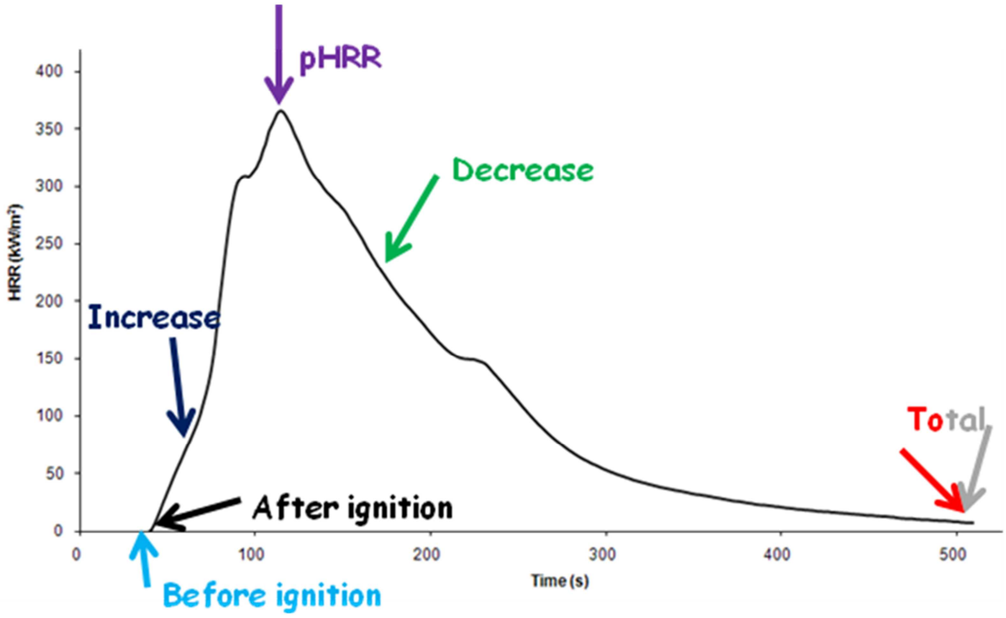

Figure 50: Schematic HRR curve showing the caracteristic times and the corresponding names choosen for shutter experiments (pHRR = peak of heat released rate)

When it is necessary to stop the cone experiment while the sample is burning and maybe reacting (from after ignition to decrease), it is a really critical point. The sample is first put away from the conical heater and quickly covered thanks to a sample holder placed upside down to stop the oxygen supply and thus leading to fast flame suppression. These residues give information on the mass loss, the expansion, the aspect of the char at those characteristic times. Samples are collected in order to perform NMR experiments (often several samples on a same residue due to heterogeneity of the char) to obtain information on the chemical composition of the char.

3.1.3 Conversion degree

The conversion degree (α) is calculated with the following formula:

$$\alpha = \frac{m_0 - m_t}{m_0 - m_f}$$

$$m_0 = \text{initial sample mass}, m_t = \text{mass at time t}$$

$$m_f = \text{final sample mass (after 8min30 of test)}$$

The mass at time t is measured on line with a balance directly placed under the sample holder in the cone calorimeter device. The device is devoted to this application so even with the heat exposure, the stability of the mass value is good and the mass precision is evaluated at ± 1 g except when it approaches zero where the accuracy is not good anymore. The residual mass is consequently calculated through the mass measured at the end of the test on a real balance.

It is noteworthy that with this formula, $\alpha = 1$ means that the experiment is finished (8 minutes 30 under the cone calorimeter) but it may remain a residue, i.e. $m_f \neq 0$.

It is possible to weight the residue collected during the shutter experiment. These data have been collected and are very reproducible with those obtained by the balance of the MLC. In the thesis only the results collected with the "on-line" balance are presented because the whole curve is obtained in that case.

3.1.4 Expansion

In order to measure the swelling of intumescent samples during cone calorimetry, a method was developed in the laboratory which consists in monitoring the expansion on-line by an infrared camera [101] (**Figure 51**). In this work, visual observations during cone calorimeter experiment indicate an important bending of the plate upon heating. This totally invalidates the swelling measurement with the IR camera because it is impossible to differentiate this bending from an expansion because of the sample holder and so to subtract it.

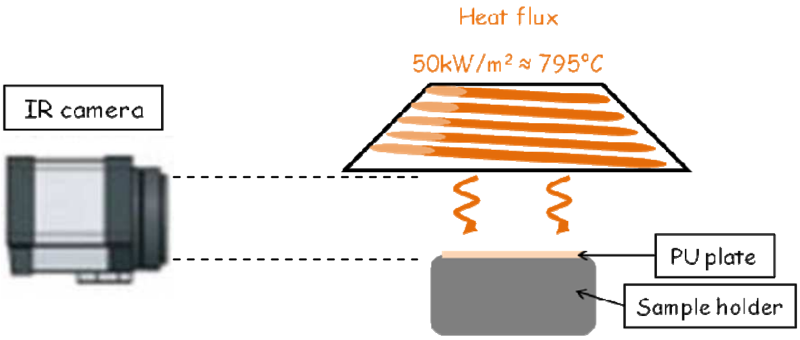

Figure 51: Experimental set-up for measuring the swelling by infrared camera

On the contrary the char samples are very stable and are preserved when cooled down, the expansion is then measured directly on the chars collected at characteristic times out of the cone during shutter experiment. This method has however several drawbacks. First it is not an on-line measurement, so modifications in the height could happen between the in-situ experiment and this measurement. Only six samples are moreover taken for a test during 8 min 30 s, it might not be representative of all the duration of the decomposition process. But to have more data, it is time and material consuming.

3.1.5 Temperature measurements

Intumescent samples are characterized by the formation of an insulating layer formed on top of the sample during its burning. During cone calorimeter experiments, a thermocouple (K type, diameter = 0.5 mm, length = 250 mm) was placed at the bottom of the PU samples (see exact location in **Figure 52**). This experiment is generally carried out with three thermocouples placed vertically at different height through a hole in the middle of the plate. For PU, it was placed horizontally instead of vertically because the hole modifies too much the burning behavior of the samples.

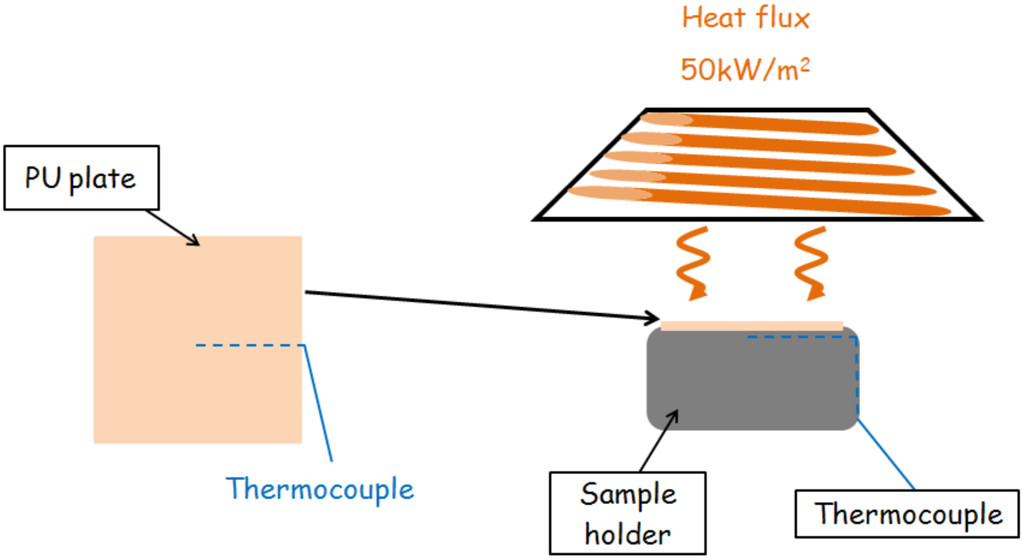

Figure 52: Schematic representation of the thermocouple placement for a temperature measurement during cone calorimeter experiment

The thermocouple is blocked with the sample holder, so that it normally does not move. This setting permits to evaluate the temperature gradients in the burning polymer and the potential barrier effect of the char formed.

3.2 Limiting oxygen index (LOI)

Limiting Oxygen Index (LOI) (Minimum Oxygen Concentration to Support Candle-like Combustion of Plastics) was measured using a Fire Testing Technology (**Figure 53**) instrument on sheets (100 x 10 x 3 mm^3) in a vertical position according to the standard ‘oxygen index’ test (ISO4589). LOI values are given in vol-% O_2 and the experiments are repeatable within ± 1 vol-%.

The LOI gives information on the relative flammability of a material because it measures the minimal oxygen concentration in an oxygen/nitrogen mixture that permits either to maintain flame combustion of the material for 3 minutes or lead to a burned length higher than 5 cm of the sample (the top of the test sample is ignited with a burner). The LOI value is the last value for which the sample burns less than 3 minutes and lead to a burned length lower than half of the barrel.

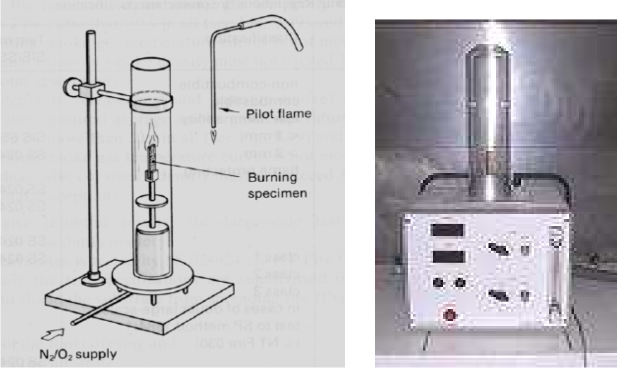

Figure 53: LOI measuring apparatus

Since air contains 21 vol-% of oxygen, it is agreed that if LOI < 21 vol-%, the material is a combustible material, and at contrary if LOI > 21 vol-%, it is a fire retarded material.

4 CONCLUSION: WORK PLAN TO UNDERSTAND THE POLYURETHANE FIRE BEHAVIOR

In this chapter, experimental techniques used to prepare and to characterize the materials and the reaction to fire of flame retarded PU castings were described. All these developments and work on the methodologies were developed via a systemic approach of the subject (some of them are very novel and have never been used before). The following chapters will use these techniques and will combine the results. The synergistic effects occurring between APP and NPs in the considered PU matrix will be evidenced and quantified by collecting the information from fire tests. Finally it is expected to propose a model for the mechanism of action leading to synergism in fire retarded PUs.

The first step of the work for understanding the synergy mechanism is to fully characterize the PU formulations once prepared. This is the purpose of the following chapter. Additives (APP and nanoparticles) are indeed incorporated to the PU matrix and this may modify the intrinsic properties of PUs. It is at least important to fully characterize the materials at time t = 0. The fire properties of the formulations will be then evaluated to quantify the synergy. The study of the thermal degradation of additives and PU formulations will finally give first clues of explanation for the fire protection mechanisms.

Chapter III - Study of PU/APP/NP systems and their fire properties

The first chapter of this thesis has established the interesting use of intumescence to flame retard PUs. It was also noticed that, even though it looks promising, not many works have been done on the synergy in intumescent PUs. That is why the investigation of a PU system containing ammonium polyphosphate (APP) as intumescent agent and nanoparticles (NP) as synergists was developed during this Ph.D.

This chapter is divided into three main sections and will focus on the characterization of the PU formulations in terms of structure, fire performances and thermal degradation. The materials will first be fully characterized. The effect of filler incorporation will then be assessed by nuclear magnetic resonance (NMR), scanning electron microscopy (SEM) and by measuring the glass transition temperature. Second, the fire properties of the formulations will be evaluated by mass loss cone calorimetry (MLC) and limiting oxygen index (LOI). A ranking of the different formulations regarding their fire properties will thus be established. Finally, the thermal analyses of the PU matrix, of the additives, of their mixtures and of filled PUs will be compared and studied.

1 CHARACTERIZATION OF THE POLYURETHANE FORMULATIONS

The first section aims at evaluating the influence of additives incorporation on the properties of the resulting PU matrix. A characterization of the materials by nuclear magnetic resonance (NMR) will characterize the formation of the PU network. The potential chemical reactions that might take place between the matrix and additives during synthesis will then be followed. The dispersion of the various additives will be investigated by scanning electron microscopy (SEM) and associated techniques. The glass transition temperature will then be measured by differential scanning calorimetry (DSC) to evaluate the potential plasticizing effect of the selected particles.

1.1 Chemical characterization of PU formulations

The reaction of the isocyanate (S2020) with the polyol (JWL440) leads to polyurethane through an urethane linkage, as shown in **Figure 54**. The ^{13}C solid state NMR spectrum of the PU is presented in **Figure 55** and the peak assignment is given in **Table 11**.

Series of bands observed under 80 ppm is assigned to aliphatic carbons. The first peak at 37 ppm is attributed to the CH_2 between the aromatic rings of the isocyanate. The other aliphatic carbons, coming from the polyol, are linked to oxygen causing their deshielding with chemical shifts between 60 and 70 ppm. Carbons linked to alcohol or ether and secondary or primary carbons can be distinguished according to their chemical shift as shown in **Table 11**. Between 110 and 140 ppm aromatic carbons appears. The carbon linked to the isocyanate function is less deshielded than the four carbons of the aromatic ring. The atom linked to the other aromatic ring via a -CH_2- bond is deshielded. The last peak at 151 ppm is characteristic of the urethane linkage.

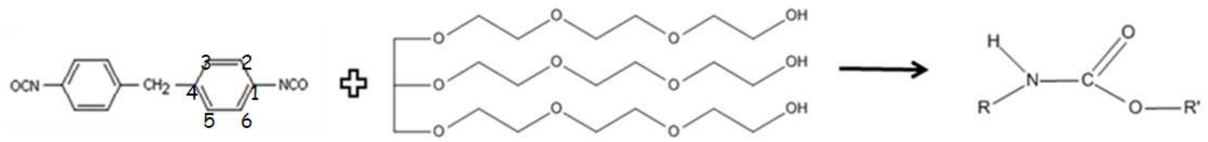

Figure 54: Reaction of the isocyanate (S2020) with the polyol (JWL440)

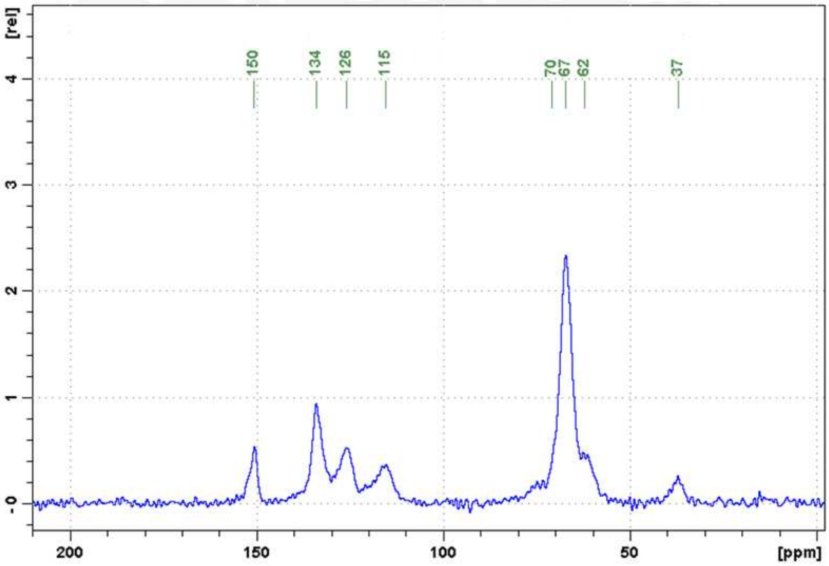

Figure 55: ^{13}C solid state NMR spectrum of PU

Table 11: Chemical shifts assignments for ^{13}C solid state NMR spectrum of PU [13, 113, 114]

Chemical shift (ppm)	Peak assignment
37	CH_2 from S 2020
62	CH_2-OH from JWL440
67	CH_2-O in the chain of JWL440
70	CH-O in the chain of JWL440
115	Aromatic C-NCO from S 2020 (1)
126	Aromatic C from S 2020 (2,3,5,6)
134	Aromatic C-CH_2 from S 2020 (4)
150	C from urethane linkage

Figure 56 gives the comparison of the ^{13}C solid state NMR spectrum of PU and PU 28%APP 2%nano MgO. The acquisition parameters and the quantity of sample put in the rotors are exactly the same for both samples. The peaks are superimposed and only differences in the intensity of the peaks can distinguish the two spectra. The same observation was made for the formulation PU

30%APP. This difference might be the result of a combined effect; first the quantity of carbon is lower in the FR formulations; and second, the polarization efficiency may be affected by the presence of additives. The cross-polarization efficiency indeed directly depends on the spin relaxation time as well as the time required for energy exchange between carbon and proton populations [115]. These parameters are depending on the molecular network of the samples which is directly dependant on the presence of additives.

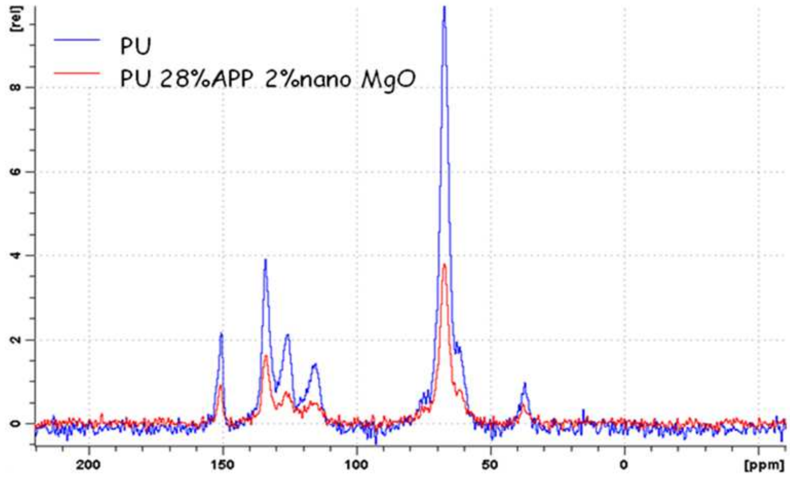

Figure 56: ^{13}C solid state NMR spectra of PU and PU 28%APP 2%nano MgO

The conclusion of this first NMR study is that the incorporation of additives (APP and nano MgO) does not influence the carbon structure of the PU matrix according to the ^{13}C NMR. This was also verified for the other NPs used within the project.

Figure 57, a shows the ^{31}P solid state NMR spectrum of APP which exhibits a double peak at -21,6 and -22,5 ppm characteristic of polyphosphate chains [116, 117]. Adding APP to PU (**Figure 57, b**), the ^{31}P NMR spectrum does not change considering the chemical shifts. This proves once again that there is no chemical interaction between the filler APP and the PU matrix. Considering the formulations containing PU, APP and NPs (**Figure 58**); the same observation can be made.

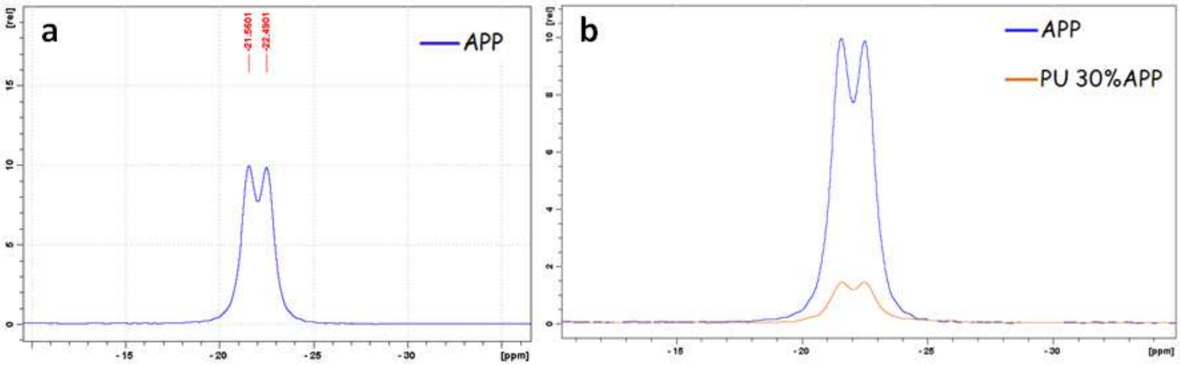

Figure 57: ^{31}P solid state NMR spectra of APP alone (a) and added in PU (b)

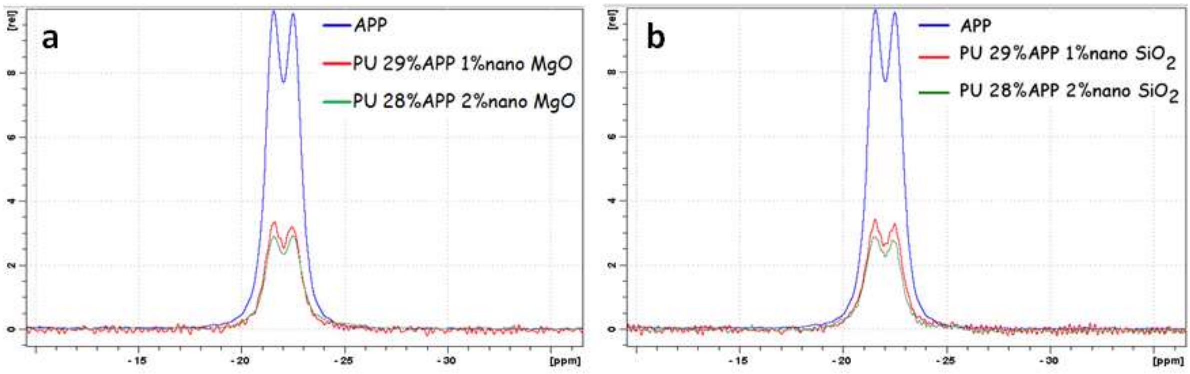

Figure 58: ^{31}P solid state NMR spectra of PU/APP/NP at different ratios (a: nano MgO, b: nano SiO_2)

As a conclusion, similarly to the conclusions made from ^{13}C NMR results, the incorporation of additives (APP and NP) does not influence the phosphorus structure of the APP in the PU matrix.

These NMR analyses showed that the selected route of synthesis of PU formulations do not induce chemical reactions between the fillers and PU. The dispersion state of the additives in the PU matrix will then be investigated.

1.2 Dispersion of additives in the PU matrix

Since there is no chemical interaction between the polymeric matrix and the additives, it is interesting to examine where the particles are located and how the network is organized. To that aim the dispersion of fillers in the PU matrix will be characterized by scanning electron microscopy (SEM), back scattering electron spectroscopy (BSE) and energy dispersive X-ray spectroscopy (EDS).

The dispersion of APP and NPs have been investigated first using SEM and BSE analysis for the formulations PU 28%APP 2%nano SiO_2 (**Figure 59**) and PU 29%APP 1%nano MgO (**Figure 60**).

These pictures first reveal that bubbles have been formed during PU preparation as we can see holes of nearly 200 µm of diameter (**Figure 59, a**). APP seems homogeneously dispersed in the PU matrix both for the formulation containing nano SiO_2 (**Figure 59, b**) and for that containing nano MgO (**Figure 60, a and b**). On the pictures, the particles size of APP lies from 5 to 40 µm, which is in accordance with the data from the supplier (D_{50} = 15 µm). The nanoparticles are also homogeneously dispersed but nanodispersion is not achieved. Aggregates and irregular distribution with some areas poor and other rich in NP can be observed (**Figure 59, c and Figure 60, c**). In the case of nano SiO_2, the aggregates lie from 100 to 800 nm whereas they are bigger with nano MgO, ranging from 200 nm to 2 µm. **Figure 59, c** also shows individual particles of nano SiO_2 with a diameter from 10 to 50 nm.

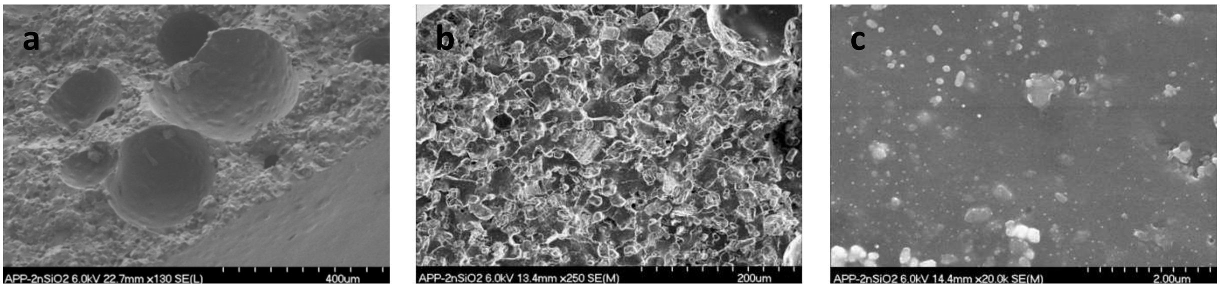

Figure 59: SEM pictures of PU 28%APP 2%nano SiO_2 taken at different magnifications (a: x130, b: x250, c: x20 000)

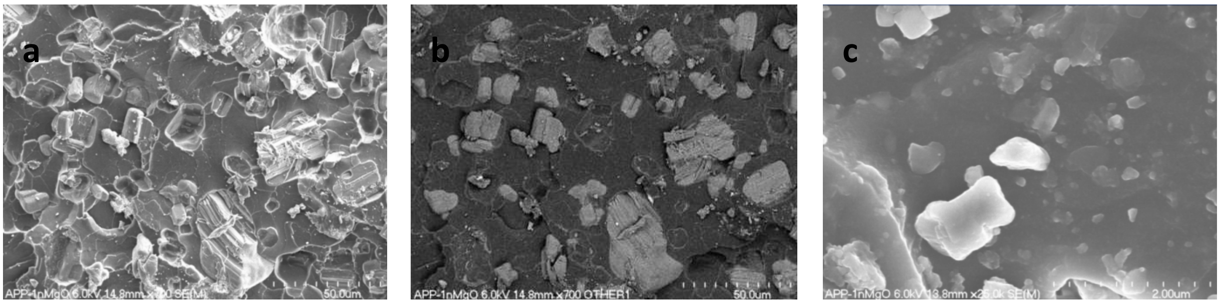

Figure 60: SEM and BSE pictures of PU 29%APP 1%nano MgO taken at different magnifications (a: SEM x700, b: BSE x700, c: SEM x25 000)

A first EDS analysis (**Figure 61**) has been performed in a global part (low magnification) of the PU 29%APP 1%nano MgO sample.

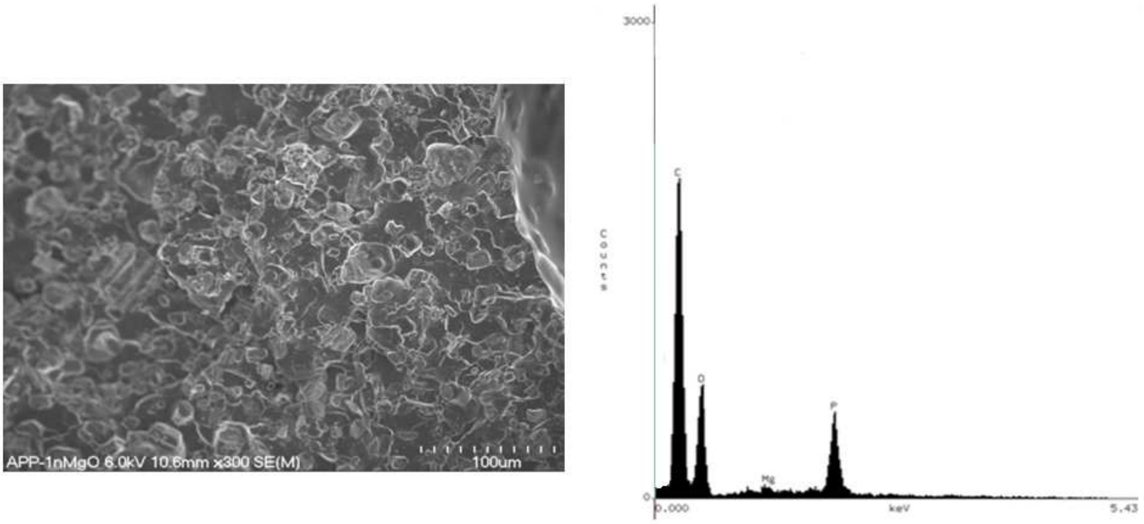

Figure 61: SEM picture and corresponding EDS spectrum of PU 29%APP 1%nano MgO

It shows that carbon, oxygen, magnesium and phosphorus are present in the observed area. The carbon peak is attributed to the carbon deposit made to perform the analysis and also to the carbon of the PU matrix. The oxygen peak comes from the PU, the magnesium oxide and also from the APP. The magnesium is added as magnesium oxide nanoparticles. Finally, the phosphorus is that of APP. Another element that should be present considering the components used to prepare the sample is the nitrogen which comes from the PU matrix and from APP. It is however quite impossible to see the nitrogen in EDS because it is a light element and the amount of nitrogen is not sufficient enough to allow its detection with our equipment.

A second EDS analysis (**Figure 62**) has been performed on the same material (PU 29%APP 1%nano MgO) but at a higher magnification. It is thus possible to isolate areas with different elements. The composition of the red mark corresponds to the PU matrix since carbon and oxygen are mainly detected. It can be noted that magnesium is also detected but at a low level. The blue mark is located on an APP particle, evidenced by oxygen and phosphorus detection. A higher magnesium concentration is detected in the PU matrix at the green mark located on a white point of the picture. It is thus possible to assume that it corresponds to MgO aggregate.

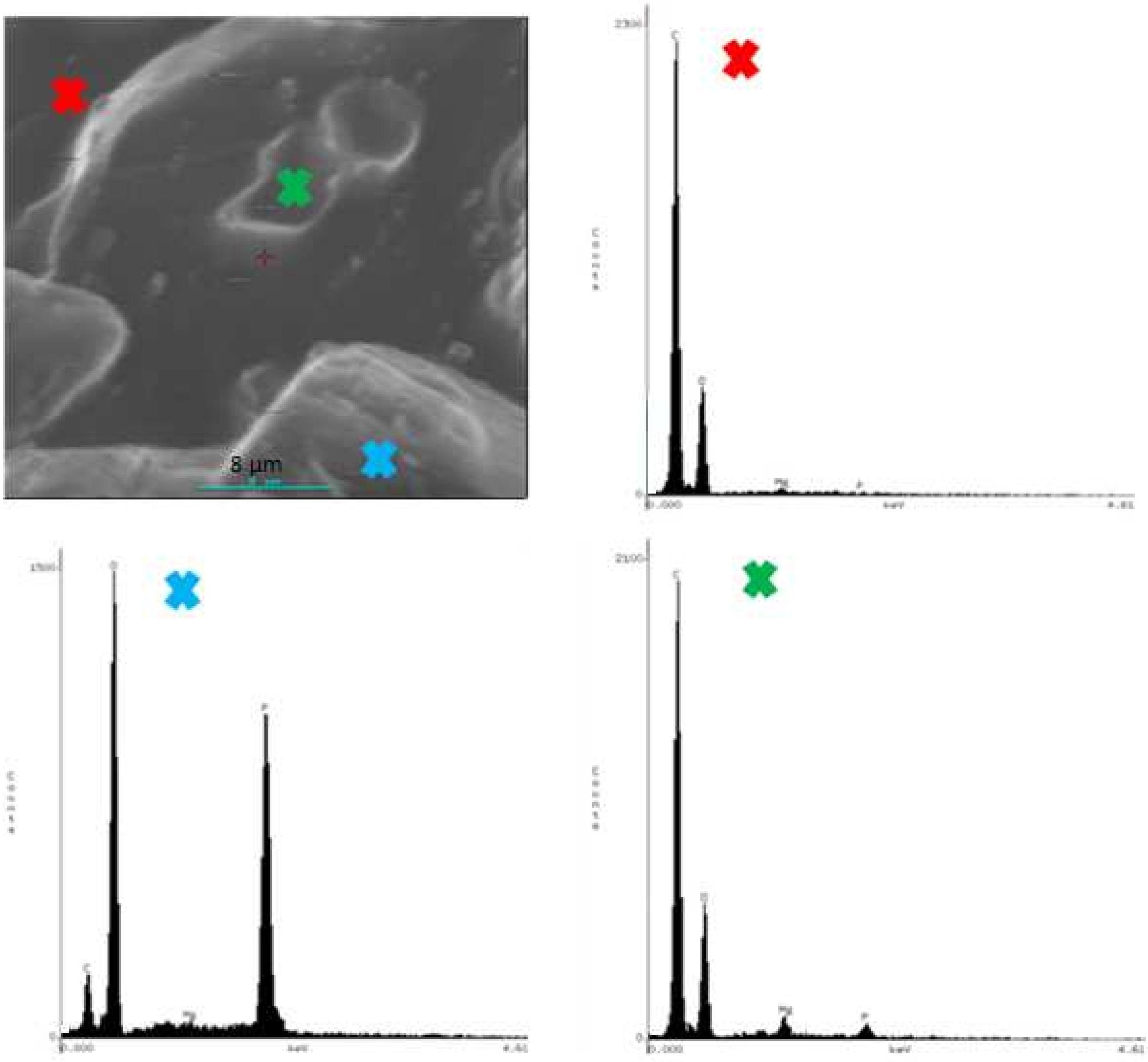

Figure 62: SEM picture and EDS spectra in selected area of PU 29%APP 1%nano MgO

This EDS analysis ensures that we can differentiate the PU matrix from the APP particles and from the nano MgO. It could thus be concluded that APP is homogeneously dispersed in the PU matrix while the NPs (MgO and SiO_2) show no nanodispersion but only microdispersion. The compatibility between the components of this formulation is however sufficient enough to get additives evenly dispersed at the micro-scale. Because of their presence directly in the PU network, these additives could impact some physical properties of the virgin material. The effect of additives on one of these properties, the glass transition temperature, will thus be discussed now. This property is particularly interesting to investigate while studying polymers because it will affect a lot their mechanical properties and consequently their field of application.

1.3 Influence of additives on the glass transition temperature

To study the influence of additives on the PU glass transition temperature (T_g), differential scanning calorimetry (DSC) has been realized. It is important to know that the incorporation of fillers, and especially NPs, often induce changes in the polymer T_g.

DSC thermograms of virgin PU and of the PU formulations are presented respectively in **Figure 63 and Figure 64**. It is first of all noteworthy that after all DSC experiments, PU samples were collected and no color change was observed; the powder just changes into a more or less compact layer. T_g is determined during the second temperature rise in the DSC cycle and the results are reported in **Table 12**.

For the virgin PU, the curve is a typical polymer DSC curve showing clearly the T_g. This curve and T_g value is impossible to compare to the literature because the term “polyurethane” is so vast that a large range of T_g are reported [12]. Each PU is unique and depends on the soft segment, hard segment, chain length, etc. and the T_g is drastically affected by those parameters.

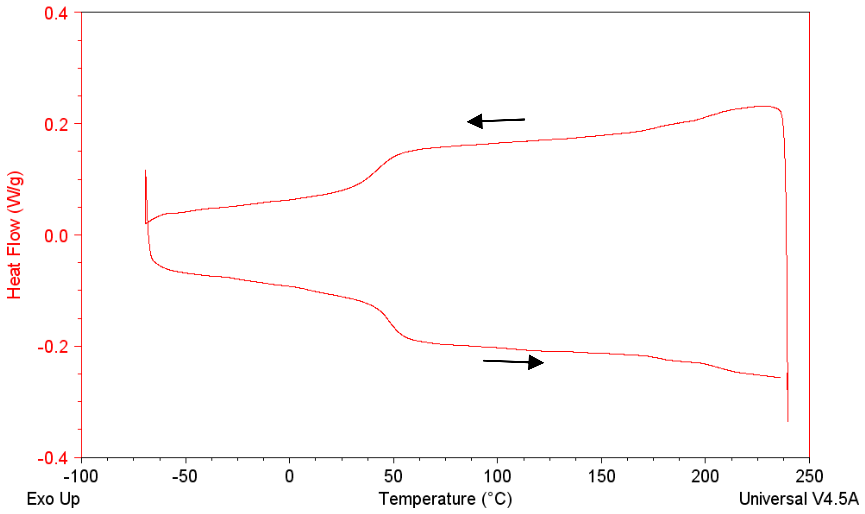

Figure 63: DSC thermogram of virgin PU (second cycle)

Two examples of DSC thermograms obtained with APP and NPs incorporated in the PU matrix are shown in **Figure 64**. For all the formulations, the same curve was obtained and the only parameter changing was the T_g.

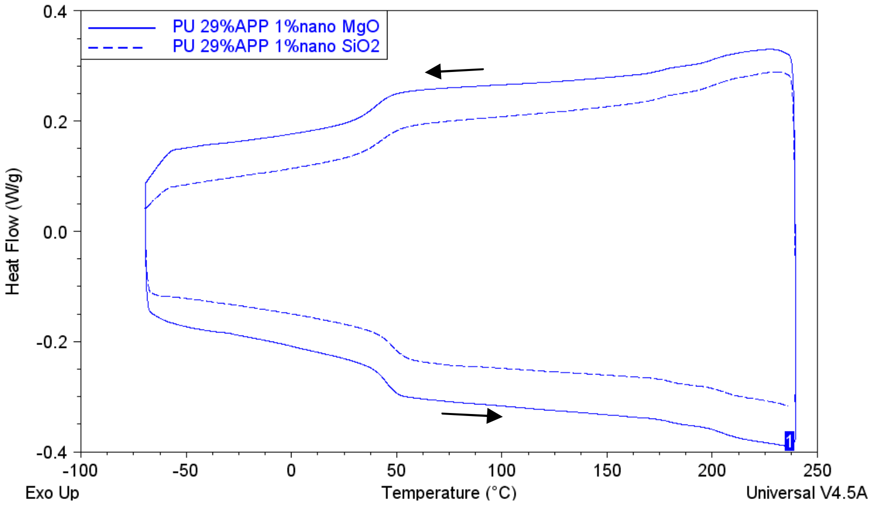

Figure 64: Comparison of second cycle DSC thermograms of PU 29%APP 1%NP (plain line: nano MgO, dash: nano SiO_2)

Table 12: Summary of T_g determined by DSC experiments (reproducibility T_g ± 1°C)

Sample	Tg (second rise in T) (°C)
PU	47
PU 30%APP	45
PU 29%APP 1%nano MgO	45
PU 28%APP 2%nano MgO	40
PU 5%nano MgO	46
PU 29%APP 1%nano SiO_2	48
PU 28%APP 2%nano SiO_2	51
PU 5%nano SiO_2	46
Polyol Jeffox WL440	/
Isocyanate S 2020	/

The virgin PU T_g (47°C) is different than that of some filled PU which demonstrates an influence of the additives on the dynamic of the polymeric chains. Additives are incorporated to the PU before polymerization of the two monomers; this could interfere during the crosslinking step and modify the chain arrangement [12]. Interactions between fillers and the polymer matrix will affect the molecular mobility at small scale as well as the flexibility of the polymer chains. The physical adsorption or chemical attachment of polymer chains to rigid particles may influence the polymer dynamics, which might furthermore modify the glass transition of the polymer chains near particle surfaces [118]. The nature of the interfacial interactions between the polymer and the incorporated particles will thus lead to different T_g values depending on the filler considered.

Regarding the DSC results (**Table 12**), nano SiO_2 and nano MgO incorporated alone in PU does not have any effect because their T_g are similar to that of the virgin polymer.

APP alone or in combination with nano MgO, seems to have a plasticizing effect on the polymer because T_g (PU 28%APP 2%nano MgO) < T_g (PU 29%APP 1%nano MgO) = T_g (PU 30%APP) < T_g (PU). This is not surprising since some phosphates based flame retardants present a plasticizing effect which can be useful depending on the field of application and the polymer considered. This plasticizing effect has already been reported in the literature for organic compounds [119, 120].

On the contrary, the combination of APP and nano SiO_2 give an increasing T_g: T_g (PU 30%APP) < T_g (PU) < T_g (PU 29%APP 1%nano SiO_2) < T_g (PU 28%APP 2%nano SiO_2). Since nano silica alone has no effect and APP alone has a plasticizing effect, this result suggests that interaction occurs between APP and nano silica in the PU matrix.

The incorporation of fillers during preparation of the PU casting modifies the glass transition temperature of the resulting material compared to the virgin polymer. A difference in the plastification state of the formulations containing APP and nano MgO or SiO_2 is particularly observed and could lead to different physical properties of the material.

The first section of this chapter showed that the incorporation of APP and NPs does not lead to chemical interactions between any of the components of the formulation. Even though NPs were used, the nanodispersion state was never reached. All the additives were however homogeneously dispersed in the PU matrix. The fillers moreover induce slight changes in the glass transition temperature of PU.

After characterizing the materials at time t = 0, an evaluation of the fire performances for all formulations will now be performed. The results collected with mass loss cone calorimeter (MLC) and limiting oxygen index (LOI) experiments will allow a ranking of the formulations.

2 EVALUATION OF THE FIRE PERFORMANCES

As already discussed, PU is known to be very flammable due to its composition made up mainly of carbon and oxygen atoms [10]. **Table 9 (p79)** reports formulations that would potentially be effective to flame retard PU. This section is devoted to the evaluation of the fire performances of these formulations. The two first parts will present the results obtained by two different fire tests: the mass loss cone calorimeter (MLC) and limiting oxygen index (LOI). The third part will summarize the data collected with the fire tests to finally quantify the synergy reached by each PU/APP/NP system.

2.1 Fire performances determined by mass loss calorimetry

The first fire test performed and presented in this section is the mass loss cone calorimeter where the sample is submitted to a heat flux of 50 kW/m^2; corresponding to a well-developed fire scenario. **Figure 65** presents the heat released rate (HRR) curves for PU, PU/APP, PU/NP and PU/APP/NP formulations using the ratios and the NPs previously selected (**Table 9 p79**). The repeatability of the experiments is generally very good and the curves plotted here are the most representative of all the tests made during this three years' work. Additionally to HRR curves, several parameters were collected at the end of the test: reduction of the peak of HRR (pHRR), total heat released (THR), expansion (obtained by measuring the char height), residual mass and pictures of final residues (**Table 13**). For a better observation of the residue, bigger size pictures are presented in **Appendix 1: Residue pictures taken at the end of a cone calorimeter test on PU, PU/NP, PU/APP and PU/APP/NP formulations p235**.

Nano gold based formulations have been tested at different ratios (PU 28%APP 2%nano gold, PU 29%APP 1%nano gold, PU 29.5%APP 0.5%nano gold) and it appears that the fire performances in cone calorimeter are equivalent in terms of HRR. The PU 29%APP 1%nano gold will consequently be the only curve presented here. Moreover for the formulation PU 28%APP 2%nano SiO_2, HRR curves of the two same samples are plotted because, only with this formulation, extreme different results can be obtained while tests are performed in the same way. The two curves represent the maximum difference obtained on two samples. These differences were reasonably attributed to a difficult synthesis of the samples leading to less homogeneous samples compared to the plates prepared with other NPs.

pHRR is the first critical parameter to compare the fire behavior of polymers. It indeed reflects if the material burns easily or not and its potential contribution to fire. As expected the virgin PU releases a lot of heat during its degradation as its pHRR is the highest (466 kW/m^2). Adding 5% of NPs (MgO or SiO_2), the fire properties according to this test are not significantly improved. At the opposite, the incorporation of 30% of APP in the polymeric matrix reduces significantly the HRR (174 kW/m^2). This corresponds to a reduction of the pHRR by 63% compared to virgin PU (**Table 13**). When NPs are used in substitution of APP a synergy is always observed. The decrease of pHRR with incorporation of nano gold and OMPOSS is of 66% and 70% respectively. This is not really a significant improvement when compare with pure APP. With MgO a larger synergistic effect can be obtained. The reduction is already better (up to 76%) for PU 25%APP 5%nano MgO and drastically higher at lower nano MgO content. The decrease of pHRR compared to virgin PU is indeed of 83% and 86% respectively for PU 28%APP 2%nano MgO and PU 29%APP 1%nano MgO. With nano silica, one sample exhibits impressively good fire properties with a 92% pHRR reduction whereas the other one is nearly not better than PU 30%APP (66% of pHRR reduction).

On the other hand there is generally no huge difference in the shape of the curves presented in **Figure 65**. Virgin PU and PU/NP may present several peaks because they are almost totally degraded during the cone calorimeter test. The combustion is thus not at a steady state but turbulent. During burning, cracks formation is observed at the surface of the sample; the flame can thus appear by these cracks leading to a non regular rate of heat released. On the contrary, samples including APP exhibit a regular and similar shape of HRR. This is due to the formation of the char which protects the underlying material and regulates the heat release during burning (see pictures in **Table 13**). The formulations 28/2 and 29/1 with nano MgO and 28/2-a with nano SiO_2 exhibit nearly no pHRR as the curve is almost flat. This is due to an efficient barrier effect of the char formed quickly after the exposition to the heat flux. Sometimes a low increase of HRR can anyway be observed on these flat curves and this is due to a default in the char surface allowing the appearance of a flame because of the formation of small hole. The case of PU 29%APP 1%nano gold is slightly different but this irregular HRR shape may rather be due to the preparation of the sample which was difficult to realize because of nano gold (bubbles, not homogeneous plate). The formation of a char is however also observed.

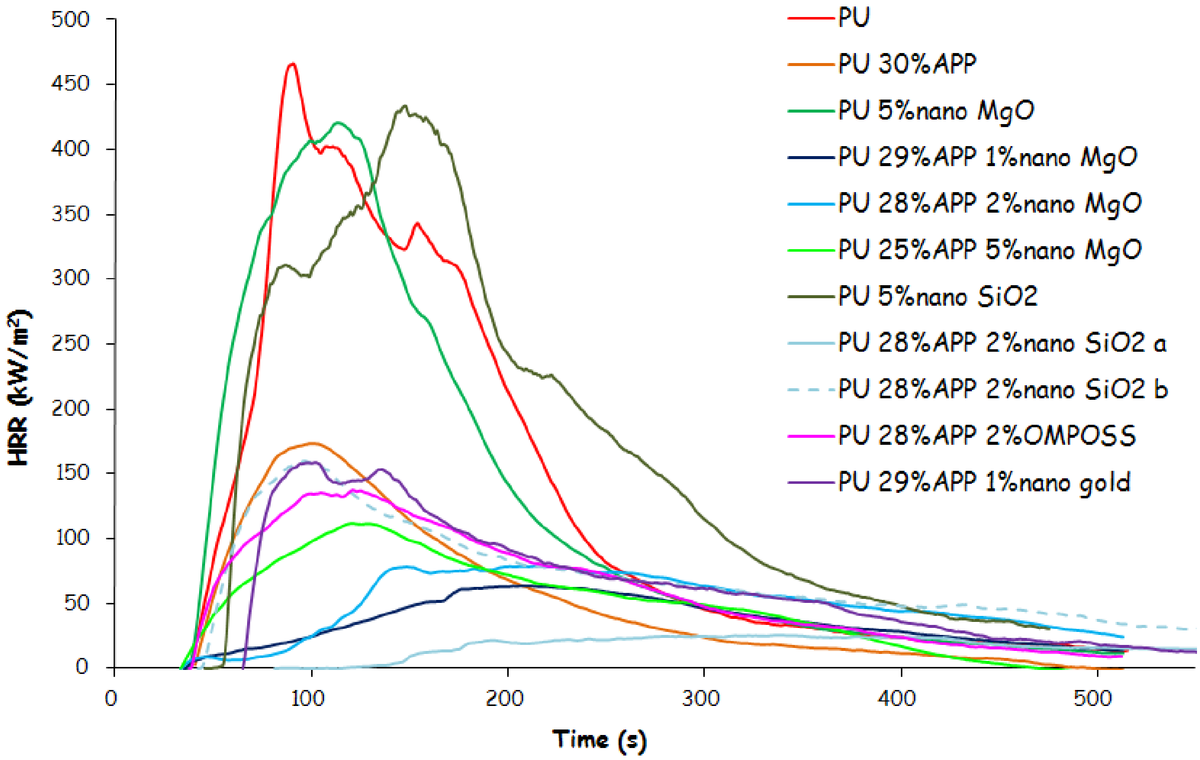

Figure 65: Superimposition of HRR curves for PU, PU 30%APP, PU 5%nano MgO, PU/APP/nano MgO (ratios 29/1, 28/2, 25/5), PU 5%nano SiO_2, PU 28%APP 2%nano SiO_2 (two different samples), PU 28%APP 2%OMPOSS and PU 29%APP 1%nano gold

For all the systems considered in this Ph.D work, the time to ignition does not change significantly (between 30 and 45 seconds) and is consequently not a critical parameter for our study. The formulation with nano gold present however a higher time to ignition (around 70 seconds) but this was mainly due to experimental problems since the plates with gold were particularly difficult to prepare and tested only twice in cone calorimeter (because of the price of the sample).

The parameters of the residues collected at the end of the test (**Table 13**) are also very interesting to compare in order to better understand the samples behavior against a fire.

PU is a carbonizing polymer and at the end of the test a black residue is observed. Its structure is disordered, full of cracks and not expanded. The addition of 5% of NPs (nano MgO or nano silica) leads to a similar char structure. The residue is in fact white for the formulation PU 5%nano MgO probably due to the presence of the inorganic particles on the top of the carbonaceous residue. There is no expansion for these materials as well. While PU and PU/NP do not present any expansion, all APP containing formulations expand, with a reference at 1100% for the material containing only APP. This expansion is attributed to the formation of a char which aims to protect the residual material from heat and mass transfers. This is verified since when there is an expansion, the fire properties observed in cone calorimetry are enhanced. The addition of OMPOSS (ratio APP/OMPOSS at 28/2) and of nano gold (ratio APP/gold at 29.5/0.5) induces a slight increase of expansion reaching 1300%. At other ratios APP/gold (29/1 and 28/2) the expansion goes up to 1500%. OMPOSS and nano gold do not provide a high expansion compared to the PU/APP system whereas by the substitution of 1 or 5% of APP by nano MgO, the expansion value grows significantly from 1100 to 1800%, and so does the fire performances regarding the decrease of pHRR. PU 28%APP 2%nano MgO give an even higher and very impressive expansion, up to 2200%. As for the HRR curve, the residue of PU 28%APP 2%nano SiO_2 is totally different depending on the sample tested. The char formation is consequently affected and the expansion varies from 1100 to 1600%. It appears in this case that the HRR behaviors and residues aspects are concomitant to characterize the fire performances. The PU 28%APP 2%nano silica HRR curve similar to that of PU 30%APP induces indeed a similar char aspect and expansion. When the fire performances are better according to the pHRR reduction, the char structure is different compared to that exhibited by PU 30%APP and a higher expansion is recorded. It is moreover possible to classify the morphology of the char by visual observation in two classes (except for virgin PU and PU/NP): PU/APP/nano MgO at ratios 29/1 and 28/2 and PU 28%APP 2%nano SiO_2 a present a different surface aspect than PU/APP and all other PU/APP/NP formulations. In the first case the surface is smooth and uniform, the color is totally grey expect from the burned part where a flame came out. The char in the second case is irregular and full of sort of worms on the surface showing that the intumescence process does not occur in the same way. This classification fits perfectly with the differences observed in HRR evolution during the test.

Because all the experiments are carried out during the same time, it was possible to present the THR values but it is not really precise because with NPs, the final temperature never reaches the value of the initial temperature even if it stops burning. By comparison between the several samples tested, the uncertainty is evaluated at 10 MJ/m^2 which means that it is impossible to differentiate the PU/APP/NP formulations based on this parameter. Virgin PU and PU/NP formulations have anyway a significantly higher THR than fire retarded PU as expected because it burns more.

Finally concerning the residual mass, values are generally concomitant with all the other parameters discussed before. For virgin polymer and PU/NP, the residual mass is low (13% for PU, 10% for PU 5%nano MgO and 16% for PU 5%nano SiO_2). The material is mostly degraded and it is thus not efficient for the fire protection. PU 29%APP 1%nano MgO, PU 28%APP 2%nano MgO and PU 28%APP 2%nano SiO_2 a show the higher mass conservation (respectively 52%, 52% and 59%). This high char yield corresponds for one part to the material forming the char but in another part to some unburned material underneath the char which has been protected as it can be seen on **Figure 66**. There are no significant differences in residual mass for PU/APP/nano gold, PU/APP/OMPOSS, PU/APP/nano silica b and PU/APP (around 45%). The only surprising results concerns the formulation PU 25%APP 5%nano MgO presenting a lower residual mass (37%) than PU 30%APP (44%). The synergy leading to higher residual mass at ratios 29/1 and 28/2 is perhaps not sufficient enough in the case of PU 25%APP 5%nano MgO to compensate the decrease of APP content. It was in particular observed that at 10 and 20 wt.% of fillers in PU, the synergy does not exist anymore with a ratio of respectively 8.33/1.67 and 16.67/3.33 (corresponding to 25/5 at 30 wt.% of fillers) [11]. This means that with a lower content of APP, higher pHRR, higher expansion and lower residual mass are obtained.

Figure 66: Picture of a slice of PU 28%APP 2%nano MgO residue taken at the end of cone calorimeter showing on the top the char and at the bottom some residual polymer

Table 13: pHRR (and its relative decrease), THR, expansion, residual mass and residue pictures of PU formulations collected after MLC test

Sample	pHRR (kW/m²)	THR (MJ/m^2)	Expansion (%)	Residual mass (%)	Residue picture	Sample	pHRR (kW/m²)	THR (MJ/m^2)	Expansion (%)	Residual mass (%)	Residue picture
PU	466 (-)	60	/	13		**PU 5%nano SiO_2**	434 (-7%)	75	/	16	
PU 30%APP	174 (-63%)	26	1100	44		**PU 28%APP 2%nano SiO_2**	160-36 (-66-92%)	17-42	1100-1600	44-59	
PU 5%nano MgO	421 (-10%)	60	/	10		**PU 28%APP 2%OMPOSS**	138 (-70%)	30	1300	42	
PU 29%APP 1%nano MgO	64 (-86%)	20	1800	52		**PU 29.5%APP 0.5%nano gold**	155 (-66%)	24	1300	45	
PU 28%APP 2%nano MgO	79 (-83%)	20	2200	52		**PU 29%APP 1%nano gold**	158 (-66%)	30	1500	46	
PU 25%APP 5%nano MgO	112 (-76%)	20	1800	37		**PU 28%APP 2%nano gold**	159 (-66%)	35	1500	48	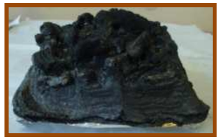

These results show that the incorporation of any selected nanoparticles whatever the ratio APP/NP leads to a synergy according to the mass loss calorimeter results, this synergy is anyway more or less important depending on the NP and the ratios used. Taking each property from MLC test into account, nano MgO incorporated in PU/APP at ratios APP/NP of 28/2 or 29/1 is indeed particularly effective.

Mass loss cone calorimeter is a test where the response of samples exposed to a radiative heat is evaluated. The interesting fire performances reached with this test might not be the same in another kind of fire test. That is the reason why another test was chosen to assess differently the fire behavior of the selected materials. This test is the limiting oxygen index (LOI) and the results obtained are discussed in the next section.

2.2 Fire performances determined by LOI

As seen in the last section, the fire properties in mass loss cone calorimeter of PU formulations depend on the intumescent system, the nanoparticles and the ratios APP/NP used. **Figure 67** summarizes the results obtained for these materials in a different fire test: the limiting oxygen index (LOI). The LOI provides different information since the heat source is provided by a flame directly applied on the sample. This test is moreover carried out in a vertical configuration. The LOI investigates the ability of a material to stop its combustion itself after ignition.

The first information is that virgin PU has a LOI of 20 vol-%, which is characteristic of a combustible material. As expected, PU exhibits high flammability as already evidenced by mass loss calorimetry. The fire performances, measured by LOI, are the same for the virgin polymer and the polymer containing 5% of NPs (MgO or SiO_2) alone, which is not a surprise as the pHRR was nearly not reduced for the material with 5% of NP compared to virgin PU. This can be due to the poor level of dispersion as it was for example the case for MMT incorporated in PP which lead to an inefficient combination [121]. It is moreover known that it is generally better to combine NPs with conventional flame retardants to reach interesting fire properties [10]. Even though the use of NPs can increase the fire properties of virgin polymer, the LOI recorded is generally not impressively high: 21.8 vol-% for incorporation of OMMT in PP [122], 20 vol-% for a sample containing 98% of EVA and 2% of LDH [123], no improvement of the incorporation of MMT in epoxy resin [124].

The addition of 30% of APP in the PU matrix enables on the contrary the material to reach a LOI value of 35 vol-%, which classify this new material as a fire retarded material.

LOI values of the PU/APP/NP formulations compared to the references PU (20 vol-%) and PU 30%APP (35 vol-%) are in agreement with the trends observed in the mass loss cone calorimeter. It indeed shows that the incorporation of any selected nanoparticles leads to a synergy because the LOI value of all PU/APP/NP formulations is significantly higher than 35 vol-%. An exception is noteworthy for the formulation PU 25%APP 5%nano MgO for which the LOI is only 26 vol-%. This could be related to the particular structure obtained under a radiant heat flux and presented in **Table 13**. The significantly lower quantity of APP contained in this sample might also be responsible for this low LOI value. This formulation is obviously influenced by the fire test conditions but this is not the case for all the other formulations. The synergy is more or less important depending on the NP and the ratios used. PU 28%APP 2%OMPOSS and PU 29.5%APP 0.5%nano gold has the same LOI value (44 vol-%) concomitant with their similar behavior in cone calorimeter. Considering the range of uncertainties PU 28%APP 2%nano SiO_2 has a higher LOI value (47 vol-%) but this is not really far from the results obtained with OMPOSS and gold. During the LOI tests no particular repeatability problems were observed with the nano silica based materials as it was the case for cone calorimeter experiments. The fire performances determined by LOI are then more reliable and it is possible to conclude that nano SiO_2 does not improve the fire performances of PU/APP systems as well as the nano MgO does. The LOI values are indeed significantly higher for PU 28%APP 2%nano MgO (52 vol-%) and PU 29%APP 1%nano MgO (51 vol-%).

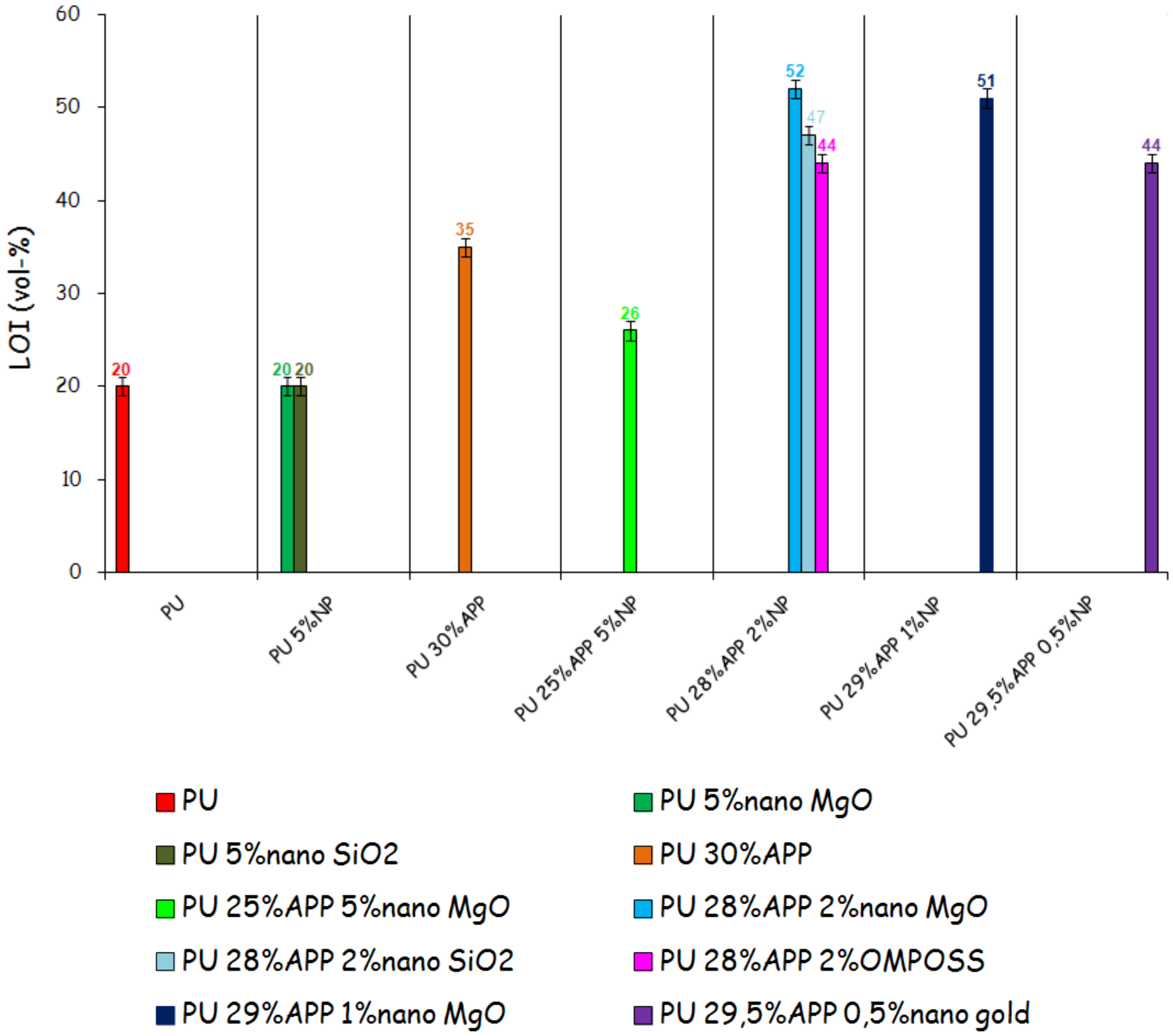

Figure 67: LOI values of PU, PU 30%APP, PU 5%nano MgO, PU 5%nano SiO_2, PU/APP/nano MgO (ratios 29/1, 28/2, 25/5), PU 28%APP 2%nano SiO_2, PU 28%APP 2%OMPOSS and PU 29.5%APP 0.5%nano gold

During the test, an intumescent behavior was observed for all samples except the virgin polymer and PU/NP. For the samples containing APP and nano MgO, a brown color was moreover noticed between the char and the unburned polymer corresponding to a partially degraded material. The formation of a char during LOI measurement as well as during the MLC test seems to play a role in the fire protection mechanism developed by the PU formulations. According to LOI values, the synergy reached by some PU/APP/NP systems is really impressive.

The LOI results will be compared to the MLC test conclusions in the next section to classify the formulations against their contribution to improve the fire performances of virgin PU.

2.3 Summary table of fire performances depending on the nanoparticles and ratios used

It has been previously evidenced that the two different fire tests performed on the PU formulations are generally in good agreement but may bring additional information and/or moderate the performances. To that aim it has been decided to judiciously compile and summarize all the data in **Table 14**.

The parameters for both tests (MLC and LOI) are presented in the first line: “pHRR, expansion, mass, aspect and LOI”. “pHRR” refers to the reduction of the pHRR compared to virgin PU, “expansion” is the swelling measured at the end of the test and “mass” corresponds to the residual mass collected at the end of the MLC test. “Aspect” is evaluated after a visual observation of the residue. Finally the LOI value is measured. According to the interpretation of cone calorimeter experiments, it was found that for our systems, a high expansion, a high mass kept and an homogeneous and compact char generally gave the best fire performances. It is noteworthy that these observations are not true for all the systems.

For each parameter, a quotation is attributed going from “--“ to “++” respectively from the worse value to the better value. To easy the reading, it was chosen to summarize this table by finally giving a mark to each formulation. This mark is calculated as follows:

- 0 point for “--“
- 1 point for “-“
- 2 points for “+”
- 3 points for “++”

The mark consequently goes from 0/15 for the worse formulation to 15/15 for the best one. When two systems reach the same mark, the ranking is done by refining all the properties. The virgin PU will be chosen as the reference and corresponds to the worse formulation with a mark of 0/15.

When adding only NPs (MgO or silica) to the PU matrix, the fire performances are not improved whereas when adding only APP, the intumescence process takes places and the mark accorded to this formulation reaches 7/15. Synergistic effects are always observed by combining APP and a small amount of NPs. Depending on the NP used and the ratio APP/NP the mark varies between 8/15 and 15/15. According to their mark going respectively from 10/15 to 8/15, PU 28%APP 2%nano SiO_2, PU 28%APP 2%nano gold, PU 29%APP 1%nano gold, PU 29.5%APP 0.5%nano gold, PU 28%APP 2%OMPOSS and PU 25%APP 5%nano MgO enhance the fire performances of PU/APP but only to a slight extent. The two best formulations are clearly PU/APP/nano MgO at ratios 28/2 and 29/1.

Table 14: Classification table of PU formulations based on parameters linked to their fire performances

Rank	Formulation	pHRR	Expansion	Mass	Aspect	LOI	Mark
1	PU 28%APP 2%nano MgO	++	++	++	++	++	15/15
2	PU 29%APP 1%nano MgO	++	++	++	++	++	15/15
3	PU 28%APP 2%nano SiO_2	+	+	+	+	+	10/15
4	PU 28%APP 2%nano gold	+	+	+	+	/	9.2/15
5	PU 29%APP 1%nano gold	+	+	+	+	/	9.2/15
6	PU 29.5%APP 0.5%nano gold	+	-	+	+	+	9/15
7	PU 28%APP 2%OMPOSS	+	-	+	+	+	9/15
8	PU 25%APP 5%nano MgO	+	++	-	+	--	8/15
9	PU 30%APP	-	-	+	+	-	7/15
10	PU 5%nano MgO	--	--	--	--	--	0/15
11	PU 5%nano SiO_2	--	--	--	--	--	0/15

The different behavior and resulting fire performances of these 12 mixtures is interesting to study in order to understand the governing parameters leading to the synergy in PU/APP/NP systems. The first relevant approach is the thermal degradation of additives and PU formulations. This will allow finding out if the mechanism of action is based on the chemistry of the system or on the physical interactions or both. Thermogravimetric analyses may indeed show stabilization between the components, in this case there would be a chemical effect and if there is no interaction, the physical route will be preferred to explain the mechanisms.

3 THERMAL DEGRADATION

The understanding of the fire properties should start by studying the thermal degradation processes involved. Even if the heat constraints used to study the thermal degradation are not representative of the fire tests conditions, they correspond to the processes involved in the first step of the combustion cycle. The polymers will first degrade whatever the heating conditions. The sample is submitted here to a convective heat from ambient temperature to 800°C. During this heating ramp, the components interact and degrade to form new structures and to yield new species. The study of the thermograms will allow seeing if chemical interactions, physical effects or both have an impact on the thermal degradation of materials.

This section is divided into three parts. In a first part, the thermal stability of the PU matrix will be studied under air and nitrogen and discussed according to the literature. Secondly the thermograms of the additives used in this Ph.D and their mixtures at different ratios will be analyzed. In the last part, the thermal stability of the additives incorporated in the PU matrix will be presented.

3.1 Thermal stability of PU

TGA has been first performed on the virgin polymeric matrix to evaluate its stability and to understand its thermal degradation process under air and nitrogen (**Figure 68**).

PU degradation [13, 14, 64, 125, 126] under air occurs in two steps, the first one starts around 250°C with a mass loss of approximately 50%. Oxygen enhances the thermal stability of PU between 390 and 560°C. Then, the rate of weight loss increases which lead to a total degradation at 675°C, due to the oxidation of the carbonaceous material previously formed. Under nitrogen, there is only one degradation step; this shows the impact of oxygen on the polymer degradation. From 300 to 400°C, the depolycondensation reaction occurs. A residue of 14% is reached at the end of the experiment.

It is known that oxygen plays an important role during polymers degradation and in most cases, the material degradation is accelerated during a thermo-oxidative step [127]; this is what is observed on **Figure 68**. It has however to be noted that according to the literature [13, 14, 125] and to previous experiments carried out at Huntsman, the first degradation step of PU is generally similar under air and under nitrogen. As the decomposition of PU occurs as a result of a multitude of physical and chemical phenomena [14], this could explain the difference observed in the considered system. The mechanism of PU thermal degradation under nitrogen is presented in **Figure 69** and indicates that the first degradation step is attributed to the urethane chain scission releasing carbon dioxide [126]. During oxidative degradation process, free radicals ($R^\bullet$) are produced and react rapidly with molecular oxygen to form peroxy radicals ($ROO^\bullet$) [14]. The peroxy radicals may further react with the PU chain and form hydroperoxides (ROOH). In the presence of heat, hydroperoxides decompose and produce more radicals that can reinitiate the decomposition of PUs; leading to a higher degradation speed of PU under oxygen. Researchers reported that the presence of oxygen does not influence the decomposition rate of PU to diisocyanates and polyols, although it affects the breakage of the polymeric chains [17] but this depends on the PU composition.

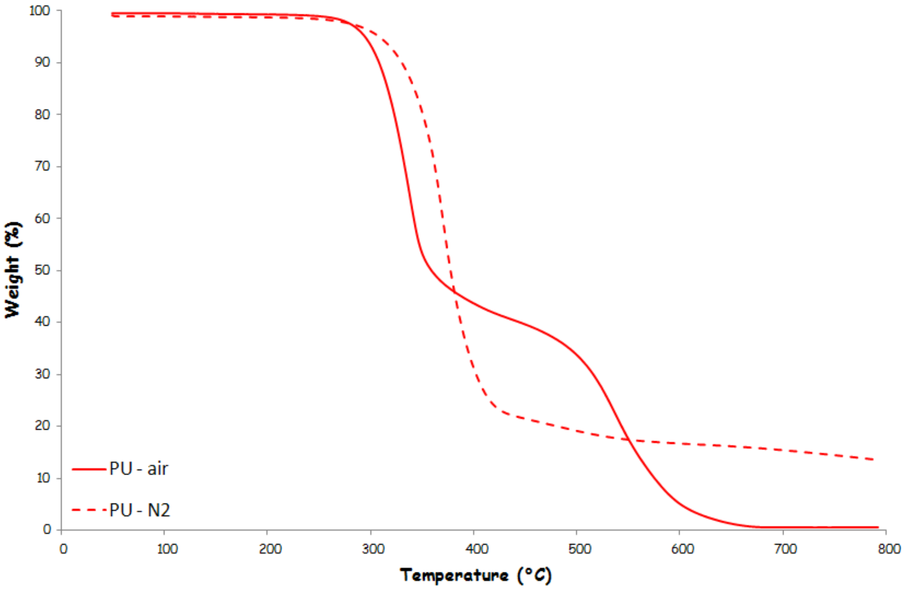

Figure 68: TG curves of virgin PU under air and nitrogen at 10°C/min

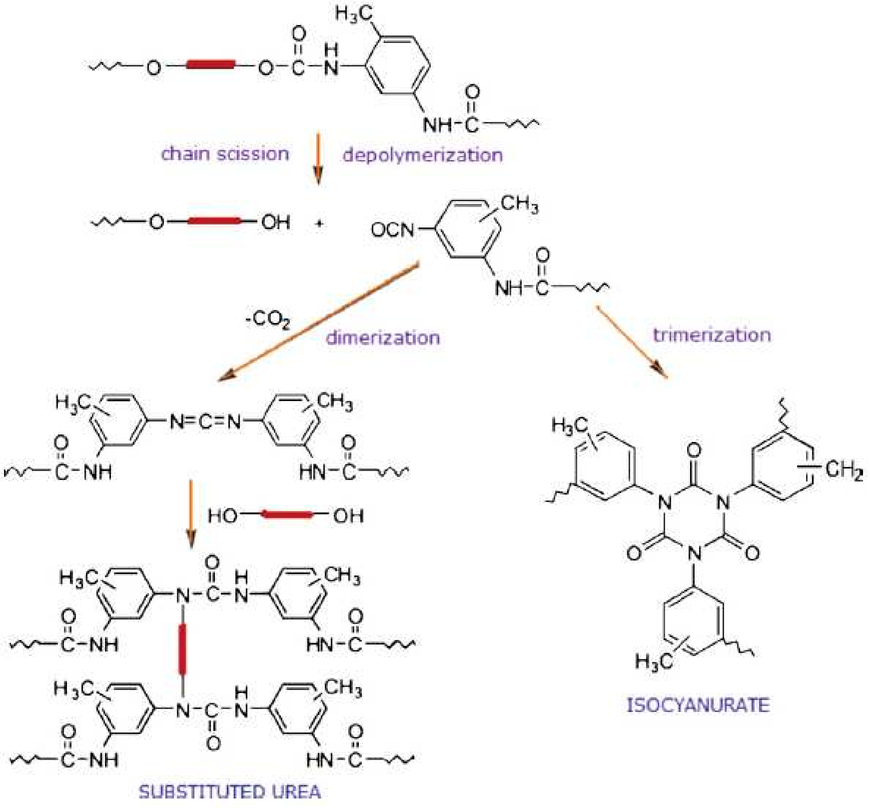

Figure 69: Mechanism of PU thermal degradation under N_2 [14, 16]

Above 650°C, there is no residue left for the virgin PU when TGA is carried out under air, this explains why in fire test the remaining mass is very low and gives no protection to the material. The incorporation of additives in this polymeric matrix should lead to higher residues giving eventually a fire protection.

3.2 Thermal degradation of additives

The additives are first submitted to thermal degradation alone to evaluate their thermal stability and then they will be mixed to examine if interactions can take place between APP and NPs. TG curves of all the additives used during this project (APP, nano MgO, nano SiO_2, nano gold and OMPOSS) are split into two graphs (**Figure 70, Figure 71**). The first one presents the results for APP, nano MgO and nano silica; and the second one compares the APP to nano gold and OMPOSS.

Concerning the APP, the degradation is similar under air and nitrogen and its mechanism has already been studied [13, 128-131]. The first degradation step starts at 300°C with the formation of ammonia and water leading to the formation of polyphosphoric acid. The second step, at 550°C, consists in the dehydration and sublimation of polyphosphoric acid in P_4O_{10}.

The nano SiO_2 does not decompose until 800°C. This result was expected since silica presents a high thermal stability [81]. Similar results were expected for the nano MgO, but a weight loss of 12-14% is observed between ambient temperature and around 400°C. The nano MgO is produced by flame spray pyrolysis and this may generate functional OH groups on part of its surface. The weight loss observed in TGA might then be a result of the degradation of those surface OH groups.

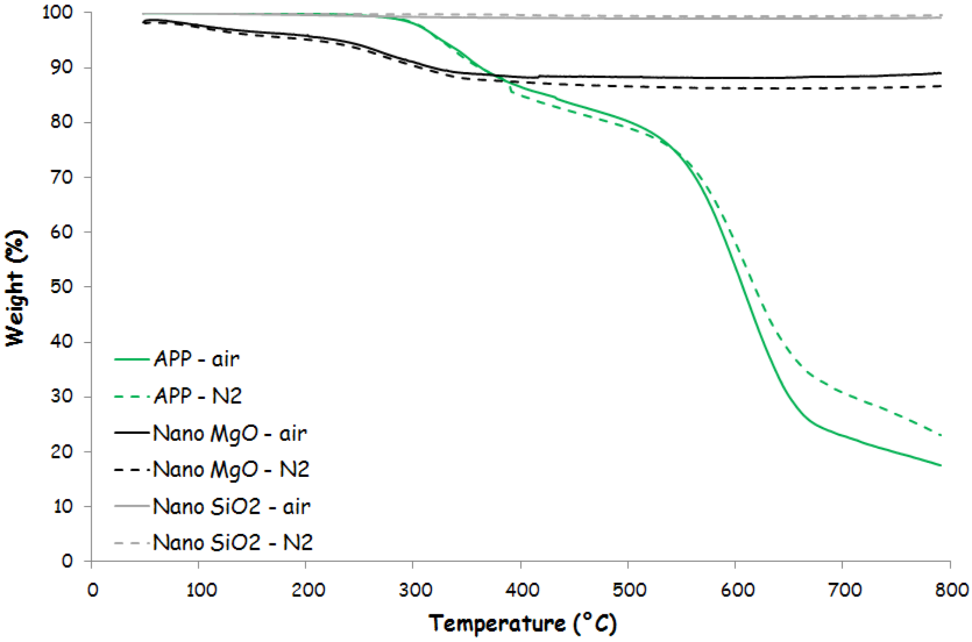

Figure 70: TG curves of APP, nano MgO and nano SiO_2 under air and nitrogen at 10°C/min

The nano gold called "bulk" corresponds to the material as received. The first degradation step is indeed due to the presence of an organic binder mixed with the gold to assist the dispersion of the particle in a polymeric matrix. A thermal treatment based on the observation of the TG curves of nano gold (bulk) was used to suppress the organic part. After that a TGA was performed on this new material called "treated". It has only been done under air because the same result is expected under nitrogen regarding the curve with the bulk material. Finally the TG curve show that nano gold is not degrading, as it was supposed to be. Note that except for TGA, the nano gold was always used as received after checking that this does not have any consequences on the results.

Finally OMPOSS has a totally different degradation pathway compared to the other NP tested because it indeed sublimates and degrades quickly from 200 to 300°C to form a small residue either under air and nitrogen [85]. The OMPOSS degradation indeed occurs in a predominant step to loose 90-95% and followed by a slow degradation of the residual material until 500°C. The OMPOSS cages break and lead to the formation of amorphous silica in the condensed phase [132]; silanols or siloxanes being released in gas phase [97].

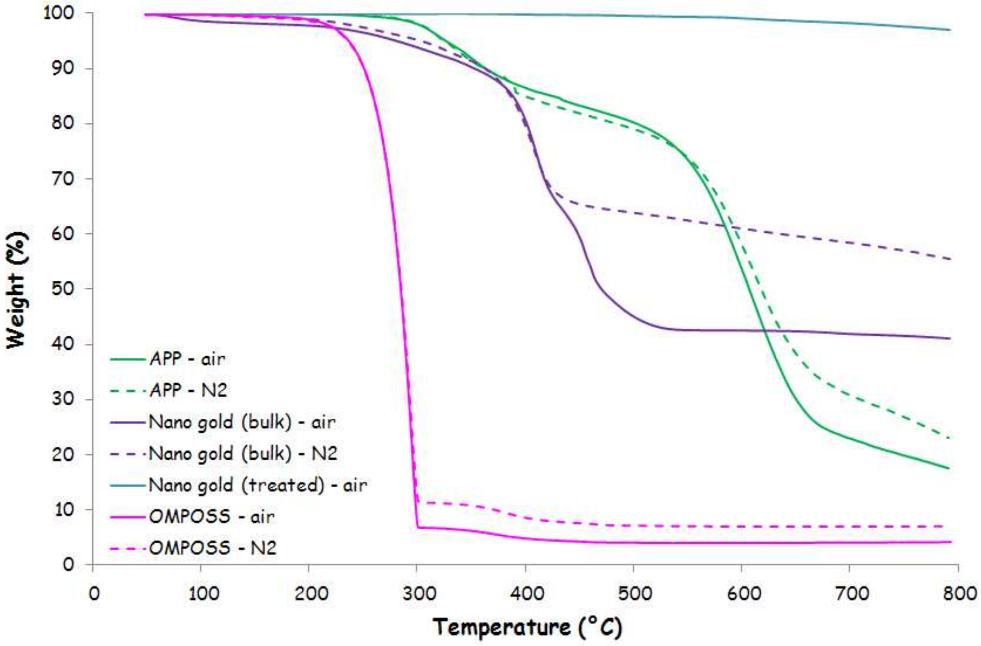

Figure 71: TG curves of APP, nano gold (bulk or treated) and OMPOSS under air and nitrogen at 10°C/min

APP degrades under air and nitrogen and its degradation mechanism is widely known. In presence of PU, this additive promotes the char formation and takes place in the intumescent process. The other additives, added at low loadings, will act as synergists. The combination of NPs with APP will thus affect the thermal degradation of the particles alone. A combination of 28% of APP and 2% of NPs is studied because it represents the ratio used to synthesize the final PU material. An exception has been made for OMPOSS which will be studied at a ratio 50/50. OMPOSS indeed sublimates and degrades before APP (**Figure 71**). If a ratio 28/2 is used and considering the small quantities involved in TGA, there is nearly no residue left that may interact with APP (verified by heating OMPOSS at 10°C/min in a furnace). The superimposition of TG curves for APP alone, the considered NP alone and the mixture APP/NP is presented in **Figure 72 until Figure 75**. On these graphs, the degradation of the mixture is always between APP and NP. Depending on the NPs used, the degradation pathway of APP is more or less affected. By a combination of APP and nano MgO, the thermal stabilization seems for instance higher compared to a combination of APP with nano silica, gold or OMPOSS. All these NPs have although an influence on the thermal degradation of the additives mixture. It could be noted that the ranking observed concerning the higher thermal stabilization follows exactly the efficiency as synergists in fire performances summarized in **Table 14 p114**.

Because of their capacities to modify the APP degradation pathway at high temperatures (T > 500°C), nano MgO and nano silica were chosen to perform a more detailed and a comparative study during TG under air and nitrogen at 10°C/min (**Figure 76**).

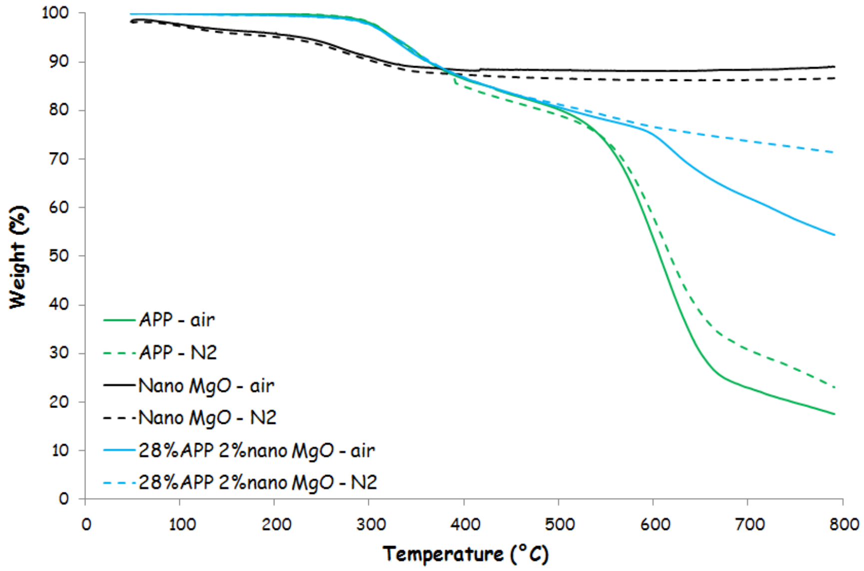

Figure 72: TG curves for APP, nano MgO and 28%APP 2%nano MgO under air and nitrogen at 10°C/min

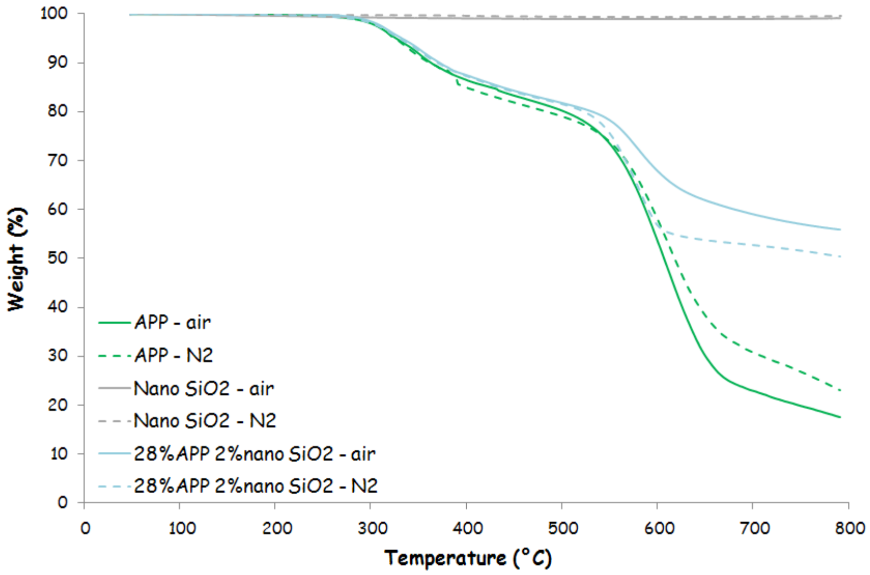

Figure 73: TG curves for APP, nano SiO_2 and 28%APP 2%nano SiO_2 under air and nitrogen at 10°C/min

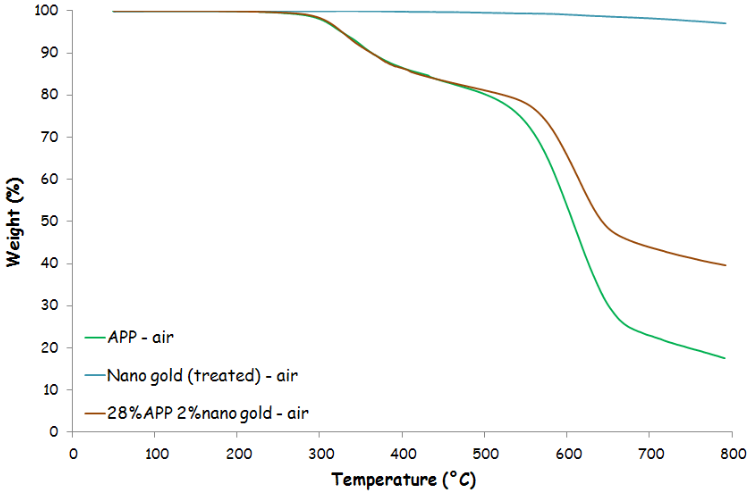

Figure 74: TG curves for APP, nano gold and 28%APP 2%nano gold under air at 10°C/min

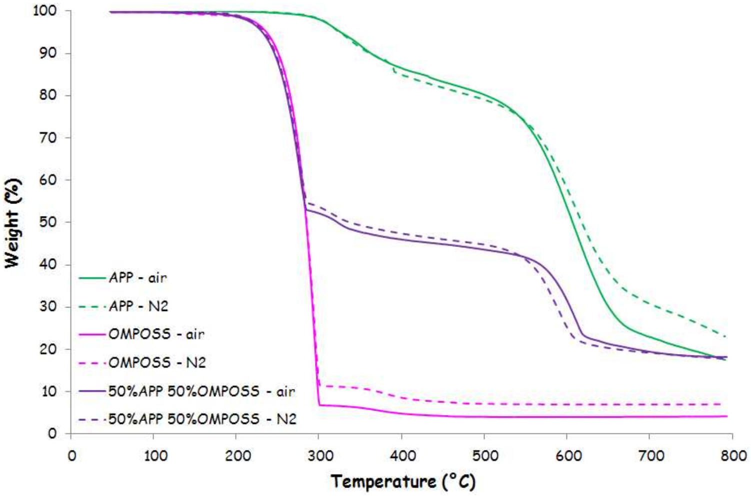

Figure 75: TG curves for APP, OMPOSS and 50%APP 50%OMPOSS under air and nitrogen at 10°C/min

Figure 76 shows the TG curves of additive mixtures at different percentages (28/2 and 29/1) under air and nitrogen. Parameters are changing step by step: the NP nature, the ratio APP/NP and the flow (air or nitrogen). This comparative study focuses only on nano MgO and nano silica because these are the most performing particles according to fire tests results (**Table 14**). It has also just been shown that MgO and silica are very effective to modify the degradation pathway of APP.

The main conclusions from **Figure 76** are: (i) nano MgO has a better stabilization effect than nano SiO_2, (ii) the residual mass is higher with a higher content of NP (except for APP/MgO under air) and (iii) higher residual mass are obtained when TGA are carried out under air (except for 28%APP 2%MgO). This evidences that MgO modifies the degradation pathway of APP in other way as silica.

Whatever the conditions and NP used, it is anyway clearly observable that a thermal stabilization of APP occurs at high temperature when combined with NP. This is why it is now interesting to evaluate the differences between experimental and simulated TG curves.

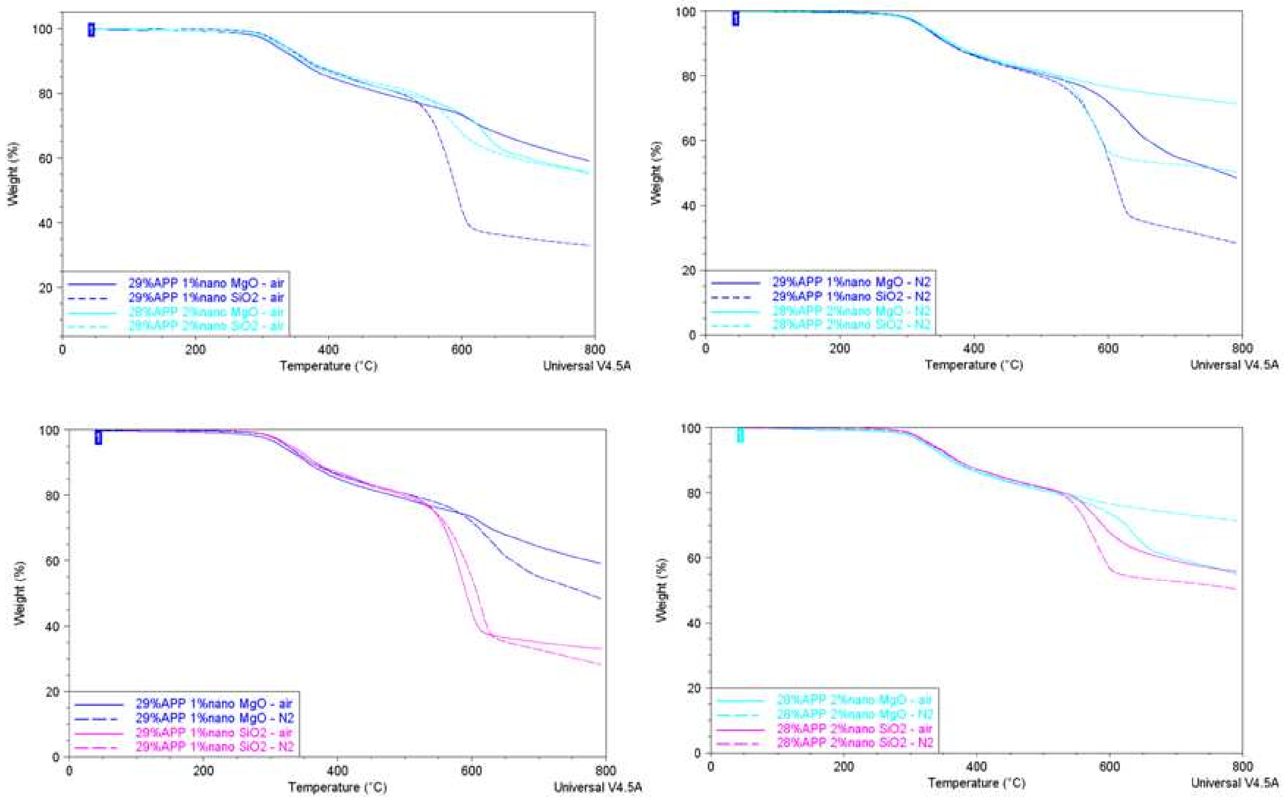

Figure 76: TG curves of APP/NP (MgO and SiO_2) mixtures under air and nitrogen at 10°C/min

It is agreed [13] when the experimental TG presents a higher mass than the simulated TG (= X% TG (APP) + Y% TG (NP)) that a stabilization of the material occurred and this is attributed, for significant mass differences, to a chemical reaction between both components of the system since heat and mass transfer are considered negligible in TG experiments. The experimental and simulated curves are plotted for all APP/NP mixtures in **Figure 77 until Figure 80**.

It is known that phosphorus is very reactive and usually forms easily phospho-X compounds [78]. For instance it has already been seen that APP and MgO reacts together to form magnesium phosphates evidenced by XRD [11]. It has also been proven that silicophosphates (SiP_2O_7) are created after heating a mixture of APP and OMPOSS [85], meaning that the silica coming from OMPOSS degradation reacts with phosphorus.

A first idea to understand the synergy mechanism was to find a nanoparticle which will not be able to react with APP thus allowing determining if the chemical reaction occurring between APP and/or its degradation products and the synergist is a critical parameter for the fire protection; nano gold was thus chosen for this purpose.

The stabilization phenomenon is clearly observed at high temperatures (after 550°C) for nano MgO (**Figure 77**), nano SiO_2 (**Figure 78**) under air and nitrogen and for nano gold under air (**Figure 79**). This means that these NPs chemically interact with APP at high temperatures at a heating rate of 10°C/min. Nano gold appears to interact with APP although this result was not expected.

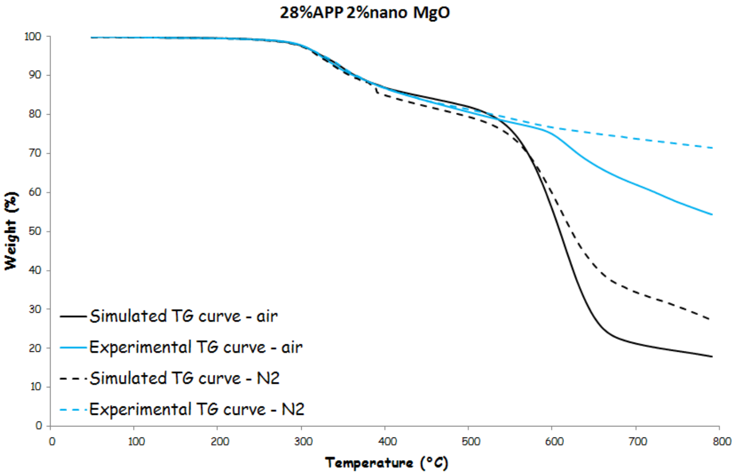

Figure 77: Simulated and experimental TG curves for the mixture APP/nano MgO at a ratio 28/2 under air and nitrogen at 10°C/min

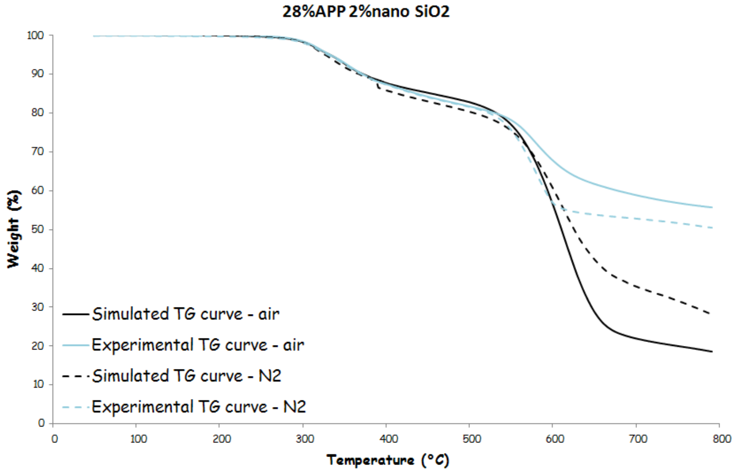

Figure 78: Simulated and experimental TG curves for the mixture APP/nano SiO_2 at a ratio 28/2 under air and nitrogen at 10°C/min

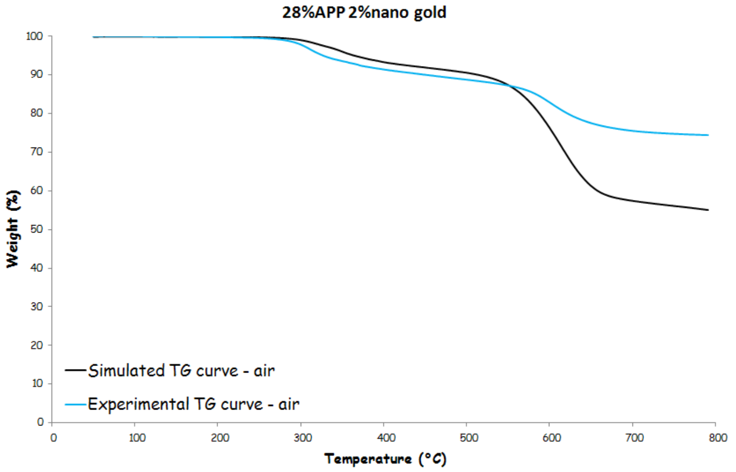

Figure 79: Simulated and experimental TG curves for the mixture APP/nano gold at a ratio 28/2 under air at 10°C/min

The case of OMPOSS (**Figure 80**) is a little bit more complicated and also very different depending on the atmosphere (air or nitrogen).

Under air, between 200 and 300°C, the experimental curve is underneath the calculated curve and after 600°C, the contrary is observed. In the first case, the sublimation of OMPOSS upon heating (between 200 and 300°C) [85] might be the origin of this difference in TG curves. During sublimation a few quantity of non degraded material may get away from the pan and this cannot be predicted by simulation. From 300 to 600°C, the curves are moreover very similar as if no chemical interactions occurred before. After 600°C, a slight stabilization on the TG curves is observed since the experimental curve is above the simulated one. APP reacts with the silica resulting from OMPOSS degradation but this represent only a small part of the material that is why the stabilization is not as high as with nano silica.

Under nitrogen, the simulated curve presents always a higher mass than the experimental curve. At low temperatures, the sublimation of OMPOSS modifies APP degradation and maybe carries along some material as it was the case under air. After 600°C, the gap between the two curves is reduced suggesting that a reaction takes place between APP and silica, coming from the degradation of OMPOSS.

At the end, either under air or nitrogen, the chemical interaction between OMPOSS and APP is in any case a predominant factor during material degradation.

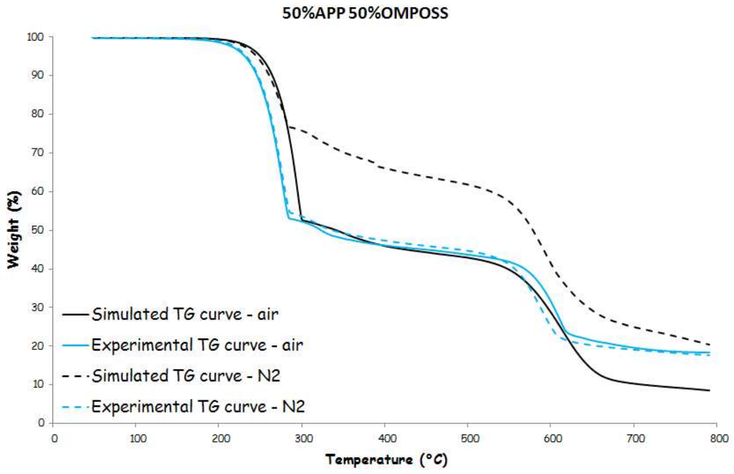

Figure 80: Simulated and experimental TG curves for the mixture APP/OMPOSS at a ratio 50/50 under air and nitrogen at 10°C/min

MgO and SiO_2 are known to react easily with APP to form respectively magnesium phosphates and silicophosphates [78]. Gold was not expected to react with APP but a stabilization is observed on TG curves thus suggesting that something might happen. To understand this, a thermal treatment (750°C for 8 minutes 30) of a mixture APP and pure nano gold (28/2) has been carried out in a furnace. From an overview of the literature, the formation of “phosphogold” has never been reported. Gold may however reacts with the nitrogen from the counter ion of APP as proposed in the literature [133]. It was not possible to perform ^{15}N solid state NMR to check this hypothesis. The quantity of sample available (due to gold price) is indeed too low to fill a 7 mm probe required to perform this ^{15}N solid state NMR experiment. A solid state NMR experiment was moreover impossible to perform because under air or with a little increase of temperature (like the one obtained during the sample spinning in NMR), the residue decomposes in two phases: a liquid phase in which the gold particles are present. To chemically characterize this residue it was thus chosen to carry out an IR spectrum (**Figure 81**). The spectrum obtained on the APP/nano gold residue is superimposed to the one of phosphoric acid because it was suspected that the liquid surrounding the gold particles was some phosphoric acid. This has been verified on **Figure 81** since the two spectra show the same peaks. Peaks are however broader for the residue but this might be due to the low quantity of sample analyzed. The mixture of APP and nano gold heated at 750°C consequently leads to phosphoric acid and gold.

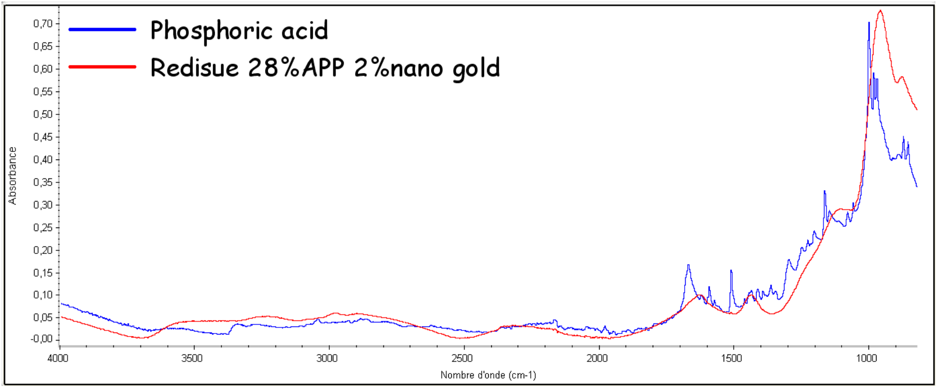

Figure 81: Transmission IR spectrum of the residue after 8 minutes 30 seconds at 700°C of a mixture APP/nano gold at a ratio 28/2 compared to phosphoric acid

The stabilization effect observed in TGA and the consequent potential chemical interactions occurring between APP and the NPs appears to be one of the clues to understand the synergy in fire properties. Other parameters than the possible reactions, such as the dispersion, the physical interactions, etc. may however be also modified and have to be kept in mind to understand the synergy. These effects of NPs observed when tested the additives alone might be different when the additives are incorporated in the PU matrix. The next part will thus study the effect of the incorporation of fillers in PU.

3.3 Thermal stability of PU formulations

The thermal stability of the PU matrix and the additives or combination of additives has been studied separately in the previous sections; the purpose of this part is to see the effect of the incorporation of fillers in PU on the thermal stability of the resulting PU formulations.

Figure 82 and Figure 83 give a comparison of the TGA results for PU, PU/APP and PU/APP/NP. **Table 15** summarizes for all the PU formulations the residual mass and the temperature corresponding to 50% weight loss. The NPs tested are nano MgO and nano SiO_2 as they allow a significantly better thermal stabilization of APP than the other NPs, as shown in the previous section. The ratios 29/1 and 28/2 have been selected because they were the most performing in fire tests.

In every case (PU/APP and PU/APP/nano MgO or nano SiO_2) the residue at 800°C is higher under nitrogen than under air, which follows the same trend as neat PU. These systems always form a residual char as high temperature residue.

The PU/APP degradation [13, 64, 130] starts at a lower temperature than the degradation of PU alone, which proves that the flame retardant modifies the PU degradation. The increase in the PU depolymerization rate is generally attributed [13, 130] to an acid catalysis due to the presence of APP. Under air, a thermally stable material is formed at around 350°C. This material shows a low degradation rate between 350 and 500°C and finally a rapid degradation in the higher temperature range with formation of a stable residue [134] (about 7%, **Table 15**) at 800°C. Under nitrogen, the behavior of PU/APP only differs from 350°C. A low degradation rate is observed in the temperature range 500-800°C leading to a residual mass of 33% (**Table 15**).

TG curves are modified in the high temperature range (T > 550°C) and under air when nanoparticles are added to the system PU/APP. The final residue is higher when 2% of NP is used and also higher with nano MgO compared to nano SiO_2. Under N_2, the PU/APP and PU/APP/NP materials seem to follow the same trend except that the mass loss at 800°C is a little bit lower for the formulation without NP (**Table 15**). However, the difference is in the range of the NP amount added in the formulation. As a consequence, under air NPs used in combination with APP in a PU matrix help the thermal stabilization effect given by the APP.

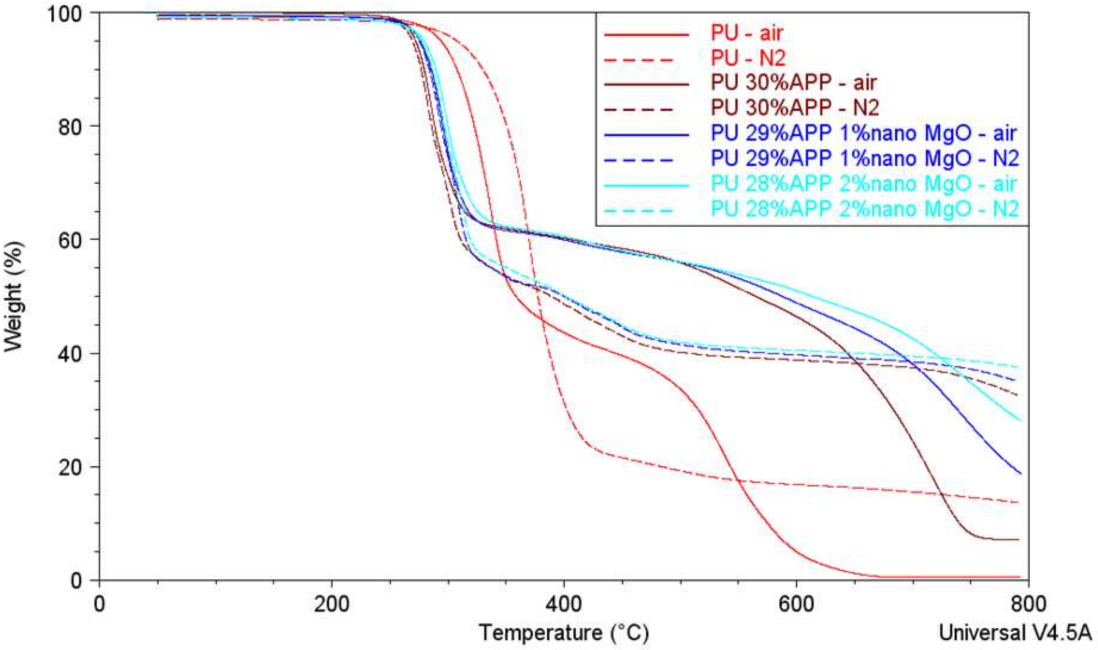

Figure 82: TG curves of PU, PU 30%APP and PU/APP/nano MgO at ratios 29/1 and 28/2 under air and nitrogen at 10°C/min

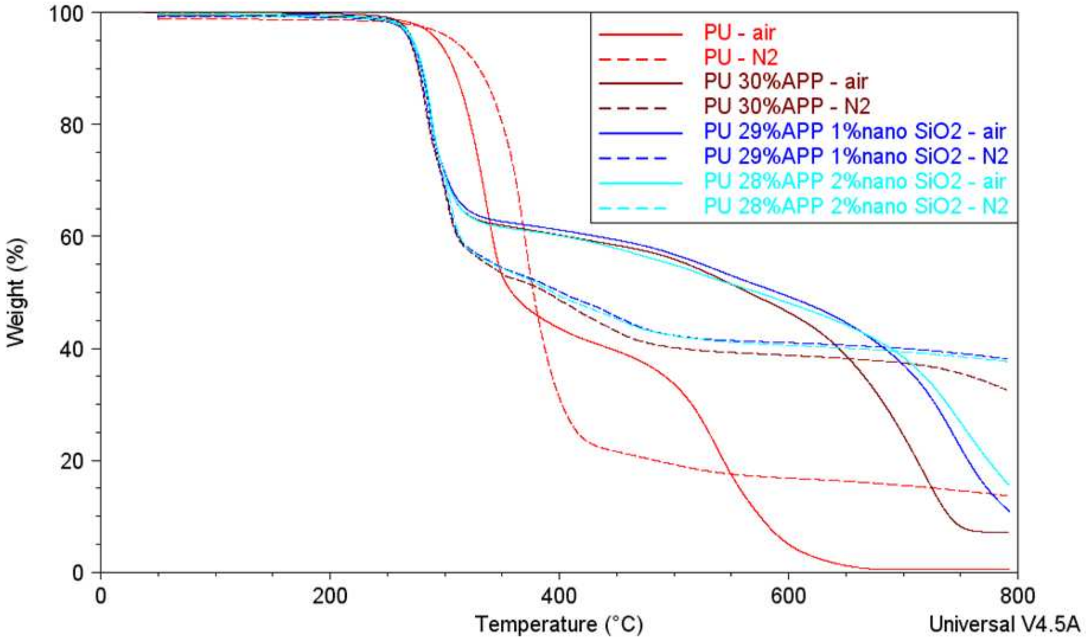

Figure 83: TG curves of PU, PU 30%APP and PU/APP/nano SiO_2 at ratios 29/1 and 28/2 under air and nitrogen at 10°C/min

Finally, **Figure 84** shows the thermograms of PU and PU/NP.

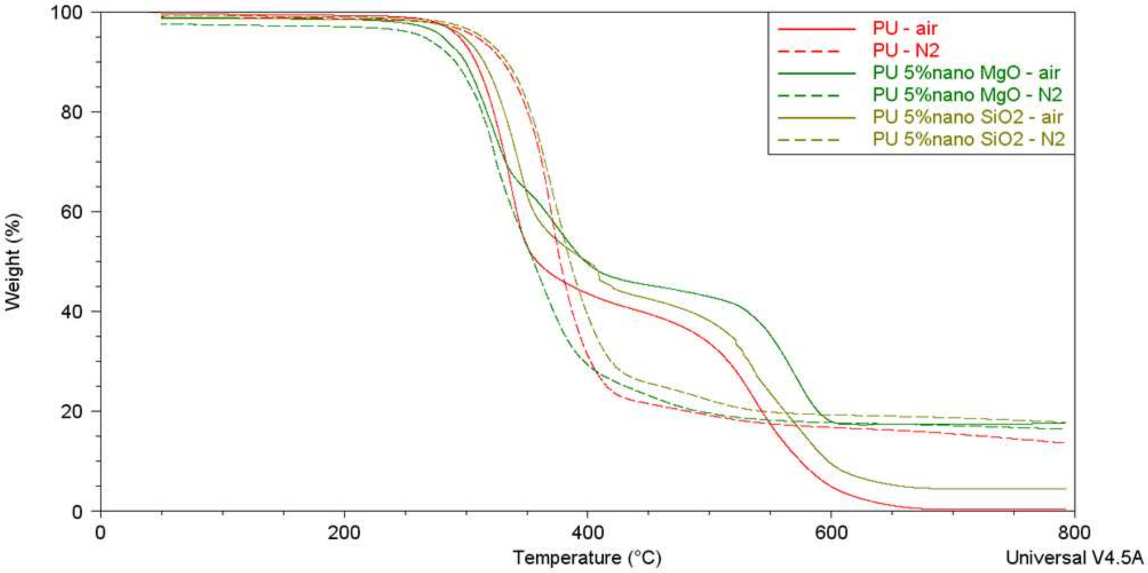

Figure 84: TG curves of PU and PU 5%NP (MgO and SiO_2) under air and nitrogen at 10°C/min

The nano SiO_2 slightly modifies the PU behavior under air or N_2; the residual mass is a little higher with nano SiO_2 but the general trend of degradation is respected.

For the nano MgO under air, the degradation is not total (a residual mass of 18% is observed at the end of the experiment, **Table 15**) at the contrary of virgin PU. This reflects the efficiency of nano MgO as additive in the PU matrix. At the end of the test, it remains some white powder in the pan, as it was the case after a cone calorimeter test (**see residue pictures in Table 13 p110**). It is assumed that the nano MgO is localized on the top of the degraded carbonaceous network. This is still an unexpected result which has never been reported in the literature and which would require further investigations but this was not the purpose of this Ph.D work. Under nitrogen, the degradation starts at a lower temperature but the same behavior and quite the same residual mass are observed compared to virgin PU.

Table 15: Residual mass and temperature at 50 wt.% (T 50%) degradation obtained from TG experiments (residual mass ± 1%, T 50% ± 10°C)

Sample	**Under air at 10°C/min**		**Under N_2 at 10°C/min**	
	Residual mass at 800°C (%)	**T 50% (°C)**	**Residual mass at 800°C (%)**	**T 50% (°C)**
PU	0	360	14	377
PU 30%APP	7	564	33	390
PU 29%APP 1%nano MgO	19	589	35	401
PU 28%APP 2%nano MgO	28	614	38	401
PU 29%APP 1%nano SiO_2	11	589	38	402
PU 28%APP 2%nano SiO_2	16	572	38	395
PU 5%nano SiO_2	2	405	18	386
PU 5%nano MgO	18	399	17	355

The incorporation of fillers modifies the thermal degradation of PU. When NPs (MgO and silica) are added alone, the degradation pathway of PU is not truly modified but the residual mass at 800°C are higher especially for MgO and under air. The incorporation of APP alone lowers at contrary the temperature of the beginning of degradation and modifies the second degradation step to finally lead to a significantly higher residual mass at 800°C. The substitution of a low amount of APP by nano MgO or nano SiO_2 induces the same modifications on the PU degradation curve but the residual mass is once again increased especially under air and with nano MgO.

The study of thermal degradation at 10°C/min of PU, additives and their mixtures, and the PU/APP/NP systems shows that the incorporation of fillers in the PU matrix contributes in the stabilization of the resulting material at high temperatures ($T > 400°C$). This is true whatever the atmosphere even if the effect is most important under air. Nano MgO, nano SiO_2 and nano gold interact with APP leading to its thermal stabilization. On the contrary OMPOSS, which sublimates, does not give higher residues. This effect of NPs on APP follows the trend observed in fire performances. While APP and NP are incorporated in the PU matrix, the stabilization effect is still observed.

4 CONCLUSION: PHENOMENON DURING THERMAL TREATMENT RELATED TO FIRE PERFORMANCES

The characterization of the synthesized materials shows first that no chemical reactions occur during the synthesis step. APP and NPs are incorporated in the PU matrix without chemical interaction between the additives and the matrix. The fillers are homogeneously dispersed in the PU matrix but no nanodispersion of the NPs was achieved. The combination of APP and NPs acts on the molecular mobility of the PU chains as the glass transition temperatures are shifted. A different effect is moreover observed by using nano MgO compared to nano silica.

Fire tests (LOI and cone calorimeter) showed first the efficiency of APP to fireproof PU. Then the substitution of APP by low quantities of NPs always lead to a synergy in fire properties as the fire tests give better results for the PU/APP/NP systems compared to the PU/APP reference. This indicates that a phenomenon should take place between APP and NPs because the PU/NP formulations do not really improve the fire performances of PU. Although the synergy is observed in all cases, a ranking of the best performances could be established as follows:

1) PU 28%APP 2%nano MgO
2) PU 29%APP 1%nano MgO
3) PU 28%APP 2%nano SiO_2
4) PU 28%APP 2%nano gold
5) PU 29%APP 1%nano gold
6) PU 29.5%APP 0.5%nano gold
7) PU 28%APP 2%OMPOSS
8) PU 25%APP 5%nano MgO

The synergy indeed depends on the NP used and on the ratio APP/NP incorporated in PU. These parameters were already found in the literature [74, 83-85, 99] to be determinant to lead to synergy as detailed in **section 2.5.2 p68**.

Virgin PU decomposes under air into two steps leading to no residue after 650°C. Under nitrogen a single step decomposition is observed and a residue of 14% stays at 800°C. The study of the thermal stability of the additives shows that APP degradation starts around 300°C and behaves in the same way under air and nitrogen to reach around 20% of residue. Nano MgO, nano silica and nano gold do not degrade since they are inorganic fillers. OMPOSS sublimates and degrades from 200 to 350°C to form a low amount of silica. A thermal stabilization of APP is obtained with the non-degraded NPs due to chemical interactions between the components. On the contrary, the interaction between APP and OMPOSS is different and leads to the lowest stabilization. It was finally demonstrated that the additives modify the degradation pathway of the virgin polyurethane leading to a thermal stabilization effect at higher temperature whatever the formulations.

It has been proved that the incorporation of APP and/or NP is not prejudicial for the PU synthesis. This section also evidenced that the improvement in fire properties should at least partially be attributed to a chemical effect since a modification of the degradation pathway of PU and its thermal stabilization were observed. This stabilization phenomenon is probably due to chemical reactions occurring between the PU matrix and the additives upon thermal constraints. This is why the next chapter is devoted to the study of the potential chemical aspects leading to the synergy between APP and NPs in PU. The chemical reactions occurring upon heating in the gas phase and condensed phase and their evolutions will thus be elucidated as well as the effect of the thermal treatment applied to the samples.

Chapter IV - Chemical aspects leading to the synergy between ammonium polyphosphate and nanoparticles in polyurethanes

As commented in the state of the art (**Chapter I, section 2.1 p48**), the flame retardants can act in gas phase, condensed phase or both [10]. In the case of the incorporation of two different fillers, a synergistic effect might be observed. Synergistic phenomena can be obtained by a combination of flame retardancy mechanisms in the condensed and gas phases [8]. APP is known to mainly act in the condensed phase as it is an efficient intumescent additive [63, 67]. The last chapter (**Chapter III, section** 2-**Evaluation of the Fire Performances p105**) showed that a small amount of inorganic filler substituted to APP in the PU formulations participates to improve the fire performances but its mechanism of action is not elucidated yet.

This section will evaluate the chemical aspects possibly leading to the synergy between APP and NPs in PU castings. The first step of elucidating the synergy mechanism is to ascertain that there is no gas phase action by performing a chemical characterization of the degradation products of PU formulations using a TGA-FTIR. Then a chemical characterization of the condensed phase will be done using solid state NMR and electron probe microanalysis (EPMA) on heat treated materials. In order to further investigate the chemical reactions involved during the condensed phase degradation, the evolution of species created during a cone calorimeter test will then be followed. To that aim the conversion degree of PU formulations will first be presented. Then the shutter experiment will be realized and the resulting NMR spectra will be analyzed. Finally the influence of heating rates on the degradation behavior of PU formulations will be detailed. Studying the kinetic of the systems is important since the right chemical reactions must occur at the right time to lead to an efficient protection. Different temperatures and heating rates are involved depending on the fire scenario considered and it is worthy to know the behavior of PU formulations in different conditions. TGA at different heating rates will be carried out and this should highlight the fact that materials could behave differently depending on thermal stresses brought by the fire test. Solid state NMR will be carried out on residues collected after different heating ramps in a furnace to examine whether chemical reactions could be affected.

This whole program leads to assess the role of chemistry in the synergy observed in fire properties between APP and NPs in PU.

1 CHEMICAL CHARACTERIZATION OF THE GAS PHASE

The incorporation of fillers modifies the thermal degradation processes of virgin PU suggesting that chemical interactions occur between the components upon heating. These modifications could take place in gas and/or condensed phase. The chemical characterization of gas phase is firstly performed thanks to TGA-FTIR and occurs in two steps. In a first part the range of temperature where gases are detected during the thermal degradation of PU formulations is determined. The second part is dedicated to the analysis of infrared spectra collected at characteristic temperatures at which gases are detected.

1.1 Evolution of gases detected during thermal degradation of PU formulations

To follow the evolution of gases evolved during the thermal degradation of PU formulations, the reference systems (PU and PU 30%APP) and the nano MgO based formulations were selected. Nano MgO was the NP leading to the highest stabilization level according to TG curves; this is why it was selected to characterize the gas phase.

The thermal degradation of PU, PU 30%APP, PU 29%APP 1%nano MgO, PU 28%APP 2%nano MgO and PU 25%APP 5%nano MgO has been examined by TGA and the gases evolved when the materials degrade are analyzed in infrared spectroscopy. A cartography of the infrared spectra is obtained with the evolution of the absorbance as a function of wavenumbers and time. The infrared spectra and mass loss can then be analyzed in parallel (**Figure 85**).

The repeatability of the experiment was good but peaks of carbon dioxide and water are always detected. These peaks are located around 650 cm^{-1}, 2350 cm^{-1} and large bands around 1600 and 3700 cm^{-1} respectively for the carbon dioxide and the water [135]. Even though the system is supposed to be closed, these components are coming from the environment since they can already be seen during the background acquisition. The presence of these characteristic peaks will consequently not be taking in account to conclude on the degradation mechanisms, the rest of the spectra can still be analyzed as usual.

The black squares on **Figure 85** represent the range of temperature or time where the main gases coming only from the degradation of the materials are detected (carbon dioxide and water are not taking into account). Peaks are observed on the infrared spectra between 350 and 575°C for virgin PU whereas the range of temperature is from 270 to around 350°C for PU 30%APP, PU/APP/NP containing 1 and 2% of nano MgO. Concerning PU 25%APP 5%nano MgO, gases are detected from 240 to 390°C. This clearly shows that degradation gases are detected at lower temperature for filled PU than for virgin PU, which is in good agreement with the TGA showing that the beginning of mass loss occurs at lower temperature for PU/APP formulations. The increase in the PU depolymerization rate is generally attributed [13, 130] to an acid catalysis due to the presence of APP. The NP do not have any additional effect on this step so the first evolving gases are detected at the same temperature for PU/APP and PU/APP/NP.

Another important difference is that for PU the gases are detected after 50% of mass loss whereas it occurs directly at the beginning of mass loss for the filled PU. The same flow rate was however used in the transfer line for all experiments. The difference might thus be due to different gases collected in both cases. The chemical composition of the gases collected will be indeed detailed in the next section.

PU

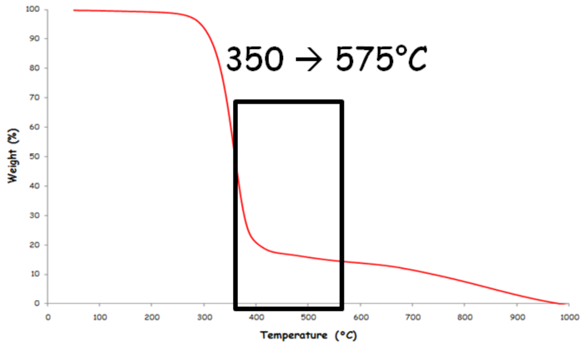

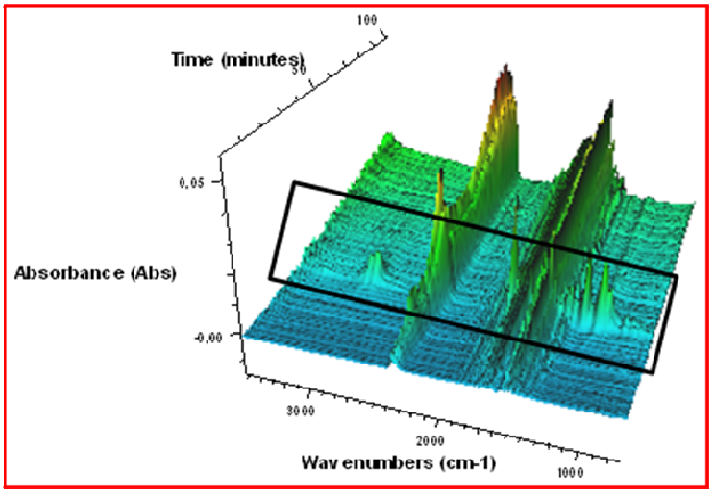

PU 30%APP

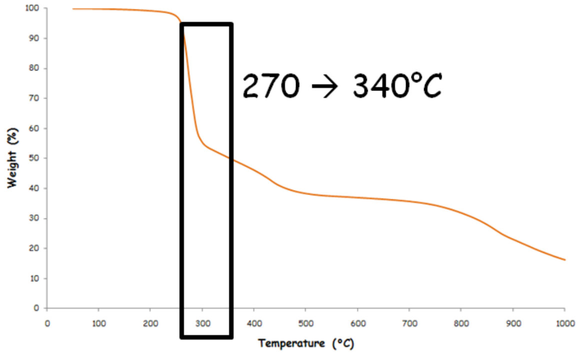

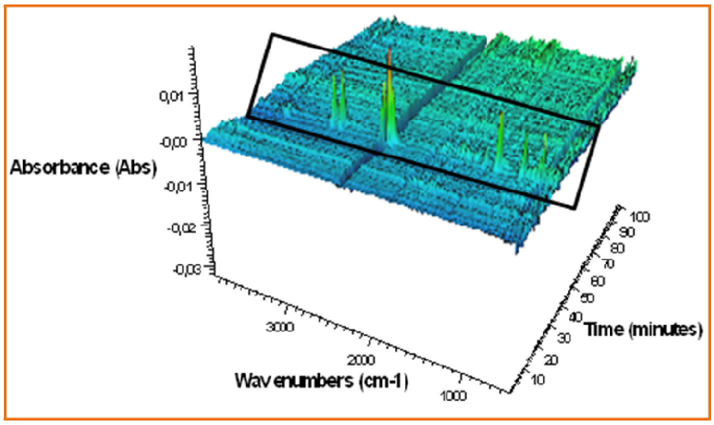

PU 29%APP 1%nano MgO

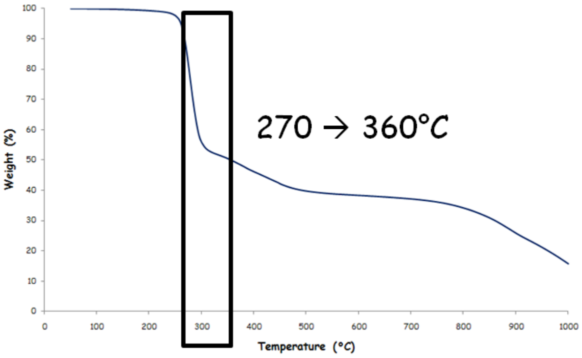

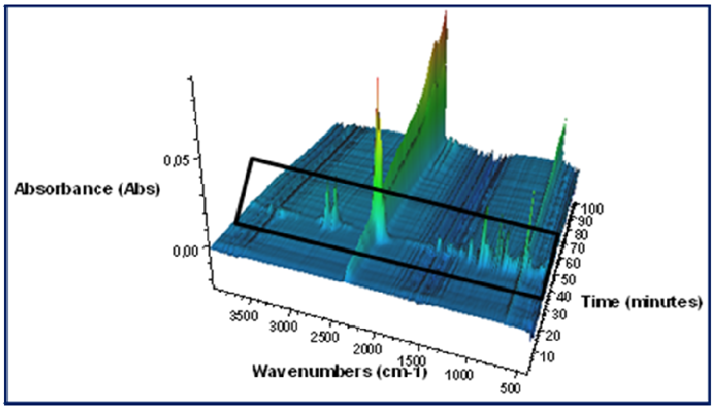

PU 28%APP 2%nano MgO

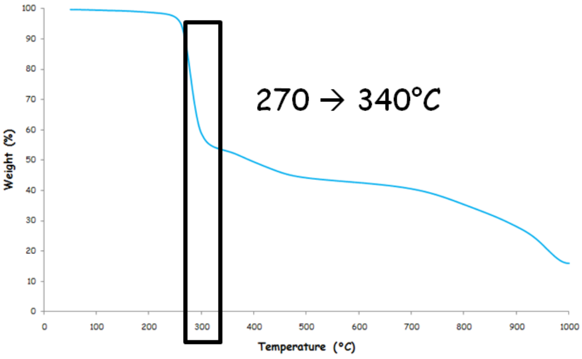

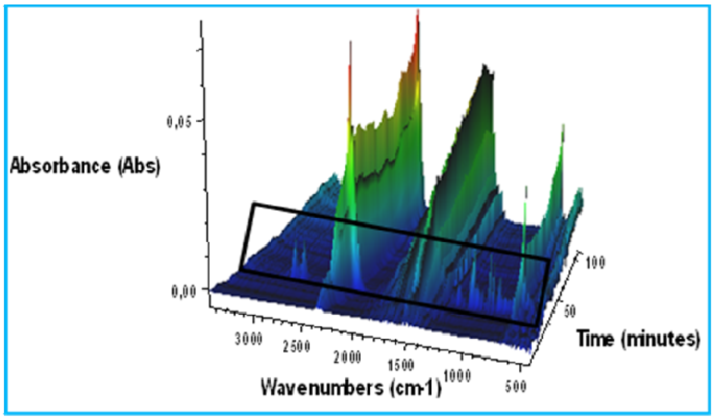

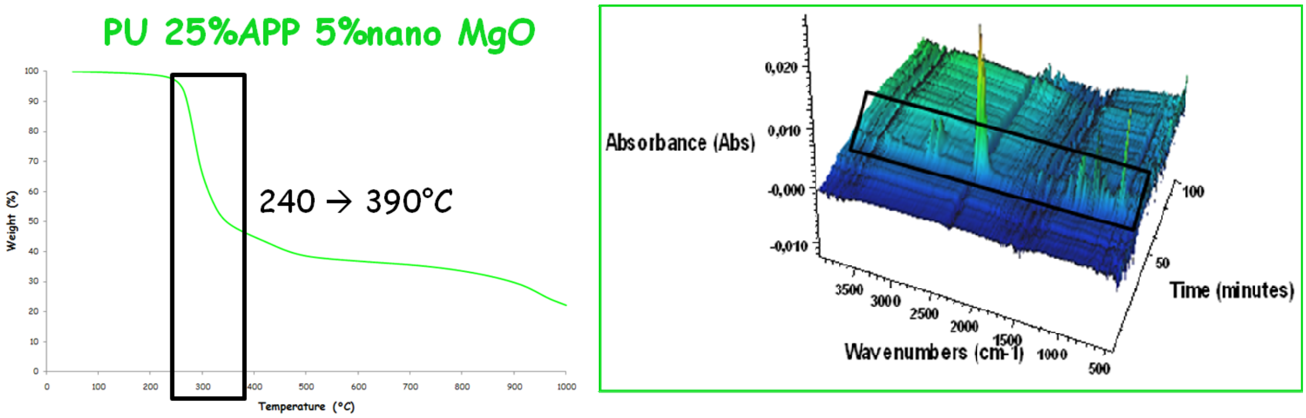

Figure 85: Curve of weight loss versus temperature and simultaneous 3D cartography of infrared spectra showing the evolution of absorbance as a function of wavenumber and time for PU, PU/APP, PU/APP/nano MgO (ratios 29/1, 28/2, 25/5) formulations

1.2 Interpretation of infrared spectra collected at characteristic temperatures

Spectra collected at a characteristic temperature are presented in **Figure 86** for all PU formulations. The temperature chosen is that at which the intensity of infrared detection is maximal and at which the spectra shows all the peaks recorded during the thermal degradation of the materials. This temperature is consequently higher for virgin PU (395°C) than for filled PU (313°C). Before and after this temperature, the same gases are evolved during the entire zone determined in the previous section but their intensity progressively increases and decreases.

Exactly the same peaks are observed for PU 30%APP and PU/APP/NP whatever the quantity of NP substituting the APP; consequently in order to ease the reading, only the PU/APP spectrum will be commented.

It is first clearly evidenced that the spectra of virgin PU and the one of filled PU are different; in particular additional peaks are detected for the second case. Some peaks are however noticeable in both cases and they could consequently be attributed to PU degradation. The additional peaks are in the same manner attributed to the effect of the filler (APP). All peaks (except carbon dioxide and water coming from the environment) are listed and assigned in **Table 16** and further discussed.

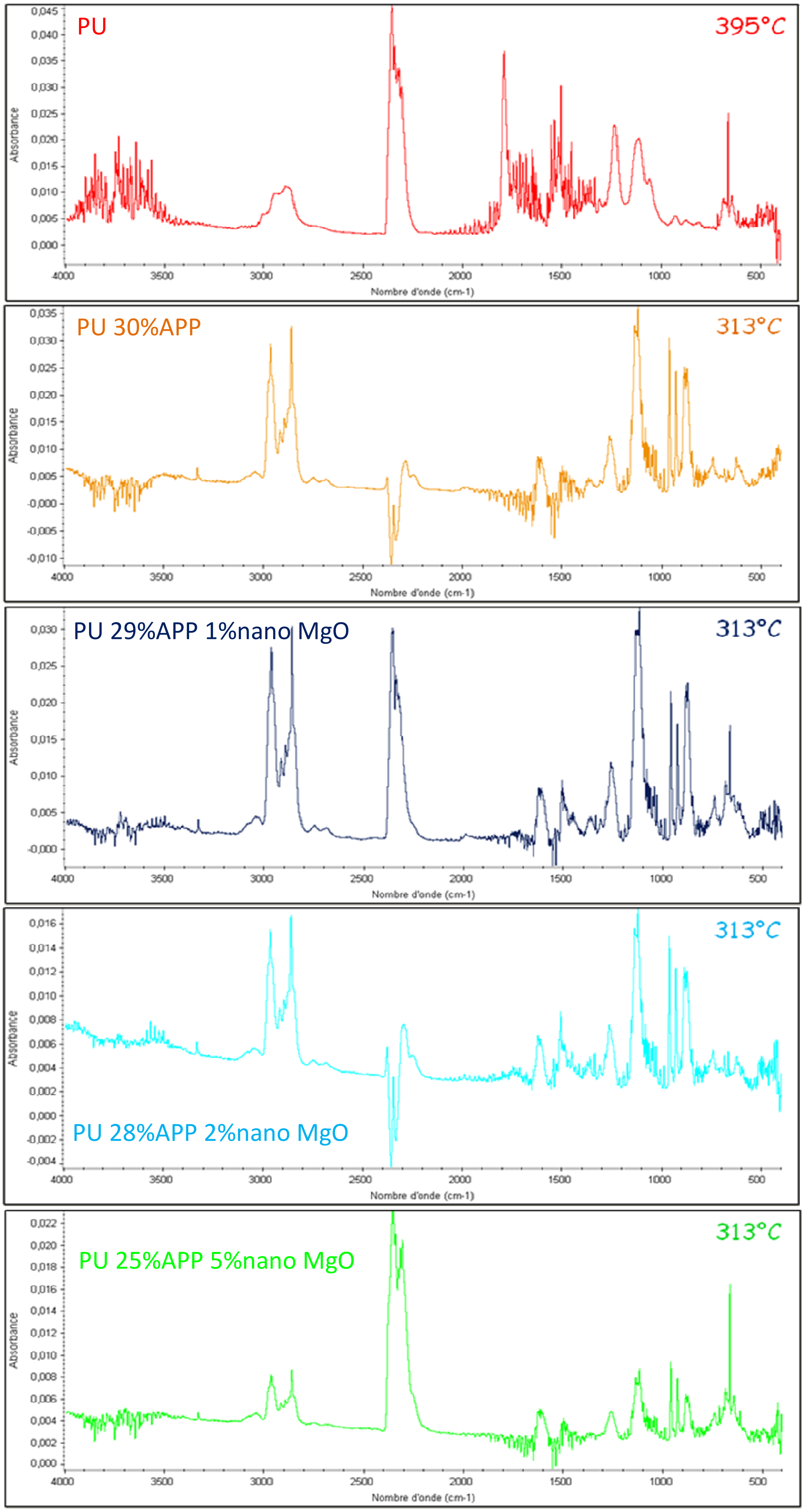

Figure 86: Infrared spectra at selected temperatures for PU formulations

Table 16: Attribution of wavenumbers from infrared spectra of gases released during degradation of virgin PU and filled PU: PU 30%APP, PU 29%APP 1%nano MgO, PU 28%APP 2%nano MgO and PU 25%APP 5%nano MgO (summarized by PU/APP(/NP))

Wavenumbers (cm^{-1})	Intensity	Peak assignment	Present in sample
3335	Medium	Stretching NH, NH_2	**PU/APP(/NP)**
Shouldering around 3000	Weak	Stretching aromatic CH	**PU** **PU/APP(/NP)**
Double peak at 2967 and 2865	Strong	Stretching aliphatic CH, CH_2	**PU** **PU/APP(/NP)**
Double peak at 2750 and 2690	Weak	P-OH, O=P-OH	**PU/APP(/NP)**
Range from 2400 to 2200	Strong	CO_2 + N=C=O	**PU** **PU/APP(/NP)**
1790	Strong	C=O	**PU**
1624 - 1510	Medium	Deformation NH, NH_2	**PU/APP(/NP)**
1260	Weak	Aliphatic C-O-C	**PU** **PU/APP(/NP)**
Double peak around 1100	Strong	Aromatic C-O-C	**PU** **PU/APP(/NP)**
970	Medium	Stretching P-O-C or NH, NH_2	**PU/APP(/NP)**
930	Medium	Stretching P-O or NH, NH_2	**PU/APP(/NP)**
Double peak at 870	Medium	Deformation P-C	**PU/APP(/NP)**

The two different mechanisms of thermal degradation observed for PU with or without APP under nitrogen are presented in **Figure 87**. In both case depolymerization of PU is observed leading to fragment detected in gas phase such as molecules containing aliphatic, aromatic CH and CH_2, C-O-C bonds from polyol and N=C=O from isocyanate [13, 130]. The transmission IR of pure polyol JWL440 has been realized and the spectrum is presented in **Figure 88**. It shows a large band around 3500 cm^{-1} attributed to the OH terminal groups, from 2900 to 2700 cm^{-1} aliphatic CH and CH_2 are found and finally the C-O-C and C-OH bonds are vibrating at 1100 cm^{-1}. Even if the techniques are different (liquid or gas sample), the peaks attributed to polyol are consistent. Through the mechanisms suggested by the literature, carbon dioxide should be released during degradation. Because of the background problems, it is impossible to confirm it but its formation seems obvious. The additional peaks recorded for the PU/APP systems are related to nitrogen and phosphorus bonds. The presence of N-H stretching and deformation is indeed characteristic to the use of APP which releases NH_3 during the first step of its degradation [129, 131]. It should also release water but this is not detectable due to the environment already containing water. Polyphosphoric acid and at higher temperature P_4O_{10} are also released during APP degradation which could explain partially the apparition of peaks around 2700 and 900 cm^{-1} characteristic of P-OH and P-O bonds. APP is moreover reacting on the PU bonds thus creating also phosphorus fragment potentially detected by the TGA-FTIR apparatus.

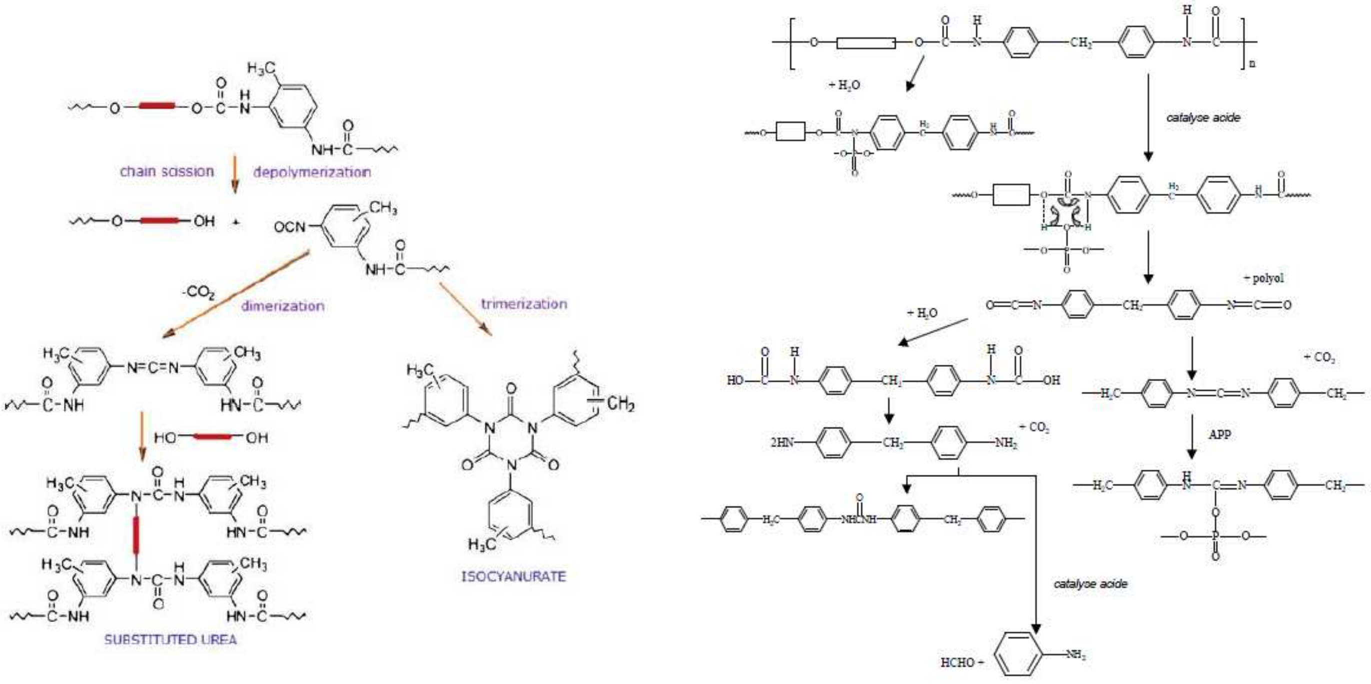

a **b**

Figure 87: Comparative mechanism of thermal degradation under nitrogen for a) virgin PU [14, 45] and b) PU/APP [13]

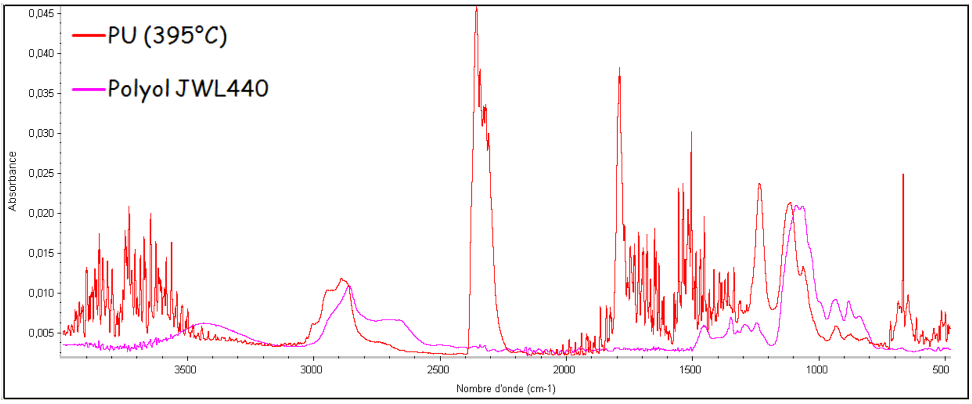

Figure 88: Transmission IR spectrum of polyol JWL440 superimposed to the one of the gases released during PU degradation

The flame retardant APP used alone or with nano MgO as synergist in PU matrix modifies the thermal degradation of PU. The range of temperature where gases are detected is narrower and begins at lower temperature. Additional gases are detected with the presence of APP such as ammonia (nitrogen bonds) and phosphorus based fragment. On the contrary no significant differences are observed between PU/APP and PU/APP/NP (whatever the ratio) gas phases, thus proving that nano MgO is not acting in the gas phase.

The synergy mechanism between APP and nano MgO is consequently not based on a gas phase mechanism. This result could be transposed to nano SiO_2 and nano gold which behave similarly according to TG experiments. The case of OMPOSS could be different because it sublimates but this sublimation prevents performing the TGA-FTIR analysis. The next part will characterize the chemistry in the condensed phase to see if, contrarily to gas phase, NPs support the formation of new species.

2 CHEMICAL CHARACTERIZATION OF THE CONDENSED PHASE

The chemical characterization of the condensed phase will allow determining the reactions involved during materials degradation. The effect of fillers in these complex processes will be investigated by solid state NMR and electron probe microanalysis (EPMA). PU, PU/APP and PU/APP/NP burnt residues will first be studied in ^{13}C, ^{31}P and ^{29}Si solid state NMR depending on the constituents of the formulation. Various NMR experiments will be designed and correlated to elucidate precisely the chemical composition of the residues. In a second part, a chemical analysis will be performed in EPMA and it will bring additional information on the composition of the condensed phase.

All the NMR and EPMA analyses have been performed on the residues collected after cone calorimetry, each sample has been exposed for 8 minutes 30 seconds (exactly) at an external heat flux of 50 kW/m^2. These conditions were fixed according to the shape of the first HRR curves performed showing that a steady state is obtained for all samples after such time of test. It was deliberately chosen to work with these samples because it is relevant to characterize, in a first approach at least, residues obtained in conditions where it was proven that the synergy occurs. The cone calorimeter provides moreover a real fire scenario.

2.1 Solid state NMR on burned residues from PU formulations

Solid state NMR is a powerful tool to characterize materials in the solid state (the integrity of the samples is not modified) and so, to determine if chemical reactions occur between the PU matrix and the component upon heating. In the last chapter (**Chapter III, section 1.1-Chemical characterization of PU formulations p97**) it has already been proven that the selected route of synthesis of PU formulations do not induce chemical reactions between the fillers and PU. The purpose of this section is to determine the chemical species present in PU formulations after a cone calorimeter test.

All PU formulations (PU, PU 30%APP, PU 5%nano MgO, PU 29%APP 1%nano MgO, PU 28%APP 2%nano MgO, PU 25%APP 5%nano MgO, PU 5%nano SiO_2, PU 28%APP 2%nano SiO_2, PU 28%APP 2%OMPOSS, PU 29.5%APP 0.5%nano gold, PU 29%APP 1%nano gold and PU 28%APP 2%nano gold) have been burnt in a standard MLC experiment and then characterized by solid state NMR. Depending on the components of each formulation, the nucleus for NMR has been judiciously chosen. PU and PU 5%nano MgO have only been characterized using ^{13}C solid state NMR. For virgin PU, there is no other interesting nucleus. For PU 5%nano MgO, ^{25}Mg NMR would have been very interesting but such acquisitions would be time consuming because of the low abundance and sensitivity of ^{25}Mg (in addition to this, the quantity of ^{25}Mg in the samples is quite low). PU/APP and PU/APP/NP have been characterized by ^{31}P NMR because all these formulations contain APP, a phosphorus based component. This will give a reference nucleus to compare the effect of each NP. Additionally to ^{31}P NMR, ^{13}C solid state NMR has also been carried out on residues from PU/APP and PU/APP/nano MgO (ratios 28/2 and 29/1). Finally ^{29}Si solid state NMR was used for PU 5%nano SiO_2, PU 28%APP 2%nano SiO_2 and PU 28%APP 2%OMPOSS.

A compilation and interpretation of all these NMR results will be provided in this section.

Figure 89 shows the ^{13}C solid state NMR spectrum of the char collected after cone calorimeter test of the formulation PU 29%APP 1%nano MgO. The same spectrum was observed with a char collected from PU, PU 5%nano MgO and PU 28%APP 2%nano MgO after cone calorimeter in the same conditions (results are not presented here). It exhibits a single peak at 127 ppm characteristic of unsaturated carbon, probably aromatic carbons. During the intumescence process, it is generally admitted that the unsaturated materials degrade and condense into aromatic structures [59, 136]. This ^{13}C solid state NMR confirms that the materials degrade to form a carbonaceous residue during a cone calorimeter test.

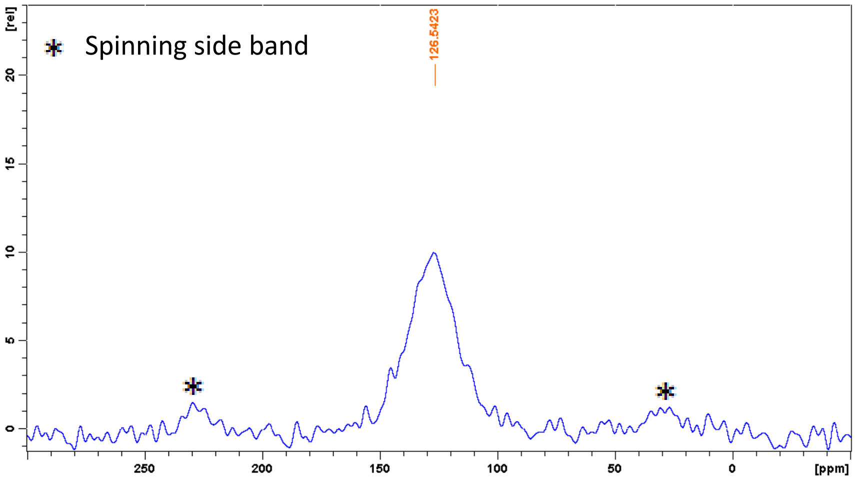

Figure 89: ^{13}C solid state NMR spectrum of the char obtained from PU 29%APP 1%nano MgO

Since it has just been chemically proven by ^{13}C solid state NMR that the carbon from the PU formulations degrades with the subsequent formation of aromatic structures, it is now necessary to investigate the role of APP and NPs in this degradation. To that aim, solid state ^{31}P NMR have been performed first on formulations containing only APP and secondly on formulations including APP and NPs.

Figure 90 compares the ^{31}P NMR spectrum of PU 30%APP before and after mass loss calorimeter experiment. A chemical modification of APP is observed as there is no more characteristic peak of polyphosphate chains (at -21.6 and -22.5 ppm) on the NMR spectrum of the char. After cone test, the spectrum of the material shows a peak at 0 ppm. This band is characteristic of PO_4 units in R_2HPO_4, RH_2PO_4 (with R = alkyl) and/or H_3PO_4 [137]. This result is in agreement with the well-known decomposition pathway of APP to phosphoric acid [13, 59, 116], suggesting that the peak at 0 ppm is H_3PO_4. Another small peak around 33 ppm is detected (only at high zoom in **Figure 90**) and attributed to phosphonic acids [138]. A series of phosphonic and phosphinic acids have been characterized by solid state ^{31}P CP/MAS NMR [138] and it appears that, depending on the chain linked to phosphorus, phosphonic acids have a chemical shift ranging between 25 and 35 ppm; the phosphinic acids are shifted to higher chemical shifts in the range 45-60 ppm. The phosphonic acids are rather unexpected since the initial flame retardant is a phosphate. Their presence suggests therefore that a reductive phenomenon occurs during the burning, while the experiment takes place under air. Karrasch et al. [139] have encountered a similar phenomenon while thermally treating a polycarbonate containing bisphenol A bis(diphenyl-phosphate). They attributed the formation of phosphonate esters to the graphitic structure of the char which could act as a possible reduction agent associated to oxygen depletion.

Thus, it suggests that phosphoric and phosphonic acids released when APP degrades enhance the fire retardancy of the materials by catalyzing the charring process. The increased fire properties exhibited by the PU 30%APP compared to virgin PU might nevertheless only be due to a physical effect since the formation of a char is observed during the cone calorimeter experiment.

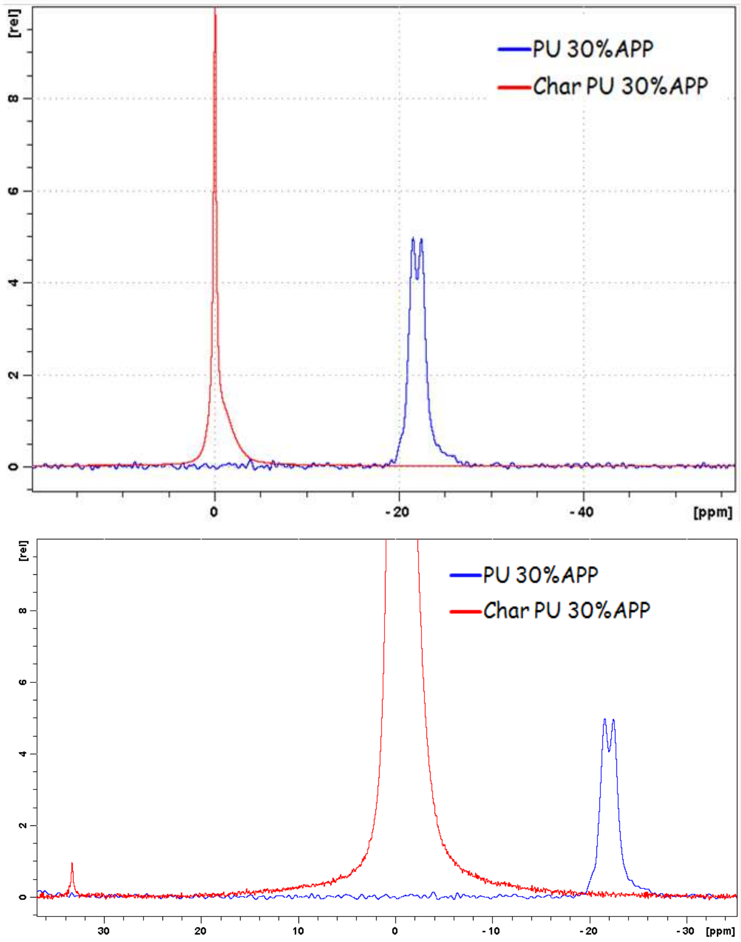

Figure 90: ^{31}P solid state NMR spectrum of PU 30%APP before and after cone calorimeter experiment (char) (top: full scale, bottom: zoom)

The PU/APP/NP ^{31}P solid state NMR was performed and the spectrum was superimposed to that of PU/APP. The goal is first to determine if there is a reaction between APP and the various NP and then to investigate the potential effect of NP on APP degradation.

Figure 91 shows the stacked ^{31}P solid state NMR spectra of the residue collected after cone calorimeter for PU/APP and PU/APP/NP formulations with all selected NP. Compared to PU 30%APP which exhibits a main peak at 0 ppm corresponding to phosphoric acid [76] and another small peak around 33 ppm attributed to phosphonic acids [138], all PU/APP/NP show additional peaks. This proves that whatever the NP used in substitution to APP and whatever the ratio, this modification has an impact on the chemical reactions occurring during degradation.

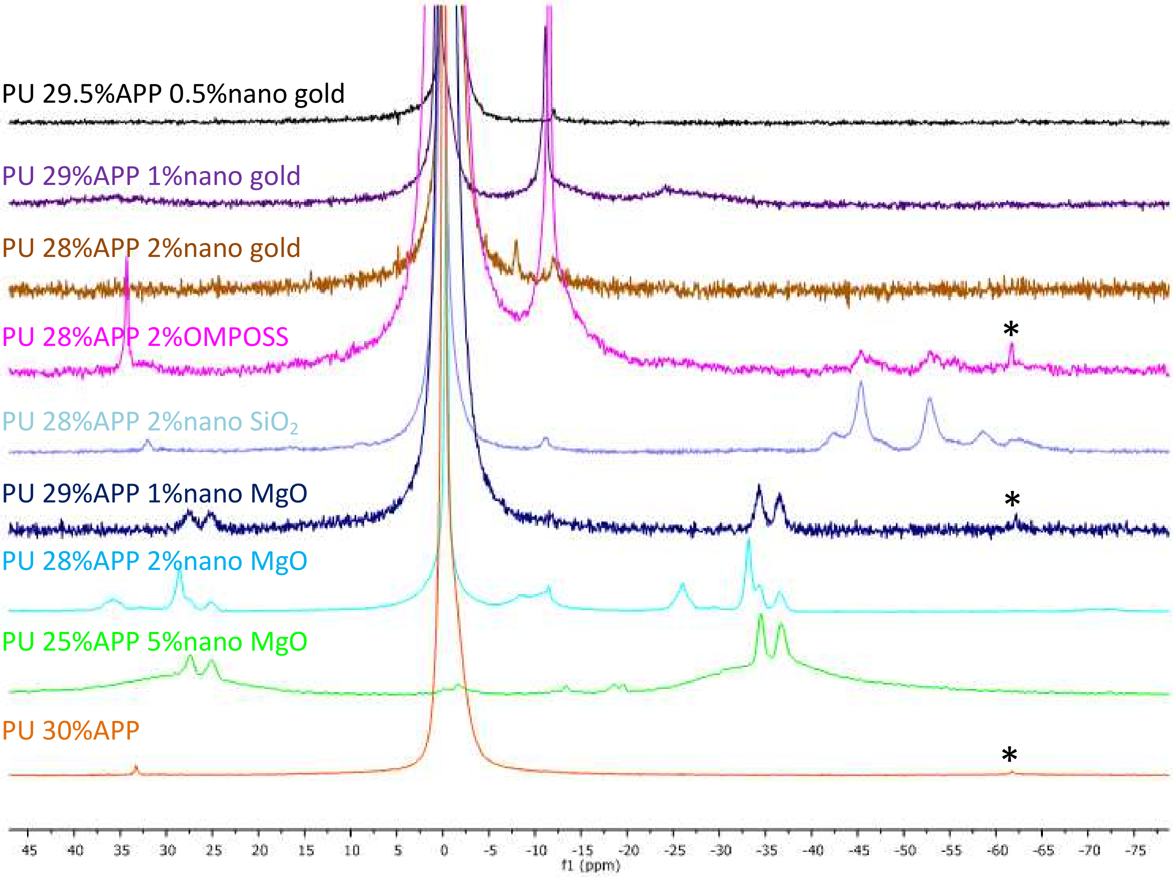

Figure 91: ^{31}P solid state NMR spectra of PU/APP and PU/APP/NP at different ratios on samples collected at the end of a cone calorimeter test (*: spinning side bands)

A peak at -11.5 ppm is for example detected in all PU/APP/NP burnt samples. In the same chemical shift area, a peak at -8 ppm is detected in the formulations containing 2%nano gold and 2%nano MgO whereas it is not detected in PU/APP. According to the previous work, these two peaks could be respectively attributed to P-O-C bonds from orthophosphates linked to an aromatic structure [76, 137] and to pyrophosphates (P-O-P bonds) [140, 141]. This differentiation is however not clear since the chemical shifts are close and depend on the phosphorus environment. It is anyway important to clearly distinguish these two peaks in order to understand the mechanisms of action of the NPs. Further NMR experiments are thus performed to ascertain the distinction between these two species.

A reference product containing similar bonds has been used to determine its chemical shift. It is more judicious to use the P-O-C bonds compared to the P-O-P bonds because it involves two different nucleuses and will consequently give only one ^{31}P NMR peak. The triphenylphosphate (structure displayed in **Figure 92**) was selected because the phosphorus is involved in P-O-C bonds with an aromatic carbon. The phosphorus is moreover linked three times to the same O-ø group.

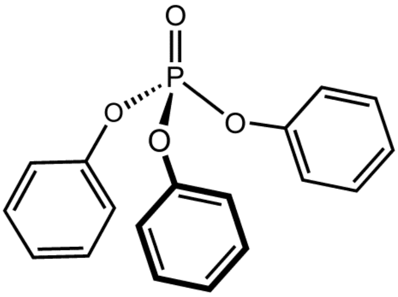

Figure 92: Chemical structure of triphenylphosphate

The ^{31}P solid state NMR spectrum of this compound is given in **Figure 93**. Only one peak (and its spinning side bands) is recorded at -13.4 ppm.

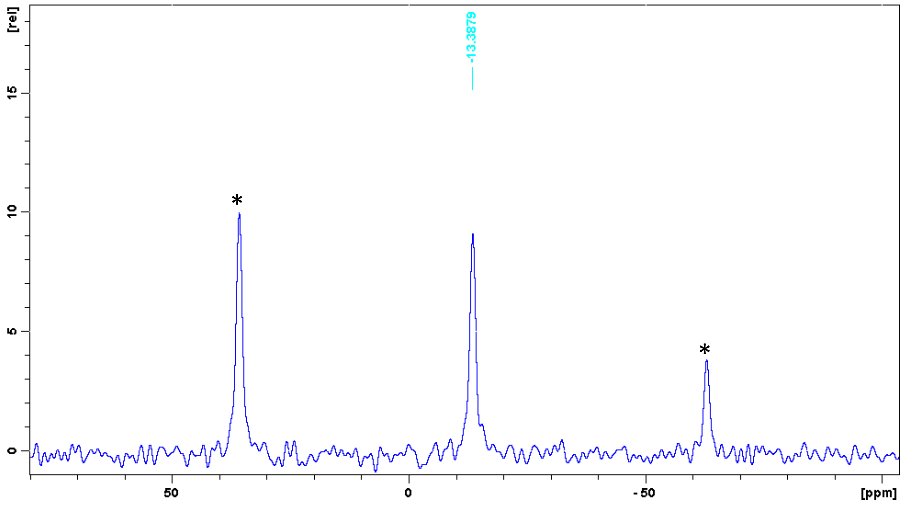

Figure 93: ^{31}P solid state NMR spectrum of triphenylphosphate (*: spinning side bands)

This chemical shift does not match with the one observed in our PU/APP/NP formulations (-11.5 ppm). The difference could be due to the higher number of aromatic rings linked to the considered phosphorus. The formation of aliphatic phosphates was for instance noticed while burning nylon 6 containing 10% of red phosphorus [142]. On the ^{31}P solid state NMR spectrum, the resonance peak was observed at -10 ppm [143]. The chemical shift of phosphorus in P-O-C bonds, recorded from -10 to -14 ppm, is decreased going from aliphatic carbon to aromatic carbon and while increasing the number of aromatic rings. In another study [139], the formation of various phenyl (bisphenol-A) phosphate esters was observed during heating; these species present a phosphorus linked two times to a O-ø group and are recorded at -12 ppm. Depending on the phosphorus environment, the NMR peak is shifted. Given that the chemical shift recorded in PU/APP/NP formulations is of -11.5 ppm, this means that the considered phosphorus is probably linked to oxygen linked to an aromatic ring. This indicates furthermore the incorporation of the phosphate into the charred network. This P-O-C bond is distinguishable from that at -8 ppm consequently attributed to pyrophosphate.

This means that in all PU/APP/NP burnt samples, species corresponding to the product of reaction between APP and PU (-11.5 ppm) without involving NPs are detected. They seem to remain undegraded at the end of the fire test at the contrary of the systems including NPs. For PU 30%APP, no peak is observed at around -11.5 ppm. It appears then that the incorporation of a small amount of any NP interferes with the reaction PU + APP. It is possible that this process occurs because the NPs modify the degradation pathway of APP thus changing its reactivity with the matrix.

The detection of pyrophosphates in PU 28%APP 2%nano gold and PU 28%APP 2%nano MgO proves that the evolution of APP in the PU matrix during thermal treatment might be affected by the presence of certain NP at particular ratios.

The PU/APP/nano MgO systems were studied in a previous work carried out in the laboratory [11] as discussed in the Chapter I. XRD analyses have been performed to investigate the reactivity between APP and nano MgO in a PU 25%APP 5%nano MgO sample degraded by cone calorimeter (spectra not shown here). Both amorphous and crystalline phases were detected and the presence of magnesium pyrophosphate ($Mg(PO_3)_2$) and magnesium phosphate ($NH_4Mg(PO_3)_3$) was particularly demonstrated. Further experiments performed by solid state ^{31}P NMR confirm this reactivity as peaks between -25 to -37 ppm attributed to magnesium phosphates are evidenced on **Figure 91** for all PU/APP/nano MgO formulations. It is noteworthy that depending on the ratio APP/NP used, the obtained magnesium phosphates created are different. A work has been carried out to try to find the exact attribution of the bands between -25 to -37 ppm.

As the formation of magnesium phosphates was suspected, some magnesium phosphates have been purchased or synthesized ($Mg_3(PO_4)_2$, H_20 and NH_4MgPO_4, H_20 from *Sigma Aldrich* and $Mg_2P_2O_7$ (α, β) was synthesized by the laboratory UCCS-UMR 8181). The strategy was to select some magnesium phosphates that may be present in our sample and to analyse them to see if their formation is evidenced in the PU/APP/nano MgO char. The ^{31}P NMR spectra were thus recorded and they are superimposed to that of the char obtained from PU 28%APP 2%nano MgO in **Figure 94**. This formulation has been chosen because it exhibits more peaks compared to the other ratios. The first comment is that the peaks of $Mg_3(PO_4)_2$, H_20 and NH_4MgPO_4, H_20 are not matching with any peaks from the char obtained from PU 28%APP 2%nano MgO. This comes from the fact that these commercial products are hydrated and thus, the chemical environment surrounding the phosphorus is affected. These different structures have their own chemical shifts which are consequently not matching with the chemical shifts of the non hydrated compounds given in the literature [144-146].

$Mg_3(PO_4)_2$ could therefore be present because its chemical shift has been recorded at -0.1 ppm [146] which could overlap with the phosphoric acid peak at 0 ppm. On the contrary considering the synthesized $Mg_2P_2O_7$ (α, β) five peaks are recorded. The peaks at -13.3 and -19.6 ppm corresponds to α-$Mg_2P_2O_7$ and the peak at -19.2 ppm is characteristic of β-$Mg_2P_2O_7$ [141, 144, 146, 147]. These peaks are not found in the spectrum of the char whereas the two last peaks are matching. These two peaks (-34 and -36 ppm) corresponds to $Mg(PO_3)_2$ [146] which is used to synthesize the $Mg_2P_2O_7$ (α, β).

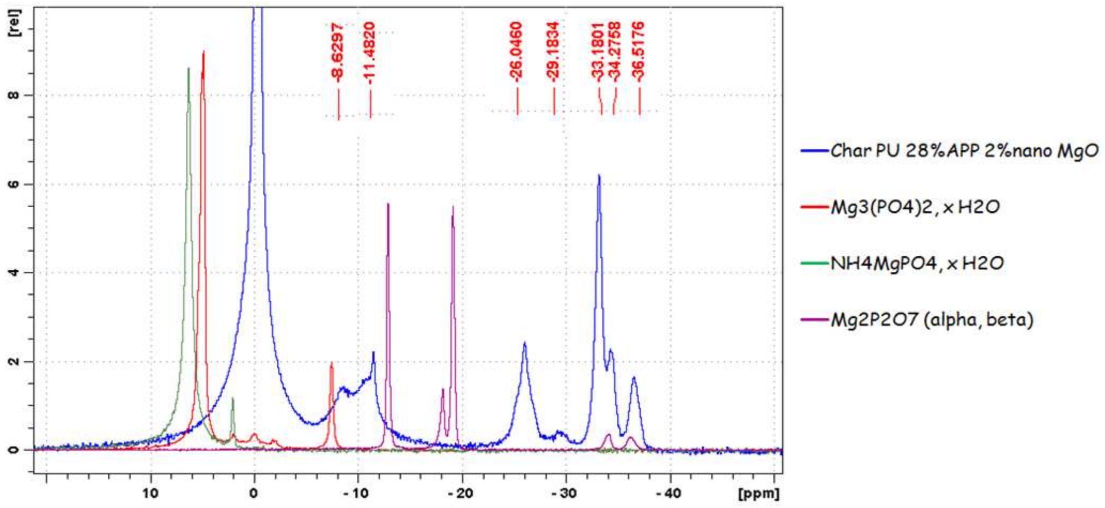

Figure 94: ^{31}P solid state NMR spectra of the char from PU 28%APP 2%nano MgO and of various magnesium phosphates

The XRD performed on the char from PU 28%APP 2%nano MgO did not bring additional information than that obtained by NMR and by XRD for the ratio 25/5. Although not all of the magnesium phosphates peaks are clearly attributed, the reaction between APP and nano MgO during mass loss calorimeter test on PU 28%APP 2%nano MgO is nevertheless evidenced.

On the other hand, the stoichiometric ratio magnesium over phosphorus is equal to 0.08 in PU 28%APP 2%nano MgO formulation. In all the magnesium phosphates that could be formed by a reaction between APP and MgO, the stoichiometric ratio magnesium over phosphorus varies between 0.33 (for $NH_4Mg(PO_3)_3$) and 1.5 (for $Mg_3(PO_4)_2$). This means that the phosphorus is always in large excess compared to the magnesium and thus from a stoichiometry point of view, all the MgO could react with the APP.

On the spectrum of PU 28%APP 2%nano silica, the collection of bands from -42 to -63 ppm could be attributed to silicophosphates species [148] similarly to what occurred in the case of nano MgO but also to P_4O_{10} in equilibrium with phosphoric acid [128]. The phosphoric acid (0 ppm), phosphonic acid (around 33 ppm) and the P-O-C bonds (-11 ppm) are also detected in this sample.

In parallel to ^{31}P solid state NMR, ^{29}Si solid state NMR has been carried out on nano SiO_2 based formulations. The aim was to prove once again the reaction between APP and nano SiO_2 with another technique than ^{31}P NMR in order to ascertain that the peaks between -40 and -60 ppm are due to the presence of silicophosphates. That is why the selected formulations were PU 5%nano SiO_2

and PU 28%APP 2%nano SiO_2, the first one contains only silica as filler while the second one contains both APP and nano SiO_2. The spectra were collected on residues obtained after a cone calorimeter experiment. The signal appears after 64 hours of acquisition and the spectra are presented and compared in **Figure 95**.

For the char PU 5%nano SiO_2 only one peak at -110 ppm is observed and corresponds to unmodified silica [149]. The structure of SiO_2 consists in a central Si surrounded by four bonds O-Si corresponding to a Q_4 structure [150]. The symbol Q_n identifies indeed the connectivity of a silicate tetrahedron with n the number of bridging oxygens (Si–O–Si) [151]. The total range of ^{29}Si chemical shifts in silicates is ranging from -60 to -120 ppm from Q_1 to Q_4 structures [149]. On the contrary for the PU/APP/nano SiO_2 formulations, no peak is detectable around -110 ppm but one peak (or maybe a double peak) around -213 ppm. By comparison with the range of chemical shifts of silicates (-60 to -120 ppm), this suggests that the species at -213 ppm is not a silicate. SiP_2O_7 has a chemical shift around -220 ppm [148]; it is a complex structure which may have six distinct Si^{VI} sites because the silicon is organized following a SiO_6 crystallographic structure. Depending on the considered site, the chemical shifts are in the range of -214 and -220 ppm [152]. SiP_2O_7 also exists in octahedral silicon coordination and the existence of two lines in the ^{29}Si NMR spectra at -213 and -215 ppm has already been observed [153]. From the literature it is clear that the species created in the char PU 28%APP 2%nano SiO_2 are silicophosphates and more precisely SiP_2O_7. Because no residual silica peak is detected according to ^{29}Si solid state NMR, this means furthermore that all nano SiO_2 reacts with APP to form silicophosphates. This clearly proves the high reactivity of APP and nano silica.

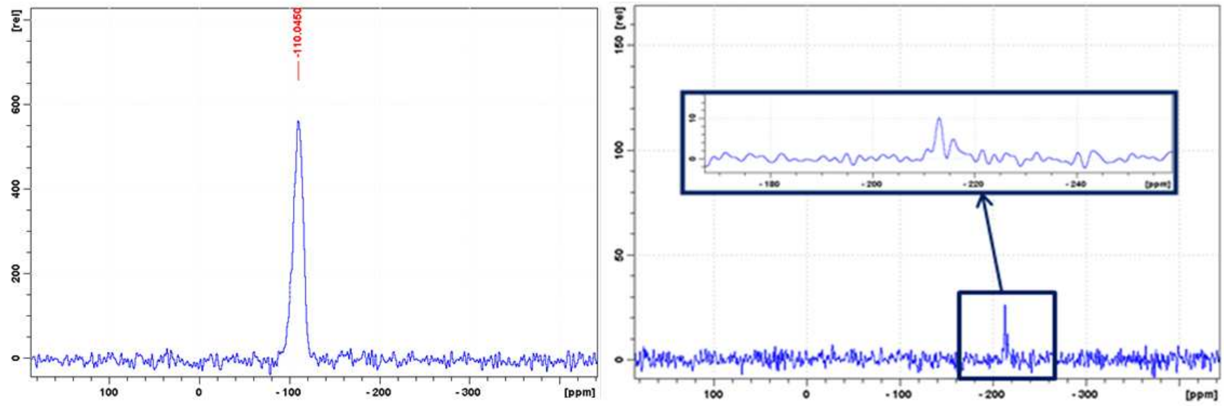

Figure 95: ^{29}Si solid state NMR spectra for char PU 5%nano SiO_2 (left) and char PU 28%APP 2%nano SiO_2 (right) collected after cone calorimeter experiment

The case of the formulation containing OMPOSS exhibits different peaks and some at very low intensity (high zoom in **Figure 91**). The TGA showed that a small residue of silica is obtained when OMPOSS degrades. Two peaks are detected at -45 and -53 ppm and might be attributed to silicophosphates [148] but also to P_4O_{10} in equilibrium with phosphoric acid [128]. By comparison with the formulation PU 28%APP 2%nano SiO_2 similar peaks are obtained at -45 and -53 ppm clearly suggesting the presence of silicophosphates. In order to prove the presence or not of silicophosphates a ^{29}Si solid state NMR was realized on this sample but unfortunately this experiment was not possible (phosphoric acid flows out of the probe during the experiment). Another possibility to assess the presence of silicophosphates is to use XRD. XRD analysis was carried out on an APP/OMPOSS mixture previously heat treated at 700 °C [85] and it revealed the presence of a crystalline phase identified as SiP_2O_7. It is then chemically possible to get silicophosphates by heating APP and OMPOSS together. The formation of silicophosphates by reaction between APP and zeolite 4A was also reported in the literature [154]. The authors found that these species were responsible for the orientation of the degradation reactions.

For all the nano gold based formulations, no products of a reaction between APP and gold is noticeable on the ^{31}P solid state NMR (**Figure 91**). Only phosphoric acid (0 ppm), P-O-C bonds (-11 ppm) and pyrophosphate (-8 ppm) for the ratio 28/2 were noticed on the spectra. For PU 29%APP 1%nano gold the presence of condensed phosphates is also evidenced by the broad band around -25 ppm [116].

This section evidenced first the development of an intumescence phenomenon as only aromatic structures are detected in ^{13}C solid state NMR for all PU formulations. The degradation of APP into phosphoric acid occurs in PU/APP formulation and is in agreement with the degradation pathway of APP. Additional phosphonic acid was also detected although its formation was unexpected. While adding NPs to the PU/APP mixture, the ^{31}P NMR spectra are different. All the NPs consequently modify the degradation pathway and/or kinetic of APP degradation and/or its reaction with the PU matrix. The contribution of APP either to give additional degradation products (pyrophosphates) or to react with the PU matrix (P-O-C bonds) has indeed been only evidenced in PU/APP/NP degradation products. Moreover some NPs (nano MgO, nano SiO_2 and OMPOSS) react with APP leading to the formation of new species. The magnesium phosphates created in PU/APP/nano MgO systems have been partially attributed. Thanks to ^{29}Si solid state NMR, it was furthermore proven that all the nano silica incorporated was used to form silicophosphates.

Even if the char was not always homogeneous, the NMR has been performed on a powder sample containing the different parts of the char randomly mixed which was judged representative of the all char. It is now interesting to characterize the chemical composition along a slice of char and to see if there is an effect of the char area considered. Another performing tool, the electron probe microanalysis, will be used for that purpose on a slice of PU/APP/nano MgO char.

2.2 Electron probe microanalysis on PU/APP/nano MgO collected after MLC test

Electron probe microanalysis (EPMA) has been used to make a mapping of the repartition of phosphorus and synergist particles in a char collected after a cone calorimeter test. The study will focus on one sample; the char obtained from PU 28%APP 2%nano MgO was chosen for several reasons: (i) it contains phosphorus and magnesium; two elements easily identified in EPMA, (ii) it is the best performing material according to fire tests (**see chapter III, section** 2-**Evaluation of the Fire**

Performances p105), (iii) its char is expanded and it is then possible to cut a slice of char with a significant height to analyze it.

Mappings of chemical composition (phosphorus and magnesium) of a slice of char from PU 28%APP 2%nano MgO were thus acquired and are presented in **Figure 96**. This char has been taken at the end of a cone calorimeter test; the conditions are the same compared to the sample analyzed by solid state NMR in the previous section. It was very difficult to cut the char and to embed it into the epoxy resin, which is required to perform the analysis. Some fragile parts (especially at the top where big bubbles are mainly observed) were broken during the sample preparation and had to be placed side by side in the epoxy resin. The slice of char is finally reconstructed to provide a mapping from the bottom to the top of the structure.

The mappings clearly show the presence of phosphorus and magnesium in the char as expected. The totally black parts observed on the pictures correspond to holes of the char as the structure is very porous (as shown on picture of the char slice in **Figure 96**). It is thus normal that phosphorus and magnesium might only be detected in the regions where some matrix is left. The scale indeed means that while going from black to red, the element is presents at a higher concentration.

Those EPMA results, in agreement with the NMR results, proves furthermore a reaction between APP and nano MgO as magnesium is generally detected in the areas where phosphorus is also found, and especially in the areas rich in phosphorus. The size of the zones which is rich in both elements also confirms a reaction between APP and nano MgO. Whereas the size of MgO aggregates was ranging from 200 nm to 2 µm in PU formulations (**Chapter III, section 1.2-Dispersion of additives in the PU matrix p100**) the phosphorus and magnesium rich zones are larger (particularly at the bottom of the char where they are measured from nearly 15 to 115 µm). This could indeed be attributed to the formation of magnesium phosphates which particle size is different and especially higher to that of isolated MgO. This particular systematic location of magnesium linked to phosphorus could also suggest that all magnesium oxide react with APP to create magnesium phosphates, as it was proven for silica.

High levels of phosphorus and magnesium are mostly located at the bottom of the sample. The quantity of these elements in fact decreases from the bottom to the top of the char, suggesting the existence of a gradient of additives in the char. An hypothesis is viable to explain this gradual repartition of phosphorus and magnesium based species: phosphorus, magnesium and/or magnesium phosphates are denser than the PU matrix but a migration of the particles occurs during the char formation. The additives are thus located at the bottom of the char, area where the char is also most compact and cohesive.

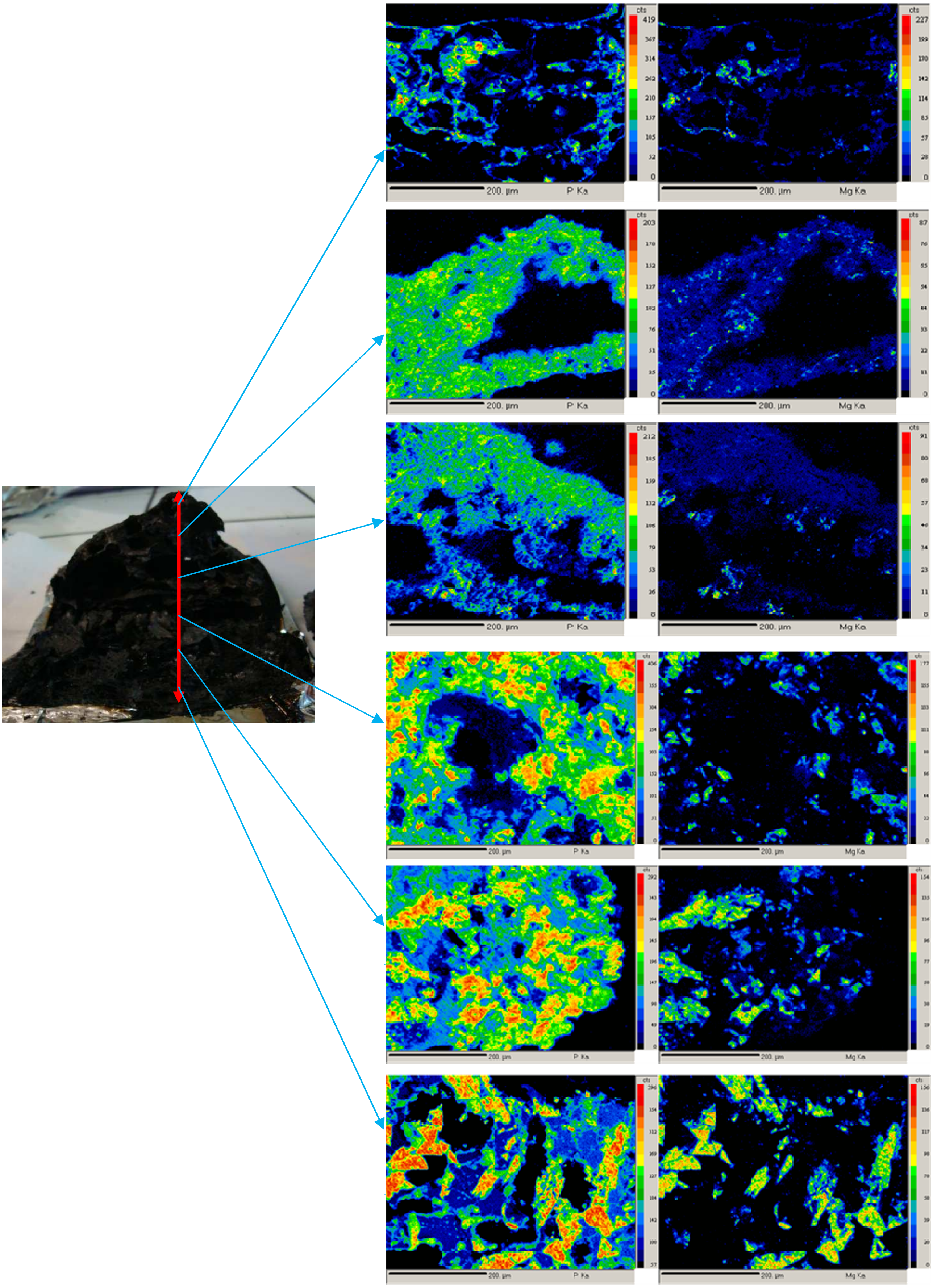

Figure 96: EPMA mappings of phosphorus (left picture) and magnesium (right picture) of a slice of char from PU 28%APP 2%nano MgO

This section proved that chemical reactions take place in the condensed phase upon heating of PU, PU/APP and PU/APP/NP formulations. Depending on the samples, it may involve the formation of a carbonaceous shield composed of aromatic carbons, the degradation of APP in phosphoric acid, phosphonic acid and pyrophosphate and the reaction between APP and NPs leading to phospho-X compounds. It clearly appears that there is a link between the species formed at the end of a cone calorimeter test and the fire properties exhibit by the formulation. Each formulation leads indeed to different chemical species and fire properties. The incorporation of NPs in intumescent PU furthermore modifies the degradation pathway and/or kinetic of APP degradation and/or its reaction with the PU matrix. Chemical reactions should consequently at least partially explain the synergy observed in fire properties between APP and NPs. It appears on EPMA pictures that the repartition in the char of created species will also induce a char structure which might be different depending on the chemical reactions involved.

This section gives consequently first evidence that chemical reactions occur between PU, APP and NPs in PU/APP/NP systems and that they should play a significant role on the synergy mechanism. The next section will go in much more details to follow and compare the species evolution during a fire test on a defined system.

3 EVOLUTION OF SPECIES FORMATION DURING THE CONE CALORIMETER

It has just been seen that chemical interactions between the components of PU/APP/NP formulations during burning are involved in the synergy mechanism. This section characterized the system at the end of a fire test; this was already a first interesting step. Since differences in chemical species have been noticed, it is now judicious to study the evolution of species formation during the cone calorimeter. To that aim “shutter experiments” (**Chapter II, section 3.1.2-Shutter experiments p93**) have been performed on PU, PU/APP and PU/APP/nano MgO. It consists in a MLC experiment stopped at characteristic times and this will allow having an overview (chemical characterization, physical observations) of the samples at different steps of degradation. The chemical species evolution will indeed be studied using solid state NMR. A similar process is conceivable by degrading materials in a furnace at a controlled temperature but it has been chosen to do it during a fire test to understand and to catch up with the real fire scenario. In order to study the synergy mechanism, the nano MgO based formulations have been chosen because all the different species were detected only in these samples: phosphoric acid, phosphonic acid, P-O-C, P-O-P, magnesium phosphates. Moreover it presents the highest synergistic effect. The influence of the ratio APP/nano MgO on the chemical species created during a fire test will moreover be evaluated.

The full cone calorimeter results for each formulation including HRR curves as a function of time, residue pictures, expansion and residual mass measured after collecting the residues are presented in **Figure 97** (**see also Appendix 2: Results obtained from shutter experiments on PU, PU/APP, PU/nano MgO and PU/APP/nano MgO formulations p241**). The pictures clearly show the evolution of the polymer to a progressively burned material whatever the concerned formulation.

PU

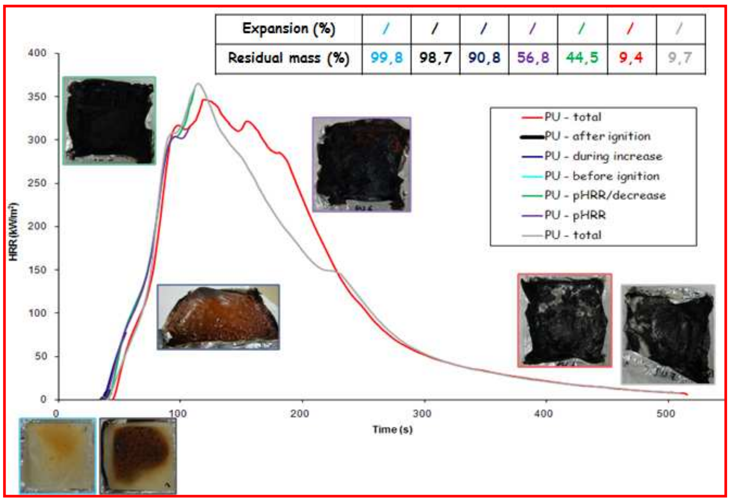

Expansion (%)	/	/	/	/	/	/	/
Residual mass (%)	99,8	98,7	90,8	56,8	44,5	9,4	9,7

PU 5%nano MgO

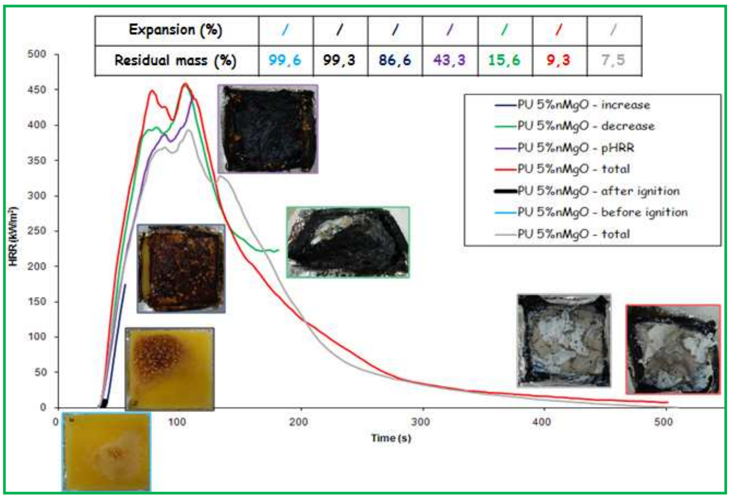

Expansion (%)	/	/	/	/	/	/	/
Residual mass (%)	99,6	99,3	86,6	43,3	15,6	9,3	7,5

PU 30%APP

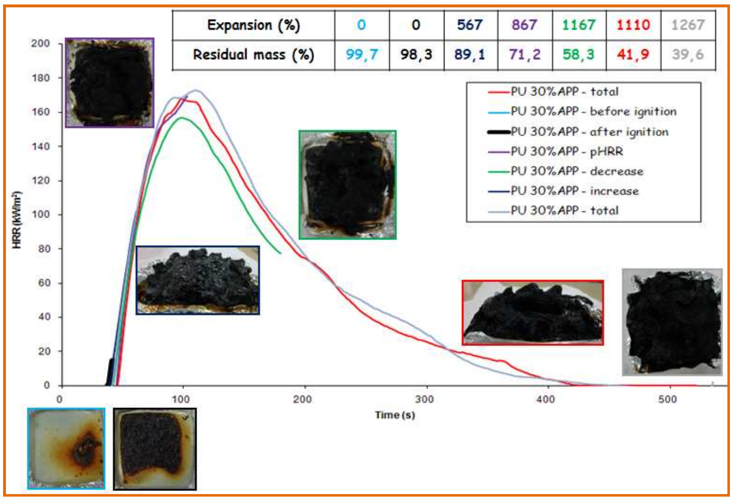

Expansion (%)	0	0	567	867	1167	1110	1267
Residual mass (%)	99,7	98,3	89,1	71,2	58,3	41,9	39,6

PU 25%APP 5%nano MgO

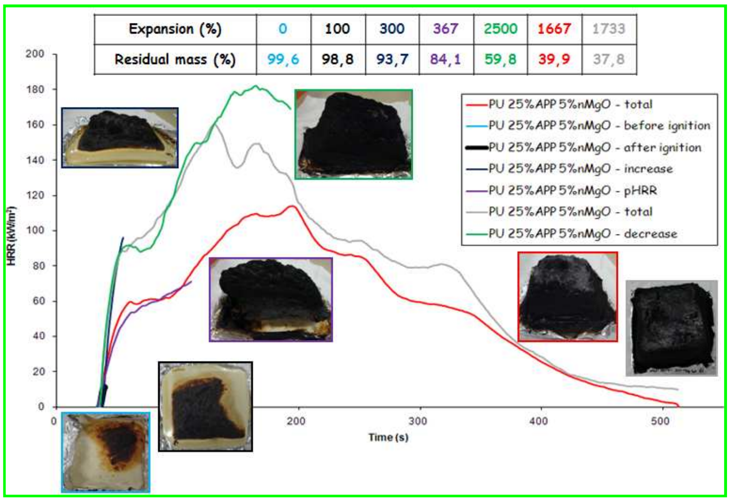

Expansion (%)	0	100	300	367	2500	1667	1733
Residual mass (%)	99,6	98,8	93,7	84,1	59,8	39,9	37,8

PU 28%APP 2%nano MgO

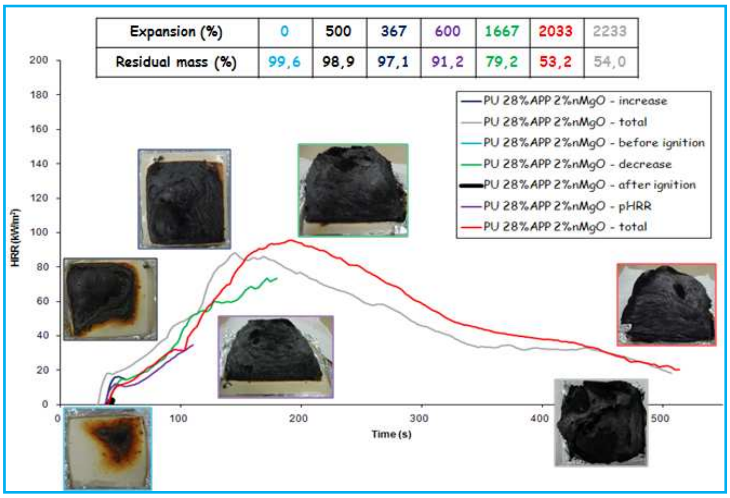

Expansion (%)	0	500	367	600	1667	2033	2233
Residual mass (%)	99,6	98,9	97,1	91,2	79,2	53,2	54,0

PU 29%APP 1%nano MgO

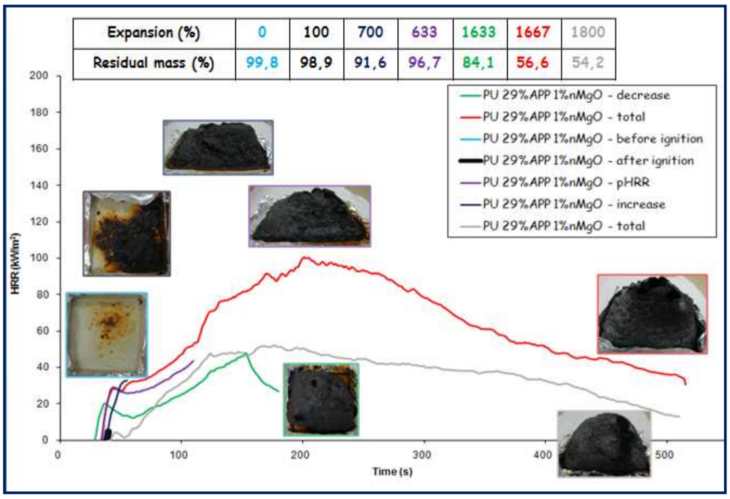

Expansion (%)	0	100	700	633	1633	1667	1800
Residual mass (%)	99,8	98,9	91,6	96,7	84,1	56,6	54,2

Figure 97: Cone calorimeter results: HRR curves, pictures, expansion and residual mass for each sample from shutter (different time of experiment) of PU, PU 5%nano MgO, PU 30%APP, PU/APP/nano MgO (ratios 29/1, 28/2, 25/5)

Seven different samples for each formulation (PU, PU/APP, PU/nano MgO and PU/APP/nano MgO at different ratios) were exposed to cone calorimeter and collected at different times as reported in **Figure 50 p93**. The “total” sample was collected twice: at the beginning and at the end of the set of experiments for each formulation, in order to evaluate the repeatability of the test. The repeatability was good for PU, PU/APP, PU/NP and PU 28%APP 2%nano MgO but not for PU 29%APP 1%nano MgO and PU 25%APP 5%nano MgO (if 10% of pHRR interval is considered as the acceptable margin error). These differences could be due to two main factors: (i) a bad dispersion of fillers in the PU matrix (linked to the constant difficulty to prepare the PU formulations) and (ii) a different char development leading to the release of more flammable gases. The general trend for HRR curve is nevertheless respected, which is the most important for the purpose of this section.

This section will now be divided into two parts, the first one will present the conversion degree at each step of the shutter experiments and the second one will detail the NMR obtained on the residue. The data concerning the expansion will be discussed in the following chapter (**Chapter V, 2.1.1-Expansion recorded during MLC experiment p177**).

3.1 Conversion degree of PU formulations during shutter experiments

The study of the conversion degree of PU formulations during a MLC test will allow knowing the degradation degree of the sample when it is collected to be analyzed in NMR. This aims to normalize the shutter experiment and thus to know more precisely at which point of degradation the sample is according to its conversion degree curve. The evolution of weight is indeed a key parameter to evaluate the processes occurring during degradation [155].

The evolution of weight as a function of time is superimposed to the HRR curves for each PU formulations in **Figure 98**. The curves are the results of an on-line measurement during cone calorimeter test whereas the residual mass was calculated through the mass measured at the end of the test on a real balance (**see explanation for these experimental details in Chapter II, section 3.1.3-Conversion degree p93**).

Nearly all the material from PU and PU 5%nano MgO formulations has burnt because only 9% of the mass remains. PU 30%APP and PU 25%APP 5%nano MgO have nearly the same value: 40 and 37% respectively and it is significantly higher for PU 28%APP 2%nano MgO (46%) and even higher for PU 29%APP 1%nano MgO where more than half of mass is preserved (53%).

The evolution of mass loss is correlated to the HRR; this is why it is particularly interesting to follow the mass to select the characteristic points for shutter experiments. Moreover the evolution of the derivative weight curves (results not shown) corresponds exactly to the opposite HRR curves. The mass loss rate observed matches with the quantity of fuel used by the samples to burn at the same time. The mass loss begins when the sample is ignited, the higher degradation rate is recorded when the HRR is increasing. Finally when the HRR decreases the mass loss rate is slowed down until the end of the experiment. The evolution of weight with the time is clearly linked to fire properties as the better the fire properties are, the less weight loss is observed.

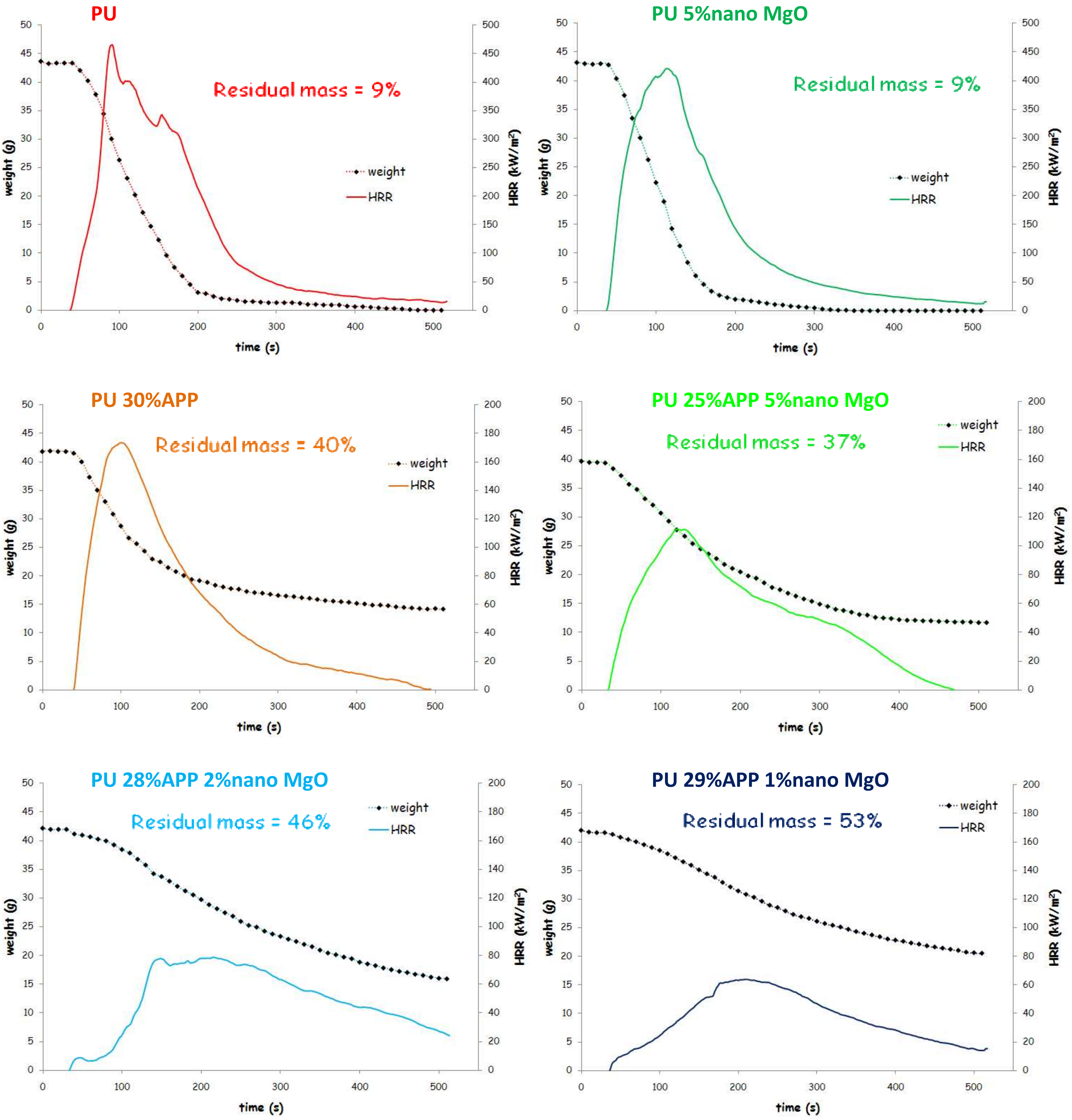

Figure 98: Superimposition of weight and HRR curves versus time for PU, PU 5%nano MgO, PU 30%APP, PU 25%APP 5%nano MgO, PU 28%APP 2%nano MgO and PU 29%APP 1%nano MgO

The conversion degree is then calculated from the weight (**see Chapter II, section 3.1.3-Conversion degree p93**) and it is presented as a function of time (**Figure 99**) for all PU formulations.

Four different behaviors are observed on this graph. First for PU and PU 5%nano MgO, the conversion starts a bit later when compare with the other samples. The conversion rate is very high, 90% of conversion are reached in 130 seconds (from 40 to 170 seconds). The 10 last percents are gained very slowly. With 30% of APP incorporated in the polymer exactly the same behavior is observed until 120 seconds but after the conversion rate is slowed down to go from 60% to 100% of conversion in 350 seconds. This could be linked to the formation of the protective intumescent char, that when formed protect the underlying material. When nano MgO is added in the PU/APP system the conversion degree starts to increase earlier (around 30 seconds), in agreement with the slightly earlier ignition time observed. This is a possible effect of nanoparticles which has already been observed [156-158]. When 5% of APP is substituted by nano MgO the rate of conversion is very progressive and 50% of conversion are reached in 140 seconds corresponding to the pHRR. The behavior for PU 28%APP 2%nano MgO and PU 29%APP 1%nano MgO is exactly the same and the conversion is really slowed down. Half of conversion degree is only reached in 200 seconds and the system is still evolving but very slowly when the test is stopped at 8 minutes 30 seconds.

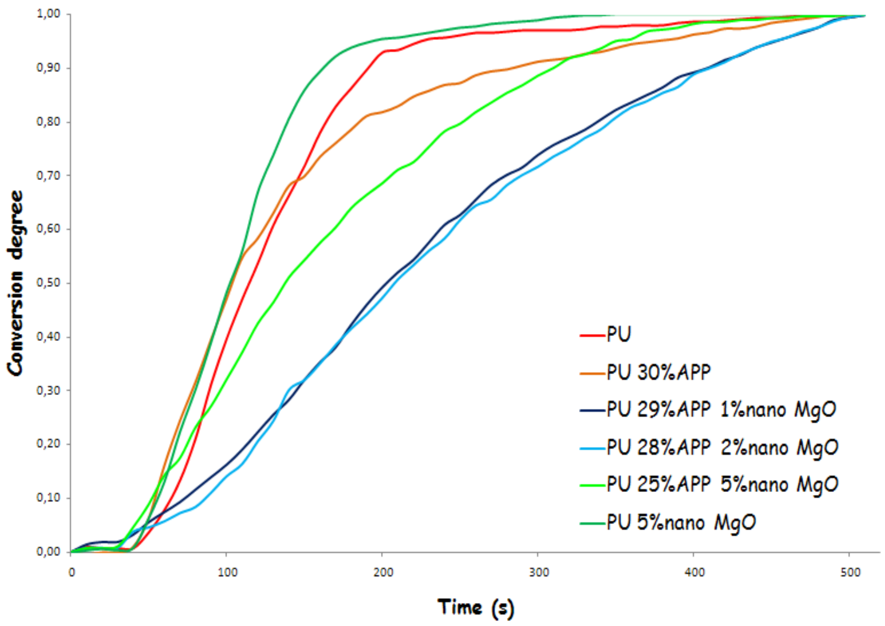

Figure 99: Conversion degree as a function of time during cone calorimeter experiment for PU, PU 30%APP, PU/APP/NP (ratios 29/1, 28/2, 25/5) and PU 5%nano MgO

The incorporation of APP and nano MgO in PU consists in a non-negligible amount of material (30%) for which the degradation is not total at the end of the cone calorimeter experiment. For PU 5%nano MgO, the amount of mineral filler is not sufficient enough to make the residual mass rises. The reactions involved in condensed phase between PU, APP and nano MgO are probably the reason why such differences in residual mass and conversion degree are observed. The products of reaction from PU + APP and APP + nano MgO are mainly present in the condensed phase compared to the PU degradation products which are released in the gas phase.

The high char yield during a fire test is important since the residual material have to protect the underlying material. This is the concept of the protection via an intumescent process. In the PU formulation, it is proved that the more mass kept the better the fire performances in cone calorimeter. The formulation PU/APP/nano MgO (at ratios 28/2 and 29/1) are indeed the most interesting according to their fire behavior in cone calorimeter (**Chapter III, section 2.1-Fire performances determined by mass loss calorimetry p106**). Additionally, the best formulations in terms of slow degradation rate are PU/APP/NP at ratios 28/2 and 29/1 followed by the ratio 25/5, and the PU/APP formulation. The same ranking is observed in fire performances. On the contrary, PU 5%nano MgO formulation, presenting a conversion degree similar to PU, does not improve the fire performances.

The study on conversion degree proves that the development of the fire protection is affected by the presence of NPs and their reactions with APP. The chemical characterization of residues collected during shutter experiments will then be detailed in the next part.

3.2 NMR analysis of residues collected from shutter experiments on PU formulations

The samples collected during the shutter experiments have been characterized by solid state NMR, the nuclei observed are carbon and phosphorus. PU 5%nano MgO has not been investigated because only ^{25}Mg NMR would have been interesting but the collection of such spectra is complex as previously discussed; and thus it has not be done. Due to the heterogeneity of partially burned material, the materials were analyzed in different parts mentioned on the graphs with top, mid or bottom; top meaning the material exposed to the heat source. On the left of the NMR spectra, the time at which the samples have been collected are reported and refer to those explained in **Figure 50 p93**. Even though all precautions have been taken to keep all the samples the same time in a dry place, it is difficult to guarantee that no species evolution happened between the MLC test and the NMR. It is anyway noteworthy that all samples have been treated in the same way and are thus comparable between each other.

Figure 100 presents the evolution of ^{13}C solid state NMR spectrum of PU with increased time of exposure under a heat flux during a cone calorimeter experiment. Before ignition, peaks characteristic of all PU bonds are found and were assigned with their chemical shifts in **Table 11 p98** in **Chapter III, section 1.1-Chemical characterization of PU formulations p97**. After ignition the bottom of the plate presents a NMR spectrum corresponding to unmodified PU, in agreement with its visual aspect. On the burnt part an enlargement of aromatic and urethane peaks is observed; this is explained by the beginning of charring and depolymerization process [76, 137]. While the experiment is going further and especially at the top of the samples, the difference between the aromatic peaks and urethane peak becomes difficult to distinguish. After the pHRR, all PU peaks totally disappear and only a broad peak is observed around 126 ppm attributed to aromatic carbons.

The carbonization occurs already on the virgin polymer and no more undegraded polymer is detected during the decrease of the HRR.

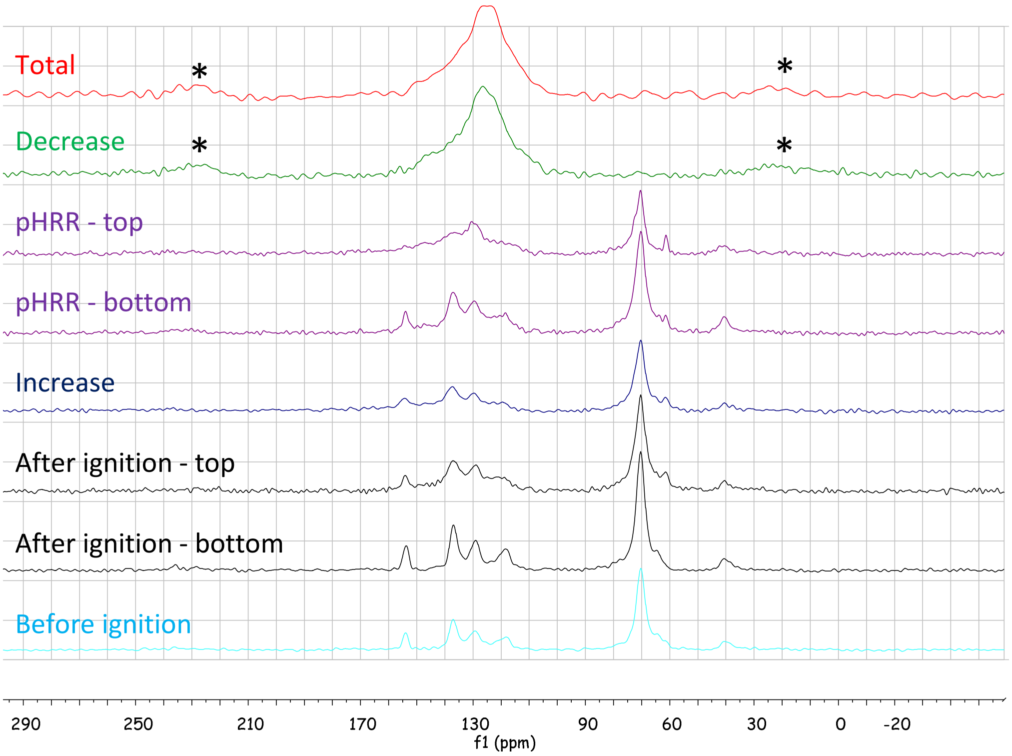

Figure 100: ^{13}C solid state NMR of PU collected at different time during cone calorimeter

The different ^{31}P solid state NMR spectra of PU 30%APP are compared in **Figure 101**. At the bottom of the first sample, a double peak at -21.6 and -22.5 ppm characteristic of polyphosphate chains [116] is observed. Before ignition, the surface exposed to the heat presents already a different NMR spectrum. Residual APP is still detected but additional peaks appear around 0 and -12 ppm. The first one is attributed to phosphoric acid, concomitant with the degradation pathway of APP [13, 129]. The second one is P-O-C bonds from orthophosphates linked to aromatic species (**see interpretation in Chapter IV, section 2.1-Solid state NMR on burned residues from PU formulations p138**), this comes from a reaction between APP and PU. After ignition the same spectra are obtained than those before ignition but APP is more degraded because there is no more residual APP in the top residue. A small peak around 33 ppm appears on the top sample after ignition, it is attributed to phosphonic acid [138]. It is noteworthy that the phosphonic acid peak is present only if there is no APP detected; suggesting that under specific conditions, all APP not used or degraded is reduced in phosphonic acid. The sample collected during the HRR increase has been analyzed in three parts. The first layer present nearly an unmodified material with APP peaks but phosphoric acid begins to appear. On the second and third layers, peaks attributed to orthophosphates linked to aromatic species (at around -12 ppm) and to phosphonic acids (around 33 ppm) appear whereas the APP bonds disappear.

At pHRR, the vitreous bottom consists of three main bands centered at 0, -11.5 and -23 ppm. They are respectively attributed to phosphoric acid, to orthophosphates linked to aromatic species and to condensed phosphates [116]. On the top, no more APP is detected but phosphonic acid is present. During decrease and at the end phosphoric acid peak is predominant, attesting the complete degradation of APP.

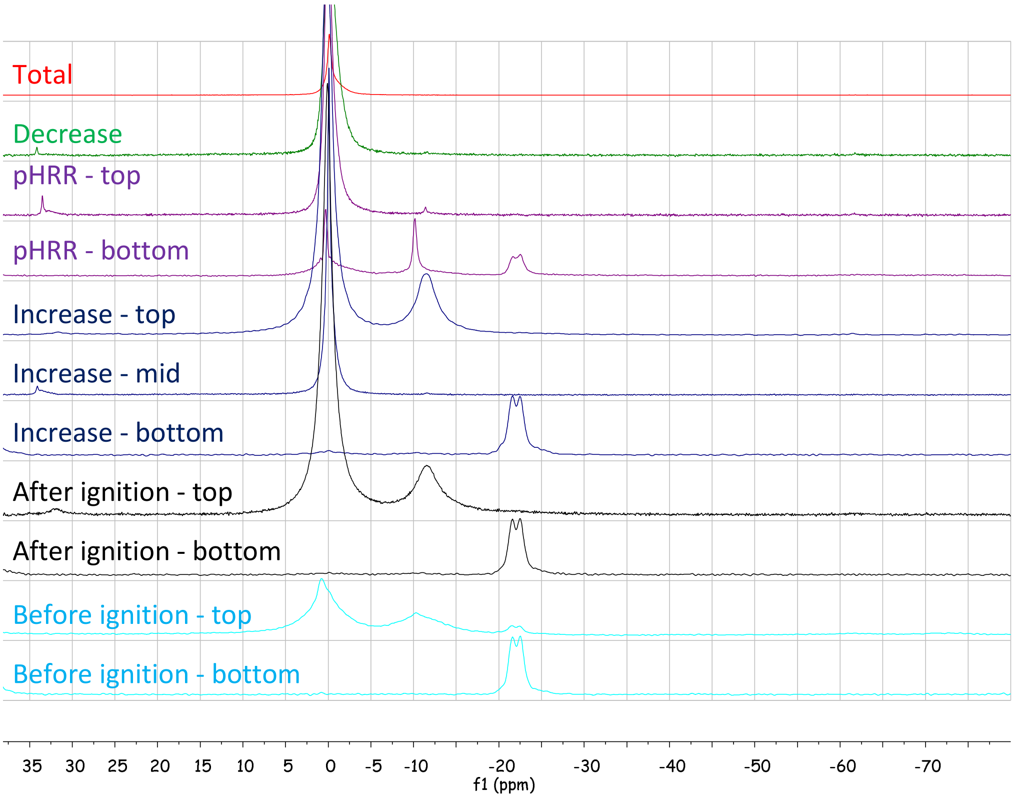

Figure 101: ^{31}P solid state NMR of PU 30%APP collected at different time during cone calorimeter

When nano MgO substitutes partially APP, the ^{31}P solid state NMR spectra were also collected before and after ignition, during the HRR increase, at the pHRR, during the decrease of HRR and at the end of the cone calorimeter experiments. The stacked spectra are shown in **Figure 102**, **Figure 103** and **Figure 104** respectively for the formulations PU 29%APP 1%nano MgO, PU 28%APP 2%nano MgO and PU 25%APP 5%nano MgO. On the phosphorus data, many similar peaks than those observed for PU 30%APP are found but additional peaks are also noticed especially from the pHRR. For the samples containing 1 and 2% of nano MgO, the same general trend of spectra is observed whereas it is really different for the sample at a ratio 25/5.

The bottom and top spectra of the three samples are similar before ignition; the bottom is only composed of APP, whereas the top is already presenting signs of APP degradation and reaction with three broad peaks centered on 0, -11 and -23 ppm. The first peak is assigned to phosphoric acid, the second to P-O-C bonds from orthophosphates linked to aromatic species and the third one to condensed phosphates or residual APP.

After ignition, the burnt materials are composed of phosphoric acid whatever the quantity of nano MgO used. A peak characteristic of phosphonic acid appears at 33 ppm only for the ratio 29/1 whereas a large band around -23 ppm corresponding to condensed phosphates or residual APP is recorded for ratios 28/2 and 25/5.

At the two lower ratios, the initial peak at -12 ppm is split into two distinct peaks or with a shoulder at -8 and -12 ppm. These two peaks are a contribution of either P-O-P from pyrophosphates and P-O-C bonds from orthophosphates linked to aromatic species. The reaction PU + APP characterized by the orthophosphates linked to aromatic species should be detected around -12 ppm and the pyrophosphates at -8 ppm (**see interpretation in Chapter IV, section 2.1-Solid state NMR on burned residues from PU formulations p138**). This means that with addition of nano MgO (at ratios 29/1 and 28/2), the formation of pyrophosphates is possible which was not the case for PU containing only APP. The magnesium oxide might indeed act as a catalyst easing the pyrophosphates formation [159]. If part of APP is degraded to form pyrophosphate, less APP will consequently be available to react with PU to form a phosphocarboneous material, thus modifying the char properties. The process of degradation and reaction of APP continues during the increase of HRR giving nearly the same peaks than those already discussed. An additional small peak at -26 ppm is detected and attributed to magnesium phosphates [144, 146]. At the pHRR, magnesium phosphates are still detected at -26 ppm and an additional peak is observed for the ratio 28/2 at -33 ppm, it is also a magnesium phosphate [145, 147, 160]. Depending on the chemical structures and environments, different magnesium phosphates are indeed detected in NMR at different chemical shifts as previously detailed. These two characteristic peaks are both detected during the decrease and at the end in PU 29%APP 1%nano MgO and PU 28%APP 2%nano MgO, in addition to phosphoric acid, pyrophosphate and orthophosphate linked to aromatic species. At the end, no more phosphonic acids are present and only a small peak of condensed phosphate is recorded.

For PU 25%APP 5%nano MgO, a broad band centered on -30 ppm is detected on the top residue during the increase, at the pHRR and during the decrease. The structure of phosphate glasses is usually described in terms of Q^n groups. Q^n groups are PO_4 tetrahedra; *n* indicates the number of bridging oxygen atoms and depends on the degree of condensation. The broad band detected around -30 ppm corresponds thus to a Q_2 and/or Q_3 structure [161, 162] and according to the broad signal, an amorphous system is expected. The presence of a number of peaks observed in the 30 to 40 ppm range and corresponding to branched orthophosphate species (polyphosphoric acid-like species) has already been observed in the literature [128]. These species are in an intermediate state between APP degradation and formation of phosphorus oxides. This broad peak might consequently be a phosphate network where magnesium oxide is embedded. This is moreover probable since this broad peak lets appear discernible magnesium phosphates peaks at higher time under cone calorimeter. The phosphoric acid peak is not well defined as well as the region where pyrophosphate and orthophosphate linked to aromatic species should be recorded. The network involving APP and nano MgO might explain why the formation of phosphoric acid, pyrophosphate and orthophosphate linked to aromatic species is modified compared to the other ratios. Magnesium phosphates are finally clearly detected at the pHRR, during the decrease and at the end of the test by peaks at -26, -34 and -36 ppm [145, 146].

It is possible to consider that at ratios 29/1 and 28/2, the chemical species involved in the degradation are the same and appears at the same time of the experiment according to the experimental uncertainties. But it exists an obvious difference with the behavior of PU 25%APP 5%nano MgO for which different magnesium phosphates and a totally different evolution of APP are observed. This difference is particularly highlighted during the HRR increase. According to cone calorimeter curves, the fire behavior of PU/APP/NP also differs depending on the ratios APP/NP only from during the HRR increase. It means that the difference between the formed chemical species is linked with the fire performances.

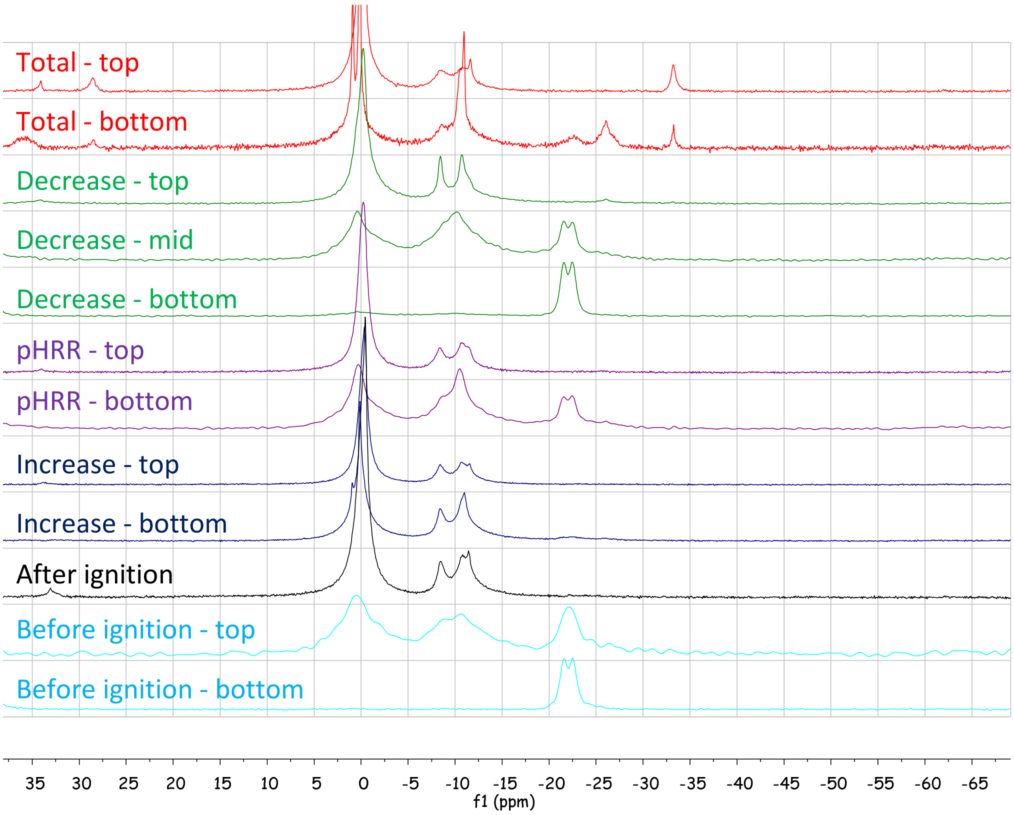

Figure 102: ^{31}P solid state NMR of PU 29%APP 1%nano MgO collected at different time during a cone calorimeter experiment

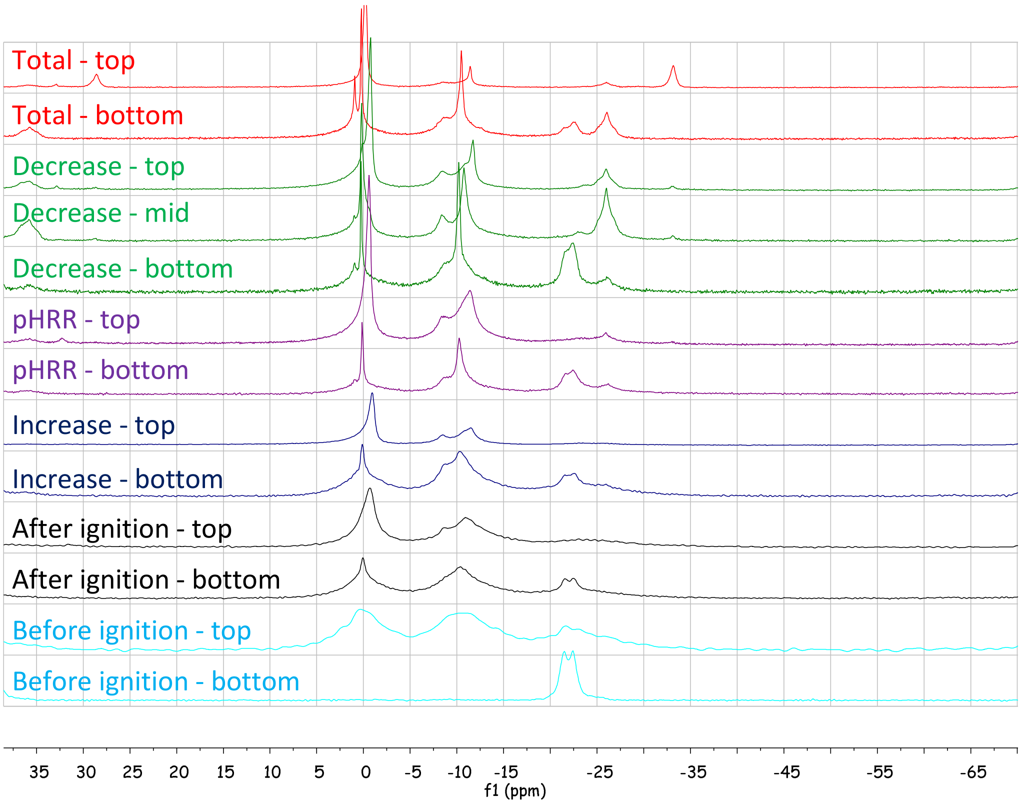

Figure 103: ^{31}P solid state NMR of PU 28%APP 2%nano MgO collected at different time during a cone calorimeter experiment

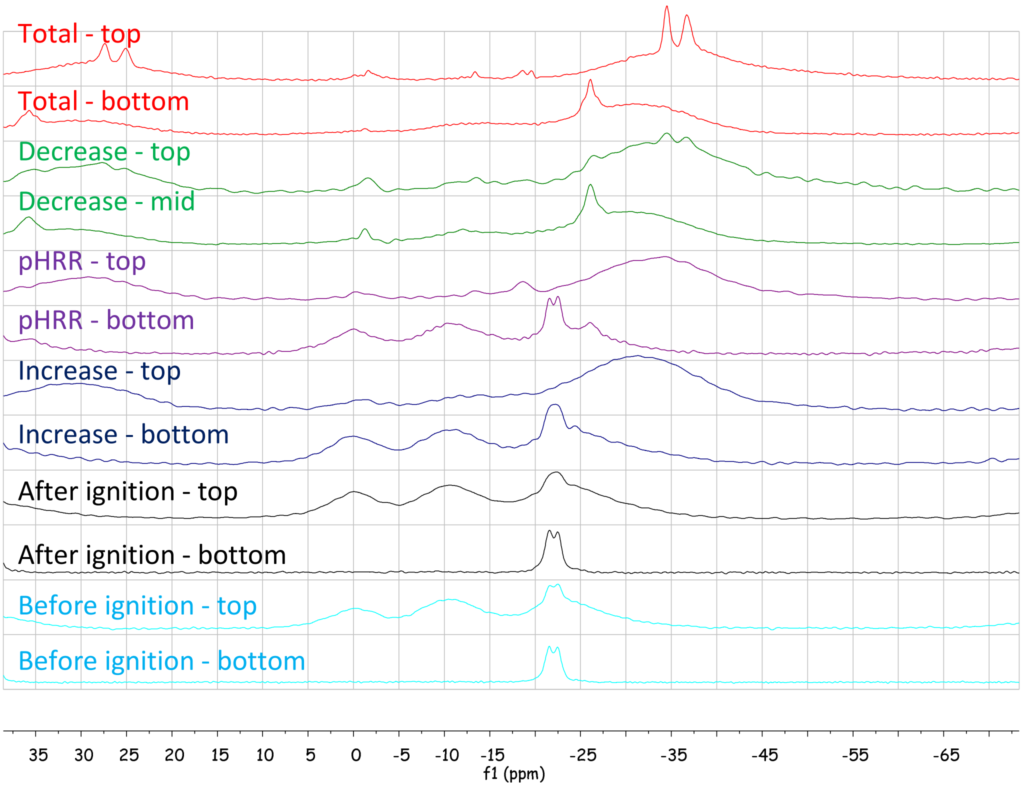

Figure 104: ^{31}P solid state NMR of PU 25%APP 5%nano MgO collected at different time during a cone calorimeter experiment

To conclude this part, the progressive charring and degradation of virgin PU has first been followed by ^{13}C solid state NMR. Then, on PU 30%APP formulations, the formation of phosphoric acid has been validated and a reaction between PU and APP is proved by the formation of orthophosphates linked to aromatic groups. A reaction between APP and nano MgO is once again clearly evidenced by the NMR characterization of residues during shutter experiment. These species appear during the increase of HRR and their presence increases as the experiment pursue. The incorporation of nano MgO leads to the formation of magnesium phosphates but also modifies the degradation pathway of APP since pyrophosphates are formed.

A clear link between the fire properties and the chemical reactions and more precisely the chemical species created in PU/APP/nano MgO systems could thus be highlighted. Virgin PU leads to bad fire performances characteristic of polymeric materials since it is mainly constituted of carbon and oxygen and consequently depolymerizes leading to flammable species. When the phosphorus based flame retardant is added, reactions occur in condensed phase with the polymer in order to create an intumescent barrier reacting with PU. This improves considerably the fire properties and decreases significantly the pHRR value. With substitution of a small quantity of APP by a synergist (nano MgO), the possibilities of reaction are even more complex. PU 29%APP 1%nano MgO and PU 28%APP 2%nano MgO present nearly the same synergy in fire properties and nearly the same evolution of chemical species during shutter experiments. PU 25%APP 5%nano MgO has intermediate fire properties between PU 30%APP and PU/APP/nano MgO at ratios 29/1 and 28/2 and the formed species are different. There is consequently clearly a link between the fire performances and the chemical species formed when burning.

The study of chemical species evolution during a cone calorimeter experiment and as a function of the location in the char (top, mid, bottom) evidenced that an intumescent char is formed and protects the residual material from a quick degradation. The more effective the intumescent protection, the better the fire properties. It is for example clearly observed that APP is preserved from degradation at the bottom of the sample up to the decrease in HRR for both 1 and 2% nano MgO containing formulations, fact which is not observed for 5%nano MgO. Thus the intumescent layer efficiency is correlated with its chemical composition which may affect its physical properties that are going to be studied in the next chapter. At the moment another aspect regarding the chemistry need to be studied; it is the influence of the heating rate. Until now the chemistry of the system has only been evaluated during or after a MLC test in which the sample is submitted to defined parameters. The heating rate is in particular very high and it could be associated to a quench since the sample is directly exposed to a radiant heat of $50kW/m^2$. If another fire test is used, different test conditions will be applied and it is thus important to know if the PU formulations will behave as it was predicted in this chapter. The most influencing and important parameter to investigate is thus the heating rate [163, 164] and its effect on the thermal stability and chemical composition of PU formulations; this is the goal of the next section.

4 INFLUENCE OF HEATING RATE ON THE DEGRADATION OF PU FORMULATIONS

This section is devoted to analyze the effect of heating rate on the degradation of PU formulations, either from a thermal point of view in a first part and also from a chemical point of view in a second part. Heating rate is a critical parameter for fire protection; different temperatures and heating rates are indeed involved depending on the fire scenario considered. The behavior of flame retarded PUs might not be similar if the samples are not tested in cone calorimeter test or LOI, where the heating rate is very high, compare to progressive increase in temperature such as the one used in fire tests such as ISO 834 (for cellulosic fire) [165] for example.

This section aims first to see if differences are observed between samples with or without NPs. Second it will evaluate on each sample if a different heating rate affect the degradation properties using ^{31}P solid state NMR. This study has been performed on two systems: PU 30%APP and PU 28%APP 2%nano MgO. This selection was made because the aim was to compare the simple intumescent systems to one sample containing NPs and exhibiting synergy in fire properties. As it has already been the case, the nano MgO based formulations are uppermost studied because they allow reaching the best fire performances in intumescent PU. The ratio 28/2 has been selected since many chemical species are detected during its degradation.

4.1 Effect of heating rate on the thermal stability of PU formulations

The thermal stability of PU formulations has been studied under air at 10°C/min in the previous chapter (**Chapter III, section** 3-**Thermal Degradation p114**). It has been first explained that the PU degradation occurs in two steps. The first step is attributed to the depolycondensation reaction; then oxygen enhances the thermal stability by developing a stable residue which is further oxidized to lead to no residue at high temperature. It has been shown that the incorporation of fillers modifies this thermal degradation. The incorporation of APP lowers indeed the temperature of the beginning of degradation and modifies the second step to finally lead to a significantly higher residual mass at 800°C. The substitution of a low amount of APP by nano MgO induces the same modifications on the PU degradation but the residual mass is once again increased.

This section presents the TG curves of PU 30%APP (**Figure 105**) and PU 28%APP 2%nano MgO (**Figure 106**) recorded at different heating rates under air. It aims to study the effect of the heating rate on the PU formulations decomposition. A wide range of heating rates was covered: 0.25, 10, 50, 100 and 150°C/min; favoring low energy reactions at low heating rate and high energy reactions at higher speed [166]. At 0.25°C/min, the data acquisition at high temperatures is difficult. After 800°C, the mass increases probably because of Archimede buoyancy (the TGA device is in vertical configuration and it is not equipped with an Archimedes' principle compensation). For PU 30%APP, the mass reached zero at 630°C; this is probably due to difficulty measurements with low mass at low speed rate.

The first degradation step is affected by the heating rate exactly in the same way for both formulations. The temperature of beginning of degradation is indeed delayed when the heating rate is increased. It is furthermore noteworthy that this delay is less and less important as the difference between two consecutive heating rates decreases (ratios are respectively of 40, 5, 2 and 1.5 from 0.25 to 150°C/min).

Then concerning the intermediate residue, its amount is not significantly modified varying the heating ramps, it suggests that there is no competitive or parallel reactions occurring during the degradation process [167, 168].

Finally during the second degradation step, PU 30%APP and PU 28%APP 2%nano MgO do not behave identically. With NPs the degradation is regularly delayed as the heating rate increases and all curves finally reach the same final residue (around 20 wt.%). This suggests that unbranched reactions are involved in the degradation mechanism [167]. On the contrary PU 30%APP weight residues are significantly different depending on the heating rate considered, suggesting competitive reaction steps [168]. A reproducible result quite surprising is however noticed at 10°C/min because the second degradation step stops at higher residual mass than expected leading moreover to a higher residual mass than the one obtained at 50 and 100°C/min. This result is not explained at the moment and would require further investigations.

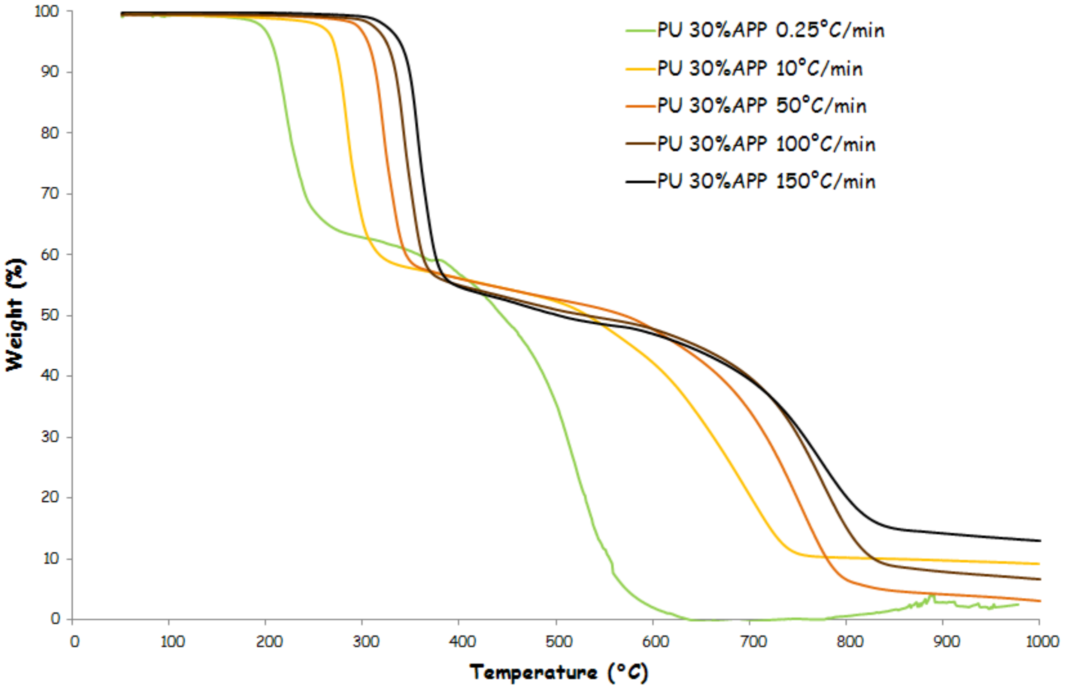

Figure 105: TG curves performed at different heating rates (0.25, 10, 50, 100, 150°C/min) on PU 30%APP under air

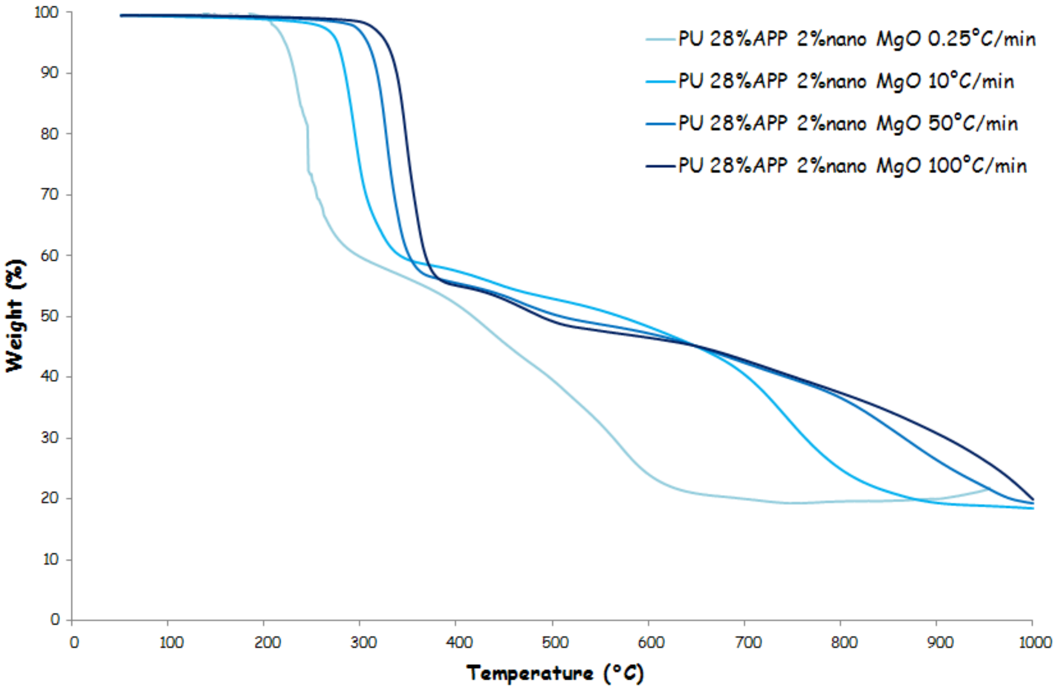

Figure 106: TG curves performed at different heating rates (0.25, 10, 50, 100, 150°C/min) on PU 28%APP 2%nano MgO under air

The second degradation step evidenced a different behavior against the variation of heating rates between the formulations with or without nano MgO while until 600°C the same conclusions can be drawn. This is particularly interesting since it corresponds exactly to the range of temperatures where stabilization occurs when nano MgO is added in the PU matrix with APP (**Chapter III, section 3.3-Thermal stability of PU formulations p124**).

The last sections showed that many chemical reactions are involved in the PU/APP/NP degradation processes. The behavior of PU 30%APP and PU 28%APP 2%nano MgO depending on the heating ramps is moreover different in TG experiments. It is now interesting to chemically characterize the residues of PU 30%APP and PU 28%APP 2%nano MgO developed at different heating rates. This will provide information on the evolution of the reactivity depending on the heating conditions.

4.2 Chemical characterization of PU formulations degraded with different heating conditions

It has just been seen that the heating rate may have an effect on PU formulations; PU 30%APP exhibit indeed different degradation pathway and residual mass depending on the heating rate whereas it is not the case for PU 28%APP 2%nano MgO. These differences in degradation processes and especially in terms of remaining mass may furthermore involve different chemical reactions and consequently degradation products. The purpose of this section is to perform a chemical characterization by ^{31}P solid state NMR of PU samples degraded in different conditions.

The conditions used to degrade PU 30%APP and PU 28%APP 2%nano MgO are reported in **Table 17**. The heating device provides a convective heat under air atmosphere and the sample used is a circle of 21 mm of diameter and 1.7 mm of thickness. In conditions (a) and (b), the sample is put in the oven at ambient temperature and the heating program starts; the sample is then taken out of the oven once the final temperature is reached. For condition (c), the sample is directly put in the oven previously heated at 700°C and it is let in for 8 minutes 30 (corresponding to the time of heat exposure in MLC test).

Table 17: Heating conditions for the degradation of PU formulations

Conditions	Heating rate (°C/min)	Temperature (°C)	Time (min)
(a)	10	500	48
(b)	10	700	68
(c)	very high	700	8.30

After these experiments, the residue is collected and analyzed by ^{31}P solid state NMR; the spectra are presented in **Figure 107 and Figure 108** respectively for PU 30%APP and PU 28%APP 2%nano MgO.

For both formulations (**Figure 107 and Figure 108**), even if all NMR spectra were acquired with the same conditions, differences are noticed on the resolution of the data. Heat treatment until 700°C ((b) and (c)) seems to make more difficult to perform the NMR experiment. The increasing broadening of the peaks from condition (a) to (b) and to (c) for each formulation is assigned to phosphorus in low symmetry surrounding probably due to non crystallized material. The presence of free radicals more or less stable in the sample may also affect the resolution of the spectra (the NMR wobble was broad and difficult to adjust). Additionally the material should be much more degraded at 700°C compared to 500°C according to TG curves, leading to a totally carbonized residue. The global phosphocarbonaceous intumescent network traps the species especially in the case of a quench because the residence time is only of 8 minutes 30. The development of a shield on the surface does not let time for reactions to take place as easily as in a progressive heating ramp. This leads to a low symmetry environment inducing broad signals.

For the PU 30%APP (**Figure 107**), whatever the heating conditions, phosphoric acid and orthophosphates linked to aromatic carbons are detected at respectively 0 and -12 ppm. For the heat treatment until 700°C, they are the only peaks recorded whereas with a 10°C/min heating rate until 500°C, phosphonic acid (33 ppm) and condensed phosphates (broad band of small intensity around -25 ppm) are also evidenced. This means that all APP was not converted into phosphoric acid in these conditions. The degradation of APP is thus affected by the heating temperature but not by the heating rate. On the contrary the formation of P-O-C bonds and consequently the reaction between APP and the PU matrix is always detected whatever the heating conditions.

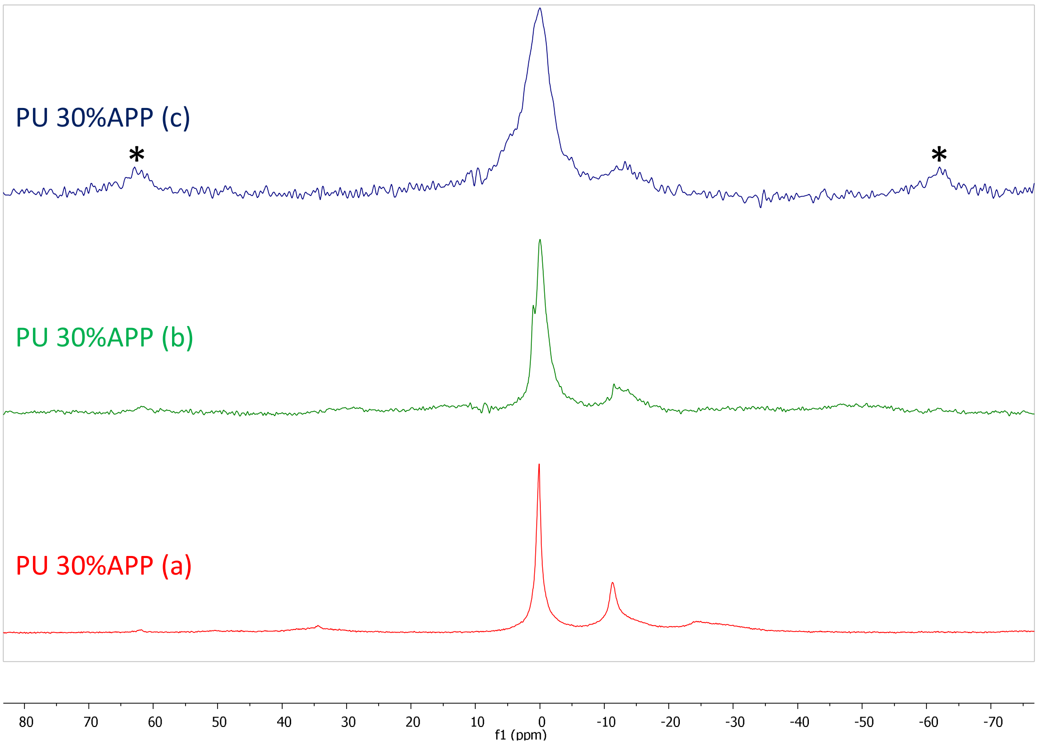

Figure 107: ^{31}P solid state NMR spectra of residue from PU 30%APP degraded with different heating conditions (a), (b) and (c)

For the PU 28%APP 2%nano MgO (**Figure 108**), three different spectra are obtained. For condition (a), four peaks are recorded and correspond to phosphoric acid at 0 ppm, orthophosphates linked to aromatic carbons around -12 ppm and two peaks corresponding to magnesium phosphates (-26 and -29 ppm). When the temperature is increased until 700°C, phosphoric acid and P-O-C bonds are still detected. Two peaks are additionally present at -34 and -36 ppm and are attributed to $Mg(PO_3)_2$ which are different magnesium phosphates compared to those formed at 500°C. In conditions (c), after a quench, the peaks characteristic of APP degradation and/or reaction with PU are not detectable anymore. This is probably due to the uncrystallized phase provided by the heat treatment. The broad peak centered around -40 ppm is very similar to the one observed on the shutter residue from PU 25%APP 5%nano MgO (**Chapter IV, section 2.1-Solid state NMR on burned residues from PU formulations p138**). It was attributed to a glassy phosphate network where magnesium oxide is embedded.

This section proves that the heating conditions affect the ^{31}P solid state NMR of both PU 30%APP and PU 28%APP 2%nano MgO. The nature of chemical species involved is always the same (phosphoric acid, orthophosphates linked to aromatic carbons, magnesium phosphates) but their environment is drastically affected by the heating rate. The stoechiometry of magnesium phosphates created depends moreover on the heating temperature. At higher treatment temperature and heating rate, the formation of non-crystallized network is favored, leading to a broadening of peaks which are consequently less precisely defined.

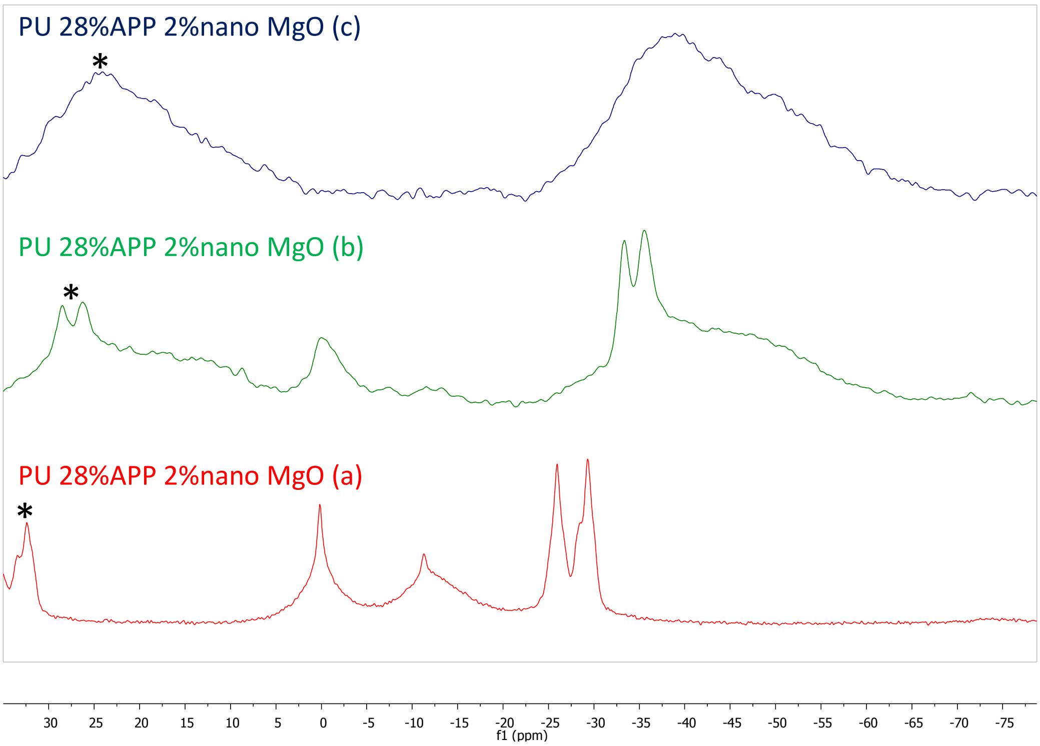

Figure 108: ^{31}P solid state NMR spectra of residue from PU 28%APP 2%nano MgO degraded with different heating conditions (a), (b) and (c)

The study of the influence of heating conditions on the degradation of PU formulations reveals first that the second step of PU degradation exhibits a different behavior against the variation of heating rates between the formulations with or without nano MgO. Since it corresponds exactly to the range of temperatures where stabilization occurs between APP and nano MgO in PU matrix, the effect of heating conditions on the chemistry of the resulting systems were secondly studied. It showed that the nature of chemical species involved is always the same but their environment is drastically affected by the heating rate.

5 CONCLUSION: CHEMICAL INTERACTIONS PARTLY RESPONSIBLE FOR THE SYNERGY

This section evidenced that the chemical interactions observed in PU/APP/NP formulations are involved in the synergy mechanism between APP and NPs in the considered PU matrix.

The PU matrix degrades and releases polyol and isocyanate fragments in gas phase. By addition of APP, the thermal degradation of PU is modified. The range of temperature where gases are detected is indeed smaller and begins at lower temperature. Additional gases are moreover detected with the presence of APP such as ammonia and phosphorus-based fragments. The synergy mechanism between APP and nano MgO is on the contrary not based on a gas phase mechanism since its composition is not affected by the presence of nano MgO.

The chemical reactions involved in the condensed phase have then been studied characterizing the residues obtained at the end of a mass loss cone calorimeter experiment. The intumescence process, leading to aromatic structures, has been evidenced in all PU formulations. The complete degradation of APP into phosphoric acid was observed for PU 30%APP. The incorporation of NPs, whatever its nature, in intumescent PU furthermore modify the chemical composition of the residues. Several mechanisms can explained those differences. Indeed, the NP could modify either the degradation pathway and/or the kinetic of APP degradation and/or its reaction with the PU matrix. Peaks corresponding to phosphonic acid, pyrophosphates and orthophosphates linked to aromatic carbons have been evidenced in PU/APP/NP residues. Reactions between APP and NPs occur as phospho-X compounds are detected in the case of MgO, SiO_2 and OMPOSS whereas nothing was detected with gold. In particular it was proven that all nano SiO_2 reacts with APP during MLC test. The repartition of species was also studied in the case of nano MgO containing systems. It reveals that high level of phosphorus and magnesium are mostly located at the bottom of the char. The formation of magnesium phosphates is moreover confirmed.

To conclude with, it has been shown that there is an obvious link between the chemical species formed in the condensed phase after burning and the fire performances exhibited by the formulation since each formulation leads to different chemical species and different fire properties.

The study of the conversion degree shows first that there is a link between a high char yield and good fire retardant properties. The mass kept during the experiment takes part in the intumescent process to form a protecting char. This phenomenon is affected by the presence of NPs and their reactions with APP, this is why shutter experiments have been performed and the residues analyzed. The progressive charring and degradation by depolymerization of virgin PU has first been followed. In PU 30%APP, the formation of phosphoric acid has been validated and a reaction between PU and APP is proved by the formation of orthophosphates linked to aromatic groups. In the case of PU/APP/nano MgO, the magnesium phosphates appear during the increase of HRR and their presence increases as the experiment pursue. The incorporation of nano MgO also leads to the formation of pyrophosphates. The influence of the ratio APP/MgO is furthermore pointed out here since the chemical species formed during the fire test are different varying the ratios.

Those results confirm that a clear link between the fire properties and the chemical reactions and more precisely the chemical species formed during PU/APP/nano MgO degradation.

Finally, the influence of heating conditions on the thermal stability and degradation pathway of PU 30%APP and PU 28%APP 2%nano MgO was finally discussed. The second degradation step evidenced a different behavior when varying the heating rates if we compare the formulations with or without nano MgO. On the other hand, the environment of chemical species formed in different conditions is drastically affected by the heating rate. At higher treatment temperature and heating rate, the formation of non-crystallized network is favored leading to a broadening of peaks. The nature of the formed magnesium phosphates also depends on the heating temperature. The heating conditions consequently play a role on the degradation of intumescent PU/APP with or without nano MgO as synergist.

In this section, it was first evidenced that the mechanism of action leading to synergy is a condensed phase mechanism. The chemistry in the condensed phase, the evolution and kinetic of formation of the chemical species takes indeed part in the synergy between APP and NPs. The synergy is however not totally elucidated by these aspects. Some questions indeed remains or need to be completed as for instance:

- why nano gold improves slightly the fire performances compared to PU 30%APP while it does not react with APP?
- why with OMPOSS the synergy is not as important as with nano silica while the same chemical species are involved?
- why a different synergy level is reached with nano MgO compared to nano SiO_2?
- why the incorporation of 1 or 2% of nano MgO lead to similar synergy and it is not the case at 5%?

Some physical properties may thus also take part in the synergy process and further explain the mechanism of action of the additives in PU. Considering the well-known intumescence process development, it will necessarily have an effect on the char aspect as we already seen on the residue pictures after MLC (**Chapter III, section 2.1-Fire performances determined by mass loss calorimetry p106**). Thus, in the following chapter, the interesting thermal barrier effect of PU formulations will be linked to char properties as its expansion, morphology and mechanical resistance.

Chapter V - Physical aspects leading to the synergy between ammonium polyphosphate and nanoparticles in polyurethanes

Chapter IV has first evidenced that the mechanism of action leading to synergy between APP and NPs in PU castings takes place in the condensed phase. The study of chemical interactions showed first that an intumescent residue is obtained while burning PU formulations. The incorporation of NPs, whatever its nature, in intumescent PU leads to the formation of additional species. APP may react with NPs to form phospho-X compounds. All the NPs furthermore modify the degradation pathway and/or the kinetic of APP degradation and/or its reaction with the PU matrix. An obvious link between the chemical species formed in the condensed phase after burning and the fire performances exhibited by the formulation was moreover assessed. Each formulation indeed leads to different chemical species and different fire properties. The chemical interactions and chemical species formed when NPs are added in intumescent PU might play a role on its physical properties and consequently on its fire performances. The intumescence process and properties of the resulting char might consequently be affected by the presence of synergist in PU/APP samples. This is particularly suspected because the pictures of the residues after cone calorimetry clearly evidence different char morphology (**see Table 13 p110 and discussion in Chapter III, section 2.1-Fire performances determined by mass loss calorimetry p106**).

This chapter will thus focus on the potential physical aspects that could lead to the synergy between APP and NPs in PU castings. This work will mainly be focused on nano MgO based formulations since they give the most interesting synergistic effect when combined with APP. PU and overall PU 30%APP will consequently be tested as references to compare the results with PU/APP/nano MgO systems. The first step of the investigation will be the evaluation of the thermal barrier effect provided by the formulations. The monitoring of insulation efficiency will first be performed on PU formulations during a cone calorimeter test and it will then be linked to the measurement of its thermal conductivity. The expansion and morphology of the char will then be analyzed. The char expansion will be monitored either during cone calorimetry or during rheological test. The morphology of the char will be studied thanks to 3D reconstructions provided by tomography. The use of this technique is relatively new in the field of flame retardancy and the results will show the possibilities offered by this powerful technique. Then a new method will be established to study the release of gases during additives degradation and compared to the TG results. It consists in recording the pressure applied on a plate while the sample is heated in the furnace of a plan/plan rheometer. Finally, the char strength of samples prepared with different heating conditions will be evaluated in a high temperature rheometer. The influence of the heating conditions on the char physical properties will thus been studied.

This approach should assess the role of the physical properties of the char in the synergy observed in fire properties between APP and NPs in PU.

1 THERMAL BARRIER EFFECT OF THE CHAR

The incorporation of fillers modifies the fire properties of virgin PU during a cone calorimeter experiment. The addition of APP allows the development of the intumescence process and thus the improvement of the fire performances of PU suggesting that the presence of a char provide a protective layer for the material. The substitution of a small quantity of APP by NPs leads to different char morphology and fire properties as well. This section will consequently investigate the thermal barrier effect provided by the different chars. The insulation efficiency will first be monitored and quantified by recording the back face temperature of samples during a cone calorimeter test. The second part is dedicated to the measurement of the thermal conductivity of PU formulations at ambient temperature and then as a function of temperature. The link between thermal conductivity and insulation efficiency will then be discussed.

1.1 Monitoring of insulation efficiency by recording temperatures in the samples

The insulation efficiency is recorded following the temperature at the back of the PU formulations with the method described in **Chapter II, section 3.1.5-Temperature measurements p95**. The thermal performance of an intumescent char is indeed determined by its insulation efficiency [169]. Evaluation of the temperature of the samples during a fire test is moreover important in order to link all data collected as a function of temperature to the results and properties determined during the fire tests [170].

HRR curves have first been plotted for all formulations and it was found that the presence of thermocouples does not modify the fire properties observed in the mass loss calorimeter.

Figure 109 presents the temperatures recorded at the back side of a sample during a cone calorimeter test on PU formulations. Before ignition (from 0 to 30 seconds, from 30 to 70°C) there is no effect of the filler on the temperature; the plate is not degraded and the behavior is consequently the same for all the samples. A huge increase of back side temperature is then observed for PU and PU 5%nano MgO because the plate is totally degraded and the thermocouple is partially in contact with the flame. For PU/APP with or without NPs, the char formation is clearly evidenced. It protects the material from the flame and plays the role of an insulative layer [61], from less to more efficient in the following order: PU 30%APP, PU 25%APP 5%nano MgO, PU 28%APP 2%nano MgO and PU 29%APP 1%nano MgO. The temperatures reached at 500 seconds are around 400°C for PU/APP/nano MgO formulations, 500°C for PU 30%APP and 650°C for PU and PU 5%nano MgO. These temperatures are the highest ones for PU/APP/nano MgO and PU/APP but not for PU and PU 5%nano MgO which reach a maximum of respectively 820°C and 750°C around 180 seconds. Taking into account the uncertainties, all the PU/APP/nano MgO have slightly the same effect to minimize the temperature increase at the back side of the plate. The PU 30%APP gives also a good protection but the performances are slightly worse than that with nano MgO in substitution of a small amount of APP. The back side temperature behavior against time is also different. A slight increase, nearly linear, is observed for PU/APP/nano MgO, there is no maximum. On the contrary, PU 30%APP formulation follows the behavior of virgin PU showing a significant increase starting at around 100 seconds up to 200 seconds but this temperature increase is slowed down by the char formation at higher time. Thus as fillers in PU, APP and a combination of APP and nano MgO do not exhibit the same protective behavior.

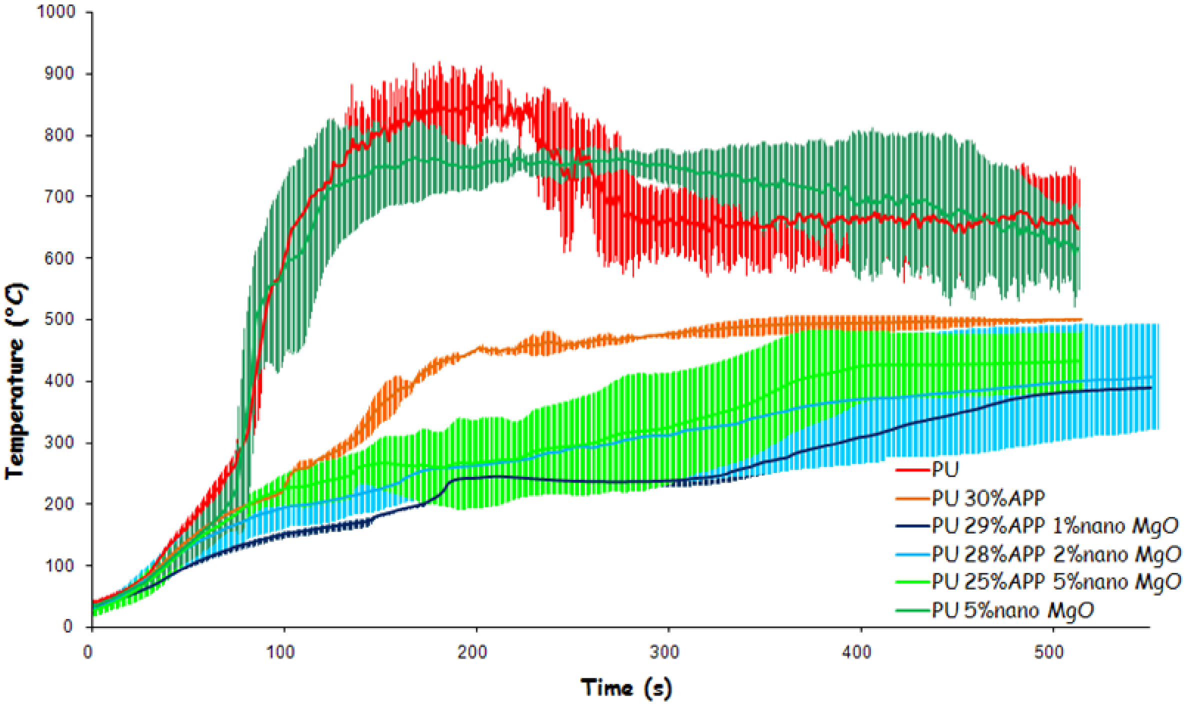

Figure 109: Back side temperatures (with vertical uncertainties based on 3 different trials) versus time recorded during cone calorimeter experiment on PU, PU 30%APP, PU/APP/NP (ratios 29/1, 28/2, 25/5) and PU 5%nano MgO

The back side temperatures evidence that APP and overall the combination of APP and nano MgO provide a thermal barrier effect attributed to the formation of a protective shield during cone calorimeter tests. A decrease of 250°C at the end and of 420°C at the maximum of the back face temperature is indeed observed for PU/APP/nano MgO formulations compared to virgin PU. From differences in PU/APP and PU/APP/nano MgO behaviors it appears that depending on the char formed, the protection is more or less efficient. Heat conductivity is one of the key factors that plays a role on the performances of coating in terms of thermal insulation [171]. Thus, it was decided to study this property on the PU formulations in the next section.

1.2 Thermal conductivity of PU formulations

Intumescent systems provide fire protection to the underlying material by the formation of an expanded char structure that leads to a significant reduced thermal conductivity, thereby contributing to the insulation function of the material. The last section evidenced that a thermal barrier effect is provided by incorporating fillers in the PU matrix. This result should be further explained studying the thermal conductivity of the PU formulations. Heat conductivity is linked to the performances of the coating since it reflects the ability of a material to conduct heat per surface and time units [172].

The thermal conductivity of virgin PU and PU containing APP and/or nano MgO has first been determined at ambient temperature by the Hot Disk method; the results are presented in **Figure 110**.

For most of industrial polymers, the thermal conductivity is at room temperature around (0.17 ± 0.04) W/K.m [12]. Generally, the thermal conductivity of a typical polymer melt is quite low, around 0.1 W/K.m, this being a thousand times less than most metals such as copper and aluminum [172]. In the case of virgin PU, the order of magnitude is in agreement with the literature. The virgin polymer has a thermal conductivity lower than those of all filled PU. Whatever the filler, the thermal conductivity of the material is similar. The thermal conductivity of solid polymers depends on the molecular structure and is influenced by polar and non-polar groups, by the degree of crystallinity, by the molecular orientation and the temperature [172]. It is important to know that the density of the material is a critical point in the measurement of thermal conductivity. The incorporation of fillers in a polymer matrix might change the density of the resulting material, thus having consequences on the thermal characteristics of the polymer. It is also possible that the filler itself has a higher thermal conductivity than the polymer, giving the filled polymer (in most cases) a higher thermal conductivity. The increase of thermal conductivity by incorporation of fillers in a polymeric matrix is a phenomenon already reported in the literature [173, 174]. The thermal conductivity of MgO measured alone is for instance very high (between 3 and 5 W/m.K) [175] compared to the one of PU formulations. According to the differences in thermal conductivity value of initial materials, it is not surprising that the filled PU will conduct differently the heat.

On the other hand, when dealing with intumescent material, it is interesting to study the evolution of thermal conductivity with increasing temperature. Very few articles in the open literature deal with the measurement of thermal conductivity at high temperature of intumescent material. This is however important because during fire tests, the temperature of the material is changing and the fire properties are partly characterized by the ability of the material to release or keep the heat. The incorporation of fillers such as flame retardant (APP) and synergist (nano MgO) give a particular burning behavior to the PU; this might be linked to their thermal conductivity evolution against the temperature which is plotted in **Figure 111**. As introduced in **Chapter II, section 2.3.4-Thermal conductivity p83**, due to experimental restrictions, the measurements were only performed on PU 30%APP and PU 28%APP 2%nano MgO. They are indeed the most important formulations in order to evaluate the synergistic effect brought by the NPs.

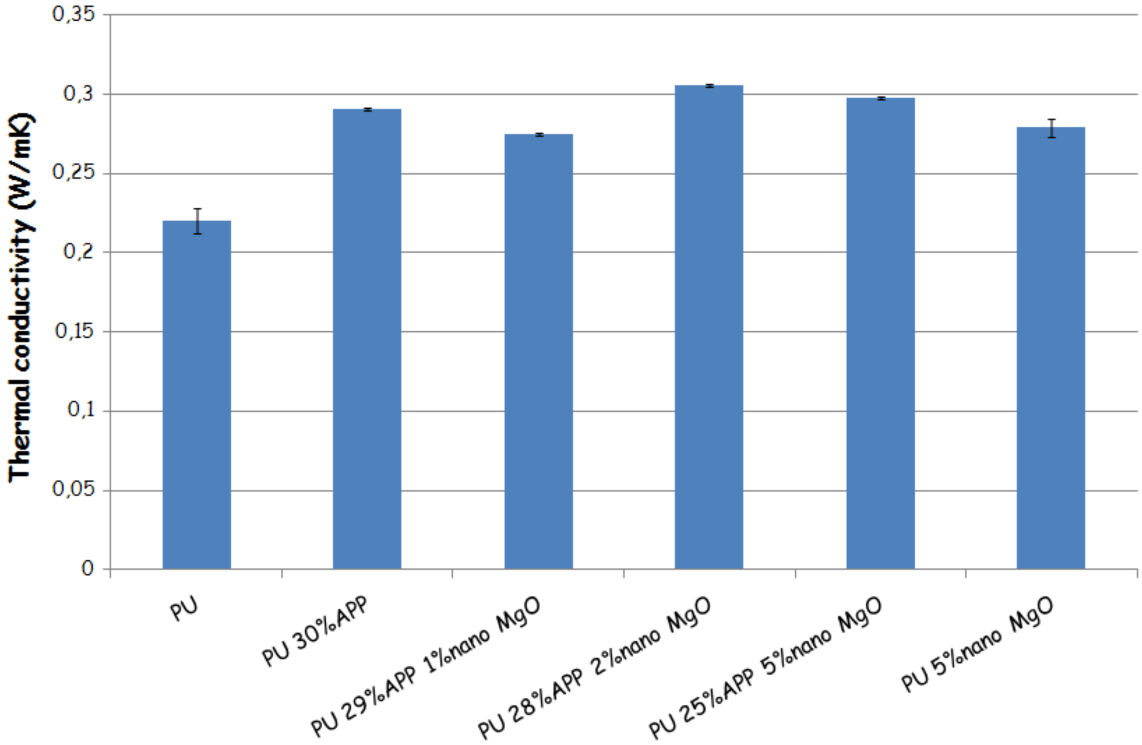

Figure 110: Thermal conductivity at ambient temperature of PU, PU 30%APP, PU/APP/nano MgO (ratios 29/1, 28/2 and 25/5) and PU 5%nano MgO *(the uncertainties take into account the repeatability between two experiments)*

The profile of the curves and order of magnitude of the thermal conductivity values (**Figure 111**) are the same for both formulations and are similar than those obtained for different fire retarded polymers already tested in the laboratory [176]. At low temperature (< 200°C), the thermal conductivity is stable; then it decreases significantly with a minimum value obtained at around 400°C. Finally the thermal conductivity increases as a function of temperature; exhibiting more or less a linear behavior after 550°C. This behavior as well as the thermal conductivity values are in total agreement with the modeling of heat transfer performed for a formulation of PP/APP/PER [177].

From ambient temperature to 200°C, the thermal conductivity of materials is not really affected by the temperature because the degradation process has not started considering the heating ramp applied to the sample (around 1.5°C/min) (**see TG curves in Chapter IV, section 4.1-Effect of heating rate on the thermal stability of PU formulations p161**). The point at 200°C was however difficult to acquire probably because of rheological modification of the PU formulations around this temperature. The thermal conductivity of the polymers indeed changes after glass transition and melting temperatures due to the greater mobility of the polymer molecules [172]. On the other hand, the viscosity modifies the contact between the probe and the material leading to different values of thermal conductivity, thus increasing the uncertainties at 200°C.

Upon heating, an intumescent material softens and produces gas that inflates the material to produce a highly porous, low thermal conductivity char [169, 178]. This is the phenomenon observed after 200°C when the thermal conductivity decreases. J.E.J Stagg [179] determined thermal conductivities of intumescent char containing 60% of fillers by numerical simulation; he demonstrated that the values vary from 0.1 W/m.K to 0.4 W/m.K from ambient temperature to 600°C. This is in the same range of values that those observed in **Figure 111** for chars filled at 30%.

The formation of the char is thus clearly evidenced by the observation of a decrease in thermal conductivity as a function of temperature and this is concomitant with the back face temperatures recorded (**Chapter V, section 1.1-Monitoring of insulation efficiency by recording temperatures in the samples p170**). During these experiments under cone calorimeter, the char expansion is however different between PU 30%APP and PU 28%APP 2%nano MgO. Since the char act as an insulative layer, the more it is expanded, the better the insulation properties if enough material is contributing to the protection. The thermal conductivity presented in **Figure 111** reveals the properties of the chars without taking the expansion into account since the thickness of the char is limited because of the sample holder. The char expansion, which is also a critical parameter for thermal insulation, will be studied in the next section of this chapter (**Chapter V, section 2.1-Monitoring of char development through its expansion p176**).

A significant difference is observed after 350°C by comparison between PU 30%APP and PU 28%APP 2%nano MgO samples. Considering that the experiments have been carried out exactly in the same way, this difference has to be linked to the samples properties, and especially to the char properties since it is already developed at 350°C. The porosity of the char is a critical parameter for the thermal conductivity properties [179]. When an intumescent formulation expands at high temperatures, numerous bubbles are created and it is clearly not possible for these bubbles to develop with the same size and to be uniformly dispersed [180]. This will affect the thermal conductivity of the materials and the value recorded at one temperature is a combination of the effect of each bubble. At 400°C, the thermal conductivity of PU 30%APP is of 0.13 W/m.K whereas the one of PU 28%APP 2%nano MgO is lower (0.05 W/m.K). The intrinsic properties of the chars developed by PU 30%APP and PU 28%APP 2%nano MgO are clearly different at 400°C. This should be due to a difference in the morphology of the char exhibited by these two formulations and this will be further studied by tomography in the next section (**Chapter V, section 2.2-Image reconstruction of char morphology by tomography p181**). According to the fact that the smaller the cells, the lower the thermal conductivity [180]; the char formed from PU 28%APP 2%nano MgO should exhibit smaller cells than the one from PU 30%APP when chars are obtained with the heating rate used in the thermal conductivity equipment.

After 400°C the thermal conductivity of both formulation increases with the temperature. Between 400 and 550°C, a second decrease of thermal conductivity is noticed around 500°C and it is more pronounced for the PU 28%APP 2%nano MgO. After that a linear increase is observed for both formulations.

Since the higher the thermal conductivity, the higher the heat transfer; the char formed from PU 30%APP should allow the material to conduct better the heat. In order for an expanded char to protect a substrate as efficiently as possible for a given heat flux, the thermal conductivity at a given thickness must be as small as possible [179]. Since the thickness is considered equivalent for both formulation due to the device used for measuring thermal conductivity, this means that the char resulting from PU 28%APP 2%nano MgO performs better to protect a substrate than the one from PU 30%APP from 400 to 800°C. This result was expected since the temperature monitored at the back side of a PU containing APP and nano MgO was lower than for PU/APP in a MLC. The evolution of the thermal conductivity of both char with the temperature is similar but their thermal barrier properties are significantly different.

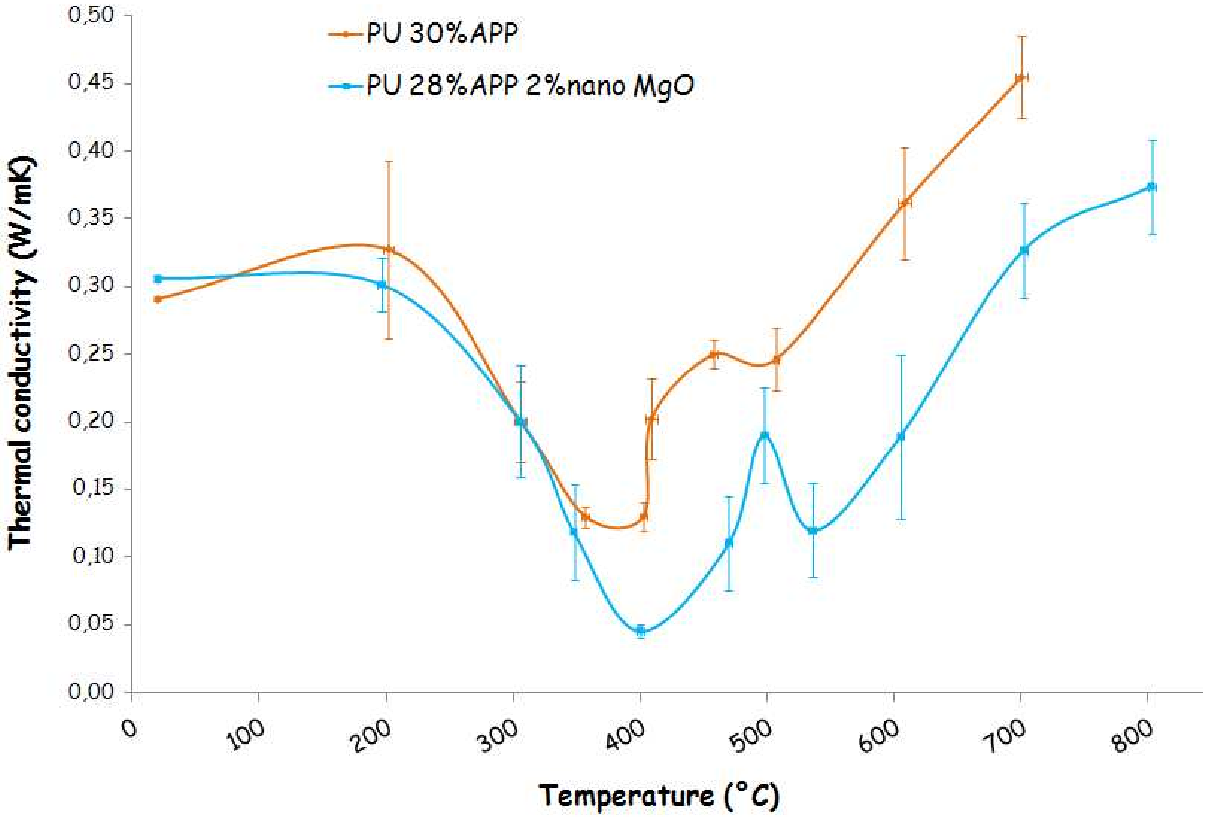

Figure 111: Evolution of thermal conductivity as a function of temperature for PU 30%APP and PU 28%APP 2%nano MgO

The study of thermal conductivity at ambient temperature and particularly as a function of temperature reveals that this parameter is linked with the insulation efficiency observed in MLC experiments. The incorporation of fillers in PU will allow the material to conduct slightly better the heat at ambient temperature. The materials behavior against a temperature increase was then monitored and shows that efficient fire protection is obtained for both PU/APP and PU/APP/nano MgO. With incorporation of APP in the PU matrix, a thermal barrier effect is observed protecting the residual material. By substitution of a small amount of APP by nano MgO, this phenomenon is also observed and further enhanced resulting in a better fire protection. This is due to the intumescence process creating chars characterized by a low thermal conductivity. In identical testing conditions, the char resulting from heat treatment of PU 28%APP 2%nano MgO performs better to protect a substrate than the one obtained from PU 30%APP in the temperature range 400 to 800°C. Since the thickness and morphology of the layer are also critical parameters for providing thermal protection to a substrate, they will be presented in the following section.

2 EXPANSION AND MORPHOLOGY OF THE CHAR

The last section has evidenced that the thermal barrier efficiency and the thermal properties of intumescent PU at high temperatures are affected by the presence of a small amount of nano MgO. This is probably due to a modification of the char properties induced by the presence of NPs. That is why the char characteristics will now be studied in this section (expansion and morphology of the chars) and the following one (mechanical behavior of the char).

This section will be organized into three parts. The first one will focus on following the char development by monitoring its expansion via two methods: the expansion is measured on shutter samples from MLC experiments or is recorded during a slow and regular temperature increase provided in a furnace. The second part will present the 3D reconstructions of chars obtained by tomography. This technique gives a full observation of the inner structure of the chars without damaging their structure. Very few studies have been performed at the moment to characterize precisely the char morphology; the work described in this part looks promising and required lots of efforts to manage to go into such details. The last section presents an original method developed to study the release of gases during additives degradation. This property may affect the morphology of chars since the flow rate and distribution of gases could interfere with the char development.

2.1 Monitoring of char development through its expansion

The intumescence process [60] consists in an increase of volume under a temperature increase, it results in the formation of an expanded multicellular barrier (the char), which is able to protect the residual material from the flame [76, 155]. If gases are not trapped during thermal decomposition, they may contribute to the development of fire (production of evolving flammable gases). On the contrary, if their trapping occurs, this should result in the swelling of the residue [85]. In particular, it was discussed in the last part that the thickness of an intumescent char is a critical parameter associated with the effective thermal conductivity to give thermal protection to a substrate [178, 179]. This section aims to quantify the swelling occurring during the intumescence process. Two techniques will be used for that purpose; the expansion will either be recorded during a cone calorimeter test or during a rheological test. In the first case, the expansion will be measured as a function of time on samples collected from the shutter experiment. In the second case, the expansion will be recorded as a function of temperature while heated in a furnace. These two results will be confronted to conclude on the swelling behavior of the samples during their char development.

2.1.1 Expansion recorded during MLC experiment

The measurement of expansion as a function of time during a cone calorimeter experiment is one way to characterize the intumescence phenomenon and to compare the different formulations together. It has been recorded on the samples collected during the shutter experiments (**see Chapter II, section 3.1.2-Shutter experiments p93 and section 3.1.4-Expansion p94 for the methods details**). The HRR curves, residue pictures and corresponding expansion data recorded are given in **Appendix 2: Results obtained from shutter experiments on PU, PU/APP, PU/nano MgO and PU/APP/nano MgO formulations p241**. The evolution of expansion as a function of time is drafted in **Figure 112**.

There is no real expansion for PU and PU 5%nano MgO; this was expected because all the ingredients required for intumescence are not present in those formulations.

On the contrary, PU/APP and PU/APP/nano MgO exhibit a volume increase as the cone calorimeter experiment is running. According to shutter results, PU/APP and PU/APP/NP do not have the same intumescence behavior since the evolution of expansion as a function of time is different for these formulations.

With NPs, the beginning of expansion occurs at a lower time compared to the sample without NPs. The same remark was made for the ignition time, leading to conclude that the decomposition process starts faster while nano MgO is incorporated in intumescent PU.

For PU/APP a huge increase is observed at the beginning of the fire test (during the first minute especially) and then the speed rate is slowed down until reaching the final expansion value of 1100% at 200 seconds.

For all PU/APP/NP formulations, a slowdown of char height is noticed between 60 and 100 seconds. This slowdown might be due to a modification of the chemical composition of the char. For example, it has been proved in the previous chapter (**Chapter IV, section 3.2-NMR analysis of residues collected from shutter experiments on PU formulations p154**) that magnesium phosphates appear during the increase and are, after that, more and more present which correspond exactly to the range of time where the slowdown appears. Maybe the magnesium phosphates or the reaction to form them induce a char reorganization leading to a char development in “two steps”. Then, in the second step, the expansion increases again until the final char height is reached. From the pHRR until the point at 180 seconds, the rate of expansion is once again high as it was during the first expansion step. Finally the char height increases slightly for PU 28%APP 2%nano MgO or even nearly stay the same until the end for PU 29%APP 1%nano MgO and PU 25%APP 5%nano MgO.

Other slight differences are moreover observed in PU/APP/nano MgO formulations depending on the ratio APP/NP considered. For PU 28%APP 2%nano MgO, the slowdown starts after ignition while it is delayed until the increase of HRR for the two other ratios. In other words, the first expansion step shows its maximum at 42 seconds for the ratio 28/2 and 55 seconds for the ratios 29/1 and 25/5. The height of the char from PU 25%APP 5%nano MgO never decreases during the cone calorimeter experiments on the contrary of the chars obtained for the two other ratios (for PU 28%APP 2%nano MgO, point “during increase” is lower than the point “after ignition” and for PU

29%APP 1%nano MgO, the point "pHRR" is lower than the point "during increase"). Then the behavior of all PU/APP/nano MgO formulations is similar except that the char height increases again after 180 seconds only for the ratio 28/2.

The final expansion discriminates once again the formulations: the char formed from PU 28%APP 2%nano MgO is the highest (2100%), then comes PU 29%APP 1%nano MgO and PU 25%APP 5%nano MgO (≈1700%) and finally PU 30%APP (1200%). This trend is in agreement with the fire properties exhibit by the formulations and discussed in **Chapter III, section 2.3-Summary table of fire performances depending on the nanoparticles and ratios used p113**.

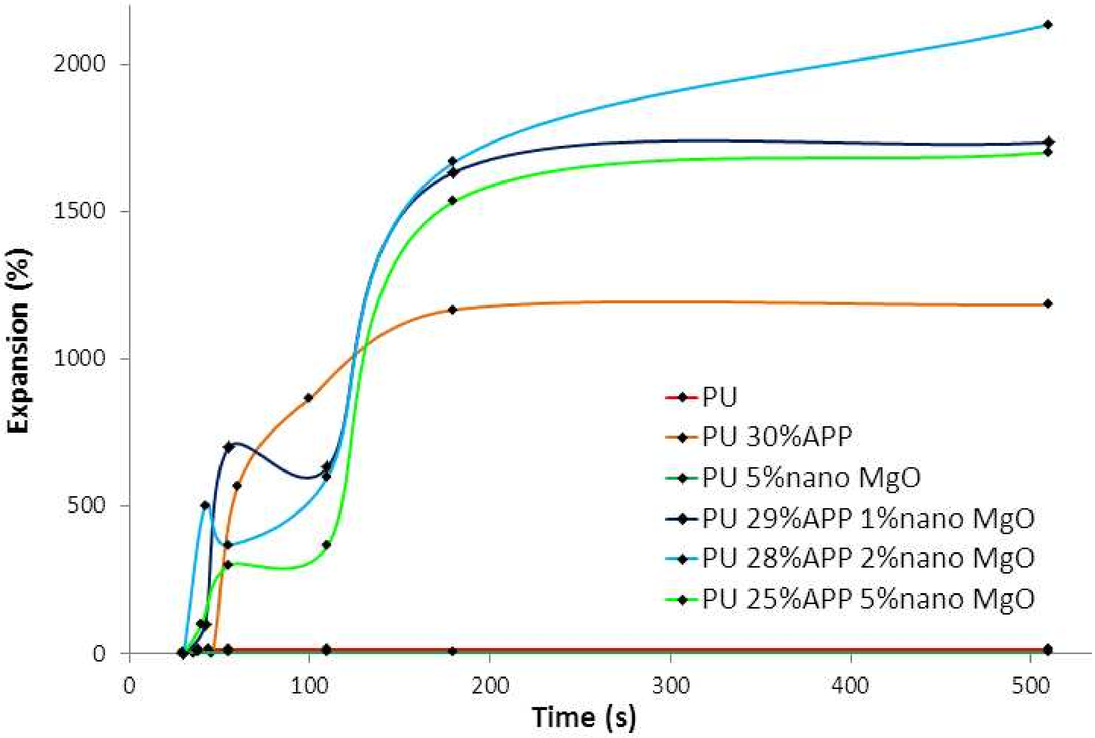

Figure 112: Expansion followed as a function of time during cone calorimeter experiment for PU, PU/APP, PU/APP/nano MgO (ratios 29/1, 28/2, 25/5) and PU/nano MgO

The different swelling behavior between the formulations is in agreement with the different char aspect observed (see residue pictures in **Appendix 1: Residue pictures taken at the end of a cone calorimeter test on PU, PU/NP, PU/APP and PU/APP/NP formulations p235**). In every case, the structure is maintained until the end of the test, attesting of a certain char hardness [110]. These first results on the swelling show that the development of the protection is drastically affected by the presence of nanoparticles; nano MgO indeed modifies the swelling process of intumescent PU and increases the height of the final structure.

2.1.2 Expansion recorded during rheological test

A second experiment was carried out to record the swelling during intumescence process. Expansion has been followed as a function of temperature on PU, PU/APP, PU/APP/NP (ratios 29/1 and 28/2) in a high temperature rheometer using a heating ramp from ambient temperature to 500°C at 10°C/min (**see conditions in Chapter II, section 2.5.2-Expansion measurements on polyurethane formulations p88**). The formulations PU 25%APP 5%nano MgO and PU 5%nano MgO has not been tested here because thin samples were required to work in the rheometer and this was very difficult to prepare at high NP content.

Even though the equipment used was optimized for our experiments (**Chapter II, section 2.5.2**-**Expansion measurements on polyurethane formulations p88**), the char formed with the heat treatment goes out by the sides of the sample holder as it could be seen on the pictures taken after the test (**Figure 113**). Moreover, since the experiments are obtained applying a normal force of the sample, the expansion values are not only representative of the expansion of the material but also of its strength. All the data were acquired in the same conditions; it is thus possible to compare the evolution of expansion versus temperature for all formulations.

In every case, charring is observed at the end of the test (T = 500°C) but the aspect and morphology is different from one sample to another. Virgin PU residue is bright black, very brittle and fragile. When APP is added, the color changes to grey but the char is still bright, sticky and a little brittle. With the incorporation of a small quantity of nano MgO, the char appears harder. These first observations will be verified and quantified in a further section measuring the strength of the char (**Chapter V, section** 3-**Mechanical Behavior of the Char p205**).

PU

PU 30%APP

PU 29%APP 1%nano MgO

PU 28%APP 2%nano MgO

Figure 113: Pictures of the residues at 500°C from PU formulations collected after rheological measurements in a high temperature rheometer

The evolution of expansion as a function of temperature is plotted in **Figure 114** for PU formulations. From 25 to 270°C, a slight linear increase in the expansion is observed, which is due to the sample holder expansion. It is nevertheless noticeable that an inflexion point is observed between 40 and 60°C, that could be attributed to the glass transition of the materials (**Chapter III, section 1.3-Influence of additives on the glass transition temperature p103**). The expansion decreases because the properties of the material change in this range of temperatures leading to a lower gap between the two plates. After 270°C, only one expansion peak is observed for the virgin PU (maximum at 375°C) whereas two peaks around 325°C and 400°C are recorded for the filled polymers. The PU expansion seems to occur slowly and its peak is observed in the range of temperature corresponding to an average value of the two peaks of degradation observed for the filled PU. The charring (charring is associated with the measured expansion) is recorded first for filled PU which is concomitant with the fact that PU/APP(/NP) degradation starts at a lower temperature than the degradation of the PU alone (**Chapter III, section 3.3-Thermal stability of PU formulations p124**). This behavior can also be linked with the shorter TTI and to the fact that expansion measured in MLC conditions starts at lower time for PU formulation. It is thus proven that the flame retardant modifies the PU degradation and consequently the intumescence phenomenon. It is quite surprising to have two expansion peaks for the filled PU if it is assumed that expansion means char formation. Two explanations for this observation are thus possible. The first peak may only be due to the release of gases that pushes the upper plate and lead to an increasing gap; and after the real charring is observed. It is also possible that a first charred structure is formed and its resistance is not sufficient enough to support the normal strength of the upper plate of the apparatus, leading it to collapse [181]. With increasing temperature the charring is reinforced and a second expansion peak is visible. In the end, with increasing temperature, the chars formed from all formulations collapse.

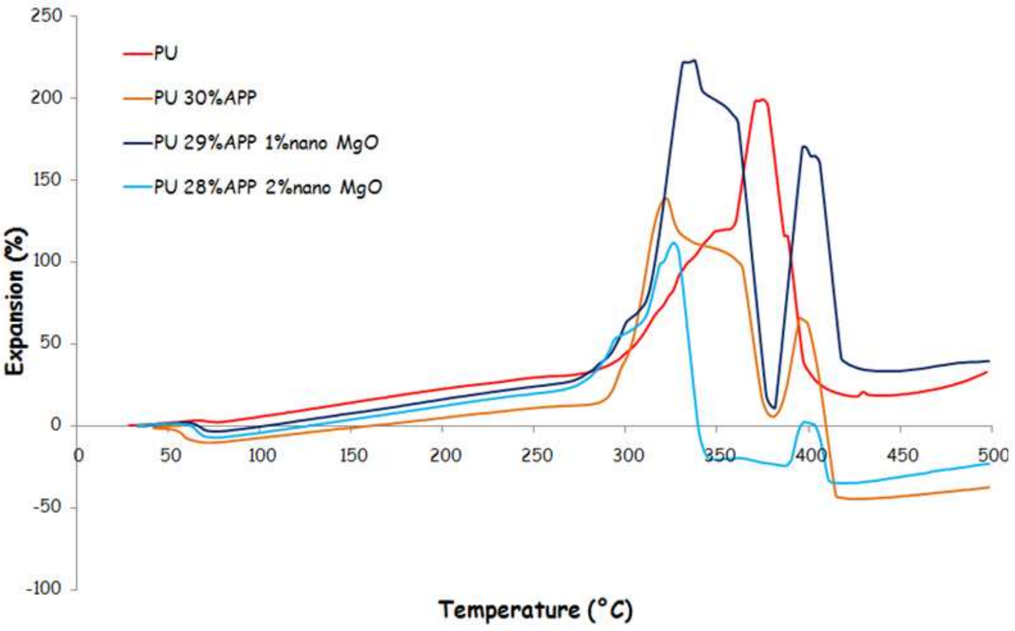

Figure 114: Evolution of expansion as a function of temperature measured at 10°C/min in a rheometer for PU, PU/APP, PU/APP/nano MgO (ratios 29/1, 28/2)

The main information to keep from this experiment is that virgin PU behaves differently from filled PU in terms of charring; especially concerning both the temperatures and behaviors. The nano MgO does not seem to have any influence on the properties of the intumescent PU until 500°C as the expansion evolution do not present any significant differences between the formulations PU/APP and PU/APP/nano MgO tested in the rheometer conditions. The char aspect is however different and this is linked to a different chemical composition of the material as evidenced in the last chapter

(**Chapter IV, section 4.2-Chemical characterization of PU formulations degraded with different heating conditions p163**).

The char development has been followed by recording the expansion as a function of time and temperature in two different heating conditions. The formulations without APP (PU and PU 5%nano MgO) does not expand during cone calorimetry since they do not contain the ingredients required for intumescence. All the formulations containing APP and eventually nano MgO, lead to the formation of a char and improve significantly the fire properties of virgin PU. By following the expansion as a function of temperature, PU/APP and PU/APP/nano MgO formulations present similar behaviors, expect in the case of MLC conditions where PU/APP present a one step behavior whereas two steps are observed for PU/APP/nano MgO. This may be the result of the different chemical species that are formed at characteristic times of the experiment as demonstrates in the previous chapter. It appears thus that expansion may have a slight effect on the synergy observed in fire performances between APP and nano MgO in PU castings. The expansion is one criterion but it is also the result of the structuring of the material upon heating. The next section will consequently deal with the char morphology of PU formulations during cone calorimeter tests. Some image reconstructions are provided by tomography and will give a full picture of the inner organization of the chars.

2.2 Image reconstruction of char morphology by tomography

This section will present the results of an innovative work to obtain a full view of intumescent systems. The **section 2.1-Fire performances determined by mass loss calorimetry p106 in Chapter III** evidenced that depending on char aspect the fire performances of PU/APP/NP formulations are modified. The char properties were indeed presented as clearly involved in the fire protection because it seems to exist an optimum char aspect (the one obtained with PU/APP/nano MgO at ratios 28/2 and 29/1) for which the fire properties are significantly better. It is then worthy to investigate the particularities of the char morphology more deeply.

Digital microscopes are a variation of a traditional optical microscope that uses optics and a charge-coupled device (CCD) camera to output a digital image to a monitor. The interesting property of this microscope is to allow getting a clear view of residues obtained after burning [85]. In order to use this technique to characterize the inner char aspect, a small piece of the interior of a char is required. With PU/APP or PU/APP/NP systems it is however impossible to cut properly a slice of char staying in one piece and consequently the use of digital microscope will be useless. In order to find an alternative to this problem and investigate the inner structure of the char, the tomography appears as the best technique since X-ray absorption tomography is a non destructive technique providing image reconstructions for a section of a three dimensional object. Apart being used for medical diagnostic tool, the tomography is quite a new technique in material science but the development of methods is constantly in progress [182, 183]. Tomography recently found its interest in fire related topics. In particular, L.G.Butler is working on developing new tools and methods for using tomography in fire retarded polymers since 2002 [184]. His research shows that it is possible to visualize key polymer additives in 3D without damaging the polymer or test sample. Consequently the first topic of interest was the dispersion of additives in the polymer matrices and many spectroscopic and mathematic tools were developed in this way [103, 104, 184-190]. To go into much more details about the polymer degradation during burning, the 3D visualization of char is now of great interest [105-107, 179]. In the few communications on the subject, the study of char and/or charring process by computing the morphology thanks to tomography give useful information to understand the processes. That is why this section is devoted to the investigation of the several char morphologies.

The selection of judicious samples to analyze was the first step of this study since the tomography experiments are expensive and time consuming. The tomography will be performed on chars developed during MLC tests. They indeed represent the highest differences between the samples. Since the goal of the project is to find out what causes the synergy between APP and NPs in a PU matrix, the formulation PU 30%APP was chosen to be compared to PU/APP/NP systems. The first selected PU/APP/NP sample is PU 28%APP 2%nano MgO because it is the best performing and widely studied formulation. The intumescence process of these two materials was furthermore studied analyzing the char at different step of the cone calorimeter test: during increase of the HRR, during decrease of the HRR and at the end of cone (**see these points characteristic in Chapter II, section 3.1.2-Shutter experiments p93 and Chapter IV, section** 3-**Evolution of Species Formation During the Cone** Calorimeter **p149**). These points were found to be interesting and enough expanded according to the data of expansion followed during a cone calorimeter test presented in the previous section. Two other parameters were found interesting to study: the effect of the ratio and of the nature of the NP; this was possible with respectively the formulations PU 25%APP 5%nano MgO and PU 28%APP 2%nano gold. The ratio 25/5 with nano MgO was preferred compared to 29/1 because the sample PU 25%APP 5%nano MgO exhibit different fire properties compared to the ratios 28/2 or 29/1. The formulation with gold was chosen because it does not react with APP during cone calorimeter experiment. All these samples lead also, at the end of a cone calorimeter test, to a different char aspect from a visual observation; that is why to investigate and to compare their morphology is relevant.

HRR curves have first been plotted for all formulations and it was found that the general trend of fire performances was respected for the samples chosen for the tomography experiments. Expansion, residual mass and visual observations are also in agreement with the data collected and presented in **Chapter II, section 2.1-Fire performances determined by mass loss calorimetry p106**. The following analyzes of char morphology have consequently been monitored on samples exhibiting the following increasing order of fire performances: PU 30%APP, PU 25%APP 5%nano MgO, PU 28%APP 2%nano gold and PU 28%APP 2%nano MgO.

The principle of tomography and its application to study chars were explained in **Chapter II, section 2.4.2-Tomography p84** but elementary informations are discussed here in order to present the results. In our case, the tomography allows the collection of two important data:

- 3D images and reconstruction of the inner structure of the char
- repartition of the fillers in the polymeric matrix

For the first point, many pictures (2000 projections by sample) were acquired and they give a repartition of matter and holes as a function of (x,y,z) in the sample thanks to a rotation over 360°C.

The second point refers to the grayvalue that will provide a mapping of particles. The grayvalue of a voxel in the reconstructed images corresponds to the average attenuation coefficient of the material inside the voxel. This means that a voxel containing only PU will show a relatively low grayvalue, while voxels containing PU and fillers will show a higher grayvalue (**refer to Chapter II, section 2.4.2-Tomography p84 for more precise explanation**).

The size of the unitary particles found in the chars (APP, nano MgO, nano gold, magnesium phosphates) are generally smaller than a voxel size (around 76 µm) which corresponds to the resolution of the image. It is then not possible to isolate the particles and to quantify them separately. The grayvalue is nevertheless affected by the presence of particles in the PU matrix that makes possible to evaluate the distribution of particles in the char.

On the pictures, this grayvalue is symbolized by a color scale to ease the visualization. The PU matrix is consequently symbolized in gray while the particles appear in a scale from yellow to red. While going from yellow to red, it means that the area considered may either contain more particles or contain particles with a higher difference of atomic number compared to the PU elements. With the selected samples, the elements present are given in **Table 18**.

The PU matrix made up of carbon, nitrogen and oxygen has consequently the lower Z and so the lower grayvalue. On the contrary phosphorus, magnesium and gold will increase the grayvalue and will appear in yellow. Magnesium and phosphorus are too close in the periodic classification to see a contrast difference between these two elements. It has moreover been proven that APP and nano MgO react together to form magnesium phosphates (**Chapter IV, section 2.1-Solid state NMR on burned residues from PU formulations p138**). It is also reasonable to suspect that all nano MgO has reacted since it was calculated that the phosphorus is in large excess compared to the magnesium. It was moreover demonstrated in the case for nano silica. Consequently for the char taken at the end of cone calorimeter, magnesium phosphates should be detected and it is unfortunately also impossible to isolate the magnesium phosphate from the phosphorus coming from APP and/or its degradation products and/or the products coming form its reaction with PU. Nano gold is significantly higher in the peridodic classification and also do not react with APP according to ^{31}P solid state NMR (**Chapter IV, section 2.1-Solid state NMR on burned residues from PU formulations p138**). This particle may thus be differentiated from APP and contributes to a higher increase in the grayvalue.

Table 18: Chemical elements present in PU/APP and PU/APP/NP formulations

	PU 30%APP	PU25%APP 5%nano MgO	PU 28%APP 2%nano MgO	PU 28%APP 2%nano gold
Carbon (Z=6)	X	X	X	X
Nitrogen (Z=7)	X	X	X	X
Oxygen (Z=8)	X	X	X	X
Magnesium (Z=12)		X	X	
Phophorus (Z=15)	X	X	X	X
Gold (Z=79)				X

All the treated images have been brought together to record a movie to see the full inner structure of the char. A CD with the 3D animations for all char samples tested is attached to this Ph.D manuscript. In order to have some illustrations of these movies directly in the text, some pictures have been extracted from the movies and are presented below. They have been taken approximately at the (x,y) slice corresponding to the higher height of the considered char (nearly the middle of the sample). At the bottom and on the sides of the samples, the aluminium foil used for cone calorimeter can be seen. It was let for the analysis because it was to difficult to get rid of it without damaging the char. The interferance of the aluminium for the grayvalue calculation is minimized due to the low quantity of aluminium and the image treatment chosen. It is moreover possible to observe that the PU plate is not totally degraded depending on the samples and the heat treatment performed. The unburned PU matrix then appears yellow because it is denser than the char. The yellow uniformity in this area prevents the detection of particles in this area. Finally, in the event of a located orange or red point, this nevertheless means that a denser particle is detected in this spot.

The graph of average grayvalue as a function of height has been recorded for each sample. The grayvalues have been extracted from the 3D sections of the chars, it is the result of an average for each (x,y) slice. In the case of curved samples or unburned polymeric matrix, the grayvalue cannot be collected at low height; the monitoring of the grayvalue is thus delayed.

These information will now be discussed in the two following sections. The first one deals with the effect of the incroporation of NPs on the morphology of intumescent PU. The second one will present the evolution of the char morphology during the intumescence process of intumescent PU with or without NPs.

2.2.1 *Effect of nanoparticles on the morphology of intumescent PU*

This first part will study the morphology of the chars taken at the end of a cone calorimeter test for PU 30%APP, PU 25%APP 5%nano MgO, PU 28%APP 2%nano gold and PU 28%APP 2%nano MgO. The aim is first to study the effect of the incorporation of NPs in PU 30%APP; of the ratio APP/NP and of the nature of the NP on the char morphology.

The pictures of the inner structure of chars collected at the end of a cone calorimeter test are presented in **Figure 115** to **Figure 118** respectively for PU 30%APP, PU 28%APP 2%nano MgO, PU 28%APP 2%nano gold and PU 25%APP 5%nano MgO. Clear differences are evidenced while looking at the inner structure of all formulations. The external char surface, which will be called “crust” in the following text, is also different depending on the samples.

The PU 30%APP morphology is characterized by an irregular surface but more homogeneous inside. An equivalent aspect is indeed obtained whatever the image considered. The inner structure is composed of big bubbles separated with thick porous walls.

The PU 28%APP 2%nano MgO presents on the contrary a regular surface of a material highly expanded. Inside the char, two distinct structures are observed: at the bottom, there are many bubbles of various sizes separated by thin walls; on the top, only one or two huge bubbles are observed. The crust aspect is also totally different compared to the PU 30%APP structure and the walls are generally thinner than the one of the PU 30%APP char. In particular the crust is very thin at the top of the char where huge bubbles are observed while the walls between bubbles are thicker at the bottom of the char where many cells are organized.

Concerning the char obtained from PU 28%APP 2%nano gold, the surface is irregular as it was the case for PU 30%APP. On the videos, it appears that many polymers remain unburned on the sides of the char. In this area, it is moreover possible to detect some orange/red points dispersed in the unburned PU matrix; this is attributed to the presence of gold. In the char, the bottom and side structure appears to be composed of small cells whereas in the middle, larger holes are visualized.

For PU 25%APP 5%nano MgO, the surface is regular and seems thicker compared to the three previous formulations and especially the PU 28%APP 2%nano MgO. The bottom of the char is not flat. The char structure is first composed of a compact layer at the bottom. Then while increasing the height, the sample is more aerated and shows some big cells. Once again a compact layer is observed around a height of 35-40 mm. Finally at the top of the char, a big hole is obtained.

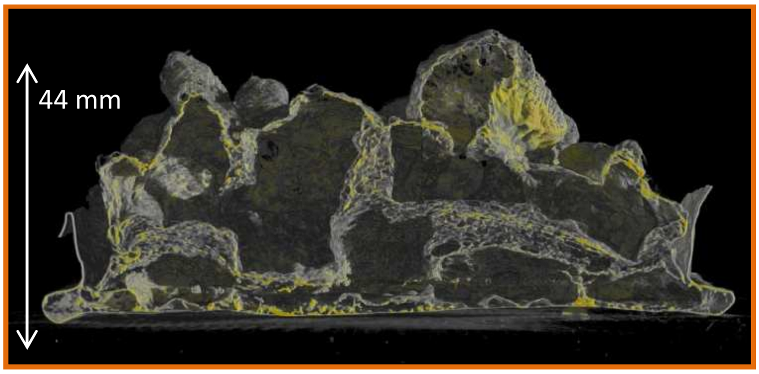

Figure 115: Picture of the inner structure of the char from PU 30%APP collected at the end of a MLC test

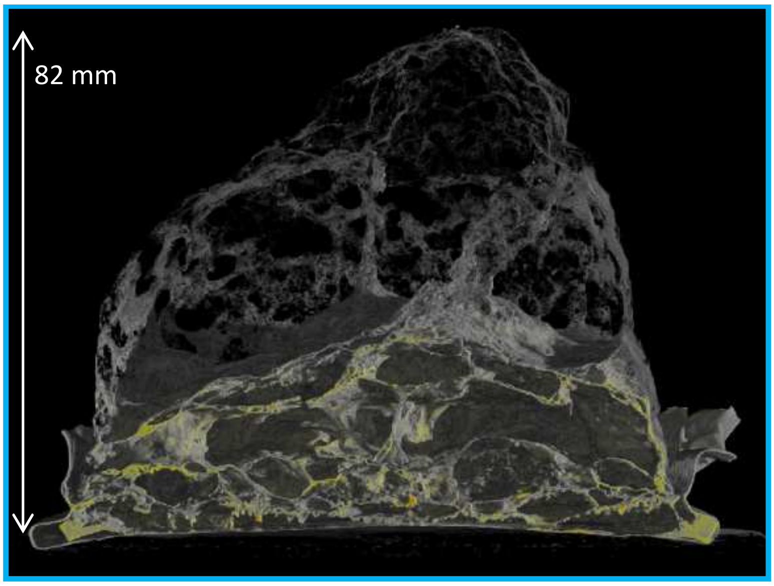

Figure 116: Picture of the inner structure of the char from PU 28%APP 2%nano MgO collected at the end of a MLC test

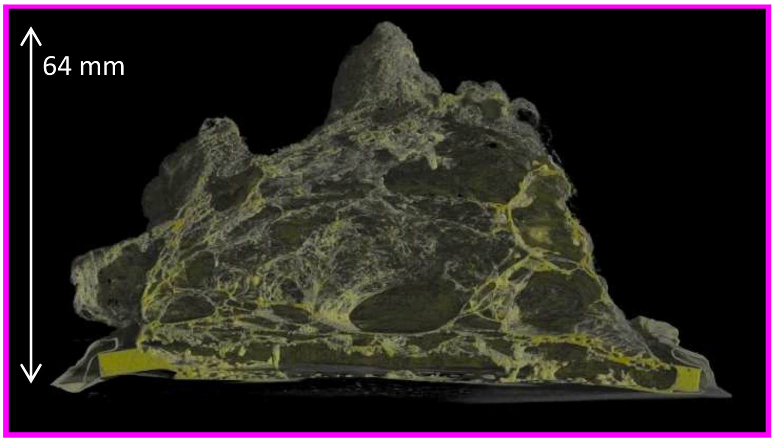

Figure 117: Picture of the inner structure of the char from PU 28%APP 2%nano gold collected at the end of a MLC test

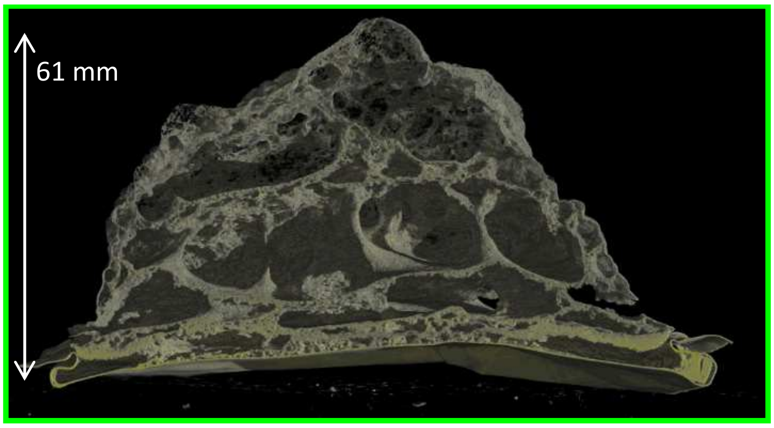

Figure 118: Picture of the inner structure of the char from PU 25%APP 5%nano MgO collected at the end of a MLC test

The incorporation of NPs, whatever its nature and amount, modifies the morphology of the char obtained with PU 30%APP at the end of a MLC experiment. The expansion, the size, number and repartition of cells, the walls thickness, the aspect and size of the crust are indeed affected by the presence of NPs. The ratio APP/NP and the nature of the NP also change the char morphology. All the materials are anyway highly porous and typical intumescent char's structure are obtained whatever the formulation [60, 78, 179]. These materials are nevertheless highly performing against fire, meaning that a compact char morphology with small cells is not crucial in our study. Especially the PU 28%APP 2%nano MgO exhibit the bigger cells and in general the less compact structure but was the better fire performing material. Since each char visualized here has different fire behavior and morphology, it is reasonable to assume a link between the morphology of the char and its fire performances. It is however difficult to establish, from these pictures, morphologic criteria leading to high fire performance materials. The only particularity found in the pictures of the char obtained from PU 28%APP 2%nano MgO is the two parts char structure with many unorganized cells at the bottom and huge voids at the top.

The study of the contrast on the pictures will be highlighted by the graph of average grayvalue versus height (**Figure 119**). This allows following the concentration profiles of the flame retardants during charring reactions [106] since the higher the average grayvalue, the higher the density.

The grayvalue is recorded from the bottom until the top of the char. The grayvalue is not recorded before around 5 mm of height because of the aluminum foil and because of the high quantity of unburned polymer, which is not representative of the fillers repartition. For PU 25%APP 5%nano MgO the recording of the grayvalue is moreover delayed; this is because the plate is not flat. The sample PU 28%APP 2%nano gold presents a global higher grayvalue (corresponding to the sum of the grayvalues at each height and equal to 16.7) than all other formulations; this is attributed to the contribution of gold having a high atomic number and thus contributing to an increase of the contrast. On the contrary the total grayvalue of PU/APP and PU/APP/nano MgO is identical (sum of grayvalues at each height equal to 7.7, 7.8 and 8.0 respectively for PU 30%APP, PU 28%APP 2%nano

MgO and PU 25%APP 5%nano MgO). This was expected since the additive loading is always equal to 30% and phosphorus and magnesium are close in the periodical classification. The differences observed on the graph for the grayvalue numbers are only due to the fact that the total height is different causing a different repartition of the grayvalue.

In every case, fillers are particularly located at the bottom of the char because the higher grayvalue is always observed at low height. The same observations were made during EPMA experiments on a char from PU 28%APP 2%nano MgO (**Chapter IV, section 2.2-Electron probe microanalysis on PU/APP/nano MgO collected after MLC test p146**). This is not surprising since, according to the videos, more matter is located at the bottom of the char leading to observe more particles. Then the quantity of fillers decreases due to an increasing number of holes in the structures. These general trends are real for all PU formulations but some differences are nevertheless observed.

For PU 30%APP, the grayvalue decreases from 5 to 16 mm approximately and then it increases with a maximum at 29 mm before decreasing again until the top of the char. The repartition of phosphorus based material is then a function of the char structure. When there are holes, no material is detected and thus the grayvalue decreases since it increases with the quantity of fillers or with the high atomic number but also with the density of materials. The average grayvalue is however always comprised between 0.1 and 0.2 after 2 mm height.

The evolution of the grayvalue as a function of height is different when NPs are incorporated in the formulation. A decrease of the grayvalue is always observed as a function of height; there is no secondary maximum as it was observed without NPs. Moreover, a plateau is observed on the top of the sample.

Concerning PU 28%APP 2%nano MgO, after a significant decrease of the grayvalue, it exhibits a plateau from 43 mm until the top of the char. At the top of the char, the fillers concentration is low and constant and this corresponds to the char area mainly constituted of big bubbles where nearly only the crust may contain some phosphorus and/or magnesium. The latest particles are then preferentially located in the bottom of the char composed of many bubbles of various sizes, more similar to the PU 30%APP morphology.

The curve for the char containing gold is more or less flat compared to the other curves. This might be due to the more heterogeneous structure exhibited by this formulation. The char morphology is indeed composed of many small bubbles especially on the sides of the sample. The decrease of filler as a function of height is regular attesting of certain char homogeneity as a function of height.

The char PU 25%APP 5%nano MgO shows a slight regular decrease of the grayvalue as a function of height. Except for the richer bottom in particles, there is no preferred location for the fillers in the char as a function of height. A slope change is nevertheless observed around 38-40 mm and this corresponds exactly to a region where the char is very dense and forms a compact layer between two aerated regions (**see video and Figure 118**).

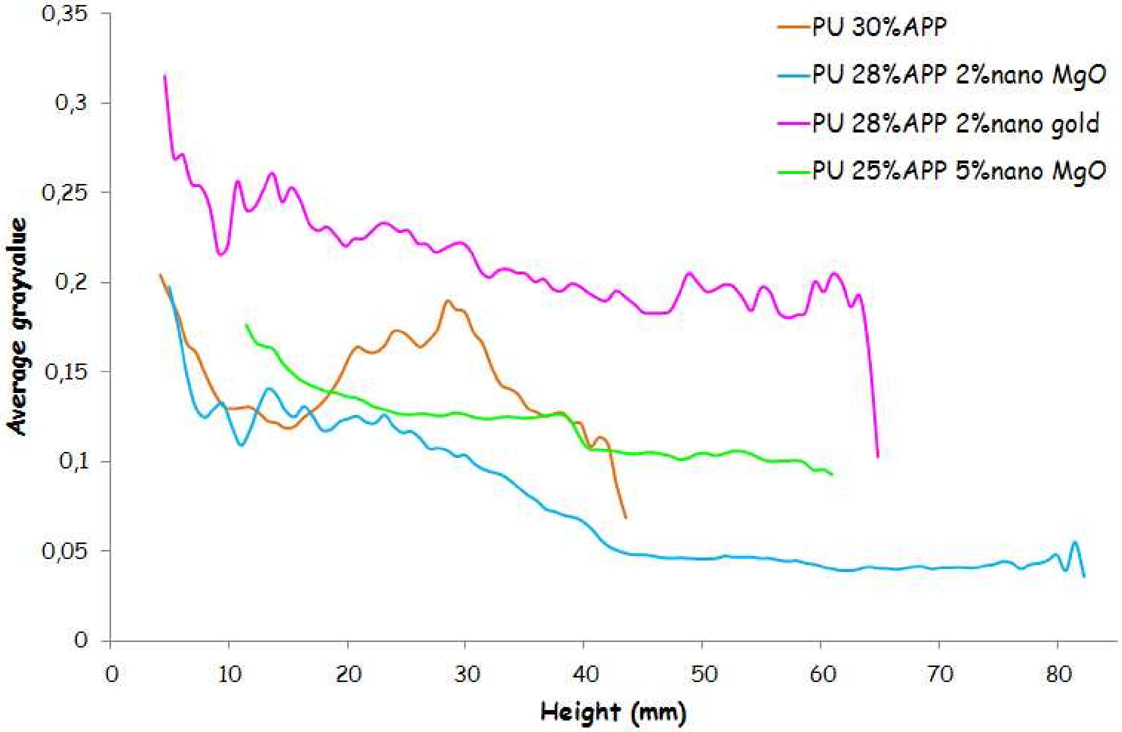

Figure 119: Average grayvalue as a function of height measured on chars collected at the end of cone calorimeter experiment for PU 30%APP, PU 28%APP 2%nano MgO, PU 28%APP 2%nano gold and PU 25%APP 5%nano MgO

While studying the repartition of particles in the degraded PU matrix, the main conclusion is that the presence of NPs affects the morphology of the intumescent formulation. The profiles of average grayvalue as a function of height are different depending on the formulation. Since each char has different fire behavior and filler repartition, it is thus possible to assume a link between the repartition of fillers in the char and its fire performances. Without NPs, the evolution of grayvalue varies due to the alternating presence of cell walls and holes. With nano gold and at a ratio APP/nano MgO 25/5, the fillers are regularly dispersed and their concentration decreases as the height increases. For the ratio APP/nano MgO 28/2, a constant filler concentration is detected in the top part of the char composed of big bubbles.

The study of the effect of NPs on the physical properties of intumescent PU revealed that they clearly affect the char morphology and the fillers repartition in the char. These properties are furthermore dependent on the nature of the NP and of the ratio APP/NP. Even if the material tested exhibits significant different fire performances, it is difficult to establish general rules regarding the optimized char morphology and/or repartition of fillers in the char.

Intumescence is a dynamic process [51, 59] which constantly evolves. The study of the char morphology at the end of cone calorimeter only gives information when the char is fully developed. The development of intumescence is thus worthy to investigate by comparing an intumescent PU with and without NPs.

2.2.2 Development of intumescence followed by tomography

To go further in the investigation of the combustion processes, volume imaging approach was adopted to visualize the 3D structure of the residue during burning [107]. The intumescence process and especially the morphology of the char during its expansion has consequently been monitored by tomography on PU 30%APP and PU 28%APP 2%nano MgO. These formulations have been stopped at characteristic times during a cone calorimeter experiment: during increase of HRR, during decrease of HRR and at the end (the last point is the one already presented and discussed in the previous section). Two comparisons can be made; the first one concerns the evolution of the structure during the development of intumescence on each sample, and the second deals with the comparison of the two formulations at a given time of the process.

The pictures approximately at the (x,y) slice corresponding to the higher height of the considered char have been extracted from the movies and are displayed in **Figure 120** and **Figure 121** respectively for PU 30%APP and PU 28%APP 2%nano MgO. These pictures show the evolution of the char structure during a cone calorimeter experiment.

During the increase of HRR, the polymeric matrix degradation is only partial. Where the material is less degraded, the PU plate still has a 3 mm thickness. This thickness decreases in the middle of the plate until reaching a minimal thickness of 1.3 mm and 1.7 mm for the formulations respectively without and with nano MgO. The plate is moreover extremely curved; this required a specific image treatment to obtain reliable grayvalue as a function of height (**Figure 122** and **Figure 123** respectively for PU 30%APP and PU 28%APP 2%nano MgO). Moreover it leads to a delayed height for starting grayvalue measurement. During the decrease of HRR, the material is still not totally degraded as the plate is still observable on the sides of the sample. In the center, PU 30%APP is totally degraded and present a char whereas for the PU 28%APP 2%nano MgO virgin material is still observed.

The char morphology of the formulations with or without nano MgO during the intumescence process is different. The videos and pictures of the evolution of the PU 28%APP 2%nano MgO char structure (**Figure 121**) show that the swelling of the sample is due to the growth of bubbles [105] versus time. On the contrary the evolution of char morphology of PU 30%APP (**Figure 120**) is a progressive swelling due to the formation of bubbles. The inner structure of the PU 30%APP char is indeed similar along the height and versus time even if more or less expanded material is obtained depending on the time of exposure on the fire test. In particular the char morphology obtained during decrease is very similar to the one obtained at the end of the test. According to PU 28%APP 2%nano MgO pictures, an aerated structure is obtained during increase and corresponds to the top structure of the final char structure. Then during decrease, a different morphology is obtained. In the core of the material and along nearly all the height, big regularly round cells are obtained and separated by thick walls. These cells seem to collapse from the decrease of HRR until the end of a cone calorimeter test perhaps because of the pressure applied by the top part of the char. This will constitute the bottom part of the final char composed of many bubbles of various sizes.

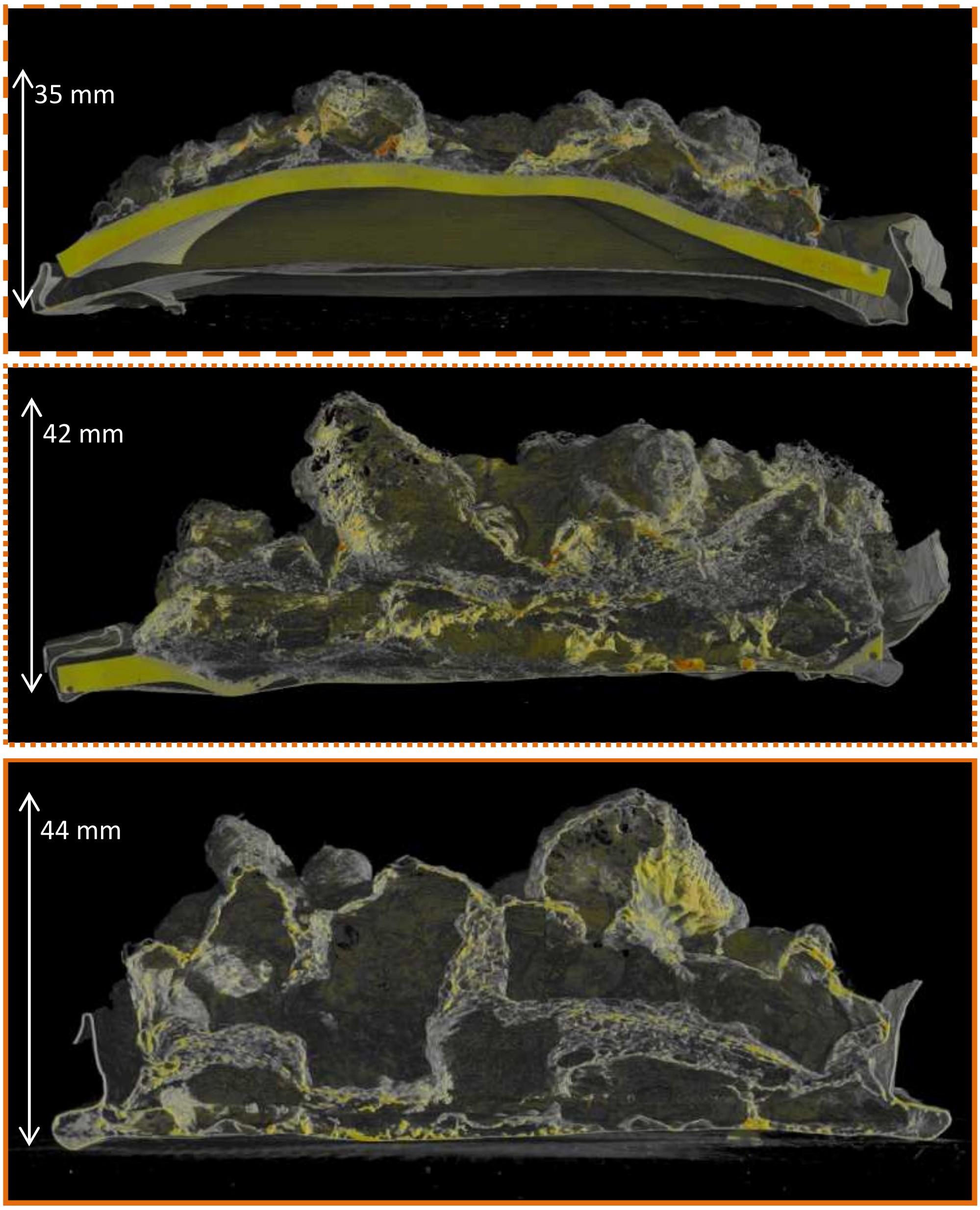

Figure 120: Evolution of the PU 30%APP char structure during a cone calorimeter test (from top to bottom: during increase, during decrease, end of cone)

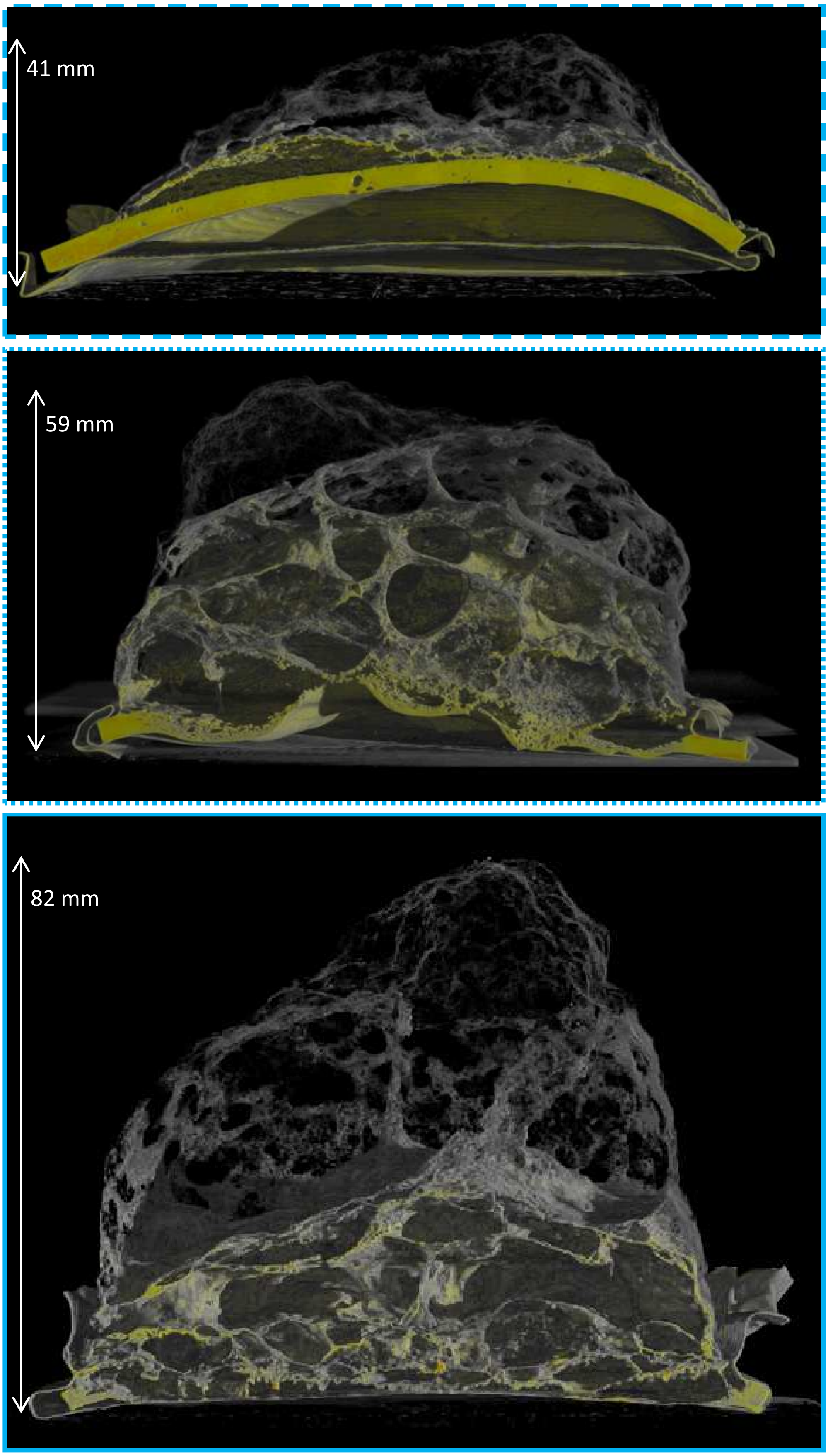

Figure 121: Evolution of the PU 28%APP 2%nano MgO char structure during a cone calorimeter test (from top to bottom: during increase, during decrease, end of cone)

As far as the repartition of particles is concerned, some differences between the two samples are also observed on the profile of average grayvalue reported as a function of height (**Figure 122** and **Figure 123** respectively for PU 30%APP and PU 28%APP 2%nano MgO). For both chars, the denser particles are anyway localized at the bottom of the char.

For PU 30%APP, the curves are very similar whatever the time during fire test between 10 and 25 mm. Before 10 mm, the curves cannot be compared due to the bending of the plates. After 25 mm, the char during increase is not far much expanded; there is thus less matter and consequently less particles causing the grayvalue to decrease until reaching the top of the char (around 35 mm). On the contrary during decrease the char is already nearly as expanded as at the end, in agreement with the data collected in this chapter (**Chapter V, section 2.1.1-Expansion recorded during MLC experiment p177**). The evolution of grayvalue is consequently similar to the one observed at the end of cone. Between 10 and 25 mm, since whatever the time of sample collection the grayvalue is similar, it means that the high density of particles located at the bottom of the final char corresponds to particles still in the unburned materials at less advanced degradation steps and especially during increase. At this latter step, APP is still detected at the bottom of the sample as it has been evidenced in **Chapter IV, section 3.2-NMR analysis of residues collected from shutter experiments on PU formulations p154**. To summarize, for PU 30%APP, the intumescence process is regular and homogeneous during cone calorimeter.

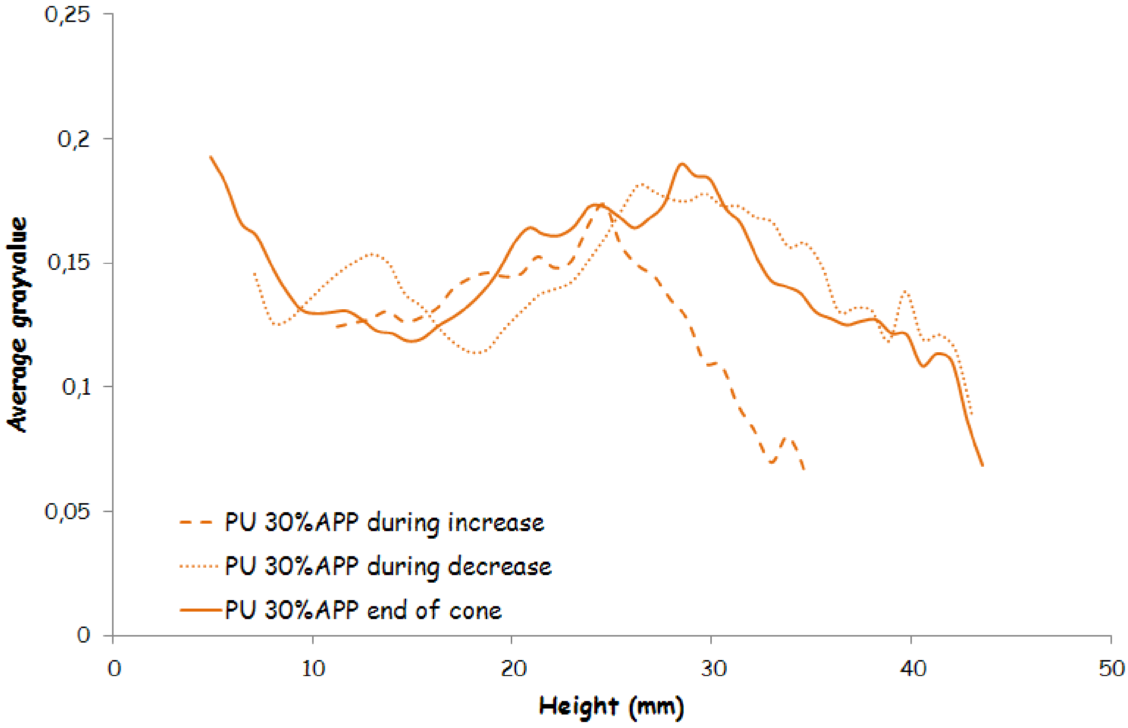

Figure 122: Average grayvalue as a function of height followed during a cone calorimeter experiment on PU 30%APP

With nano MgO, the intumescence process occurs in a different manner. Before 12 mm, the samples are not comparable since the plate is curved and/or unburned. The curve of the grayvalues versus height is also stopped when the maximum height is reached: from 42 mm to 83 mm respectively for material collected during increase to the residue obtained at the end. Between 12 and 42 or 60 mm, the shapes of the curves are similar except for the profile during increase from 25 to 42 mm. The top of the char during increase is significantly poorer in particles than the average material. This is concomitant with the fact that a huge void is observed on the video or picture (**Figure 121**). A similar plateau is obtained at the end of cone after 43 mm and was already attributed in the last section to a char area mainly constituted of big bubbles where nearly only the crust may contain some phosphorus and/or magnesium. The grayvalues are however different depending on the time of exposure to the cone. The grayvalues during increase are always lower than the one obtained at the end and the contrary is observed for the grayvalues recorded during decrease. During increase, the particles are mainly located in the unburned polymer causing lower grayvalues. During decrease, it appears on the contrary that all phosphorus and magnesium are already present in the char and mainly located at the bottom. It has moreover already been proven that phosphorus and magnesium react to form magnesium phosphate from the pHRR (**Chapter IV, section 3.2-NMR analysis of residues collected from shutter experiments on PU formulations p154**). It is thus possible that this reaction involves more particles which are consequently used to form the char. The char height is however lower during decrease compared to the end of cone, leading all particles to be concentrated in a smaller volume explaining thus the higher grayvalues recorded. The big regularly round cells observed (**Figure 121**) are consequently rich in phosphorus and magnesium. From during decrease to the end, the particles already present in the char will follow the char expansion and morphology changes leading to observe a plateau until the maximal expansion. To summarize, the intumescence process on PU 28%APP 2%nano MgO seems to occur in two distinct steps. At first, very aerated area containing a low amount of fillers are created and this will compose the upper part of the final char. In a second step, many bubbles are formed and they are rich in phosphorus and magnesium and probably correspond to magnesium phosphates. These bubbles will further reorganized in order to create the bottom part of the final char.

The intumescent behavior is much more complex in the case of nano MgO containing formulation and lead to a more complex char structure. The fire properties of PU 30%APP are highly enhanced by the substitution of a small amount of APP by nano MgO and part of the explanation could be based on the char morphology that varies during the fire test.

It is now possible to superimpose and to compare the profile of grayvalue as a function of height for PU 30%APP and PU 28%APP 2%nano MgO during increase and during decrease (**Figure 124**). For the end of cone calorimeter, these two formulations have already been compared in the last section.

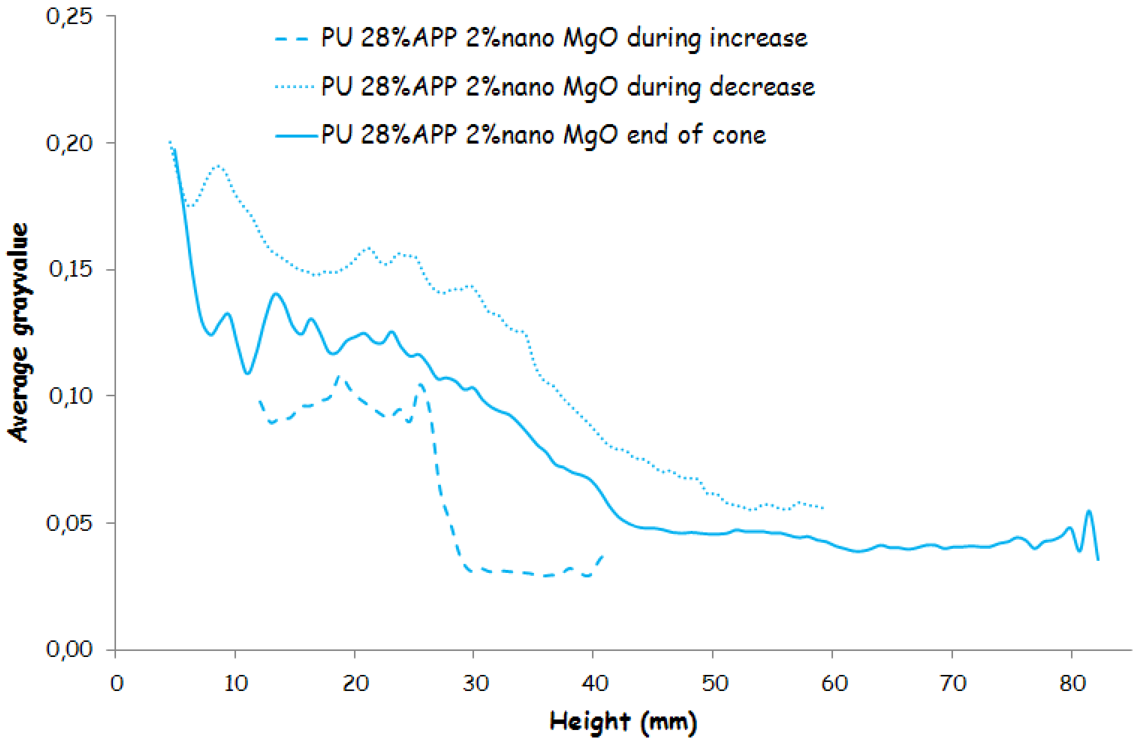

Figure 123: Average grayvalue as a function of height followed during a cone calorimeter experiment on PU 28%APP 2%nano MgO

By comparison of the two formulations collected during increase, the same shape of curve is observed until 30 mm height. After the sharp decrease in grayvalues, there is no char anymore (34 mm) in the case of PU 30%APP while a stable value is observed for PU 28%APP 2%nano MgO until the top of the char (42 mm). This means that the particles are mostly located in the bottom of the char and the top of the char is mostly composed of voids and degraded matrix. This latter area is predominant for the formulation with NP compared to the one without, attesting of different char morphology at the beginning of the intumescence process. The grayvalues are moreover significantly higher for PU/APP compared to PU/APP/nano MgO. Since the same quantity of fillers (phosphorus and magnesium quite equivalent regarding the impact on the grayvalue) has been introduced during synthesis in the PU, it means that a higher amount of fillers are involved in the charring process during increase of the HRR curve in the case of PU 30%APP. In other words, more particles are going from the unburned polymer to the char when there is no NP. This should be linked to a faster degradation of the PU matrix containing only APP. This concept of faster degradation in the case of PU 30%APP compared to PU 28%APP 2%nano MgO is concomitant with many other results:

- better thermal insulation and thermal conductivity properties for the char PU 28%APP 2%nano MgO (**Chapter V, section 1-Thermal Barrier Effect of the Char p170**) leading to higher temperatures at the bottom of the char for PU 30%APP
- different chemical species are formed during cone calorimeter experiment (**Chapter IV, section 3.2-NMR analysis of residues collected from shutter experiments on PU formulations p154**) and in particular the presence of NPs leads to a modification of the degradation pathway and/or kinetic of

APP degradation and/or its reaction with the PU matrix (**Chapter IV, section 2.1-Solid state NMR on burned residues from PU formulations p138**)

- a slowdown was observed in the evolution of expansion as a function of time with nano MgO while it was regular without NP (**Chapter V, section 2.1.1-Expansion recorded during MLC experiment p177**)

During the decrease of HRR, the comparison between the two samples is similar to the one made at the end of cone calorimeter test described in the previous section. The repartition of phosphorus based material is concomitant with the structure for PU 30%APP. With nano MgO, a significant progressive decrease of the grayvalue is recorded as a function of height from the bottom to the top of the char. The concentration of fillers is decreasing while reaching the top of the char although the structure is similar all over the char. This time, the grayvalues for both formulations are in agreement with the quantity of fillers incorporated in the PU matrix. It means that the differences in degradation processes are no longer observed according to the quantity of fillers present in the char.

The study of fillers repartition in the char during the intumescence process revealed an effect of the presence of nano MgO in the intumescent formulation PU 30%APP. At the beginning of the development of intumescence in cone calorimeter experiment, a faster degradation of PU 30%APP is noticed. After the decrease of HRR, the intumescence process is nearly finished (especially for PU 30%APP) and finally leads to two different final structures.

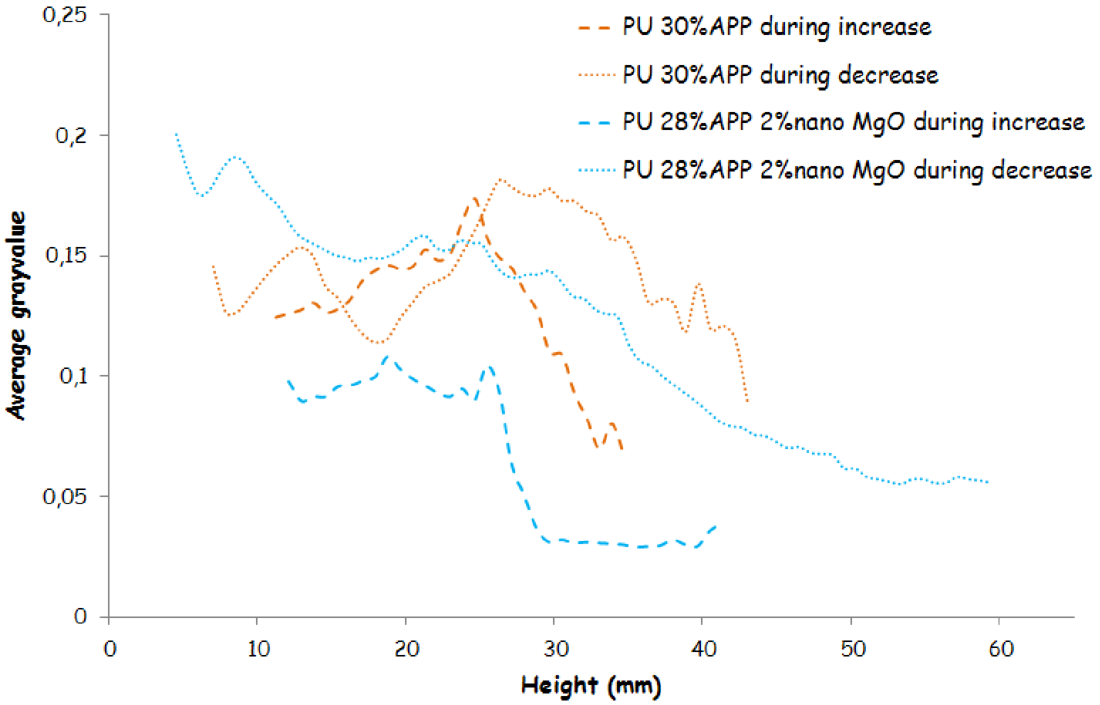

Figure 124: Average grayvalue as a function of height during increase and during decrease of HRR for PU 30%APP compare to PU 28%APP 2%nano MgO

The use of tomography provided major information on the char morphology and the repartition of fillers in degraded PU matrix.

At the end of a cone calorimeter experiment, the incorporation of NPs affects the char morphology and the fillers concentration profiles along the depth. These properties are furthermore dependent on the nature of the NP and on the ratio APP/NP.

The intumescent behavior is much more complex in the case of nano MgO containing formulation and leads to a more complex char structure. Good correlation with the monitoring of expansion is noticed. The PU 30%APP intumesces regularly and lead to an homogeneous char composed of big bubbles separated by thick walls whereas the PU 28%APP 2%nano MgO char grows in two steps: at first a very aerated area is formed and will compose the upper part of the final char, then bubbles are formed and will further reorganize at the bottom of the char. A faster degradation is additionally evidenced without nano MgO and is totally concomitant with other results previously discussed.

The fire properties of PU 30%APP are enhanced by the substitution of a small amount of APP by NPs. The tomography helped to evidence that part of the explanation is based on the char morphology and development of intumescence during the fire test. It appears more precisely that all chemical and physical properties are linked and only a combination of optimized parameters can lead to the synergy between APP and NPs in PU matrix.

On the other hand, the morphology exhibited by the intumescent PU formulations is a result of a swelling and blowing mechanism leading to the formation of cells of different size. The fillers incorporated in PU participate to this bubbles development to a certain extent depending on the fillers or combination of filler used. Upon thermal stress, the fillers degrade and/or react leading to the release of gases which are “used to build the intumescent structure”; the increasing internal pressure from degradation gases allows the char to expand. A new method has thus been developed to investigate at the laboratory scale the flux of gases released during the additives degradation (APP, nano MgO and their mixture). This study will be particularly relevant to further understand the differences in char morphology and intumescence process between PU/APP and PU/APP/nano MgO formulations.

2.3 Development of a new method to study the gas released during additives degradation

It is widely known that in intumescent systems, blowing or swelling agents are conventionally used [10, 51, 60] and releases gases that enable the char to expand [13, 59]. Swelling and blowing must moreover occur at the right time and temperature to be efficient in case of fire [60, 145]. The previous section showed that the char morphology is affected by the composition of fillers used in the PU matrix. It suggests thus that depending on the gas flow, the char development might be influenced.

The idea was consequently to record the pressure of gas released during degradation. The gases released during PU, PU/APP and PU/APP/nano MgO degradation has already been monitored by TGA-FTIR (**Chapter IV, section** 1-**Chemical Characterization of the Gas Phase p131**) but the equipment did not allow quantification. The comparison was only made on the nature of the chemical species and they were the same for PU/APP and PU/APP/nano MgO systems. The aim now is to study the effect of the additives themselves and to compare their ability to release gases. Moreover in such an experiment, only a few milligrams of materials are used and thus diffusion processes are assumed to be negligeable.

Thus, a high temperature rheometer was used to evaluate the gas flow released when the additives degrade. Its use is obviously in that case very unique and unusual regarding its primary function but the same principle as the one used to measure the char expansion as a function of temperature on PU formulations was used. A normal strength is applied on the sample and the gap evolution is recorded while the temperature is linearly increased. This will be linked to the release of gases that push away the upper plate (**method fully described in Chapter II, section 2.5.1-Method to study the additives degradation p87**).

By testing only the additives (APP, nano MgO and their mixture), the idea was to see if it is possible to detect a modification with temperature upon normal strength. Testing separately the matrix and the additives was interesting because it excludes the direct effect of the charring. The contribution of additives is therefore analyzed more precisely.

The section will now be divided into two parts. The first one will present the results of gases released during the degradation of APP and of the mixtures APP/nano MgO. In a second part, those results will be compared to those obtained in TGA.

2.3.1 Evolution of gases released during additives degradation

The additives used in PU formulations (APP, nano MgO and their mixture) have been tested through rheological means to investigate their behavior upon degradation. In particular the monitoring of gases released during the additives degradation is of interest and will be possible studying the evolution of the gap increase as a function of the temperature (**see Chapter II, section 2.5.1-Method to study the additives degradation p87 for the method details**).

The distance between the bottom and upper plate during the experiment is recorded versus temperature. The release of gases will lead to an increase in the upper plate and thus of the gap. On **Figure 125**, APP and the mixtures APP/nano MgO in different ratios exhibit different behaviors when the temperature increases. Nano MgO alone was tested with the same method but the results were not reliable because some nano MgO may escape from the bottom plate due to its low density and consequently high volatility. The curves for APP and for the mixtures APP/nano MgO was on the contrary repeatable. It is then possible to ascertain that the differences observed on **Figure 125** are significant.

The evolution of the gap with the temperature for the sample holder alone (without any sample) shows a linear increase from the beginning to 500°C, this is due to the linear thermal expansion of steel. All the samples present nearly the same linear increase from 25 to around 250°C, which is only due to the sample holder deformation.

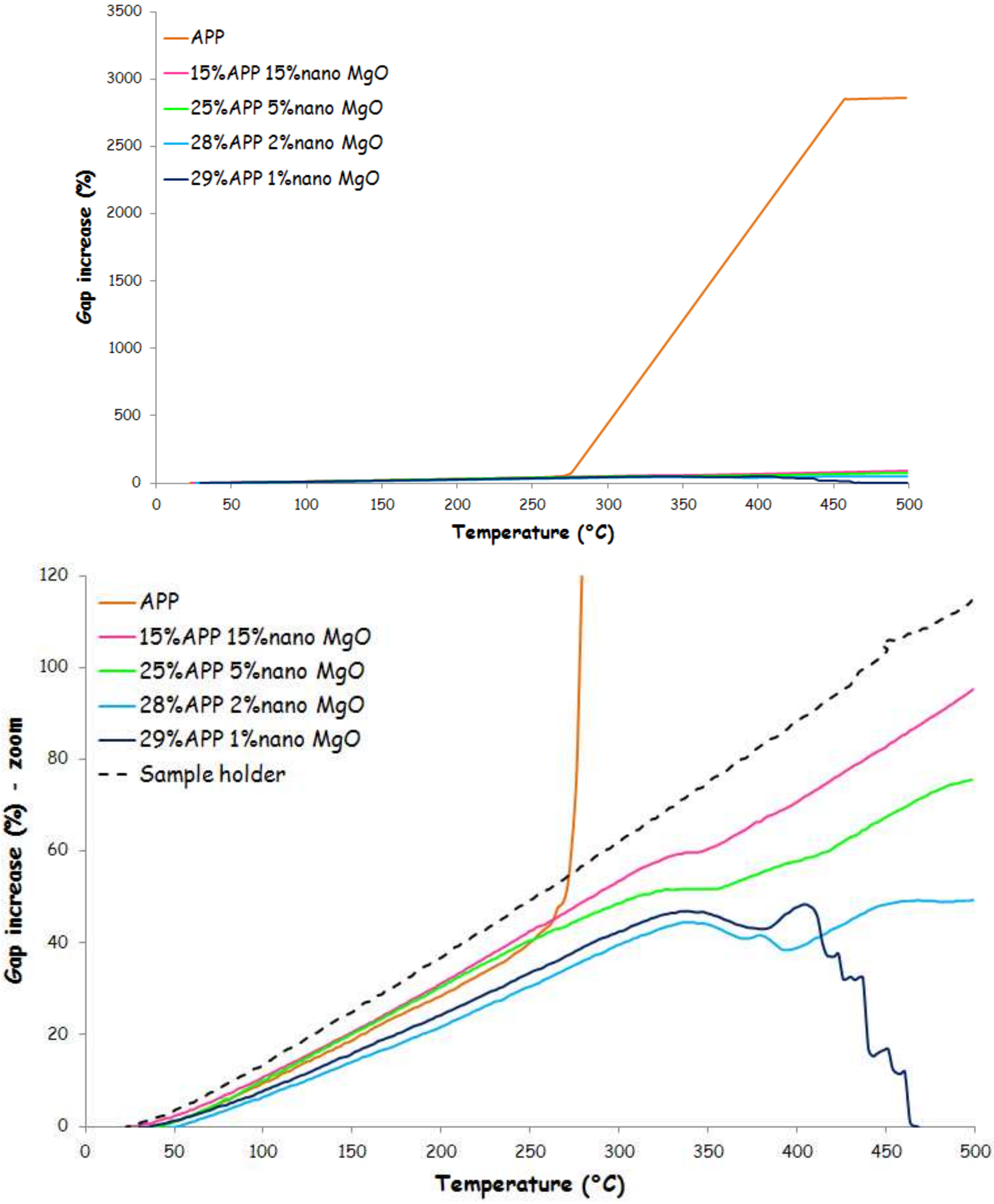

Figure 125: Curve of gap increase as a function of temperature for the additives used in PU formulations measured in a high temperature rheometer (top: full scale, bottom: zoom)

Then a huge increase in the gap is observed for APP leading to a plateau at 3000% (this value corresponds to experimental limitation). The residue is not swelled when collected after the test and considering that it is just APP, it might not have swelled during the experiment as well. The recorded gap increase is consequently due to gases released during degradation that push the upper plate.

When nano MgO is added to APP, whatever the ratio, the gas recorded through the gap increase is slowed down. It appears that nano MgO regulates the pressure flow released during the degradation of APP. At ratios 15/15 and 25/5, a slowing down is observed around 300-350°C, and the gap starts to increase again with the same previous slope at higher temperature. For the ratios 28/2 and 29/1 on the contrary a significant decrease of the gap is observed, especially with 1% of nano MgO for which the gap increase reaches zero. This is concomitant with the aspect of the residue: at ratios 15/15 and 25/5 no degradation is observed (the powder remained and is just a little more compact) whereas for 28/2 and 29/1 mixtures, the residue is sticky and hard (vitreous state).

It is known that magnesium and phosphorus react easily to create magnesium phosphates upon heating. This reaction should affect the gases released during APP degradation, leading to regulate the pressure flow. The properties of the glassy network formed upon heating might indeed be responsible for the gas flow recorded with the rheometer. Indeed, it is reported that the glasses composed only of phosphate chains (case of APP) possess a low viscosity and a small tendency to crystallize [191]. On the contrary, the incorporation of MgO, Al_2O_3 and TiO_2 results in a strengthening of the glass network and hence, increases the viscosities and notably decreases the tendency to crystallize [191, 192]. In the case of the mixture 28%APP 2%nano MgO, the magnesium/phosphate glass created are thus stronger, more compact and the gases evolved during APP degradation are consequently trapped by the structure. This is not the case for the low viscosity glass created during APP degradation which molten structure let the gases escape easily. This has been evidenced by visually following the degradation of APP and 28%APP 2%nano MgO (**Figure 126**). The residue obtained with APP present many bubbles from which the gases could escape whereas the residue obtained with the mixture APP/nano MgO is very cohesive and the gases have been trapped in this network. On the curve of gap increase, this phenomenon results in a slow down of the gap increase recorded for APP after 250°C provided by the presence of nano MgO. The higher viscosity of the degraded material created by the mixture 28%APP 2%nano MgO causes even more a gap decrease because the gas species are trapped in the glassy network which progressively degrades at higher temperature.

Figure 126: Residue picture after a thermal treatment from 25 to 400°C at 10°C/min on APP (right) and 28%APP 2%nano MgO (left)

It is moreover known that the stoichiometry of the magnesium phosphates depends on the ratio APP/nano MgO (see calculation of the ratios for different magnesium phosphates in **Chapter IV,**

section 2.1-Solid state NMR on burned residues from PU formulations p138); this could explain why the profile of gap increase as a function of temperature is different. The magnesium/phosphate glasses have different viscosity properties depending on their composition and thus affect their relative ability to release gases. Whatever the magnesium/phosphate glass created, it is still more efficient than the phosphate glass to trap degradation gases leading to small values of gap increase as a function of temperature.

This section has just evidenced that nano MgO regulates the gas flow when APP degrades. It appears to have a particular interaction between APP and nano MgO at low content in nano MgO (typically 28/2 and 29/1). This should be linked with the chemical interactions occurring between APP and nano MgO.

By extrapolation, with certain additives in PU, there might be more or less pressure in the matrix during heating and this might be correlated to the different char aspect observed between the formulations PU/APP or PU/APP/nano MgO described previously in this chapter (**Chapter V, section 2.2-Image reconstruction of char morphology by tomography p181**). The pressure applies on a surface at a given time by the release of species in the char PU 30%APP is indeed higher than that induced by the degradation products of PU 28%APP 2%nano MgO. The char PU 30%APP is consequently less structured (especially its crust) and composed of large cells. The tomography has moreover shown that higher phosphorus and/or magnesium containing materials are detected in the char at the beginning of the intumescent process compared to the PU 28%APP 2%nano MgO formulation. This observation is in total agreement with the fact that APP degradation products, when used alone, are easily and rapidly released.

Since the additives degradation has already been followed by TGA (**Chapter III, section 3.2-Thermal degradation of additives p117**), the obtained results could be compared to those obtained here.

2.3.2 Correlation between additives degradation followed by TGA or by rheological means

The last section presented an innovative method to study the release of gases during additives degradation by rheological means. A new method always needs to be validated by other reliable data. This is the purpose of the following text which will correlate the data obtained during additives degradation studied in TGA or by rheological means.

The TGA and the gas release monitored in the rheometer have been performed as far as possible in the same conditions (10°C/min, under air), leading them comparable on the range of temperature from 50 to 500°C. However it has to be noted that the size of the sample differs in both technique.

The superimposition of TG curves and gap curves as a function of temperature for APP and 28%APP 2%nano MgO are presented respectively in **Figure 127** and **Figure 128**. The weight derivative curves are also provided. This comparison has only been made for APP and 28%APP 2%nano MgO. They illustrate the best the phenomenon of modification of gases released by incorporation of nano MgO in APP since for 29%APP 1%nano MgO, the explanation is the same than with a ratio 28/2.

In the case of APP, the huge gap increase (due to high pressure of the degradation products) starts with the beginning of mass loss (**Figure 127**). On the TGA, this step has been attributed to the release of ammonia and water leading to the formation of polyphosphoric acid [13, 59, 129]. This proves a clear correlation between TGA and gap increase and further confirms our assumption (the gap increase is due to gases released). The increase of gases released in the rheometer then continues with the mass loss observed on TG curves. Since the presence of the plateau at 3000% is not reliable (**Chapter V, section 2.3.1-Evolution of gases released during additives degradation p198**), the end of the curves cannot be commented.

The change in the linearity of the gap curve (only due to the sample holder) is delayed of around 100°C compared to the beginning of mass loss for the additives mixture containing 28% of APP and 2% of nano MgO (**Figure 128**). The decrease of gap starts indeed at the maximum slope of the derivative TG curve. The release of ammonia and water leading to the formation of polyphosphoric acid is affected by the presence of nano MgO even at low content. These species are nevertheless released according to the TG curves but their pressure is lower. This means that a different degradation process occurs. It illustrates once again the fact that nano MgO, used in a ratio 28/2, modifies the degradation of APP from 250 to 500°C.

It would have been expected to see differences in the values and/or the slope of the curves of the derivative TG curves for PU 30%APP and PU 28%APP 2%nano MgO since their gas released behavior was totally different. It is however not the case as it can be seen on **Figure 127 and Figure 128** presenting derivative weight values around 0.15 %/°C in both case. Thus, the role of MgO on the monitoring of gap increase in the rheometer is no longer evidenced by TGA. The only difference between the conditions of the experiment performed in TGA compared to the one performed in the rheometer is the size of the sample. With a higher quantity of powder, as in the case of the rheometer, it is possible that the viscosity of the glass created during the experiment has an impact on the release of gas and this might not be detected with the 10 mg used in TG experiments.

According to the TGA, it has been shown that the stabilization of APP by nano MgO occurs after 500°C (**Chapter III, section 3.2-Thermal degradation of additives p117**), a range of temperature which cannot be analyzed with the rheometer. It is possible that a reaction between APP and nano MgO occurs at lower temperature (it has been indeed proven in **Chapter IV, section 4.2-Chemical characterization of PU formulations degraded with different heating conditions p163** that reactions occur between APP and nano MgO in the PU casting at 500°C). It could thus explain the stabilization of the pressure flow of the gases released by APP degradation around 250°C. Unfortunately it cannot be verified on the residues after TGA and/or rheometer because the glassy residue is stuck in the sample holder.

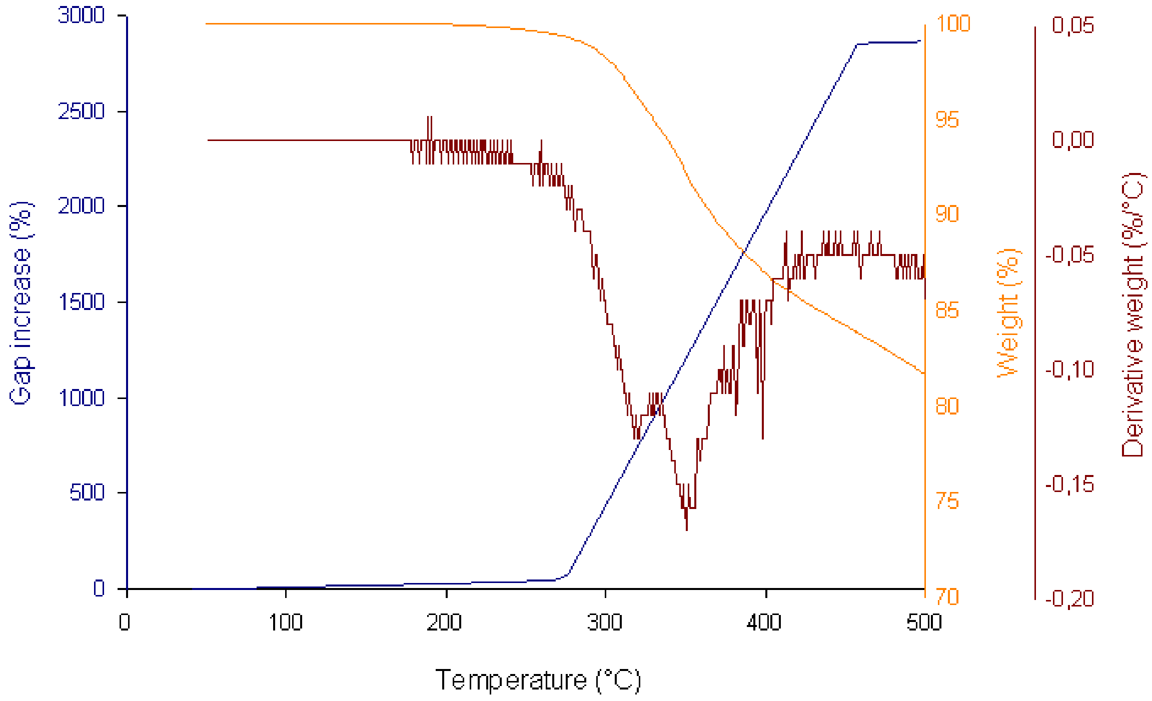

Figure 127: Gap increase versus temperature superimposed to TG curves (weight + derivative weight = f (temperature)) for APP

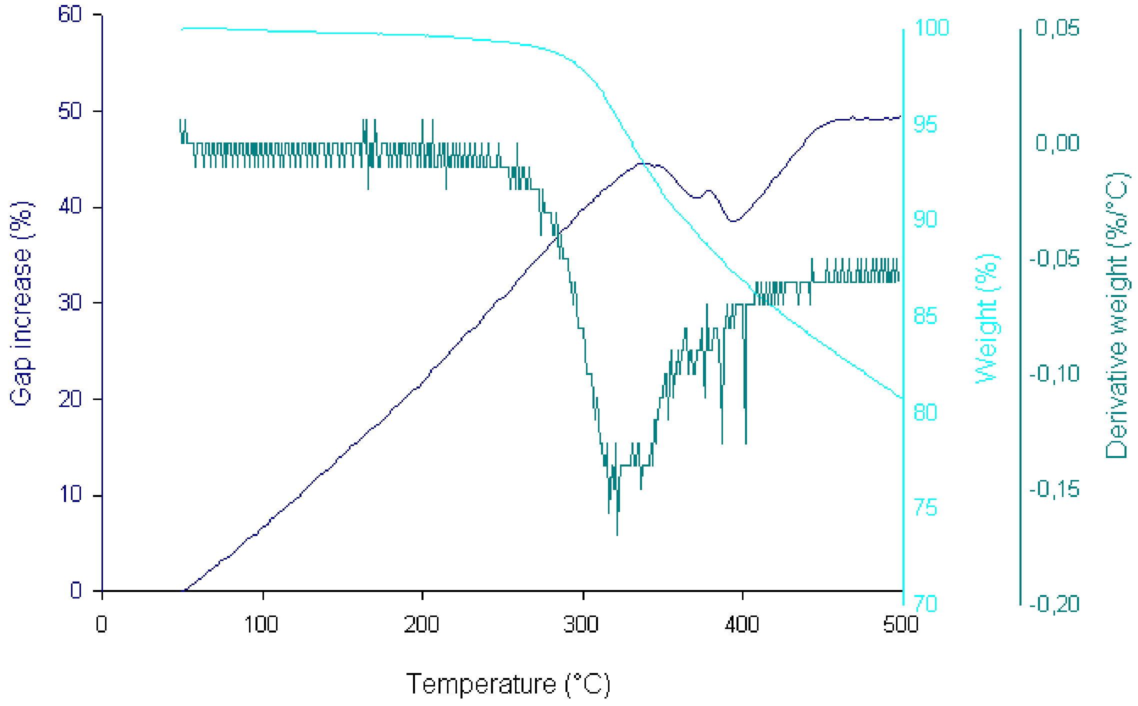

Figure 128: Gap increase versus temperature superimposed to TG curves (weight + derivative weight = f (temperature)) for 28%APP 2%nano MgO

The study of gases released during additives degradation showed that the degradation processes involved are different if there is nano MgO in combination with APP or not. In particular it was found that nano MgO regulates the gas flow when the additives degrade. The char morphology could furthermore be correlated with those results since the crust of the char PU 30%APP is less structured compared to the one obtained from PU 28%APP 2%nano MgO. Part of the explanation of synergy in fire performances is thus elucidated because higher amount of gases could escape from the char of PU 30%APP compared to PU 28%APP 2%nano MgO. This is moreover consistent with a faster degradation of the PU 30%APP, proposed from tomography results, since the degradation products are released faster in the burning front. The regulation of the gas flow exhibited with nano MgO might probably be a consequence of the chemical interactions occurring between APP and nano MgO.

This section has fully investigated the expansion and morphology of PU/APP and PU/APP/NP chars which represent critical parameters for intumescent systems.

The char development has first been followed recording the expansion as a function of time and temperature in two different heating conditions. The formulations PU and PU 5%nano MgO does not expand during cone calorimetry as expected. Following the expansion as a function of temperature with a heating ramp of 10°C/min, it was impossible to discriminate PU/APP and PU/APP/nano MgO formulations. The charring process allow however a distinction between PU/APP with or without nano MgO when the expansion is followed as a function of time during a cone calorimeter experiment. A slowdown is observed at the beginning of intumescence when nano MgO is incorporated in the formulation while the expansion evolves progressively in the case of PU 30%APP.

The tomography has then been used to evaluate the char morphology and the concentration profiles of fillers in degraded materials. The incorporation of NPs, their nature and content, affects the char morphology and the fillers distribution in the char at the end of a cone calorimeter experiments. The intumescent behavior is much more complex in the case of nano MgO containing formulation and leads to a more complex char structure. The PU 30%APP intumesces regularly whereas the PU 28%APP 2%nano MgO char grows in two steps leading to different final char structures. A faster degradation is additionally evidenced without nano MgO since more filler are detected in the char PU 30%APP at the beginning of the intumescence process.

The study of gases released during additives degradation, in agreement with TGA results, revealed that the degradation processes involved for APP with or without nano MgO are different. In particular it was found that nano MgO regulates the gas flow released by APP during its degradation especially at low content in nano MgO.

The fire properties of PU 30%APP are enhanced by the substitution of a small amount of APP by NPs. The expansion measurement, the tomography, the study of gases released during additives degradation are concomitant to evidence that part of the explanation is based on the physical properties of the char. It appears more precisely that all chemical and physical properties are linked and only a combination of optimized parameters can lead to synergy between APP and NPs in PU matrix.

The last physical property of the char to investigate is its mechanical behavior. The mechanical resistance of the char is indeed a significant factor in fire properties because the char destruction can occur leading to a lost of the protective behavior of the intumescent shield. Many external influences such as wind, mechanical action of fire or convective air flow may apply pressure on the char which have to be resistant enough to give the best fire properties. The following section will characterize the mechanical strength of the char resulting from PU formulations and prepared in different conditions. The influence of these different conditions used to develop the char will be particularly discussed as well as the influence of the presence of nano MgO.

3 MECHANICAL BEHAVIOR OF THE CHAR

Rheological properties are important for the development of intumescence in polymers. These properties depends on the degradation and/or reaction of polymer, additives and their combination [60, 78]. In particular the mechanical resistance of the char is a significant factor because in conditions of fire, char destruction may happen by means of external influence such as wind, mechanical action of fire or convective air flows [60]. If a char has good structural, morphological and heat insulative properties but is easily destroyed under a mechanical action, its efficiency is totally lost in the turbulent regime of combustion. The incorporation of NPs in PU/APP intumescent formulation was already proven to modify many char properties as the thermal barrier performances, the expansion, the morphology of the char and the intumescent process development. The presence of NPs could furthermore impact the mechanical properties of the resulting char and really need to be studied [193]. In particular, the porosity of the char has been evidenced as one of the main factors influencing the mechanical stability [110-112].

This section will thus be divided into two parts. The first one will deal with the evaluation of the mechanical strength of PU/APP/nano MgO chars prepared by different methods. The second part will go into much more details in order to identify the parameters affecting the char strength. The methods used to record the mechanical properties of char are fully described in **Chapter II, section 2.5.3-Mechanical strength of char p88**. The study of the mechanical behavior of the char has only been performed on PU, PU/APP and PU/APP/nano MgO samples because firstly, it was difficult to prepare the samples required for this kind of analysis and secondly, the nano MgO based formulations are the one particularly studied in this Ph.D work due to their best fire performances. In particular, after evaluating the mechanical behavior of the chars with the conventional mechanical test used at the laboratory [13, 60, 194], the following work will only focus on the systems PU 30%APP and PU 28%APP 2%nano MgO which will be compared together. This comparison will highlight the differences in the mechanical properties of the resulting chars and particularly their behavior against the conditions of char development.

3.1 Evaluation of the mechanical strength of chars prepared by different methods

When the viscosity varies during the temperature increase while the intumescence process develops, the internal structure of the charred material may also be modified as seen in the previous section. It is the characteristics of this structure that lead to the efficiency of fire protection [194, 195]. A good balance between enough resistant and not too hard char needs to be found. It is indeed necessary that the intumescent shield do not break during fire but on the contrary if it is too hard, the creation and propagation of cracks may lead to a rapid degradation of the material [60]. The porosity of the char has also to be taken in account since studies showed that one of the main factors influencing the mechanical stability is the char porosity, the smaller the pores size the better the char strength [110-112]. In particular, it has been evidenced that the pore sizes in the char vary with or without NPs. The mechanical characteristics of the chars will then be described in this part and linked to the other physical properties already commented before.

The evolution of char strength as a function of gap has first be monitored (method RF-HR500-500-o, it corresponds to the heating device-heating rate at heat treatment temperature-measurement temperature-sample characteristics, **see the precise signification of the method in Table 10 p91**) on PU, PU 30%APP, PU 29%APP 1%nano MgO and PU 28%APP 2%nano MgO; the graphs are plotted in **Figure 129**. The strength can be assimilated to a destruction force. When the strength is high, it means that the underlying material resists at the pressure applied on its surface. 1600 g is the maximum provided by the equipment. On the contrary, for a low resistant material, the strength required to destroy it will be low. Two extreme cases can thus be discussed. First if a material is extremely hard, the strength recorded will immediately jump until 1600 g when the upper plate will touch it. Second, if a material is not resistant at all, the strength recorded will be very low while the upper plate is damaging the char until its total destruction. The gap corresponds to the distance between the upper and bottom plates of the rheometer. It indicates first the char height (first gap at which the strength has a significant value over zero) and then at which distance the char exhibit a more or less powerful resistance on the upper plate of the rheometer. When the measurement of the strength cannot be done anymore because of the maximum force reached, the gap will be named the critical gap. The graphs of char strength as a function of gap are thus very rich in information concerning the mechanical resistance of the structured chars. Pictures of the residues after testing are additionally interesting to study and allow to corroborate the information obtained with the graphs.

The first graph (**Figure 129**) shows that the mechanical properties of PU char drastically depends on the fillers used since the evolution of strength as a function of gap is totally different depending on the considered formulation.

Virgin PU indeed leads to a very fragile char that is destroyed without any resistance between 8 and 3 mm gap. The observation of the residue at the end of the test (**Figure 130**) clearly shows that the material has been totally broken and the pieces of broken char are just staying at the bottom of the rheometer plate. This explains why the strength drastically increases around 3 mm of gap; it only corresponds to the force of the pieces compacted in the sample holder after the char destruction as already described in the literature [194].

The char exhibited by PU/APP/NP formulations are relatively fragile. They are destroyed by a small pressure from the upper plate. The strength increases regularly from 16 mm until approximately 5 mm showing a progressive resistance of the char which finally totally collapses. The incorporation of APP and nano MgO leads nevertheless to a slight improvement in the mechanical strength of PU char. The mechanical resistance is also slightly higher for the ratio 28/2 compared to the ratio 29/1. The critical gap values vary in the same way. The residues collected after test consist in a collection of small resistant pieces of char in both cases, as seen on **Figure 130**. This material is bright grey whereas it was darker in the case of virgin PU. The properties and aspect of the char are consequently largely affected by the presence of fillers.

The PU/APP char is on the contrary a very resistant material. There is indeed no destruction at all of the char and the critical gap of 14 mm corresponds to the char height. This is confirmed by the aspect of the char after the experiment (**Figure 130**) which seems to be intact. The surface of this char is homogeneous and bright grey. However, the material is composed of a thick crust and under the crust, a big bubble is observed. This is not in agreement with the literature which reported that the smaller the pores size the better the char strength [110-112] but in that case a hard crust is formed. The case of the char of PU 30%APP is very particular since the structure developed here is not the same as that observed in the previous sections. It appears that the conditions used here to develop the PU 30%APP char seem to lead to a char with a particular mechanical behavior and this needs to be further investigated.

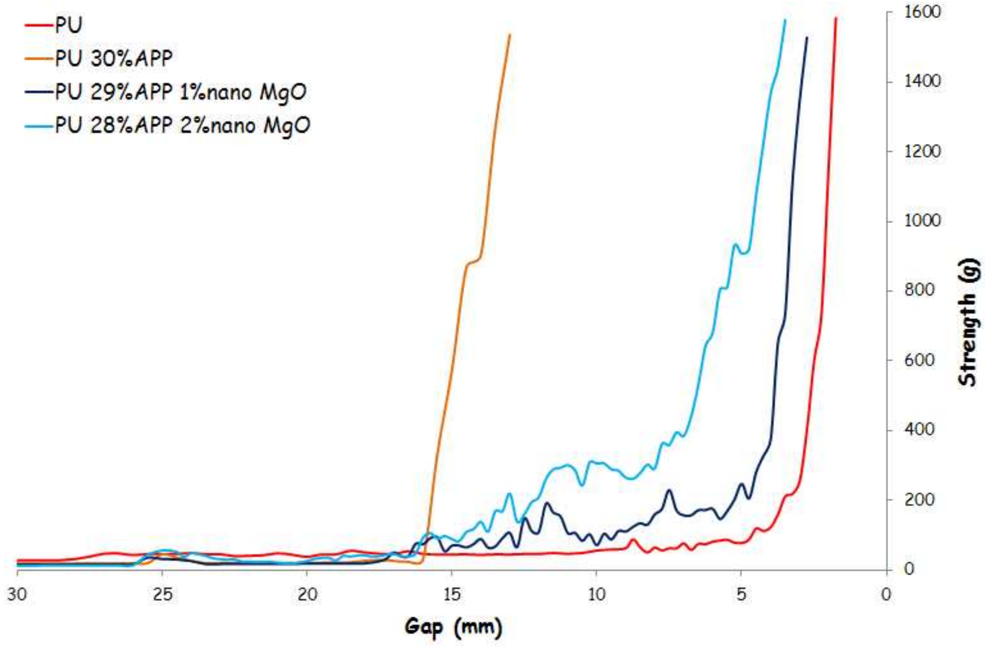

Figure 129: Evolution of char strength as a function of gap for PU, PU 30%APP, PU 29%APP 1%nano MgO and PU 28%APP 2%nano MgO prepared by method RF-HR500-500-o

Figure 130: Pictures of residues collected after measuring the strength as a function of gap on samples prepared by the method RF-HR500-500-o (from left to right: PU, PU 30%APP, PU 29%APP 1%nano MgO, PU 28%APP 2%nano MgO)

Unexpected results have just been obtained concerning the mechanical strength and morphology of PU/APP char. The conditions to develop the char required for the test (method RF-HR500-500-o) are suspected to be responsible of these results. To that aim it was chosen to follow the evolution of char strength as a function of gap on chars developed in a typical cone calorimeter experiment (50 kW/m² during 8 minutes 30 on a 10x10x0.3 cm^3 plate corresponding to the method MLCi-Q-AT-☐). The method RF-HR500-500-o indeed represents a simulation to know the mechanical resistance of chars while the method MLCi-Q-AT-☐ concerns the samples behavior in a real case where the fire performances have been evaluated (**Chapter III, section 2.1-Fire performances determined by mass loss calorimetry p106**).

Figure 131 compares the evolution of strength as a function of gap for PU 30%APP and PU 28%APP 2%nano MgO developed in the conditions of method MLCi-Q-AT-☐ and the corresponding residue pictures obtained during and after the mechanical test are presented in **Figure 132**. Significant expansion are reached thus requiring to start the recording of strength at higher gaps, up to 88 mm for the char PU 28%APP 2%nano MgO for instance.

For both chars the evolution of strength oscillates significantly during the experiment; this is in total agreement with the char morphology observed in **Chapter V, section 2.2.1-Effect of nanoparticles on the morphology of intumescent PU p185**. The irregularity of the strength measurement is linked to the cellular structure. This can moreover be seen on the pictures of the residue after the test (**Figure 132**) in particular for PU 28%APP 2%nano MgO. It appears, as suspected from tomography data, that the thin upper layer of the char is easily broken at around 85 mm and after a big hole (no big strength modification) is observed until approximately 40 mm. After that, the two chars start to exhibit the irregular strength increase related with their inner structures composed of cells of different size.

There are not much differences in the mechanical behavior of PU/APP and PU/APP/nano MgO chars except the significantly higher expansion exhibited by the char containing nano MgO but this has already been discussed in this chapter (**2.1-Monitoring of char development through its expansion p176**).

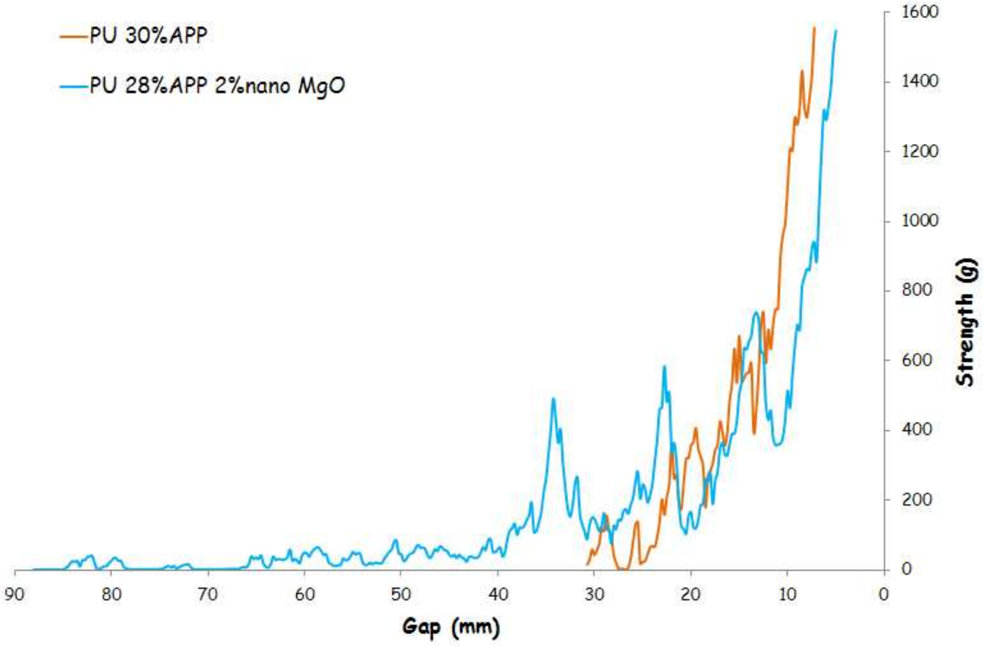

Figure 131: Evolution of char strength as a function of gap for PU 30%APP and PU 28%APP 2%nano MgO prepared by method MLCi-Q-AT-☐

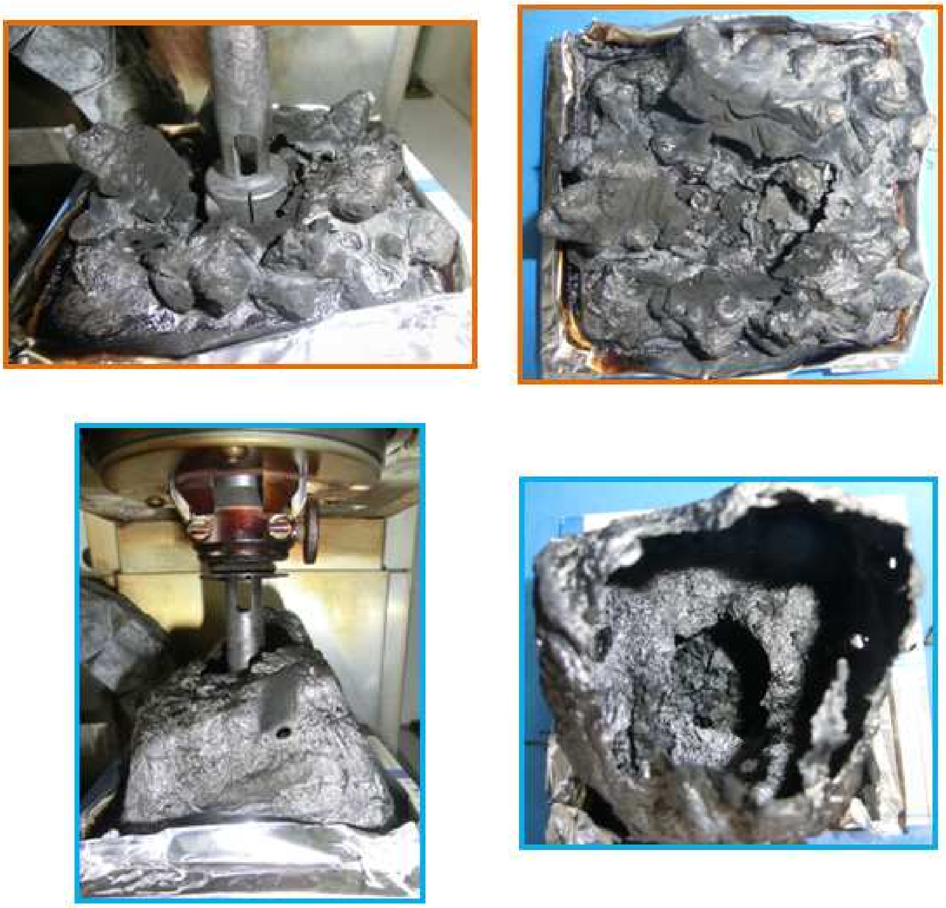

Figure 132: Pictures of chars prepared by method MLCi-Q-AT-☐ during (left) and after (right) strength measurement (top: PU 30%APP, bottom: PU 28%APP 2%nano MgO)

There is consequently not a significant influence of the incorporation of nano MgO on the mechanical strength of the char prepared by a standard cone calorimetry experiment. The better fire performances reached by the incorporation of nano MgO are consequently not a consequence of differences in char strength. It is moreover noteworthy that although the chars are not very strong, the fire protection mechanism required for cone calorimetry and LOI is effective.

Even if the mechanical properties of the chars have not a direct impact on the synergy mechanism, PU 30%APP and PU 28%APP 2%nano MgO may however behave differently in specific conditions as seen with the method RF-HR500-500-o. These differences have thus to be studied and further discussed. The behavior exhibited by the PU 30%APP formulation prepared with the method MLCi-Q-AT-□ give this time an expected result (quite fragile cellular char according to visual and qualitative observations of char strength) and it confirms the fact that the conditions to develop the char required for the method RF-HR500-500-o are responsible for the previous unexpected results. The evolution of char strength as a function of gap is moreover plotted and compared for these two methods in **Figure 133**; this will allow a more precise identification of the parameters responsible for these radically different mechanical properties.

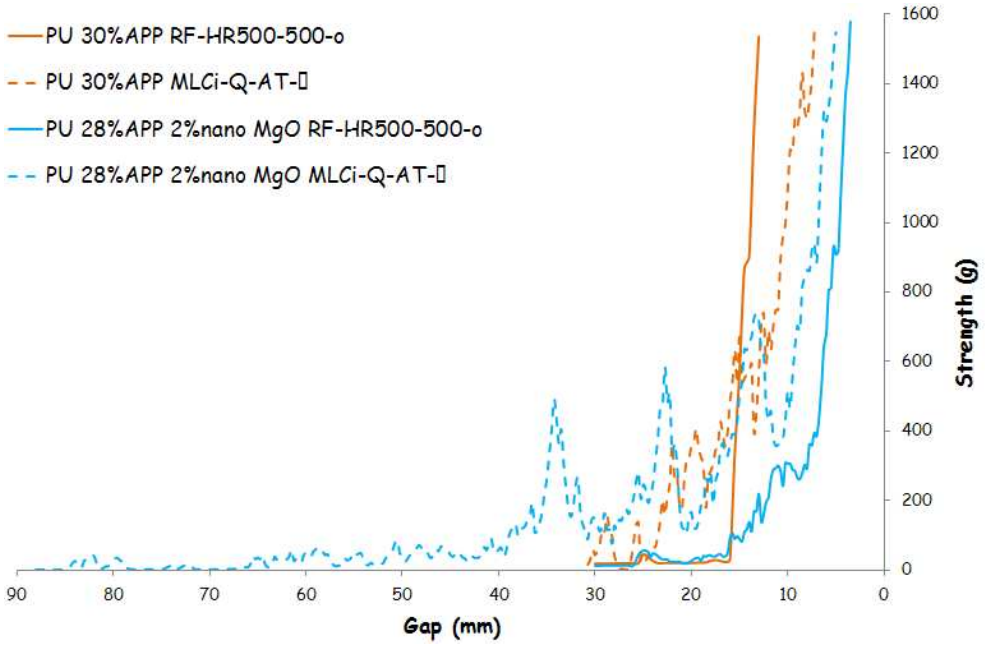

Figure 133: Comparison of the evolution of char strength as a function of gap for PU 30%APP and PU 28%APP 2%nano MgO prepared in rheometer or in cone calorimeter (methods RF-HR500-500-o versus MLCi-Q-AT-□)

In **Figure 133**, the recorded strength is different depending on the method for the same formulations or on the formulation for a same method. For the PU 30%APP, the differences are significantly highlighted since with the method RF-HR500-500-o, a very resistant char was obtained while with the method MLCi-Q-AT-□, the char is weaker. This leads to totally different evolution of the strength as a function of gap and critical gap values. These differences are not so important with nano MgO. The critical gap values are indeed considered as equivalent and the char strength is not drastically different from one method to another. In any case, **Figure 133** illustrates that depending on the method used, the char properties will be affected and the two formulations tested are not modified to the same extent; PU 30%APP is indeed more influenced by the conditions used to prepare the char.

Several parameters are modified while changing from method RF-HR500-500-o to MLCi-Q-AT-☐ and one or more of them could affect the mechanical behavior of the PU formulations. The following section will now aim to identify more precisely which parameters are crucial when dealing with the mechanical properties. It will also be particularly interesting to draw rules leading to the formation of strong chars.

3.2 A governing parameter potentially affecting char properties: the heating rate

The last section evidenced that the heating conditions have a significant impact on the mechanical resistance of the resulting chars; the aim of this section is first to identify the parameters affecting the mechanical properties and second to draw rules leading to the formation of strong chars. This is an interesting and very complete study but it is not related to the main topic of this manuscript which is to investigate the synergy mechanism between APP and NPs. It was indeed shown that the mechanical properties of the chars have not a direct impact on the synergy mechanism. The work carried out to find the governing parameters affecting char properties will then be detailed in **Appendix 3: Study of the parameters governing the mechanical behavior of PU 30%APP and PU 28%APP 2%nano MgO chars p249** and only the main conclusion will be given in this section.

To summarize the information obtained by the study of the mechanical behavior of char, it was showed first that the chars developed in the rheometer could be discriminated by their mechanical strength. Virgin PU is very fragile and collapses very easily. Higher destruction force is required to make PU/APP/nano MgO char (ratios 28/2 and 29/1) collapse but the material is still fragile, especially at a ratio 29/1. An unexpected resistance is exhibited by the char PU 30%APP. These results, related to char aspects, suggest that the char strength might be affected by some external parameters depending on the conditions used to develop the chars. It was then decided to investigate the mechanical behavior of sample prepared by cone calorimetry in different conditions on PU 30%APP and PU 28%APP 2%nano MgO. The chars PU 30%APP and PU 28%APP 2%nano MgO developed by a standard cone calorimetry experiment (method MLCi-Q-AT-☐) have equivalent mechanical resistance even if a higher expansion is observed for the formulation containing nano MgO. The oscillation in char strength values reflects the char morphology widely studied by tomography in the last section, which is composed of char walls alternatively with empty area due to its inner structure composed of many cells of different sizes.

It was then shown that the char strength is affected by some external parameters depending on the conditions used to develop the chars. With or without nano MgO in intumescent PU, the parameters affecting the mechanical properties are moreover totally different.

The investigation of nine different methods to develop the char was done in order to find the parameters affecting the mechanical behavior of the different chars (**Table 19**). It was thus evidenced that neither the presence of flame nor the heating type (convective or radiative heat) influences the char strength of both PU formulations. It has been however highlighted that it is required to control perfectly the heating conditions since different behaviors were observed when samples have been degraded in two furnaces (convective heat in both case) surrounding by different environments. The temperature at which the mechanical test is realized is of importance as well as the samples characteristics (size, shape, thickness and sample holder properties).

It was finally evidenced that for a same sample prepared in the same furnace and tested at ambient temperature, PU 30%APP and PU 28%APP 2%nano MgO behave totally differently. The heating rate is a critical parameter for the char strength of PU 30%APP and the heating temperature has a slight impact if a heating ramp was used. The resistance of PU 30%APP char is indeed favored by a slow heating rate (10°C/min) and lower heating temperatures (500°C). On the contrary, the mechanical properties of PU 28%APP 2%nano MgO are never influenced neither by the heating rate nor by the heating temperature.

Table 19: Summary table of the governing parameters potentially affecting char strength

Methods compared	**Parameter investigated**	**Effect on PU 30%APP char strength**	**Effect on PU 28%APP 2%nano MgO char strength**
MLCi-Q-AT-o versus MLCØi-Q-AT-o	Flame	No	No
MLCi-Q-AT-o versus MLCi-Q- AT-□	Sample characteristics	Yes	Yes
MLCi-Q-AT-o versus TO-Q700-AT-o	Heating type	No	No
TO-HR500-AT-o versus RF-HR500-AT-o	Furnace type	Yes	Yes
RF-HR500-500-o versus RF-HR500-AT-o	Measurement temperature	Yes	Yes
TO-HR700-AT-o versus TO-HR500-AT-o	Heating temperature	Yes (stronger char at lower temperature)	No
TO-Q700-AT-o versus TO-Q500-AT-o	Quench temperature	No	No
TO-HR700 (or 500)-AT-o versus TO-Q700 (or 500)-AT-o	Heating rate	Yes (stronger char at slow heating rate)	No

Since the mechanical strength of chars developed by cone calorimetry from PU 30%APP and PU 28%APP 2%nano MgO was equivalent while the fire performances were different, it means that the mechanism of synergy between APP and NP in PU is consequently not a result of mechanical properties. It is anyway important to remember that it has only been proved for cone calorimetry and the conclusions might be different in other fire tests. In particular the incorporation of nano MgO in intumescent PU has nevertheless a considerable impact on the development of chars submitted to different heating conditions (heating temperature and overall heating rate). It appears that nano MgO is a sort of stabilizer of the char structure since it is almost never affected by external heating conditions. The char PU 28%APP 2%nano MgO is indeed always quite fragile and only small pressures are required to lead it collapse. On the contrary, without nano MgO, opposite char structure and consequently mechanical behavior may be observed especially by changing the heating rate. These behavior differences against heating rate are consistent with the influence of heating rates on the degradation of PU 30%APP and PU 28%APP 2%nano MgO studied in **Chapter IV, section** 4-**Influence of Heating Rate on the Degradation of PU Formulations p161**. The range of temperature studied with the mechanical behavior investigation (≥ 500°C) corresponds indeed to a range of temperature where the combination of APP and NP exhibits a stabilization effect evidenced by TGA.

4 CONCLUSION: SOME PHYSICAL INTERACTIONS RESPONSIBLE FOR THE SYNERGY

This section evidenced that some of the physical properties of PU/APP/NP formulations are involved in the synergy mechanism between APP and NPs in the considered PU matrix.

The effective fire protection of PU/APP and PU/APP/nano MgO formulations compared to PU and PU/nano MgO was linked to the thermal barrier effect induced by the chars developed in cone calorimeter. The back face temperature of PU plates indeed evidenced a decrease of 250°C at the end of the test by the incorporation of a mixture APP/nano MgO in the virgin PU.

The incorporation of fillers increases the thermal conductivity of virgin PU at ambient temperature, thus leading to a faster heat transfer. Under the temperature increase, the intumescence process then occurs and creates chars characterized by a low thermal conductivity. The evolution of the thermal conductivity with temperature of PU 30%APP and PU 28%APP 2%nano MgO is similar but their values are significantly different. The intrinsic properties of the chars developed by PU 30%APP and PU 28%APP 2%nano MgO are clearly different at and after 400°C. At a similar expansion, these two chars have different morphology resulting in thermal conductivity differences.

The char development has then been followed by monitoring the expansion. By following the expansion as a function of temperature during a 10°C/min heating ramp, it was impossible to discriminate PU/APP from PU/APP/nano MgO formulations. On the contrary, if the expansion is monitored as a function of time during a cone calorimeter experiment, the incorporation of nano MgO plays a role on the charring process and on the final expansion values. A slowdown is observed at the beginning of intumescence with nano MgO while the expansion evolves progressively without nano MgO.

The use of tomography provided major information on the char morphology, char structuring and repartition of fillers in degraded PU matrix. It was proven that the incorporation of NPs affects both the char morphology and the fillers repartition at the end of a cone calorimeter test and this depends on the nature of the NP and the ratio APP/NP. The intumescence behavior and the final char structure are moreover much more complex in the case of PU 28%APP 2%nano MgO compared to PU 30%APP. The last one intumesces regularly and leads to a homogeneous char whereas with nano MgO, the char grows in two steps concomitantly with the expansion measurement leading to an inner char structure in two parts. A faster degradation is additionally evidenced without nano MgO. The synergy mechanism between APP and NP in PU is consequently partly due to the char morphology and the development of intumescence.

The study of gases released during additives degradation thanks to an innovative method reveals furthermore that the degradation processes involved are different if there is nano MgO in combination with APP or not. Nano MgO regulates the gas flow when APP degrades due to the formation of a dense glassy network, especially at low content in nano MgO. It was thus evidenced that the char morphology can be correlated with this pressure released by the additives. The crust of the char PU 30%APP is indeed far less structured than the one obtained from PU 28%APP 2%nano MgO. This is moreover in agreement with the faster degradation of PU 30%APP since the degradation products are released faster in the burning front.

In our study, the char morphology, its expansion and thermal conductivity appear intimately related to design a material with high thermal barrier effect. It is known that intumescent systems provide fire resistance to the underlying material by its expansion and formation of a char that leads to a significant reduced thermal conductivity, thereby contributing to the insulation function of the material. Higher expansion and lower thermal conductivity are observed for the system PU 28%APP 2%nano MgO compared to PU 30%APP which then protect better the substrate leading to better fire performances.

The study of the mechanical behavior of chars revealed that the char strength highly depends on the PU formulations tested and on the conditions used to develop the chars. The chars PU 30%APP and PU 28%APP 2%nano MgO tested after cone calorimetry exhibit an equivalent mechanical resistance even if an higher expansion is noticed by the formulation containing nano MgO. This proved that the synergy mechanism between APP and NP in PU in cone calorimetry conditions is not governed by the mechanical resistance of the chars. A correlation between the char strength as a function of char height and the char morphology was moreover highlighted.

With or without nano MgO in intumescent PU, the parameters affecting the mechanical properties are moreover totally different. The presence of flame and the heating type (convective or radiative heat) were never influencing the char strength of both PU formulations. The temperature at which the mechanical test is realized is of importance as well as the samples characteristics (size, shape, thickness and sample holder properties). It was finally evidenced that PU 30%APP and PU 28%APP 2%nano MgO behave totally differently regarding the heating conditions imposed. The heating rate is a critical parameter for the char strength of PU 30%APP and the heating temperature has a slight impact if a heating ramp is used. The resistance of PU 30%APP char is indeed favored by a slow heating rate (10°C/min) and lower heating temperatures (500°C). On the contrary, the mechanical properties of PU 28%APP 2%nano MgO are never influenced neither by the heating rate nor by the heating temperature and always exhibit a poor mechanical resistance. The incorporation of nano MgO has then a stabilizer role for the char structure concomitant with the regulation of pressure flow and finally governing the char structure.

In this chapter, it was validated that the physical properties of chars are clearly taking part in the synergy process between APP and NP in the considered PU matrix. The higher thermal barrier effect provided by the low thermal conductivity PU 28%APP 2%nano MgO char is first evidenced. The expansion, the char morphology and its development during the intumescence process are affected by the presence of NP and the ratio APP/NP and consequently have a role in the synergy process. All these physical char properties must be linked to the chemical species present in the char since different physical properties as well as chemical properties are identified in PU/APP and PU/APP/NP chars. Even if the poor char strength exhibited in cone calorimetry does not depend on the presence of nano MgO in intumescent PU, stronger char might be obtained by changing the heating conditions. The resistance of PU 30%APP char is indeed favored by a slow heating rate and low heating temperatures. On the contrary, the mechanical properties of PU 28%APP 2%nano MgO are never influenced by the heating conditions. The char morphology is consequently different.

A combination of chemical and physical phenomena appears to be required to lead to a synergy between APP and NP in our PU matrix. This will be further discussed in the following general conclusion in order to draw general rules associated to well define governing parameters for preparing PUs with enhanced flame retardancy.

GENERAL CONCLUSION

The work described in this Ph.D thesis was carried out in the frame of the collaborative project between ENSCL/UMET-ISP and Huntsman and had two main objectives. The first one was to explain the synergy in fire performances observed between APP and NPs in the considered PU matrix. The second one was to draw general rules and find the governing parameters for preparing PUs with enhanced flame retardancy.

PUs are indeed interesting polymers due to their designable composition and thus properties but their use is currently limited due to the fire risks they occasioned. The main goal of the project was therefore to understand the flame retardancy mechanism of fillers in a model PU casting in order to widen the knowledge to all filled PU systems. According to the literature and requirements from Huntsman, the system studied was thus composed of a specific PU matrix, a phosphorus based intumescent flame retardant (APP) and selected NPs. The reaction to fire of these systems was investigated and interactions between PU, APP and NPs were identified. Then, different methods were developed and different experiments were carried out to fully understand the mechanisms of action of APP/NPs combination.

First, selected fillers were incorporated in the PU matrix and the resulting materials were first characterized in terms of chemical composition, dispersion, glass transition temperature, reaction to fire and thermal stability. Since PU, PU/APP and PU/APP/NP exhibit different fire performances and different mechanisms of thermal degradation, it was decided to investigate further the parameters affecting the behavior of PU formulations upon heating either in fire conditions or with heating ramps. It was evidenced that both chemical and physical interactions were involved in the fire protection mechanisms. These parameters and their effect on the fire protection mechanisms are listed in **Table 20**. This table summarizes the results presented in this Ph.D thesis and aims to give the following information:

- which parameter(s) allow(s) playing on the fire performances of PU? This corresponds to the comparison between PU and PU/APP
- which parameter(s) play(s) a role on the synergy mechanism? This corresponds to the comparison between PU/APP and PU/APP/NP
- what are the conditions leading to the best FP?

In **Table 20**, each parameter is taken separately but the understanding of the fire protection mechanism is based on a combination of all parameters. It allows nevertheless highlighting the parameters involved in the synergy mechanism between APP and NPs in the PU matrix.

Table 20: Summary table presenting the parameters evaluated to understand the fire protection mechanisms (FP = fire performances and NT stands for not tested)

Parameter evaluated	Effect on FP?	Role on synergy?	Conditions for optimized FP
Chemical reaction during synthesis	No	No	/
Dispersion	Yes	No	Only homogeneous dispersion required, nanodispersion not necessary
Glass transition temperature	No	No	/
Nature of NP	/	Yes	MgO better than SiO_2 better than gold better than OMPOSS
Ratio APP/NP	/	Yes	Nano MgO: 28/2 ≈ 29/1 better than 25/5; nano gold: 28/2 better than 29/1 and better than 29.5/0.5
Modification of the thermal degradation pathway	Yes	No	Beginning of PU degradation catalyzed by APP but no effect of NP
Thermal stabilization	Yes	Yes	Higher thermal stabilization is better
Chemical composition of gas phase	Yes	No	Phosphorus and nitrogen based components in gas phase lead to better FP but no additional gases with NPs
Chemical composition of the condensed phase	Yes	Yes	
- species formed during APP degradation	Yes	Yes	Better if presence of phosphonic, phosphoric acid, P-O-C and P-O-P
- reaction APP + PU	Yes	No	Better FP if reaction APP + PU
- reaction APP + NP	/	Yes	Better FP if reaction APP + NP
- nature of phospho-X compounds	/	Yes	Magnesium phosphates better than silicophosphates
Kinetic of APP degradation	/	Yes	Better if P-O-P and P-O-C formed: only observed if NP is present
Char yield	Yes	Yes	Better FP if higher mass kept
Effect of heating conditions on thermal stability	NT	Yes	Same final residue whatever the heating rate leads to better FP
Thermal conductivity at ambient temperature	Yes	No	Higher thermal conductivity at ambient temperature gives better FP
Thermal conductivity of the char	NT	Yes	Lower thermal conductivity char favors increased FP
Char expansion	Yes	Yes	Higher char leads to better FP

Evolution of char height	/	Yes	Presence of a slowdown at the beginning of char expansion improves the FP
Char morphology	/	Yes	A structure in two parts with a bottom composed of many small cells improves the FP
Repartition of fillers in the char	/	Yes	A progressive decrease of fillers in the char gives better FP
Inner char structure development	/	Yes	Not regular char development leads to better FP
Degradation kinetic according to quantity of PU plate left during MLC	NT	Yes	Slower degradation rate favors increased FP
Flow of gases released	NT	Yes	A controlled and slow flow for gases released during degradation gives better FP
Mechanical strength of char	Yes	No	Under certain conditions the formation of a strong char (increased FP) is possible with PU/APP but not PU/APP/NP
Effect of heating conditions on mechanical behavior	NT	Yes	If there is no effect of the heating conditions on the mechanical behavior, the FP are better

The synergy mechanism exhibited by PU/APP/NP formulations leading to high fire performances can now be explained.

The nature of NP and the ratio APP/NP are the first important parameters to select because they will affect all the other properties.

The thermal stability provided by the PU/APP/NP formulations is the result of many reactions occurring in the condensed phase: the NPs can change the species formed during APP degradation, they can also change the kinetic of APP degradation and finally NPs may react with APP to lead to new phospho-X compounds (for instance magnesium phosphate in the case of MgO). These reactions evidenced in the condensed phase totally depend on the NP and on the ratio APP/NP. The thermal stability, provided by the specific reactions, gives a high char yield; that allow the development of the intumescence mechanism.

The char developed during the intumescence process has different properties depending if NPs are added or not in the formulation and this is linked to the chemical species present in the condensed phase. These properties are the thermal conductivity of the char, the char expansion and the char morphology. A lower thermal conductivity, a higher char expansion and a smaller cell based morphology obtained in the case of the PU 28%APP 2%nano MgO char compared to the PU 30%APP char give enhanced flame retardancy. The better thermal barrier effect provided by the incorporation of nano MgO in the intumescent formulation consequently delays the degradation of the underlying PU matrix.

The evolution of char height and the inner char structure development are totally linked and evidence a two steps process with nano MgO compared to a regular evolution without nano MgO. In particular a slowdown in the PU/APP/nano MgO char expansion speed is noticed and should be linked to a difference in the rheological properties of the materials that could not be measured due to experimental limitations. The influence of rheological properties is anyway strongly supported by the fact that nano MgO added to APP forms a non porous glassy structure, thus “regulating” the pressure flow of gases released during APP degradation. This explains as well why the external char surface of PU 30%APP is so irregular compared to the one of PU 28%APP 2%nano MgO.

The degraded fillers present in the char have different chemical composition and were formed at different moment during the MLC test and are then differently dispersed in the char. The heating conditions affect differently the formulations PU 30%APP and PU 28%APP 2%nano MgO; in particular their thermal stability and the mechanical strength of their char. The nano MgO generally acts as a stabilizer leading the degradation of the material less affected by the external conditions.

To summarize, the incorporation of NPs in intumescent PU leads to the formation of specific chemical species at specific times that enable the development of a stable intumescent structure with optimized properties. This mechanism is responsible for the synergy observed in fire performances between APP and NPs in the considered PU matrix; the synergistic effect is linked to the NP and the ratio APP/NP selected.

The synergy mechanism occurring between APP and NPs in a PU matrix has been widely investigated and elucidated during this Ph.D work. The governing parameters of the synergy have been evidenced by a range of techniques; in particular some are new in this research field. General rules based on the governing parameters have moreover been drawn to design PUs with high fire protection performances.

OUTLOOK

As it has just been seen in the general conclusion, new methods have been successfully set up during this Ph.D work in order to identify the governing parameters of the synergy between APP and NPs in PU. The synergy mechanism has thus been mainly elucidated but it is still possible to go deeper to understand even better some parts of the mechanism.

First, it would be interesting to complete some experiments to characterize even better the PU/APP/NP systems. Then, the extension of the work to other application such as the use of PU as fire protective coating should be considered. Finally, a quantitative approach should be worth to perform in order to model and further design an optimized intumescent system.

To go further in the understanding of the phenomena occurring during the degradation of PU formulations, the characterization of the materials regarding their chemistry, the kinetics and the rheology should be completed.

In particular, the development of new NMR sequences allowing attributing more easily the ^{31}P solid state NMR signals is currently under investigation. The better assignment of the peaks between -5 and -15 ppm is of particularly interest because the formation of pyrophosphates and/or P-O-C bonds results in different fire protection mechanisms. A double cross polarization sequence is giving promising results on a reference molecule: the phenylphosphinic acid.

The kinetic of formation of the degradation products from PU/APP and PU/APP/NP is important to be detailed. In particular, it was noticed during the Ph.D work that the thermal degradation of PU 30%APP and PU 28%APP 2%nano MgO is differently affected by the heating rate. This could furthermore be linked to different fire properties depending on the heating constraints of different fire tests and thus this should be further investigated.

Finally, as it has been evidenced in this Ph.D thesis, the rheology of the systems appears to be a key factor in the protection mechanism. A method to characterize reliably the viscosity of the formulations upon degradation is required to understand better the phenomenon.

Because of the cooperation with an industrial partner, Huntsman, one of the goals of this Ph.D work was also to provide commercially suitable systems. The Ph.D work was performed on a PU casting with a specific composition to ease the understanding of the phenomenon occurring. A patent on the use of MgO in combination with intumescent flame retardants in PUs has been filed and will be published in September 2012. Thanks to the governing parameters evidenced during the Ph.D work, it is indeed possible to design commercially suitable products. The next step is thus to develop the concept for all kind of PU-based materials in order to manufacture flame retarded polymers.

One of the ideas of the project was to use the PU/APP/NP formulation to act as a fire protective coating to protect PU foams or steel structure for example. The formulation PU 28%APP 2%nano MgO has been tested according to the ISO 834 fire test for cellulosic fire [165]. The evolution of the temperature against the time has been recorded and is presented and compared to another intumescent PU based system in **Figure 134**. The formulation PU 28%APP 2%nano MgO is able to protect the steel plate and the back face temperature does not exceed 500°C (temperature corresponding to the acceptable limit for temperature increase) until around 1800 seconds but the protection is not as efficient as in the case of the other PU based system (500°C reached after 4000 seconds).

Even if the PU/APP/NP system was very efficient in cone calorimetry and LOI, it is not as efficient when dealing with the fire protection measured according to the ISO 834 test. This is probably due to the different thermal stress engaged in the furnace test; it is more severe compared to MLC or LOI. Heating rate is indeed a critical parameter for fire protection; different temperatures and heating rates are involved depending on the fire scenario considered. It is clearly shown here that this affect the thermal barrier effect provided by the PU formulations. The quantification of the effect of the governing parameters is now required to go further in the comprehension of the material behavior submitted to an external heating source.

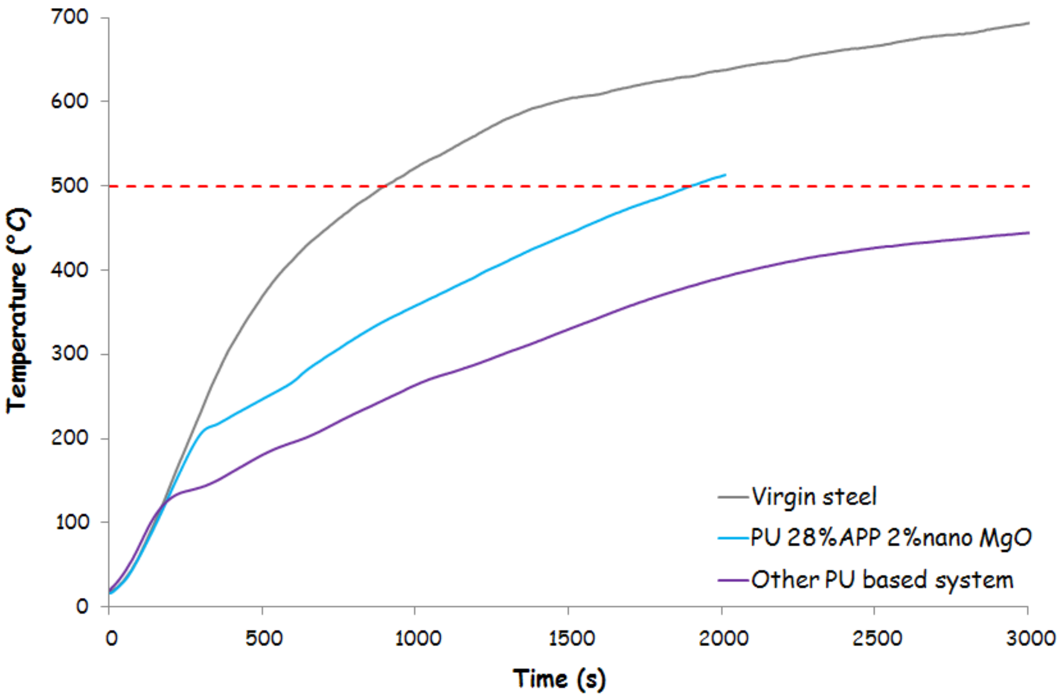

Figure 134: Time-Temperature curves obtained under ISO834 conditions for virgin steel, the formulation PU 28%APP 2%nano MgO and another PU based system coated on steel plates (around 1600-1700 µm of thickness)

Finally, the work carried out on the understanding of the synergy mechanism could be used to develop a model in order to find, whatever the system, the "ideal" NP giving high fire performances through a synergistic effect. In particular by the precise quantification of the governing parameters, designing by simulation an optimized intumescent system will be possible.

This approach should involve a deeper kinetic analysis to model the phenomenon observed by changing the thermal stresses (different fire tests). The effect of the heating rate should thus be extrapolated to predict the behavior of the material whatever the heating constraints.

In parallel, an analysis of the cells size and distribution in the char developed in different conditions might be done using the results from tomography. The porosity of the charred structure for example should be calculated using image analyses and this will give an overview of the inner structure that could be use in numerical models.

All the governing parameters should be linked in a multicomponent model which will predict the behavior of the material under a temperature increase. The final aim of the simulation is to be able to design an optimized intumescent system containing a polymeric matrix, an intumescent additive and a NP acting as synergist. After the investigation of the properties of the primary compounds of a system, the parameters could be injected in the model developed and this model will predict the suitable NP to use in this particular case.

Some issues are still observed to provide a suitable commercially application for the PU/APP/NP systems developed in this Ph.D work but the current efforts will probably help to resolve them. In particular all the methods developed and the governing parameters detailed in this Ph.D work are really required to go further in the research on the flame retardancy of intumescent systems.

REFERENCES

1. J.TROITZSCH, M.LE_BRAS and S.BOURBIGOT, *International Plastic Flammability Handbook - Fundamentals*, ed. H.G. Publications. 2004.
2. O.BAYER, W.SIEFKEN, H.RINKE, L.ORTHNER and H.SCHILD, *A process for the production of polyurethanes and polyureas*, I.G. Farben, Editor. 1937.
3. G.WOODS, *The ICI Polyurethanes book*. 1990: ICI Polyurethanes and John Wiley & sons.
4. ADEME. *Etude du marché du polyuréthane et état de l'art de ses techniques de recyclage*. 2003.
5. G.PAL and H.MACSKASY, *Plastics: their behavior in fires.* Elsevier New York, 1991.
6. M.M.HIRSCHLER, *Polyurethane foam and fire safety.* POLYM ADVAN TECHNOL, 2008. **19**: p. 521-529.
7. R.DELOBEL. *L'ignifugation : les différentes stratégies*. in *Actes du 6ième Congrès Européen sur l'Ignifugation desMatériaux Polymères*. 1997. Lille.
8. S.BOURBIGOT and S.DUQUESNE, *Fire retardant polymers: Recent developments and opportunities.* J MATER CHEM, 2007. **17**(22): p. 2283-2300.
9. D.WANG and C.A.WILKIE, *Fire Properties of Polymer Nanocomposites*, in *Fire Properties of Polymer Composite Materials*, A.P.MOURITZ and A.G.GIBSON, Editors. 2006, Springer.
10. F.LAOUTID, L.BONNAUD, M.ALEXANDRE, J-M.LOPEZ-CUESTA and P.DUBOIS, *New prospects in flame retardant polymer materials : from fundamentals to nanocomposites.* MAT SCI ENG R, 2009. **63**: p. 100-125.
11. F.SAMYN, *Development of polyurethane with improved reaction to fire - Polyurethane containing intumescent additives and nanoparticles*. 2009.
12. J-P.TROTIGNON, J.VERDU, A.DOBRACZYNSKI and M.PIPERAUD, *Matières plastiques : structures-propriétés, mise en oeuvre, normalisation*, ed. Nathan. 1996.
13. S.DUQUESNE, *Etude des procédés d'ignifugation de substrats polymères par revêtements intumescents - Application aux polyuréthanes* 2001, UNIVERSITE DES SCIENCES ET TECHNOLOGIES DE LILLE: Lille.
14. D.K.CHATTOPADHYAY and D.C.WEBSTER, *Thermal stability and flame retardancy of polyurethanes.* PROG POLYM SCI, 2009. **34**: p. 1068-1133.
15. Z.S.PETROVIC, Z.ZAVARGO, J.H.FLYNN and W.J.MACKNIGHT, *Thermal degradation of segmented polyurethanes.* J APPL POLYM SCI, 1994. **51**: p. 1087-1095.
16. S.V.LEVCHIK and E.D.WEIL, *Thermal decomposition, combustion and fire-retardancy of polyurethanes—a review of the recent literature.* POLYM INT, 2004. **53**: p. 1585-1610.
17. R.BILBAO, J-F.MASTRAL, J.CEAMANOS and M-E.ALDEA, *Kinetics of the thermal decomposition of polyurethane foams in nitrogen and air atmospheres.* J. Anal. Appl. Pyrolysis, 1996. **37**(1): p. 69-82.
18. J.LEFEBVRE, B.BASTIN, M.LE_BRAS, S.DUQUESNE, R.PALEJA and R.DELOBEL, *Thermal stability and fire properties of conventional flexible polyurethane foam formulations.* POLYM DEGRAD STABIL, 2005. **88**: p. 28-34.
19. J.S.BABIEC_JR., J.J.PITTS, W.L.RIDENOUR and R.J.TURLEY, *HOW TO EFFECTIVELY FLAME RETARD FLEXIBLE URETHANE FOAMS: TETRAKIS (2-CHLOROETHYL)ETHYLENE DIPHOSPHATE.* 1975.
20. W.WITTEBECKER, D.DAEMS and U.WERTHER, *Performance of polyurethane building products in fires.* Brochure ISOPA (European Isocyanate Producers Association).
21. European_Flame_Retardants_Association, *How do flame retardants work ?* 2006.
22. GOLIATH, *Flame retardants: improving fire safety for plastics products.* PLAST ENG, 2006.

23. F.SCHAPMAN, B.YOUSSEF, E.ABOUT_JAUDET and C.BUNEL, *Ignifugation de polyurethanes I. Utilisation d'un polyol insature modifie par le 1-thioethyl diethylphosphonate.* EUR POLYM J, 2000. **36**: p. 1865-1873.
24. W.EL_KHATIB, B.YOUSSEF, C.BUNEL and B.MORTAIGNE, *Fireproofing of polyurethane elastomers by reactive organophosphonates.* POLYM INT, 2003. **52**: p. 146-152.
25. B.YOUSSEF, B.MORTAIGNE, M.SOULARD and J.M.SAITER, *Fireproofing of polyurethane by organophosphonates.Study of degradation by simultaneously TG/DSC.* J THERM ANAL CALORIM, 2007. **90**: p. 489-494.
26. Z.E.JOLLES and D.M.JONAS, *Flame-retardant liquid surface coating compositions*. 1968, Berk Ltd.: Great Britain.
27. M.KAWADA and S.TANIUCHI, *Fire-resistant agents*. 1970, Daiichi Kogyo Seiyaku Co., Ltd.: Japan.
28. M.MODESTI and A.LORENZETTI, *Flame retardancy of polyisocyanurate-polyurethane foams: use of different charring agents.* Polym. Degrad. Stab., 2002. **78**(2): p. 341-347.
29. F.SAMYN, *Compréhension des procédés d'ignifugation du polyamide 6 - Apport des nanocomposites aux systèmes retardateurs de flamme phosphorés*. 2007, UNIVERSITE DES SCIENCES ET TECHNOLOGIES DE LILLE: Lille.
30. A.GHAREHBAGHI, R.BASHIRZADEH and Z.AHMADI, *Polyurethane flexible foam fire resisting by melamine and expandable graphite: Industrial approach.* J CELL PLAST, 2011. **47**(6): p. 549–565.
31. H.SINGH and A.K.JAIN, *Ignition, combustion, toxicity, and fire retardancy of polyurethane foams: a comprehensive review.* J. Appl. Polym. Sci., 2009. **111**(2): p. 1115-1143.
32. C.M.DICK, C.DENECKER, J.J.LIGGAT, M.H.MOHAMMED, C.E.SNAPE, G.SEELEY, C.LINDSAY, B.ELING and P.CHAFFANJON, *Solid state 13C and in situ 1H NMR study on the effect of melamine on the thermal degradation of a flexible polyurethane foam.* POLYM INT, 2000. **49**: p. 1177-1182.
33. M.THIRUMAL, D.KHASTGIR, G.B.NANDO, Y.P.NAIK and N.K.SINGHA, *Halogen-free flame retardant PUF: Effect of melamine compounds on mechanical, thermal and flame retardant properties.* Polymer Degradation and Stability, 2010. **95**(6): p. 1138-1145.
34. A.KOENIG, A.MALEK, U.FEHRENBACHER, G.BRUNKLAUS, M.WILHELM and T.HIRTH, *Silane-functionalized flame-retardant aluminum trihydroxide in flexible polyrethane foam.* J CELL PLAST, 2010. **46**(5): p. 395-413.
35. U.A.PINTO, L.L.Y.VISCONTE, J.GALLO and R.C.R.NUNES, *Flame retardancy in thermoplastic polyurethane elastomers (TPU) with mica and aluminum trihydrate (ATH).* POLYM DEGRAD STABIL, 2000. **69**: p. 257-260.
36. J.LINDHOLM, A.BRINK, C-E.WILEN and M.HUPA, *Cone calorimeter study of inorganic salts as flame retardants in polyurethane adhesive with limestone filler.* J. Appl. Polym. Sci., 2012. **123**(3): p. 1793-1800.
37. D.BARAL, P.P.DE and G.B.NANDO, *Thermal characterization of mica-filled thermoplastic polyurethane composites.* POLYM DEGRAD STABIL, 1999. **65**: p. 47-51.
38. S.BENLI, U.YILMAZER, F.PEKEL and S.OZKAR, *Effect of Fillers on Thermal and Mechanical Properties of Polyurethane Elastomer.* J APPL POLYM SCI, 1998. **68**: p. 1057-1065.
39. G.FONTAINE, T.TURF and S.BOURBIGOT, *Salen copper complexes: a novel flame retardant for thermoplastic polyurethane.* ACS SYM SER, 2009. **1013**: p. 329-340.
40. B.K.KIM, J.W.SEO and H.M.JEONG, *Preparations and properties of polyurethane nanocomposites with organoclay or nanosilica.* J POLYM ENG, 2009. **29**: p. 27-38.
41. R.KOZLOWSKI, M.A.HASSAN, B.OBIDZINSKI, A.B.SHEHATA and M.AMER, *Newly Modified MMT and Its Application with Intumescent Additives as New Flame Retardant System for Polyurethane Polymer.* POLYM-PLAST TECHNOL, 2008. **47**(9): p. 902-909.
42. Z.XU, X.TANG and J.ZHENG, *Thermal Stability and Flame Retardancy of Rigid Polyurethane Foams/Organoclay Nanocomposites.* POLYM-PLAST TECHNOL, 2008. **47**(11): p. 1136-1141.

43. M.MODESTI, A.LORENZETTI, S.BESCO, D.HRELJA, S.SEMENZATO, R.BERTANI and R.A.MICHELIN, *Synergism between flame retardant and modified layered silicate on thermal stability and fire behaviour of polyurethane nanocomposite foams.* POLYM DEGRAD STABIL, 2008. **93**: p. 2166-2171.
44. M.BERTA, A.SAIANI, C.LINDSAY and R.GUNARATNE, *Effect of Clay Dispersion on the Rheological Properties and Flammability of Polyurethane-Clay Nanocomposite Elastomers.* J APPL POLYM SCI, 2009. **112**: p. 2847-2853.
45. M.BERTA, C.LINDSAY, G.PANS and G.CAMINO, *Effect of chemical structure on combustion and thermal behaviour of polyurethane elastomer layered silicate nanocomposites.* POLYM DEGRAD STABIL, 2006. **91**: p. 1179-1191.
46. M.MODESTI, A.LORENZETTI and S.BESCO, *Influence of Nanofillers on Thermal Insulating Properties of Polyurethane Nanocomposites Foams.* POLYM ENG SCI, 2007: p. 1351-1358.
47. B.SON, T-S.HWANG and D-C.GOO, *Fire-retardation properties of polyurethane nanocomposite by filling inorganic nano flame retardant.* POLYMER, 2007. **31**: p. 404-409.
48. H.MAHFUZ, V.K.RANGARI, M.S.ISLAM and S.JEELANI, *Fabrication, synthesis and mechanical characterization of nanoparticles infused polyurethane foams.* COMPOS PART A-APPL S, 2004. **35**: p. 453-460.
49. Gy.MAROSI, Gy.BERTALAN, P.ANNA, I.RAVADITS, Sz.SZABO, S.BOURBIGOT, M.LE_BRAS and R.DELOBEL, *Polyphosphate flame retardants in polyolefins.* Recent Adv. Flame Retard. Polym. Mater., 2000. **11**: p. 154-163.
50. H.TRAMM, C.CLAR, P.KUHNEL and W.SCHUFF, *Fireproofing of wood*, RuhrchemieAktiengesellschaft, Editor. 1938: Germany.
51. H.L.VANDERSALL, *Intumescent coating systems, their development and chemistry.* J FIRE FLAMMABILITY, 1971. **2**: p. 97-140.
52. A.BALLISTRERI, G.MONTAUDO, C.PUGLISI, E.SCAMPORRINO and D.VITALINI, *Intumescent flame retardants for polymers. I. The poly(acrylonitrile)-ammonium polyphosphate-hexabromocyclododecane system.* J APPL POLYM SCI, 1983. **28**(5): p. 1743-1750.
53. G.MONTAUDO, E.SCAMPORRINO and D.VITALINI, *Intumescent flame retardants for polymers. II. The polypropylene-ammonium polyphosphate-polyurea system.* J POLYM SCI POL CHEM, 1983. **21**(12): p. 3361-3371.
54. G.CAMINO, L.COSTA and L.TROSARELLI, *Mechanism of intumescence in fire retardant additives for polymers.* Polymer Preprints (American Chemical Society, Division of Polymer Chemistry), 1984. **25**(1).
55. G.CAMINO, L.COSTA and L.TROSARELLI, *Study of the mechanism of intumescence in fire retardant polymers. Part I. Thermal degradation of ammonium polyphosphate-pentaerythritol mixtures.* POLYM DEGRAD STABIL, 1984. **6**(4): p. 243-252.
56. G.CAMINO, L.COSTA and L.TROSARELLI, *Study of the mechanism of intumescence in fire retardant polymers. Part II. Mechanism of action in polypropylene-ammonium polyphosphate-pentaerythritol mixtures.* POLYM DEGRAD STABIL, 1984. **7**(1): p. 25-31.
57. G.CAMINO, L.COSTA and L.TROSARELLI, *Study of the mechanism of intumescence in fire retardant polymers. Part III. Effect of urea on the ammonium polyphosphate-pentaerythritol system.* POLYM DEGRAD STABIL, 1984. **7**(4): p. 221-229.
58. G.CAMINO, L.COSTA, L.TROSARELLI, F.COSTANZI and G.LANDONI, *Study of the mechanism of intumescence in fire retardant polymers. Part IV. Evidence of ester formation in ammonium polyphosphate-pentaerythritol mixtures.* POLYM DEGRAD STABIL, 1984. **8**(1): p. 13-22.
59. S.BOURBIGOT and S.DUQUESNE, *Intumescent based flame retardant*, in *Fire retardancy of polymeric materials*, C.A.WILKIE and A.B.MORGAN, Editors. 2009, Wiley.
60. M.JIMENEZ, *Etude des mécanismes de protection et de réaction au feu dans les revêtements intumescents. Application aux resines époxydiques*. 2006, UNIVERSITE DES SCIENCES ET TECHNOLOGIES DE LILLE: Lille.
61. S.BOURBIGOT, M.LE_BRAS, S.DUQUESNE and M.ROCHERY, *Recent Advances for Intumescent Polymers.* MACROMOL MATER ENG, 2004. **289**: p. 499–51.

62. M.LE_BRAS, M.BUGAJNY, J-M.LEFEBVRE and S.BOURBIGOT, *Use of polyurethanes as char-forming agents in polypropylene intumescent formulations.* POLYM INT, 2000. **49**: p. 1115-1124.

63. X-Y.MENG, L.YE, X-G.ZHANG, P-M.TANG, J-H.TANG, X.JI and Z-M.LI, *Effects of Expandable Graphite and Ammonium Polyphosphate on the Flame-Retardant and Mechanical Properties of Rigid Polyurethane Foams.* J APPL POLYM SCI, 2009. **114**: p. 853-863.

64. S.DUQUESNE, M.LE_BRAS, S.BOURBIGOT, R.DELOBEL, H.VEZIN, G.CAMINO, B.ELING, C.LINDSAY and T.ROELS, *Expandable graphite: a fire retardant additive for polyurethane coatings.* FIRE MATER, 2003. **27**: p. 103-117.

65. K.SHEN and B.SCHILLING. *Recent advances with expandable graphite in intumescent flame retardant technology* Available from: http://www.nyacol.com/exgraphadv.htm.

66. S.DUQUESNE, M.LE_BRAS, S.BOURBIGOT, R.DELOBEL, G.CAMINO, B.ELING, C.LINDSAY, T.ROELS and H.VEZIN, *Mechanism of Fire Retardancy of Polyurethanes Using Ammonium Polyphosphate.* J APPL POLYM SCI, 2001. **82**: p. 3262–3274.

67. S.DUQUESNE, R.DELOBEL, M.LE_BRAS and G.CAMINO, *A comparative study of the mechanism of action of ammonium polyphosphate and expandable graphite in polyurethane.* POLYM DEGRAD STABIL, 2002. **77**: p. 333–344.

68. C.Y.H.CHAO, *Comparison of the Thermal Decomposition Behavior of a Non-Fire Retarded and a Fire Retarded Flexible Polyurethane Foam with Phosphorus and Brominated Additives.* J FIRE SCI, 2001. **19**: p. 137-156

69. M.MODESTI and A.LORENZETTI, *Improvement on fire behaviour of water blown PIR–PUR foams: use of an halogen-free flame retardant.* EUR POLYM J, 2003. **39**: p. 263-268.

70. X-C.BIAN, J-H.TANG, Z-M.LI and Xiang-Cheng Bian, 2,3 Jian-Hua Tang,2 Zhong-Ming Li1, *Flame Retardancy of Hollow Glass Microsphere/Rigid Polyurethane Foams in the Presence of Expandable Graphite.* J APPL POLYM SCI, 2008. **109**: p. 1935-1943.

71. S.DUQUESNE, M.LE_BRAS, S.BOURBIGOT, R.DELOBEL, G.CAMINO, B.ELING, C.LINDSAY and T.ROELS, *Thermal degradation of polyurethane and polyurethane/expandable graphite coating.* POLYM DEGRAD STABIL, 2001. **74**: p. 493-499.

72. S.DUQUESNE, M.LE_BRAS, S.BOURBIGOT, R.DELOBEL, F.POUTCH, G.CAMINO, B.ELING, C.LINDSAY and T.ROELS, *Analysis of Fire Gases Released from Polyurethane and Fire-Retarded Polyurethane Coatings.* J FIRE SCI, 2000. **18**: p. 456-482.

73. S.BOURBIGOT, T.TURF, S.BELLAYER and S.DUQUESNE, *Polyhedral oligomeric silsesquioxane as flame retardant for thermoplastic polyurethane.* POLYM DEGRAD STABIL, 2009. **94**: p. 1230–1237.

74. D.SCHARF, R.NALEPA, R.HEFLIN and T.WUSU, *Studies on flame retardant intumescent char: part I.* FIRE SAFETY J, 1992. **19**(1): p. 103-17.

75. G.F.LEVCHIK and S.V.LEVCHIK, *Mechanism of complex fireproofing compounds action in polyamide 6:ammonium phosphate-inorganic filler.* Dokl. Akad. Nauk Belarusi, 1996. **40**(5): p. 74-77.

76. S.BOURBIGOT, M.LE_BRAS, R.DELOBEL, R.DECRESSAIN and J-P.AMOUREUX, *Synergistic effect of zeolite in an intumescence process: Study of the carbonaceous structures using solid-state NMR.* J CHEM SOC FARAD T, 1996. **92**(1): p. 149-158.

77. S.BOURBIGOT, M.LE_BRAS, R.DELOBEL, P.BREANT and J-M.TREMILLON, *4A zeolite synergistic agent in new flame retardant intumescent formulations of polyethylenic polymers - study of the effect of the constituent monomers.* POLYM DEGRAD STABIL, 1996. **54**: p. 275-287.

78. S.BOURBIGOT. *Intumescence: an older concept for future applications*. in *13th edition of the european Meeting on Fire retardant Polymers FRPM* 2011. Turin, Italy.

79. S.BOURBIGOT, M.LE_BRAS, F.DABROWSKI, J.W.GILMAN and T.KASHIWAGI, *PA-6 Clay Nanocomposite Hybrid as Char Forming Agent in Intumescent Formulations.* FIRE MATER, 2000. **24**: p. 201-208.

80. A.LAACHACHI, M.COCHEZ, E.LEROY, M.FERRIOL and J-M.LOPEZ-CUESTA, *Fire retardant systems in poly(methyl methacrylate): Interactions between metal oxide nanoparticles and phosphinates.* POLYM DEGRAD STABIL, 2007. **92**: p. 61-69.
81. P.WEI, J.HAO, J.DU, Z.HAN and J.WANG, *An Investigation on Synergism of an Intumescent Flame Retardant Based on Silica and Alumina.* J FIRE SCI, 2003. **21**: p. 17-28.
82. G.F.LEVCHIK, S.V.LEVCHIK and A.I.LESNIKOVICH, *Mechanisms of action in flame retardant reinforced nylon 6.* POLYM DEGRAD STABIL, 1996. **54**: p. 361-363.
83. S.V.LEVCHIK, G.F.LEVCHIK, G.CAMINO and L.COSTA, *Mechanism of action of phosphorus-based flame retardants in nylon 6. II. Ammonium polyphosphate/talc.* J. Fire Sci., 1995. **13**(1): p. 43-58.
84. S.V.LEVCHIK, G.F.LEVCHIK, G.CAMINO, L.COSTA and A.I.LESNIKOVICH, *Mechanism of action of phosphorus-based flame retardants in nylon 6. III. Ammonium polyphosphate/manganese dioxide.* Fire Mater., 1996. **20**(4): p. 183-190.
85. C.GERARD, *Contribution of nanoparticles to the flame retardancy of epoxy resins* 2011, UNIVERSITE LILLE 1 SCIENCES ET TECHNOLOGIES Lille.
86. Gy.MAROSI, A.MARTON, P.ANNA, G.BERTALAN, B.MAROSFOI and A.SZEP, *Ceramic precursor in flame retardant systems.* Polym. Degrad. Stab., 2002. **77**(2): p. 259-265.
87. F.SAMYN, S.BOURBIGOT, S.DUQUESNE and R.DELOBEL, *Effect of zinc borate on the thermal degradation of ammonium polyphosphate.* THERMOCHIM ACTA, 2007. **456**: p. 134-144.
88. D.DELAVAL, *Développement et caractérisation de systèmes intumescents retardateurs de flamme pour polypropylène recyclés issu des véhicules usagés*. 2009, UNIVERSITE DES SCIENCES ET TECHNOLOGIES DE LILLE: Lille.
89. Z.WU, W.SHU and Y.HU, *Synergist Flame Retarding Effect of Ultrafine Zinc Borate on LDPE/IFR System.* J APPL POLYM SCI, 2007. **107**: p. 3667-3674.
90. G.FONTAINE and S.BOURBIGOT, *Intumescent polylactide: A nonflammable material.* J. Appl. Polym. Sci., 2009. **113**(6): p. 3860-3865.
91. A.P.KUMAR, D.DEPAN, N.S.TOMER and R.P.SINGH, *Nanoscale particles for polymer degradation and stabilization—Trends and future perspectives.* PROG POLYM SCI, 2009. **34**: p. 479–515.
92. M.LE_BRAS and S.BOURBIGOT, *Mineral fillers in intumescent fire retardant formulations - criteria for the choice of a natural clay filler for the ammonium polyphosphate/pentaerythritol/polypropylene system.* Fire Mater, 1996. **20**(1): p. 39-49.
93. F.DABROWSKI, M.LE_BRAS, L.CARTIER and S.BOURBIGOT, *The use of clay in an EVA-based intumescent formulation. Comparison with the intumescent formulation using polyamide-6 clay nanocomposite as carbonisation agent.* J. Fire Sci., 2001. **19**(3): p. 219-241.
94. J-F.HAN, D-Y.WANG, Y.LIU and Y-Z.WANG, *A intumescent flame-retardant polypropylene system and its burning behaviors.* Gaofenzi Cailiao Kexue Yu Gongcheng, 2009. **25**: p. 138-141.
95. C.MANZI-NSHUTI, J.M.HOSSENLOPP and C.A.WILKIE, *Comparative study on the flammability of polyethylene modified with commercial fire retardants and a zinc aluminum oleate layered double hydroxide.* POLYM DEGRAD STABIL, 2009. **94**: p. 782-788.
96. S.DUQUESNE, F.SAMYN, S.BOURBIGOT, P.AMIGOUET, F.JOUFFRET and K.SHEN, *Influence of talc on the fire retardant properties of highly filled intumescent polypropylene composites.* POLYM ADVAN TECHNOL, 2008. **19**: p. 620-627.
97. A.VANNIER, *Procédés d'ignifugation du poly(éthylènetéréphtalate) - application textile*. 2008, UNIVERSITE DES SCIENCES ET TECHNOLOGIES DE LILLE: Lille.
98. L.SONG, Y.HU, Y.TANG, R.ZHANG, Z.CHEN and W.FAN, *Study on the properties of flame retardant polyurethane/organoclay nanocomposite.* POLYM DEGRAD STABIL, 2005. **87**: p. 111-116.
99. M.LIN, B.LI, Q.LI, S.LI and S.ZHANG, *Synergistic effect of metal oxides on the flame retardancy and thermal degradation of novel intumescent flame-retardant thermoplastic polyurethanes.* J APPL POLYM SCI, 2011. **121**(4): p. 1951-1960.

100. X.SHAN, P.ZHANG, L.SONG, Y.HU and S.LO, *Compound of Nickel Phosphate with Ni(OH)(PO4)2- Layers and Synergistic Application with Intumescent Flame Retardants in Thermoplastic Polyurethane Elastomer.* Ind. Eng. Chem. Res., 2011. **50**(12): p. 7201-7209.
101. Y.PAUL, *Evaluation de la résistance au feu de revêtements pour la protection de substrats metalliques - Conception de tests à l'échelle laboratoire*. 2006, CONSERVATOIRE NATIONAL DES ARTS ET METIERS DE LILLE.
102. Q.DONG, C.GAO, Y.DING, F.WANG, B.WEN, S.ZHANG, T.WANG and M.YANG, *A polycarbonate/magnesium oxide nanocomposite with high flame retardancy.* J APPL POLYM SCI, 2012. **123**(2): p. 1085-1093.
103. K.HAM, H.A.BARNETT and L.G.BUTLER, *Burning Issues in Tomography Analysis.* COMPUT SCI ENG, 2008: p. 78-81.
104. H.A.BARNETT, K.HAM, J.T.SCORSONE and L.G.BUTLER, *Synchrotron X-ray Tomography for 3D Chemical Distribution Measurement of a Flame Retardant and Synergist in a Fiberglass-Reinforced Polymer Blend.* J PHYS CHEM B, 2010. **114**: p. 2-9.
105. L.G.BUTLER, K.HAM, B.JENKINS, B.YERGLER and H.A.BARNETT. *3D Imaging of Slow Processes with Synchrotron X-Ray Tomography: Flame Retardant, Polystyrene and Heat Pulses*. in *64th Southwest Regional Meeting of the American Chemical Society*. 2008. Little Rock, AR, US.
106. L.G.BUTLER, K.HAM and R.W.HALLL. *Time-Dependent X-ray Tomography Imaging of Flame Retardants in Polymer Blends*. in *Joint 66th Southwest and 62nd Southeast Regional Meeting of the American Chemical Society*. 2010. New Orleans, LA, US.
107. A.GONZALEZ, A.DASARI, B.HERRERO, E.PLANCHER, J.SANTAREN, A.ESTEBAN and S.-Z. LIM, *Fire retardancy behavior of PLA based nanocomposites.* POLYM DEGRAD STABIL, 2012. **97**: p. 248-256.
108. V.CNUDDE, B.MASSCHAELE, M.DIERICK, J.VLASSENBROECK, L.VAN_HOOREBEKE and P.JACOBS, *Recent progress in X-ray CT as a Geosciences Tool.* APPL GEOCHEM, 2006. **21**(5): p. 826-832.
109. L.A.FELDKAMP, L.DAVIS and J.KRESS, *Practical cone beam algorithm.* J OPT SOC AM, 1984. **1**: p. 612-619.
110. A.BERLIN, N.A.KHALTURINSKIJ, I.S.RESHETNIKOV and M.Y.YABLOKOVA, *Some aspects of mechanical stability of intumescent chars.* Special Publication - Royal Society of Chemistry, 1998.
111. A.BERLIN, I.RESHETNIKOV, M.Y.YABLOKOVA and N.KHALTURINSKIJ. in *Proc. of 6th european meeting on fire retardancy of polymers*. 1997. Lille.
112. I.RESHETNIKOV, M.Y.YABLOKOVA, E.POTAPOVA, N.KHALTURINSKIJ, V.CHERNYH and L.MASHLYAKOVSKY, *Mechanical stability of intumescent chars.* J APPL POLYM SCI, 1998. **67**(10): p. 1827-1830.
113. J.D.MAO, A.SCHIMMELMANN, M.MASTALERZ, P.G.HATCHER and Y.LI, *Structural features of a bituminous coal and their changes during low-temperature oxidation and loss of volatiles investigated by advanced solid state NMR spectroscopy.* ENERG FUEL, 2010. **24**: p. 2536-2544.
114. T.M.DUNCAN, *A compilation of chemical shift anisotropies*. 1990.
115. F.BERGER, M.WEINMANN, F.ALDINGER and K.MUELLER, *Solid-State NMR Studies of the Preparation of Si-Al-C-N Ceramics from Aluminum-Modified Polysilazanes and Polysilylcarbodiimides.* Chem. Mater., 2004. **16**(5): p. 919-929.
116. M.JIMENEZ, S.DUQUESNE and S.BOURBIGOT, *Intumescent fire protective coating: Toward a better understanding of their mechanism of action.* THERMOCHIM ACTA 2006. **449**: p. 16-26.
117. S.BOURBIGOT, *Utilisation de la RMN de l'état solide pour la déformulation*. 2009.
118. C.G.ROBERTSON, C.J.LIN, M.RACKAITIS and C.M.ROLAND, *Influence of Particle Size and Polymer-Filler Coupling on Viscoelastic Glass Transition of Particle-Reinforced Polymers.* Macromolecules (Washington, DC, U. S.), 2008. **41**(7): p. 2727-2731.
119. J.T.HOWARTH and A.A.MASSUCCO, *Flame Resistant Elastic Elastomeric Fibers*, M.S. Center, Editor. 1972: USA.

120. O.B.PRAVEDNIKOVA, O.S.DUTIKOVA, I.M.KARELINA and L.S.GAL'BRAIKH, *Effect of phosphonic acid salt derivatives on the fireproofing indexes of plasticized polyvinyl chloride.* Fibre Chem., 2009. **41**(2): p. 85-87.
121. G.MAROSI, A.MARTON, A.SZEP, I.CSONTOS, S.KESZEI, E.ZIMONYI, A.TOTH, X.ALMERAS and M.LE_BRAS, *Fire retardancy effect of migration in polypropylene nanocomposites induced by modified interlayer.* POLYM DEGRAD STABIL, 2003. **82**: p. 379-385.
122. L.LIU, S.WEI and X.LAI, *In situ synthesis and characterization of polypropylene/polyvinyl acetate-organophilic montmorillonite nanocomposite.* J. Appl. Polym. Sci., 2012. **124**(5): p. 4107-4113.
123. B.RAMARAJ and K.R.YOON, *Thermal and Physicomechanical Properties of Ethylene-vinyl Acetate Copolymer and Layered Double Hydroxide Composites.* J APPL POLYM SCI, 2008. **108**: p. 4090-4095.
124. A.TOLDY, N.TOTH, P.ANNA and G.MAROSI, *Synthesis of phosphorus-based flame retardant systems and their use in an epoxy resin.* POLYM DEGRAD STABIL, 2006. **91**: p. 585-592.
125. L.BUSTAMANTE_VALENCIA, *Experimental and numerical investigation of the thermal decomposition of materials at three scales: application to polyether polyurethane foam used in upholstered furniture*. 2009: Poitiers.
126. J.LEFEBVRE, *Modélisation et simulation de la dégradation thermique de mousses de polyuréthane: application à la compréhension de leur comportement au feu*. 2003, UNIVERSITE DES SCIENCES ET TECHNOLOGIES DE LILLE: Lille.
127. X.ALMERAS, F.DABROWSKI, M.LE_BRAS, R.DELOBEL, S.BOURBIGOT, G.MAROSI and P.ANNA, *Using polyamide 6 as charring agent in intumescent polypropylene formulations II. Thermal degradation.* Polym. Degrad. Stab., 2002. **77**(2): p. 315-323.
128. M.BUGAJNY, S.BOURBIGOT, M.LE_BRAS and R.DELOBEL, *The origin and nature of flame retardance in ethylene-vinyl acetate copolymers containing hostaflam AP 750* POLYM INT, 1999. **48**: p. 264-270.
129. R.DELOBEL, M.LE_BRAS, N.OUASSOU and F.ALLISTIQSA, *Thermal behaviors of ammonium polyphosphate-pentaerythritol and ammonium pyrophosphate-pentaerythritol intumescent additives in polypropylene formulations* J FIRE SCI, 1990. **8**: p. 85-108.
130. J.H.SAUNDERS, *Reactions of isocyanates and isocyanate derivatives at elevated temperatures* RUBBER CHEM TECHNOL, 1959. **32**: p. 337-345.
131. N.GRASSIE and M.ZULFIQAR, *The effect of the fire retardant ammonium polyphosphate on the thermal degradation of a polyurethane*. DEVELOPMENTS IN POLYMER STABILISATION. Vol. 1. 1979: G Scott Ed.
132. A.FINA, D.TABUANI, F.CARNIATO, A.FRACHE, E.BOCCALERI and G.CAMINO, *Polyhedral oligomeric silsesquioxanes (POSS) thermal degradation.* Thermochim. Acta, 2006. **440**(1): p. 36-42.
133. M.AUFRAY and A-A.ROCHE, *Is gold always chemically passive?* Appl. Surf. Sci., 2008. **254**(7): p. 1936-1941.
134. M.BUGAJNY, M.LE_BRAS, S.BOURBIGOT and R.DELOBEL, *Thermal behaviour of ethylene±propylene rubber/polyurethane/ammonium polyphosphate intumescent formulation - a kinetic study.* POLYM DEGRAD STABIL, 1999. **64**: p. 157-163.
135. *Encyclopedia of Industrial Chemical Analysis*. p. 263-319.
136. S.BOURBIGOT, M.LE_BRAS and R.DELOBEL, *Carbonization mechanisms resulting from intumescence - Part II. Association with an ethylene terpolymer and the ammonium polyphosphate-pentaerythritol fire retardant system* CARBON, 1995. **33**(3): p. 283-294.
137. S.BOURBIGOT, M.LE_BRAS and R.DELOBEL, *Carbonization mechanisms resulting from intumescence association with the ammonium polyphosphate-pentaerythritol fire retardant system.* CARBON, 1993. **31**(8): p. 1219-1230.
138. R.K.HARRIS, L.H.MERWIN and G.HAGELE, *Solid state nuclear magnetic resonance study of a series of phosphonic and phosphinic acids.* J CHEM SOC FARAD T 1, 1989. **85**(6): p. 1409-1423.

139. A.KARRASCH, E.WAWRZYN, B.SCHARTEL and C.JAGER, *Solid-state NMR on thermal and fire residues of bisphenol A polycarbonate/silicone acrylate rubber/bisphenol A bis(diphenyl-phosphate)/(PC/ SiR/BDP) and PC/SiR/BDP/zinc borate (PC/SiR/BDP/ZnB) - Part I: PC charring and the impact of BDP and ZnB.* POLYM DEGRAD STABIL, 2010. **95**(12): p. 2525-2533.

140. H.ASSAAOUDI, I.S.BUTLER, J.KOZINSKI and F.BELANGER-GARIEPY, *Crystal structure, vibrational spectra and thermal decomposition study of a new, dicationic, acidic pyrophosphate: KHMgP2O7· 2H2O.* J CHEM CRYSTALLOGR, 2005. **35**(10): p. 809-820.

141. D.PROCHNOW, A-R.GRIMMER and D.FREUDE, *Solid-state NMR studies of 17O-enriched pyrophosphates.* SOLID STATE NUCL MAG 2006. **30**: p. 69-74.

142. G.F.LEVCHIK, S.V.LEVCHIK, G.CAMINO and E.D.WEIL, *Fire retardant action of red phosphorus in nylon 6*, in *Fire retardancy of polymers - The use of intumescence*. 1998, The Royal Society of Chemistry.

143. D.G.GORENSTEIN, *Phosphorus-31 NMR. Principles and application*. 1984, Orlando: D.G.GORENSTEIN, Academic press.

144. F.FAYON, D.MASSIOT, K.SUZUYA and D.L.PRICE, *31P NMR study of magnesium phosphate glasses.* J NON-CRYST SOLIDS, 2001. **283**: p. 88-94.

145. M.A.ARAMENDIA, V.BORAU, C.JIMENEZ, J.M.MARINAS, F.J.ROMERO and J.R.RUIZ, *Characterization by XRD, DRIFT, and MAS NMR Spectroscopies of a Mg2P2O7 Catalyst.* J COLLOID INTERF SCI 1998. **202**: p. 456-461.

146. G.TRICOT, *Investigation and better understanding of the role of phosphates in the inhibition mechanism of catalysed oxidation of C/C composite materials*. 2005, USTL: Lille.

147. M.FEIKE, R.GRAF, I.SCHNELL, C.JAGER and H.W.SPIESS, *Structure of Crystalline Phosphates from 31P Double-Quantum NMR Spectroscopy.* J AM CHEM SOC, 1996. **118**: p. 9631-9634.

148. R.DUPREE, D.HOLLAND and M.G.MORTUZA, *Six coordinated silicon in glasses.* NATURE, 1987. **328**: p. 416-417.

149. E.LIPPMAA, M.MAGI, A.SAMOSON, G.ENGELHARDT and A.R.GRIMMER, *Structural studies of silicates by soli state high resolution ^{29}Si NMR.* J AM CHEM SOC, 1980. **102**: p. 4889-4893.

150. M.C.DAVIS, D.C.KASEMAN, S.M.PARVANI, K.J.SANDERS, P.J.GRANDINETTI, D.MASSIOT and P.FLORIAN, *Q(n) Species Distribution in K2O·2SiO2 Glass by 29Si Magic Angle Flipping NMR.* J. Phys. Chem. A, 2010. **114**(17): p. 5503-5508.

151. C.E.TAMBELLI, J.F.SCHNEIDER, N.P.HASPARYK and P.J.M.MONTEIRO, *Study of the structure of alkali-silica reaction gel by high-resolution NMR spectroscopy.* J. Non-Cryst. Solids, 2006. **352**(32-35): p. 3429-3436.

152. J.F.STEBBINS and M.KANZAKI, *Local structure and chemical shifts for six coordinated silicon in high pressure mantle phases.* SCIENCE. **251**: p. 294-298.

153. I.L.MUDRAKOVSKII, V.M.MASTIKHIN, V.P.SHMACHKOVA and N.S.KOTSARENKO, *High resolution solid state ^{29}Si and ^{31}P NMR of silicon-phosphorus compounds containing six coordinated silicon.* CHEM PHYS LETT, 1985. **120**(4,5): p. 424-426.

154. S.BOURBIGOT, M.LE_BRAS, R.DELOBEL and L.GENGEMBRE, *XPS study of an intumescent coating. II. Application to the ammonium polyphosphate/pentaerythritol/ethylenic terpolymer fire retardant system with and without synergistic agent.* Appl. Surf. Sci., 1997. **120**(1/2): p. 15-29.

155. I.RESHETNIKOV, A.ANTONOV, T.RUDAKOVA, G.ALEKSJUK and N.KHALTURINSKIJ, *Some aspects of intumescent fire retardant systems.* POLYM DEGRAD STABIL, 1996. **54**(2-3): p. 137-141.

156. A.LAACHACHI, D.RUCH, F.ADDIEGO, M.FERRIOL, M.COCHEZ and J-M.LOPEZ-CUESTA, *Effect of ZnO and organo-modified montmorillonite on thermal degradation of poly(methyl methacrylate) nanocomposites.* POLYM DEGRAD STABIL, 2009. **94**: p. 670–678.

157. G.BEYER, *Flame retardancy of nanocomposites based on organoclays and carbon nanotubes with aluminium trihydrate.* POLYM ADVAN TECHNOL, 2006. **17**: p. 218–225.

158. T.ISHIKAWA, T.UENO, Y.WATANABE, K.MIZUNO and K.TAKEDA, *Flame Retardancy of Polybutylene Terephthalate Blended with Various Oxides.* J APPL POLYM SCI, 2008. **109**: p. 910-917.

159. S.BOURBIGOT, F.CARPENTIER, M.LE_BRAS and R.DELOBEL, *Interaction FR additives/polymer - application to the EVA-Mg(OH)2-zinc borate system*, in *Additives '99, International Conference, 8th*. 1999: San Francisco.

160. M.A.ARAMENDIA, V.BORAU, C.JIMENEZ, J.M.MARINAS, F.J.ROMERO and J.R.RUIZ, *XRD and Solid-State NMR Study of Magnesium Oxide–Magnesium Orthophosphate Systems.* J SOLID STATE CHEM 1998. **135**: p. 96-102.

161. D.S.BRAUER, C.RUESSEL and J.KRAFT, *Solubility of glasses in the system P2O5-CaO-MgO-Na2O-TiO2: Experimental and modeling using artificial neural networks.* J. Non-Cryst. Solids, 2007. **353**(3): p. 263-270.

162. G.WALTER, J.VOGEL, U.HOPPE and P.HARTMANN, *The structure of CaO-Na2O-MgO-P2O5 invert glass.* J. Non-Cryst. Solids, 2001. **296**(3): p. 212-223.

163. S.BOURBIGOT, R.DELOBEL, M.LE_BRAS and D.NORMAND, *Comparative study of the integral TG methods used in the invariant kinetic parameter method. Application to the fire-retardant polypropylene.* J. Chim. Phys. Phys.-Chim. Biol., 1993. **90**(10): p. 1909-28.

164. V.MAMLEEV, S.BOURBIGOT, M.LE_BRAS and J.LEFEBVRE, *Three model-Free methods for calculation of activation energy in TG.* J. Therm. Anal. Calorim., 2004. **78**(3): p. 1009-1027.

165. International_Organization_for_Standardization, *International standard ISO 834-1 Fire-resistance tests-elements of building construction. Part 1. General requirements*. 1999: Geneva.

166. O.CERIN, *Develoment and characterization of a novel flame retardant EVM-based formulation: investigation and comprehension of the flame retardant mechanisms*. 2010, UNIVERSITE DES SCIENCES ET TECHNOLOGIES DE LILLE: Lille.

167. S.VYAZOVKIN, A.K.BURNHAM, J.M.CRIADO, L.A.PEREZ-MAQUEDA, C.POPESCU and N.SBIRRAZZUOLI, *ICTAC Kinetics Committee recommendations for performing kinetic computations on thermal analysis data.* Thermochim. Acta, 2011. **520**(1-2): p. 1-19.

168. S.BOURBIGOT, J.W.GILMAN and C.A.WILKIE, *Kinetic analysis of the thermal degradation of polystyrene-montmorillonite nanocomposite.* POLYM DEGRAD STABIL, 2004. **84**: p. 483-492.

169. J.E.J.STAGGS, *Numerical Characterization of the Thermal Performance of Static Porous Insulation Layers on Steel Substrates in Furnace Tests.* J. Fire Sci., 2011. **29**: p. 177-192.

170. B.SCHARTEL and A.WEISS, *Temperature inside burning polymer specimens: pyrolysis zone and shielding.* Fire Mater., 2010. **34**(5): p. 217-235.

171. G.T.LINTERIS, *Numerical simulations of polymer pyrolysis rate: Effect of property variations.* Fire Mater., 2011. **35**(7): p. 463-480.

172. N.SOMBATSOMPOP and A.K.WOOD, *TEST APPARATUS/MATERIAL PROPERTIES: Measurement of Thermal Conductivity of Polymers using an Improved Lee's Disc Apparatus.* POLYM TEST, 1997. **16**: p. 203-223.

173. Z.ZHANG, Y.LI-LEI, A.KUKOVECZ, Z.KONYA, J.BIELECKI and J.LIU, *Characterization of CNT enhanced conductive adhesives in terms of thermal conductivity.* ECS Trans., 2012. **44**(1, China Semiconductor Technology International Conference 2012): p. 1011-1017.

174. S.HAN and D.D.L.CHUNG, *Increasing the through-thickness thermal conductivity of carbon fiber polymer-matrix composite by curing pressure increase and filler incorporation.* Compos. Sci. Technol., 2011. **71**(16): p. 1944-1952.

175. G.A.SLACK, *Thermal conductivity of MgO, Al2O3, MgAl2O4, and Fe3O4 crystals from 3° to 300°K.* Phys. Rev., 1962. **126**: p. 427-41.

176. B.GARDELLE, S.DUQUESNE, V.RERAT and S.BOURBIGOT, *Thermal Degradation and Fire Performance of Intumescent Silicon-based Coatings*, in *American chemical society*. 2012: San Diego (US).

177. S.BOURBIGOT, S.DUQUESNE and J-M.LEROY, *Modeling of heat transfer of a polypropylene-based intumescent system during combustion.* J. Fire Sci., 1999. **17**(1): p. 42-56.

178. J.E.J.STAGGS, R.J.CREWE and R.BUTLER, *A theoretical and experimental investigation of intumescent behaviour in protective coatings for structural steel.* Chem. Eng. Sci., 2012. **71**: p. 239-251.
179. J.E.J.STAGGS, *Thermal conductivity estimates of intumescent chars by direct numerical simulation.* Fire Saf. J., 2010. **45**(4): p. 228-237.
180. J.YUAN, *Intumescent coating performance on steel structures under realistic fire conditions*. 2009, UNIVERSITY OF MANCHESTER.
181. C.RETI, *Procédés d'élaboration de matériaux biosourcés à propriétés retard au feu améliorées - Application à l'acide polylactique*. 2009, UNIVERSITE LILLE I SCIENCES ET TECHNOLOGIES: Lille.
182. L.G.BUTLER, B.SCHILLINGER, K.HAM, T.A.DOBBINS, P.LIU and J.J.VAJO, *Neutron imaging of a commercial Li-ion battery during discharge: Application of monochromatic imaging and polychromatic dynamic tomography.* Nucl. Instrum. Methods Phys. Res., Sect. A, 2011. **651**(1): p. 320-328.
183. A.P.KAESTNER, B.MUNCH, P.TRTIK and L.G.BUTLER, *Spatio-temporal computed tomography of dynamic processes.* SPIE Optical engineering, 2011.
184. L.G.BUTLER, K.HAM, H.JIN and R.L.KURTZ, *Tomography at the Louisiana State University CAMD synchrotron: applications to polymer blends.* Proc. SPIE-Int. Soc. Opt. Eng., 2002. **4503**(Developments in X-Ray Tomography III): p. 54-61.
185. K.HAM, H.JIN, R.AL_RAOUSH, X.XIE, C.S.WILLSON, G.R.BYERLY, L.S.SIMERAL, M.L.RIVERS, R.L.KURTZ and L.G.BUTLER, *Three-Dimensional Chemical Analysis with Synchrotron Tomography at Multiple X-ray Energies: Brominated Aromatic Flame Retardant and Antimony Oxide in Polystyrene.* Chem. Mater., 2004. **16**(21): p. 4032-4042.
186. H.A.BARNETT, K.HAM and L.G.BUTLER, *The 3D chemical distribution of a flame retardant in a fiberglass-reinforced polymer blend as measured with synchrotron x-ray tomography.* Proc. SPIE-Int. Soc. Opt. Eng., 2006. **6318**(Developments in X-Ray Tomography V): p. 631821/1-631821/9.
187. L.G.BUTLER, K.HAM and H.A.BARNETT. *3D Chemical imaging with synchrotron X-ray tomography*. 2006: American Chemical Society.
188. L.G.BUTLER. *Synchrotron X-ray tomography of flame retardants in polymers*. 2007: American Chemical Society.
189. K.HAM, H.A.BARNETT and L.G.BUTLER, *Synchrotron X-ray tomography of flame retardants in polymers.* Polym. Prepr. (Am. Chem. Soc., Div. Polym. Chem.), 2007. **48**(2): p. 519.
190. H.A.BARNETT, C.McFERRIN, R.W.HALL and L.G.BUTLER. *Diffusion of flame retardants in polystyrene: Simulations and measurements with synchrotron X-ray tomography*. 2008: American Chemical Society.
191. P.WANGE, J.VOGEL, S.KNOCHE and C.RUESSEL, *Crystallization and viscosity of phosphate melts in the system Na2O-CaO-MgO-P2O5-Al2O3-TiO2.* Glass Sci. Technol. (Offenbach, Ger.), 2004. **77**(4): p. 172-176.
192. A.KISHIOKA, T.MIYAISHI and M.KINOSHITA, *Viscosity of alkali aluminophosphate glass.* Yogyo Kyokaishi, 1979. **87**(8): p. 422-9.
193. M.JIMENEZ, S.DUQUESNE and S.BOURBIGOT, *Characterization of the performance of an intumescent fire protective coating.* Surf. Coat. Technol., 2006. **201**(3-4): p. 979-987.
194. J.CIRET, *Investigation of intumescent coatings for fire protection - Application to jet-fire*. 2010, UNIVERSITE DES SCIENCES ET TECHNOLOGIES DE LILLE: Lille.
195. P.ANNA, Gy.MAROSI, S.BOURBIGOT, M.LE_BRAS and R.DELOBEL, *Intumescent flame retardant systems of modified rheology.* Polym. Degrad. Stab., 2002. **77**(2): p. 243-247.

APPENDICES

Appendix 1: Residue pictures taken at the end of a cone calorimeter test on PU, PU/NP, PU/APP and PU/APP/NP formulations

This appendix shows at larger scale the information already provided in **Chapter III, section 2.1-Fire performances determined by mass loss calorimetry p106**. All PU formulations have been tested in a mass loss calorimetry test and this appendix present the pictures of the residues collected at the end of this test.

Figure 135: Picture of the PU residue at the end of a cone calorimeter test

Figure 136: Picture of the PU 30%APP residue at the end of a cone calorimeter test

Figure 137: Picture of the PU 5%nano MgO residue at the end of a cone calorimeter test

Figure 138: Picture of the PU 29%APP 1%nano MgO residue at the end of a cone calorimeter test

Figure 139: Picture of the PU 28%APP 2%nano MgO residue at the end of a cone calorimeter test

Figure 140: Picture of the PU 25%APP 5%nano MgO residue at the end of a cone calorimeter test

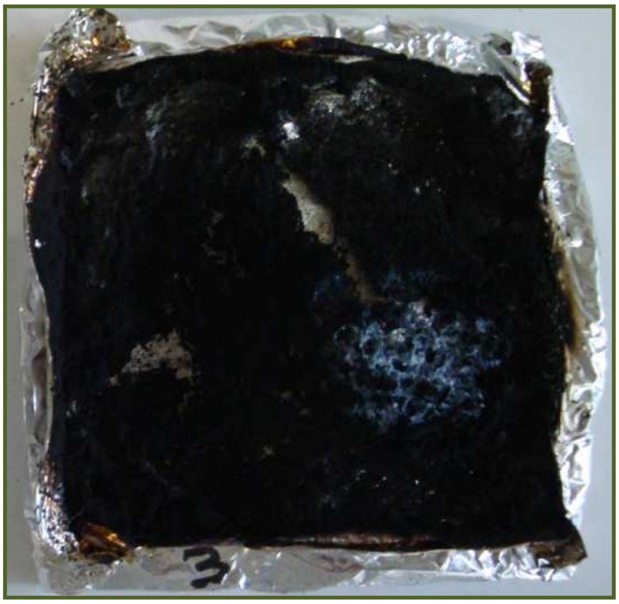

Figure 141: Picture of the PU 5%nano SiO$_2$ residue at the end of a cone calorimeter test

Figure 142: Picture of the PU 28%APP 2%nano SiO$_2$ residues at the end of a cone calorimeter test

Figure 143: Picture of the PU 28%APP 2%OMPOSS residue at the end of a cone calorimeter test

Figure 144: Picture of the PU 29.5%APP 0.5%nano gold residue at the end of a cone calorimeter test

Figure 145: Picture of the PU 29%APP 1%nano gold residue at the end of a cone calorimeter test

Figure 146: Picture of the PU 28%APP 2%nano gold residue at the end of a cone calorimeter test

Appendix 2: Results obtained from shutter experiments on PU, PU/APP, PU/nano MgO and PU/APP/nano MgO formulations

This appendix shows at larger scale the information already provided in **Chapter IV, section** 3-**Evolution of Species Formation During the Cone** Calorimeter **p149**. For respectively PU, PU 5%nano MgO, PU 30%APP, PU25%APP 5%nano MgO, PU 28%APP 2%nano MgO and PU 29%APP 1%nano MgO, the HRR curves stopped at characteristic times are plotted and the corresponding pictures, expansion and residual masses are also given.

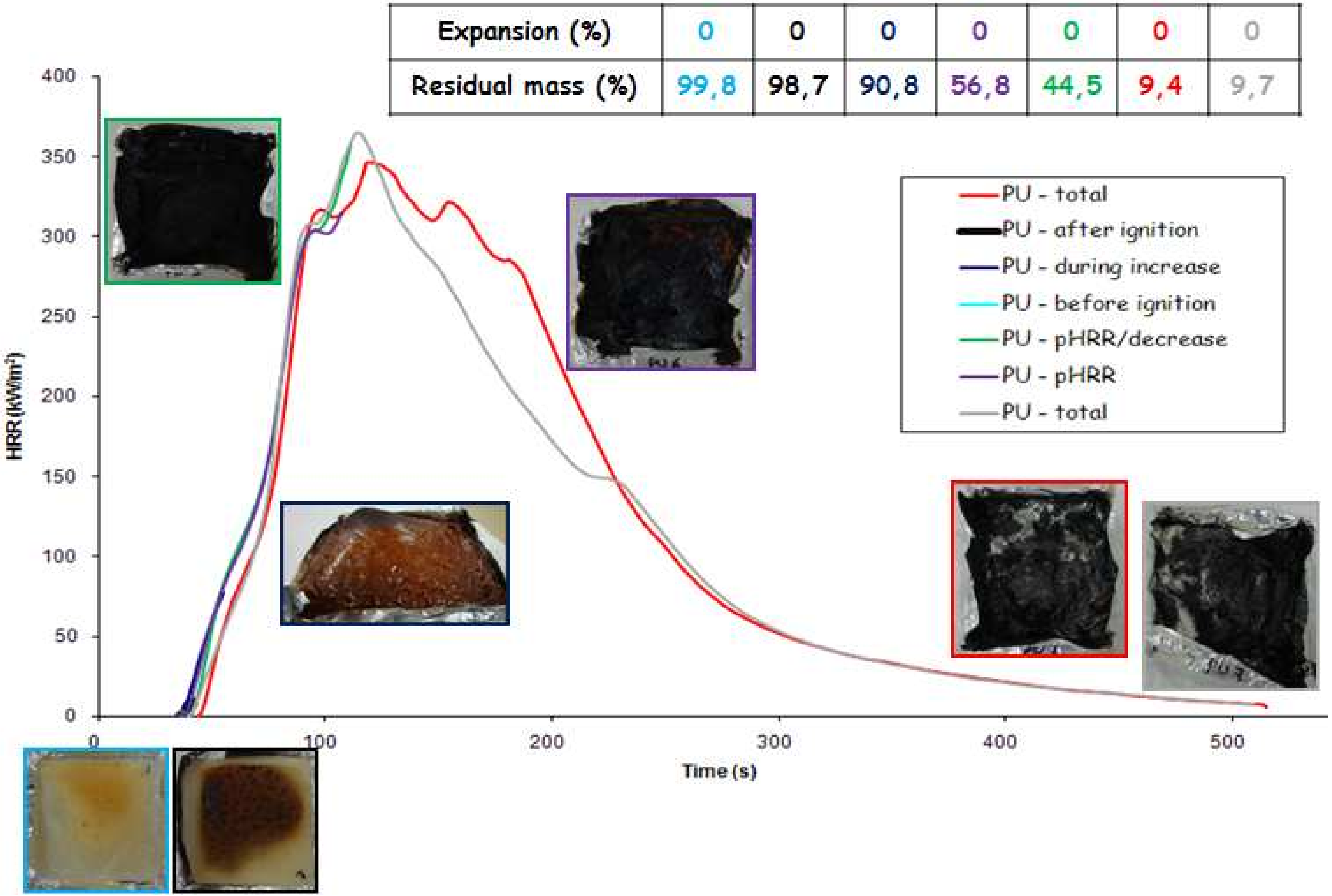

Expansion (%)	0	0	0	0	0	0	0
Residual mass (%)	99,8	98,7	90,8	56,8	44,5	9,4	9,7

Figure 147: Cone calorimeter results from shutter experiments on PU

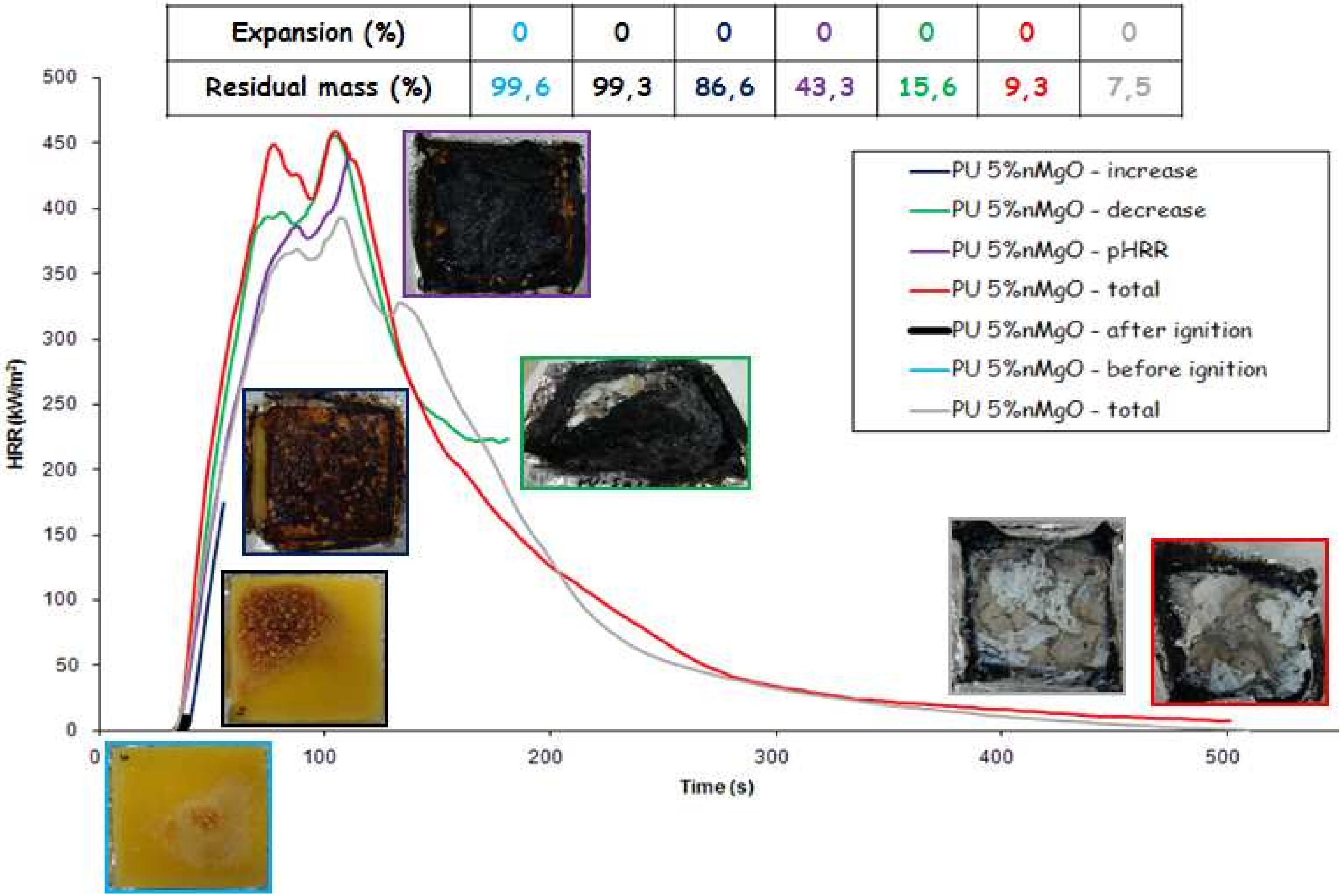

Expansion (%)	0	0	0	0	0	0	0
Residual mass (%)	99,6	99,3	86,6	43,3	15,6	9,3	7,5

Figure 148: Cone calorimeter results from shutter experiments on PU 5%nano MgO

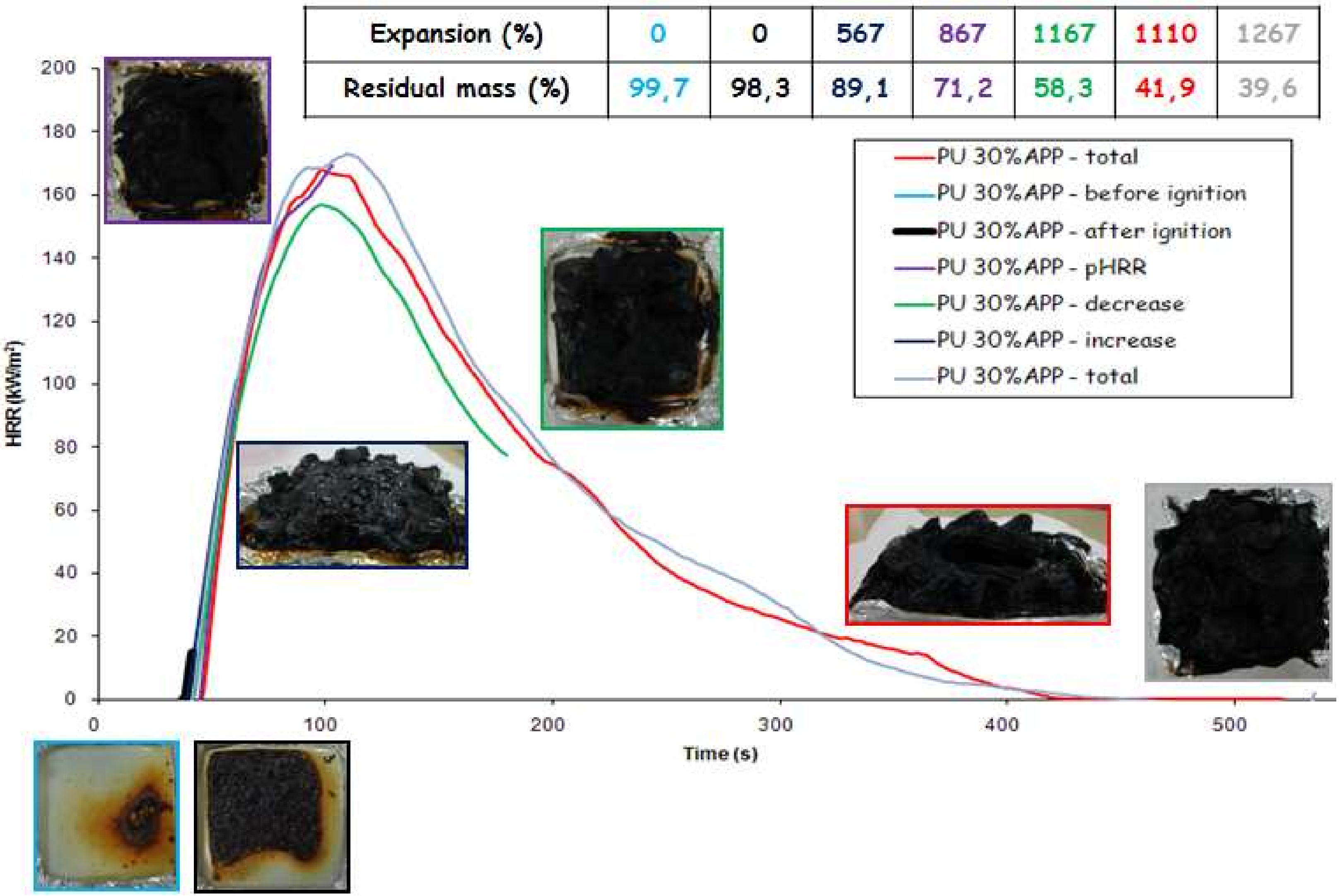

Expansion (%)	0	0	567	867	1167	1110	1267
Residual mass (%)	99,7	98,3	89,1	71,2	58,3	41,9	39,6

Figure 149: Cone calorimeter results from shutter experiments on PU 30%APP

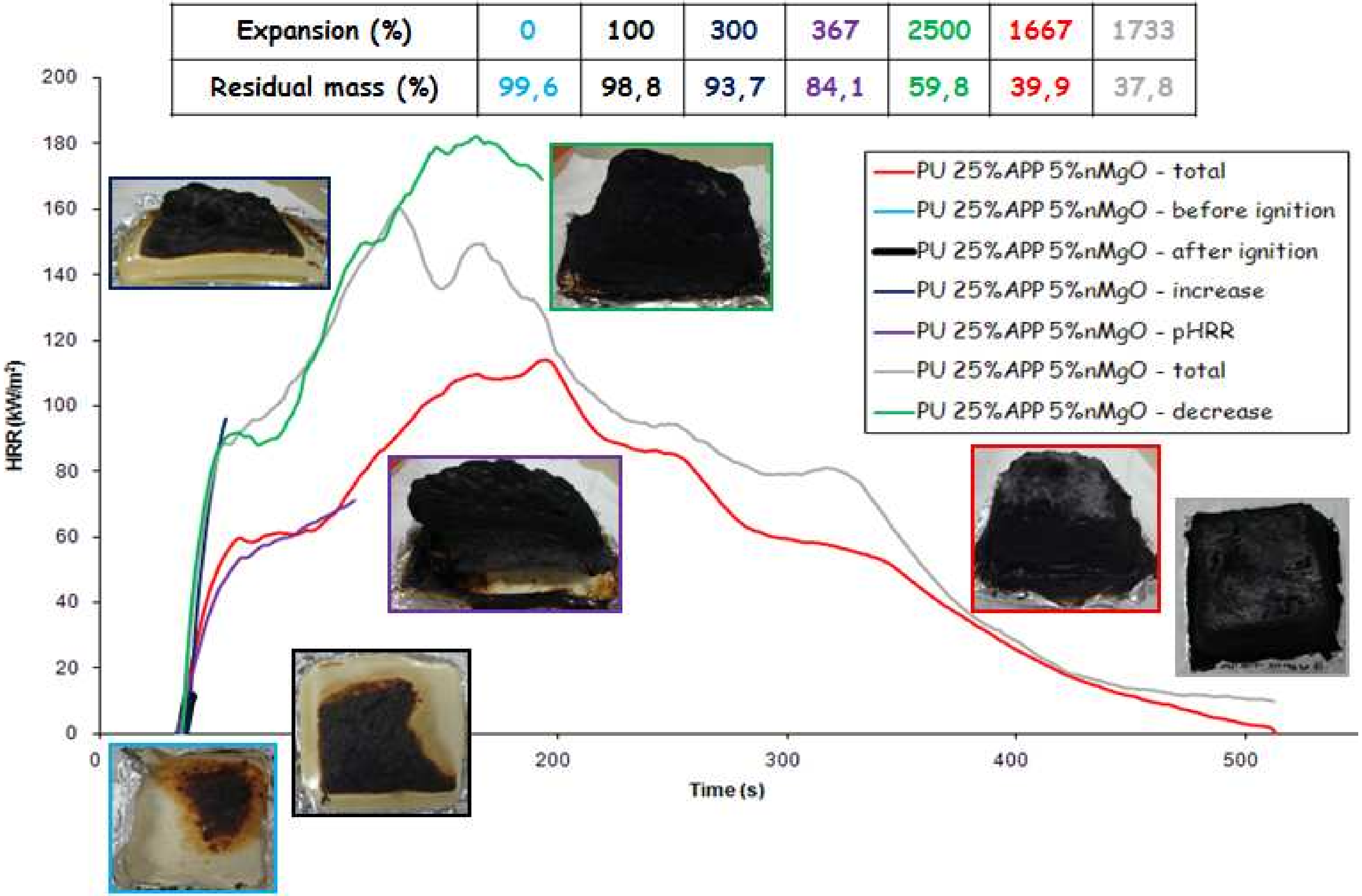

Expansion (%)	0	100	300	367	2500	1667	1733
Residual mass (%)	99,6	98,8	93,7	84,1	59,8	39,9	37,8

Figure 150: Cone calorimeter results from shutter experiments on PU 25%APP 5%nano MgO

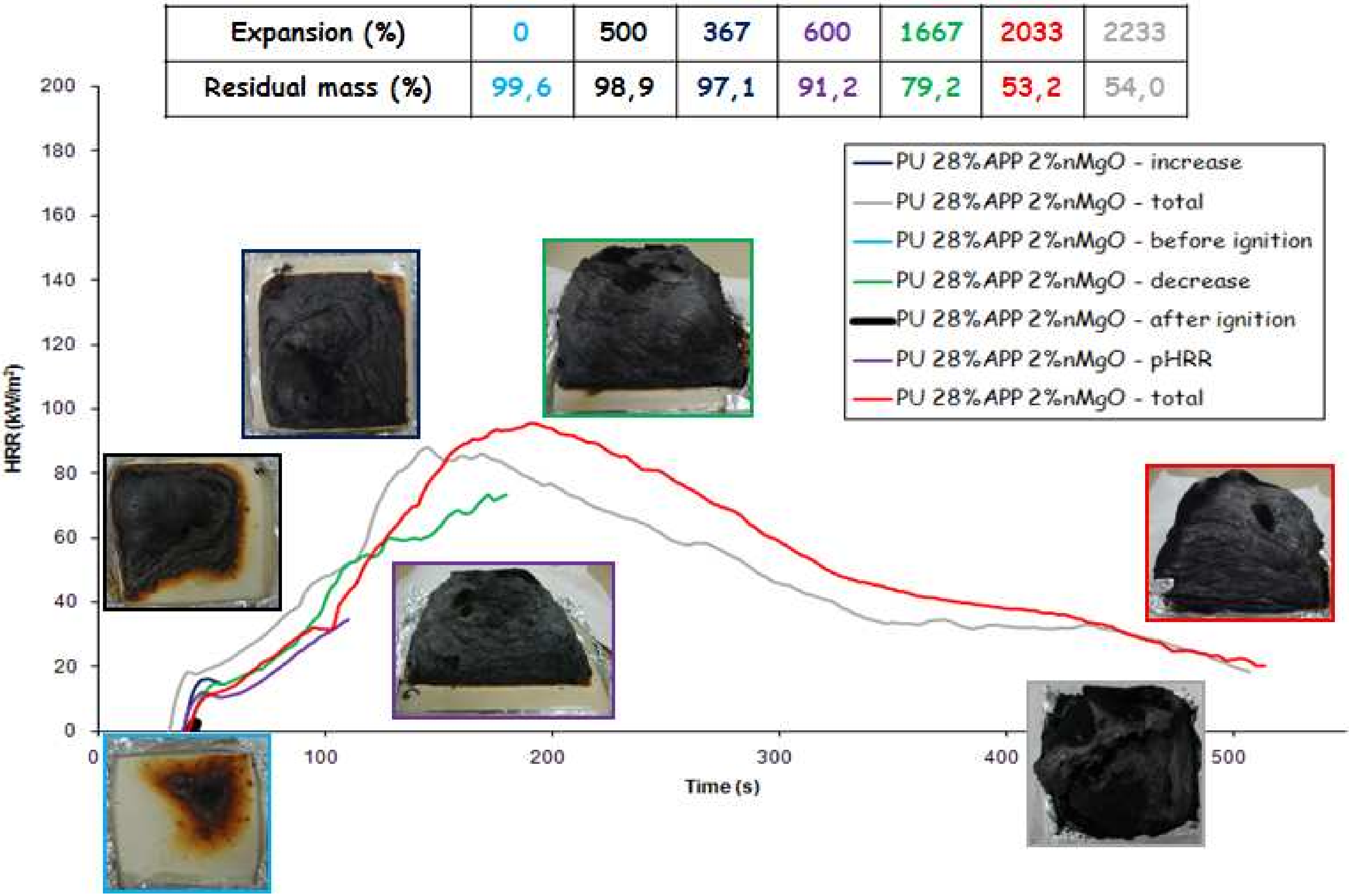

Expansion (%)	0	500	367	600	1667	2033	2233
Residual mass (%)	99,6	98,9	97,1	91,2	79,2	53,2	54,0

Figure 151: Cone calorimeter results from shutter experiments on PU 28%APP 2%nano MgO

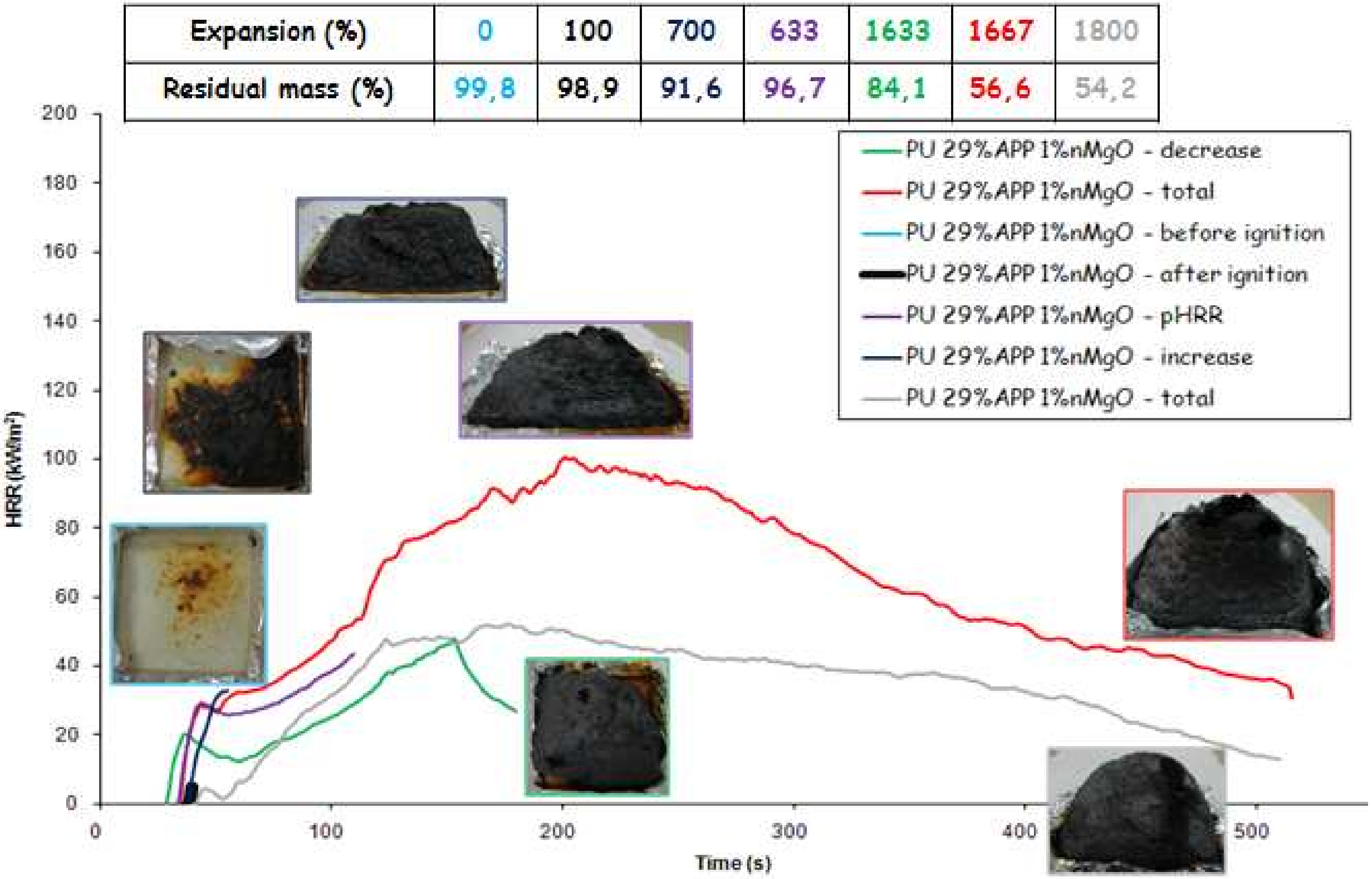

Expansion (%)	0	100	700	633	1633	1667	1800
Residual mass (%)	99,8	98,9	91,6	96,7	84,1	56,6	54,2

Figure 152: Cone calorimeter results from shutter experiments on PU 29%APP 1%nano MgO

Appendix 3: Study of the parameters governing the mechanical behavior of PU 30%APP and PU 28%APP 2%nano MgO chars

The mechanical behavior of chars obtained by heating PU formulations in the rheometer was studied in **Chapter V, section 3.1-Evaluation of the mechanical strength of chars prepared by different methods p206**.

It revealed the formation of an unexpected strong char for PU 30%APP. The char strength of a standard cone calorimeter char was consequently measured and the formation of a weaker char was observed. Several parameters are modified while changing from one method to another (methods RF-HR500-500-o versus MLCi-Q-AT-☐, **see the precise signification of the method in Table 10 p91**) and one or more of them could affect the mechanical behavior of the PU formulations. A list of these parameters can thus be established:

- heating device
- heating rate
- heating temperature
- measurement temperature
- presence of flame (ignition)
- sample characteristics (size, shape, thickness, presence of “walls” from the sample holder)

The following discussion will now aim to identify more precisely which parameters are crucial when dealing with the mechanical properties. It will also be particularly interesting to draw rules leading to the formation of strong chars.

The first important parameter to evaluate is the presence of a flame. A standard cone calorimeter test requires indeed the use of an ignition spark. For the method RF-HR500-500-o, it is impossible to ignite the sample and moreover prohibited in order not to damage the rheometer furnace. A standard cone calorimeter is thus performed for the method MLCi-Q-AT-o with exactly the same procedure but without the ignition (method MLCøi-Q-AT-o).

The evolution of char strength as a function of gap is then recorded and plotted in **Figure 153**. It reveals that for both methods, the same trend and the same critical gap is obtained; leading to the conclusion that the flame does not influence the mechanical properties of any of the chars. The pictures (**Figure 154**) of the final residues are in agreement with the plotted data; the same totally degraded and compacted residues are obtained whatever the method. The formulation containing nano MgO was just a little more expanded without ignition (it is evidenced on **Figure 153** and **Figure 154**) but this is not significant as far as the mechanical properties are concerned. The method MLCi-Q-AT-o will consequently now be taken as the reference to do further method comparisons but it must be reminded that same results were obtained without ignition.

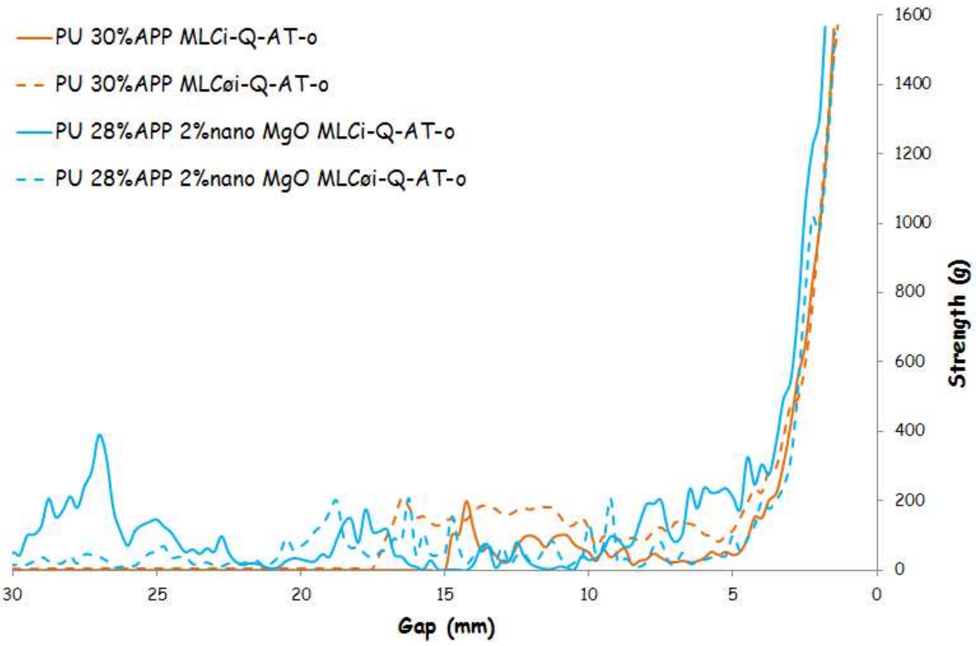

Figure 153: Comparison of the evolution of char strength as a function of gap for PU 30%APP and PU 28%APP 2%nano MgO prepared in cone calorimeter with or without ignition (methods MLCi-Q-AT-o versus MLCøi-Q-AT-o)

Figure 154: Pictures of residues collected after measuring the strength as a function of gap on samples prepared by methods MLCi-Q-AT-o (full line) and MLCøi-Q-AT-o (dash line) (left: PU 30%APP, right: PU 28%APP 2%nano MgO)

In order to study the influence of the samples characteristics, the idea was to develop a char under the cone calorimeter from a thin circular sample directly in the sample holder used for measuring char strength. The char strength is then measured with the rheometer at ambient temperature.

The evolution of char strength as a function of gap has thus been superimposed for the methods MLCi-Q-AT-o and MLCi-Q-AT-□ in **Figure 155**. The mechanical behaviors are totally different depending on the method used, signifying that the samples characteristics have an effect on the char strength. The measured destruction force and the critical gap values are much lower in the case of the small circular sample compared to the standard cone calorimeter sample. This means that for both formulations, the char developed in cone calorimeter is most resistant if it is a 10x10x0.3 cm^3 sample. The higher critical gap value may although only be due to the higher quantity of material present with this bigger sample. In any case it can be seen that depending on initial sample characteristics, the reaction of the char to a mechanical constraint is significantly modified.

The samples characteristics varying between the two methods are the size, the thickness, the shape and the presence of "walls" from the sample holder. When the sample holder surrounds the PU casting, this indeed changes drastically the char development as it can be seen in **Figure 156**. The residues after performing the method MLCi-Q-AT-o are really different compared to the one coming from MLCi-Q-AT-☐ (**Figure 132**). It should have been time consuming to analyze each parameter of sample characteristics individually and it is not a top priority for our work. The important conclusion to remind here is that the mechanical strength of the char obtained from PU 30%APP and PU 28%APP 2%nano MgO is affected by the sample characteristics (size, shape, thickness of the sample and sample holder configuration).

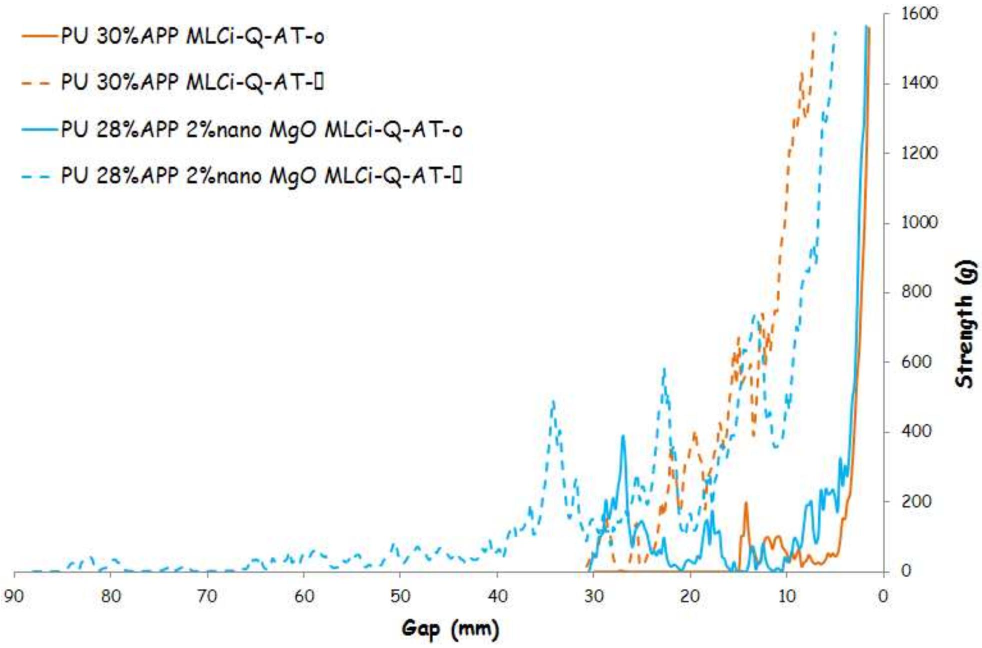

Figure 155: Comparison of the evolution of char strength as a function of gap for PU 30%APP and PU 28%APP 2%nano MgO with samples of different characteristics (methods MLCi-Q-AT-o versus MLCi-Q-AT-☐)

Figure 156: Pictures of residues collected after degradation with method MLCi-Q-AT-o (left: PU 30%APP, right: PU 28%APP 2%nano MgO)

It was then decided to compare the method RF-HR500-500-o to the method MLCi-Q-AT-o (**Figure 157**) in order to evaluate the influence of the heating conditions (heating device, heating temperature, heating rate and measurement temperature). Significant differences are noticeable regarding the measured destruction forces and the critical gap values. PU 30%APP is drastically affected by the heating conditions since a highly resistant material is obtained with the method RF-HR500-500-o whereas the evolution of strength versus gap of a typically fragile material is recorded after performing the method MLCi-Q-AT-o on PU/APP sample. With nano MgO the differences between the two methods are less obvious but still exist. Higher strength values and a higher critical gap are required to break the char from method RF-HR500-500-o. For both PU formulations, a stronger char is obtained with the conditions provided by the method RF-HR500-500-o. This can moreover be deduced by comparing the pictures of the residues after measuring the strength as a function of gap presented in **Figure 158**.

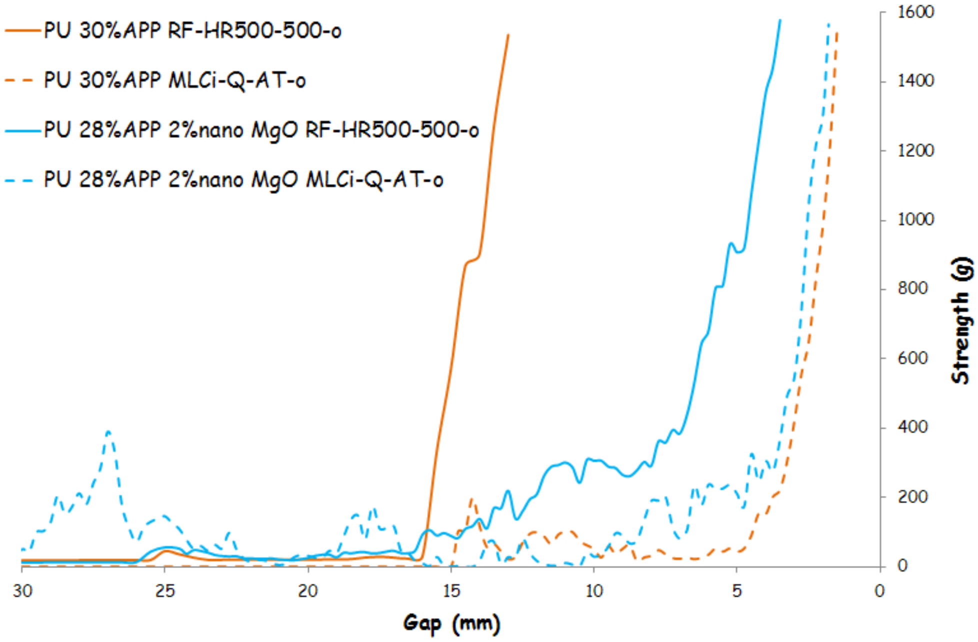

Figure 157: Comparison of the evolution of char strength as a function of gap for PU 30%APP and PU 28%APP 2%nano MgO heated in different conditions (methods RF-HR500-500-o versus MLCi-Q-AT-o)

A totally unmodified char is obtained for PU 30%APP after mechanical test in the case of method RF-HR500-500-o whereas a totally unstructured broken char is compacted at the bottom of the plate in the case of method MLCi-Q-AT-o. With this last method, the mechanically tested char PU/APP/nano MgO has the same aspect compare to the one obtained for PU/APP. This reinforces the fact that the evolution of char strength as a function of gap is similar and especially according to the critical gap value for the method MLCi-Q-AT-o. The pictures observation confirms once more that the heating conditions drastically affect the mechanical behavior of the resulting char; this is overall pronounced for PU 30%APP.

Figure 158: Pictures of residues collected after measuring the strength as a function of gap on samples prepared by methods RF-HR500-500-o (full line) and MLCi-Q-AT-o (dash line) (left: PU 30%APP, right: PU 28%APP 2%nano MgO)

By comparison between the mechanical properties exhibited by chars prepared in the rheometer (RF-HR500-500-o) or in a standard MLC test (MLCi-Q-AT-☐), it was obvious that the different conditions lead to different char strength whatever the formulation considered. It was first proven that there is no influence of the presence of flame (forced versus self-ignition). Then the samples characteristics (size, shape, thickness, and sample holder properties) were responsible of changes in the mechanical properties of chars. The final influencing parameter studied was the heating condition which refers to the heating device, the heating temperature, the heating rate and the measurement temperature. While modifying the heating conditions, the mechanical properties of char are largely different and especially without nano MgO. This needs to be further analyzed by dissociating the parameters including in the heating conditions. The purpose of the following discussion is thus to determine the effect of the heating device, the measurement temperature, the heating temperature and finally the heating rate on the mechanical strength of PU 30%APP and PU 28%APP 2%nano MgO chars.

Another heating device than those previously used (rheometer furnace and cone calorimeter) was used to control the heating conditions. The tubular oven was required because it allows playing on the heating rates and treatment temperatures. The temperature in the rheometer is indeed limited to 500°C and with the cone calorimeter, the standard procedure implies to fix a heat flux but the heating rate is not controlled. New methods are consequently put in place to investigate the potential effects of the heating conditions on the char strength of PU 30%APP and PU 28%APP 2%nano MgO. Those experiments will now only be performed on small and thin circular PU plates since it has been evidenced in the last section that the samples characteristics interfere in the mechanical strength. The pictures of the residues collected after the heating step but before the mechanical test are given in **Appendix 4: Pictures of PU 30%APP and PU 28%APP 2%nano MgO chars developed by different methods before mechanical strength measurement p263**.

The change of heating device might have consequences on the mechanical strength of chars; this is why it is the first parameter studied here.

The cone calorimeter with or without ignition provides a radiative heat thanks to the external cone heater placed above the sample whereas the rheometer furnace and the tubular oven give a convective heat spreading the entire sample. Two samples were tested after heat treatment in the cone calorimeter or in the tubular oven (respectively methods MLCi-Q-AT-o and TO-Q700-AT-o), the corresponding curves of strength versus gap are plotted in **Figure 159** for PU/APP and PU/APP/nano MgO. The other conditions were as fas as possible identical. A direct exposure (more or less like a quench) of the sample has effectivelty been performed in the tubular oven preheated at 700°C. In the cone calorimeter, the precise temperature of the quench is not known but the temperature at the top of the plate was measured by a thermocouple during a cone calorimeter experiment (results not shown in this manuscript) and the value was generally close to 700°C.

The curves and the residue pictures (**Figure 160**) reveal that very comparable results are obtained by using the methods MLCi-Q-AT-o and TO-Q700-AT-o. The strength and critical gap values are very similar for both method and both formulations and a low resistant material is always created. This is furthermore attested by the totally degraded material observed after the test which is totally compacted in the rheometer plate.

This first study proves that there is no influence of the heating type (radiative heat versus convective heat) on the strength of PU 30%APP and PU 28%APP 2%nano MgO chars.

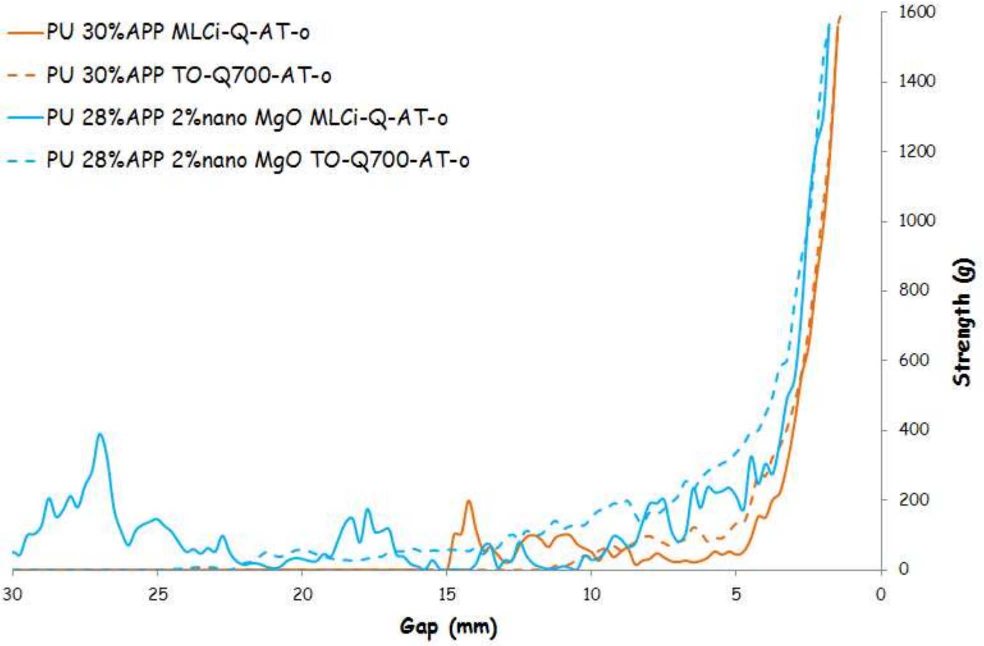

Figure 159: Influence of heating type (comparison of methods MLCi-Q-AT-o and TO-Q700-AT-o) on the evolution of char strength as a function of gap for PU 30%APP and PU 28%APP 2%nano MgO

Figure 160: Pictures of residues collected after measuring the strength as a function of gap on samples prepared by methods MLCi-Q-AT-o (full line) and TO-Q700-AT-o (dash line) (left: PU 30%APP, right: PU 28%APP 2%nano MgO)

Slow heating rate of 10°C/min have been provided either by the tubular oven but also by the rheometer furnace. The method RF-HR500-500-o is not relevant to compare to the method TO-HR500-AT-o because two parameters are changing from one method to the other. The furnace type and the measurement temperature are indeed different in these two methods. A new experiment is then performed and consists in heating until 500°C at 10°C/min the sample in the rheometer furnace, letting then the char cool down and after measuring its mechanical behavior at ambient temperature, this is the protocol of the method RF-HR500-AT-o. It is consequently possible to evaluate first the effect of the furnace type and then of the measurement temperature.

The resulting char strength after methods TO-HR500-AT-o and RF-HR500-AT-o is presented in **Figure 161**. Contrarily to what was observed by using different heating device (the cone calorimeter and the rheometer furnace), it appears with the curves that the mechanical properties of the chars are affected by the furnace type: rheometer furnace versus tubular oven.

The char obtained from PU 30%APP is more resistant when prepared in the tubular oven than when prepared in the rheometer furnace. The char is less expanded with the method RF-HR500-AT-o but when the upper plate of the rheometer touches the char, it exhibits a strong resistance and slightly collapse with high strength. The char is nevertheless not totally destroyed at the end of the test as it can be seen on **Figure 162**.

With additional nano MgO in the formulation, the ranges of gap where the highest strength are observed are different but the critical gap is similar (**Figure 161**). The residues pictures (**Figure 162**) show also a different aspect; in particular the color is very different. Both chars have anyway been destroyed even if the profile of the curve varies from one method to another.

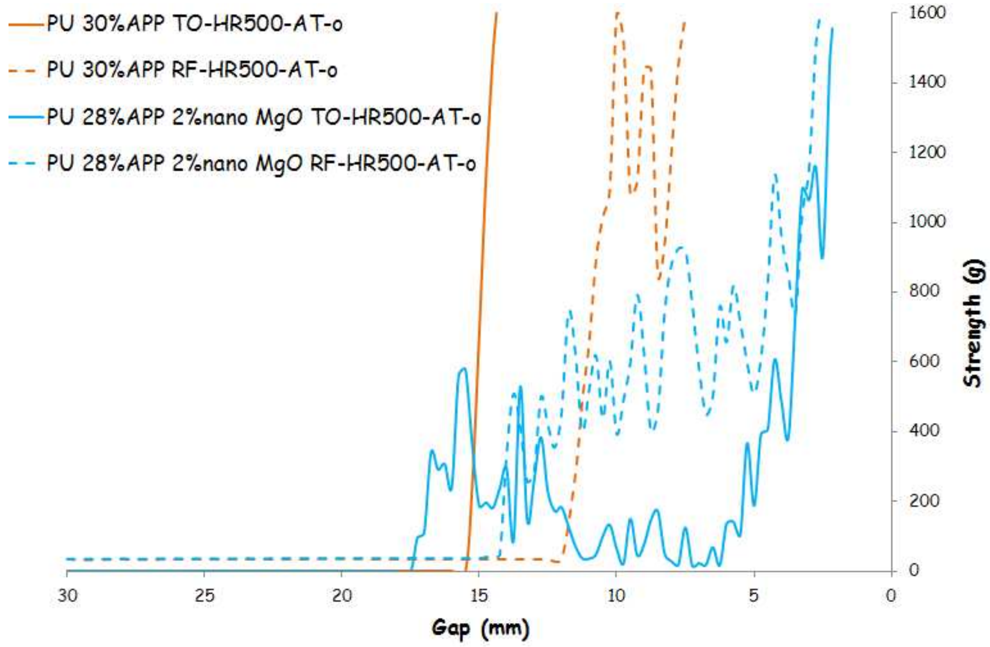

Figure 161: Influence of the furnace (comparison of methods TO-HR500-AT-o and RF-HR500-AT-o) on the evolution of char strength as a function of gap for PU 30%APP and PU 28%APP 2%nano MgO

Figure 162: Pictures of residues collected after measuring the strength as a function of gap on samples prepared by methods TO-HR500-AT-o (full line) and RF-HR500-AT-o (dash line) (left: PU 30%APP, right: PU 28%APP 2%nano MgO)

The differences observed by changing the type of furnace used (convective heating in both case) should rather be due to different conditions than to a real effect of the furnace itself. The temperature in the tubular oven is indeed not perfectly controlled, the air flux around the furnaces and also the global environement were moreover totally different leading to uncontrolled exterior influences. The general trend of mechanical resistance is however as expected in both furnaces: PU 30%APP char is resistant whereas PU 28%APP 2%nano MgO char collapses under strength. This experiment aimed to show that the mechanical properties are very sensitive to many parameters and everything needs to be perfectly studied in order to draw reliable conclusions. The comparisons are consequently more relevant if the exact same experimental conditions were used; this is why the following experiments will only be compared if the same furnace was used.

In order to study the consequences of the measurement temperature on the char strength of PU 30%APP and PU 28%APP 2%nano MgO, the profile of strength as a function of gap has been plotted for the methods RF-HR500-500-o and RF-HR500-AT-o in **Figure 163**. The corresponding pictures of the residues after the test are given in **Figure 164**. Quite the same observations can be made than the one made by comparing the methods TO-HR500-AT-o and RF-HR500-AT-o.

The measurement temperature (500°C versus ambient temperature on cooled down chars) influences the mechanical strength of chars; and overall of PU 30%APP char. This is not a surprising result since the intumescence is a dynamic process [51, 59] and the char morphology, composition and rheology may still be modified during an isotherme at high temperature or during a cooling down to work at ambient temperature.

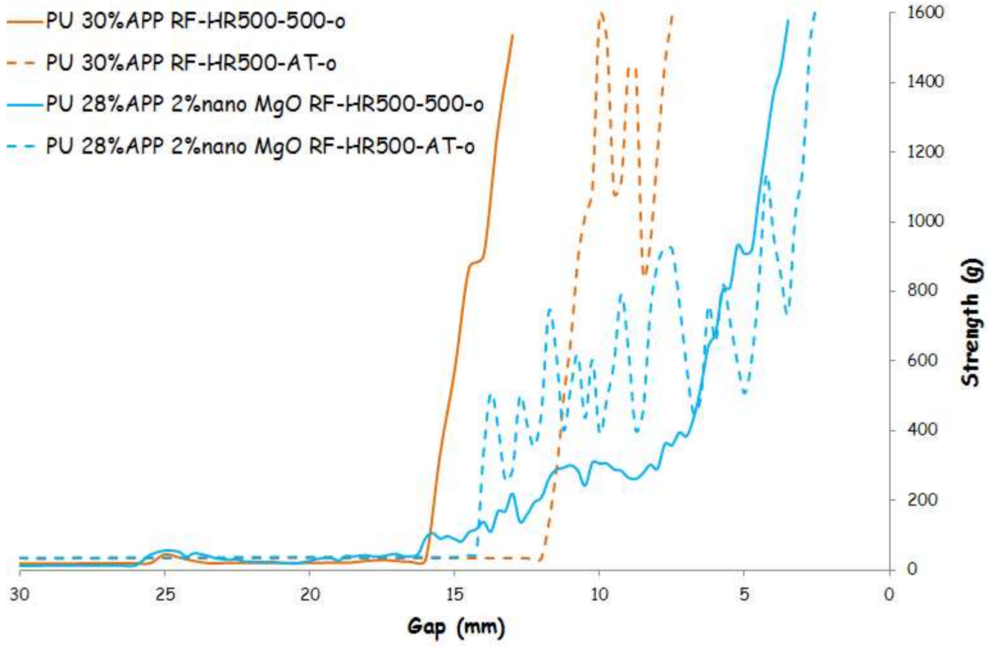

Figure 163: Influence of the measurement temperature (comparison of methods RF-HR500-500-o and RF-HR500-AT-o) on the evolution of char strength as a function of gap for PU 30%APP and PU 28%APP 2%nano MgO

Figure 164: Pictures of residues collected after measuring the strength as a function of gap on samples prepared by methods RF-HR500-500-o (full line) and RF-HR500-AT-o (dash line) (left: PU 30%APP, right: PU 28%APP 2%nano MgO)

Since we are now aware that the samples characteristics, the furnace used and the measurement temperature have an impact on the mechanical test, the following experiments will only be performed with small, thin circular samples, in the tubular oven and at ambient temperature.

The two criteria that still need to be tested are the heating temperature and the heating rate; it will be discussed in the following talk.

To test the effect of the heating temperature, the sample will be heated at 500°C or 700°C. It is moreover possible to reach these temperatures either with a slow heating ramp of 10°C/min or with a quench by placing directly the sample at the desired temperature. Two comparisons have consequently been made: first with a heating ramp, the method TO-HR700-AT-o is compared to the method TO-HR500-AT-o and second with a quench, the method TO-Q700-AT-o is compared to the method TO-Q500-AT-o. The graphs and residue pictures with the heating ramp are presented respectively in **Figure 165** and **Figure 166** while for the quench, the results are provided in **Figure 167** and **Figure 168**.

On **Figure 165**, the behavior of the samples versus a different heating temperature varies depending on the formulation considered. With nano MgO, the char strength is not affected by the heating temperature since the whole profile of strength versus gap (including the strength and critical gap values) are very similar for both methods. The final residue aspect looks also very similar on **Figure 166**. On the contrary, PU/APP has different char strength depending on the heating temperature (500 versus 700°C). At 500°C, once the upper plate of the rheometer is in contact with the char, the force recorded is saturating attesting of a strong char (**Figure 165**). The expansion is lower at 700°C and the char is slightly weaken by the pressure applied. This mechanical resistance difference is furthermore evidenced by looking at the residue pictures in **Figure 166**; it can be seen that the same char residue is obtained but it was softer at 700°C. It was already the case for the char obtained after the furnace test and before the mechanical test as it can be seen by comparing **Figure 174** and **Figure 175** in the **Appendix 4: Pictures of PU 30%APP and PU 28%APP 2%nano MgO chars developed by different methods before mechanical strength measurement p263**. For both PU 30%APP chars developed at different heating temperature, the mechanical strength is still very good compared to the one exhibited by PU/APP/nano MgO samples.

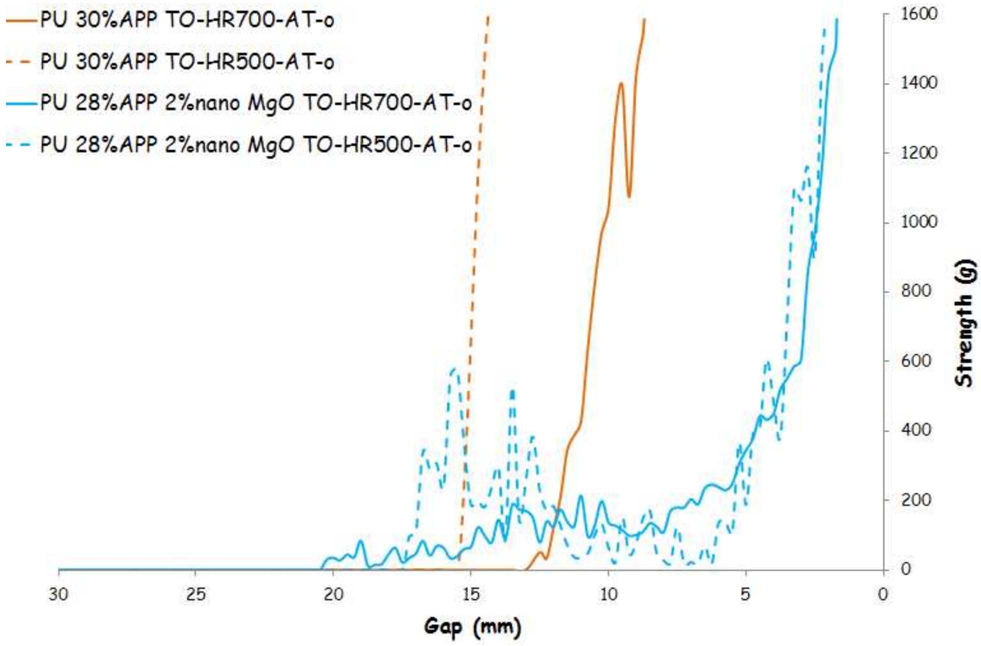

Figure 165: Influence of heating temperature after a 10°C/min heating ramp (comparison of methods TO-HR700-AT-o and TO-HR500-AT-o) on the evolution of char strength as a function of gap for PU 30%APP and PU 28%APP 2%nano MgO

Figure 166: Pictures of residues collected after measuring the strength as a function of gap on samples prepared by methods TO-HR700-AT-o (full line) and TO-HR500-AT-o (dash line) (left: PU 30%APP, right: PU 28%APP 2%nano MgO)

After a quench, things do not happen as after a heating ramp as it is presented in **Figure 167** and **Figure 168**. This time neither PU 30%APP nor PU 28%APP 2%nano MgO are affected by the heating temperature. The four samples behave quite identically according to the graph of char strength as a function of gap (**Figure 167**) and their corresponding residue pictures (**Figure 168**). In every case, the chars are totally destroyed by a very low destruction force.

To conclude, with nano MgO, the char strength is poorly affected by the heating temperature whereas without nano MgO, the mechanical properties of the char depend on the heating temperature when the char is developed with a heating ramp. The lower temperature favours a stronger char for PU 30%APP since degradation is lower at low temperature.

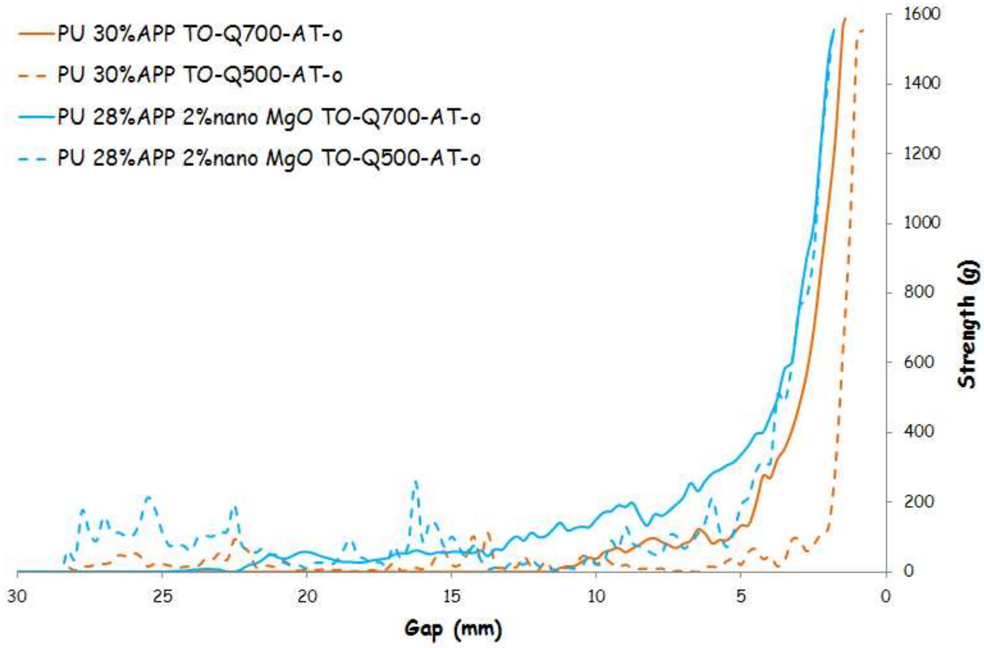

Figure 167: Influence of the quench temperature (comparison of methods TO-Q700-AT-o and TO-Q500-AT-o) on the evolution of char strength as a function of gap for PU 30%APP and PU 28%APP 2%nano MgO

Figure 168: Pictures of residues collected after measuring the strength as a function of gap on samples prepared by methods TO-Q700-AT-o (full line) and TO-Q500-AT-o (dash line) (left: PU 30%APP, right: PU 28%APP 2%nano MgO)

The final parameter to study is the effect of the heating rate on the mechanical behavior of PU 30%APP and PU 28%APP 2%nano MgO chars. As it was previously done for studying the influence of the heating temperature, the effect of the heating rate will be described at two different heating temperatures. This leads to compare together first the methods TO-HR700-AT-o and TO-Q700-AT-o and second the methods TO-HR500-AT-o and TO-Q500-AT-o. The evolution of char strength as a function of gap and the residue pictures are respectively presented in **Figure 169** and **Figure 170** for the results at 700°C and in **Figure 171** and **Figure 172** for the results at 500°C.

When the samples are heated until 700°C, the char strength is largely affected by the heating rate but only for the PU 30%APP system. The char is a little weakened by the pressure applied as it can be seen on **Figure 170**. On the contrary, when PU 30%APP is submitted to a quench until 700°C, the resulting char is very fragile and breaks very easily as it can be seen on **Figure 170**. For PU

28%APP 2%nano MgO, the two curves of strength as a function of gap (**Figure 169**) are very similar as well as the residue pictures (**Figure 170**).

When the samples are heated until 500°C only, exactly the same conclusions are obtained that at higher temperature.

The study of the mechanical strength of the char as a function of heating rate demonstrated that the incorporation of nano MgO modified the behaviors of the corresponding chars. Whatever the heating temperature, the PU 30%APP is highly influenced by the heating rate whereas the PU 28%APP 2%nano MgO is not affected at all. For PU 30%APP, the slow heating rates (10°C/min) particularly favors a strong char.

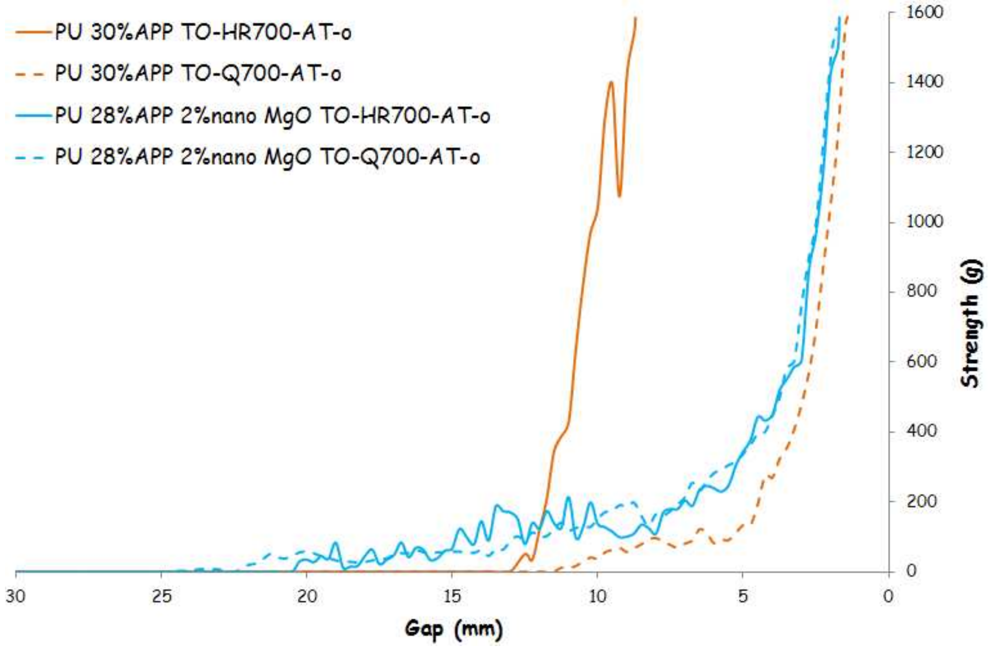

Figure 169: Influence of the heating rate until 700°C (comparison of methods TO-HR700-AT-o and TO-Q700-AT-o) on the evolution of char strength as a function of gap for PU 30%APP and PU 28%APP 2%nano MgO

Figure 170: Pictures of residues collected after measuring the strength as a function of gap on samples prepared by methods TO-HR700-AT-o (full line) and TO-Q700-AT-o (dash line) (left: PU 30%APP, right: PU 28%APP 2%nano MgO)

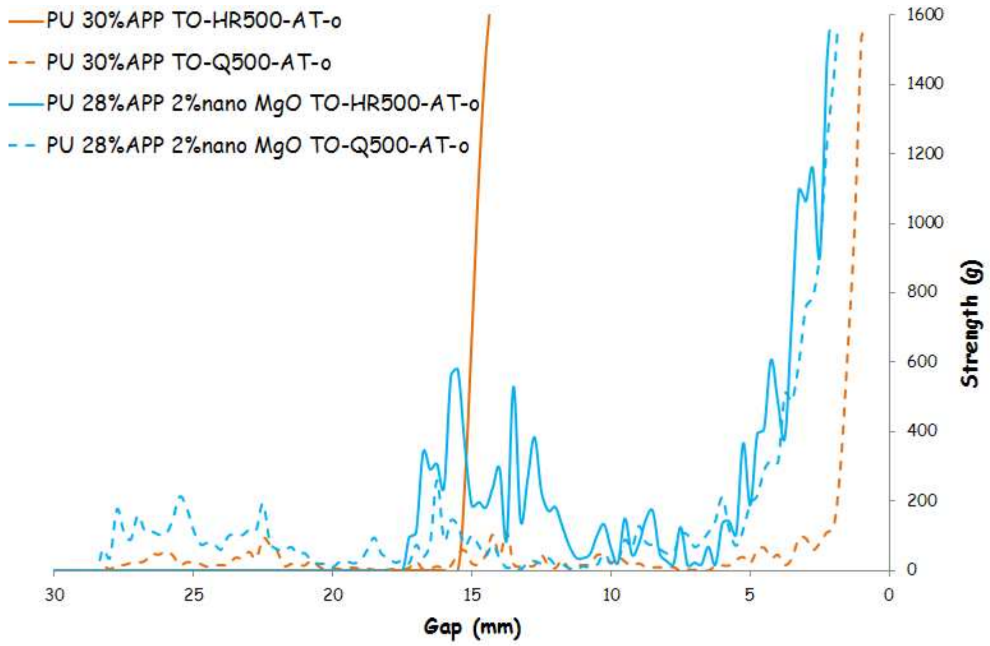

Figure 171: Influence of the heating rate until 500°C (comparison of methods TO-HR500-AT-o and TO-Q500-AT-o) on the evolution of char strength as a function of gap for PU 30%APP and PU 28%APP 2%nano MgO

Figure 172: Pictures of residues collected after measuring the strength as a function of gap on samples prepared by methods TO-HR500-AT-o (full line) and TO-Q500-AT-o (dash line) (left: PU 30%APP, right: PU 28%APP 2%nano MgO)

The study of mechanical behavior of char proved that significantly different char strength can be obtained depending on on the formulation considered and the conditions used to develop the char. This was always evidenced by both the profile of expansion as a function of gap and the residue pictures. The main conclusions of the complete study detailed here are given in **Chapter V, section 3.2-A governing parameter potentially affecting char properties: the heating rate p211**.

Appendix 4: Pictures of PU 30%APP and PU 28%APP 2%nano MgO chars developed by different methods before mechanical strength measurement

In order to evaluate the parameters affecting the mechanical behavior of the PU 30%APP and PU 28%APP 2%nano MgO chars, several methods to develop them have been put in place. The methods and their name codes are described in **Chapter II, section 2.5.3-Mechanical strength of char p88** and the results are discussed in **Chapter V, section 3.2-A governing parameter potentially affecting char properties: the heating rate p211**. This appendix presents the residue pictures taken after the development of the char and before undergoing the mechanical test.

Figure 173: Pictures of residues collected after degradation with method MLCi-Q-AT-o (left: PU 30%APP, right: PU 28%APP 2%nano MgO)

Figure 174: Pictures of residues collected after degradation with method TO-HR700-AT-o (left: PU 30%APP, right: PU 28%APP 2%nano MgO)

Figure 175: Pictures of residues collected after degradation with method TO-HR500-AT-o (left: PU 30%APP, right: PU 28%APP 2%nano MgO)

Figure 176: Pictures of residues collected after degradation with method TO-Q700-AT-o (left: PU 30%APP, right: PU 28%APP 2%nano MgO)

Figure 177: Pictures of residues collected after degradation with method TO-Q500-AT-o (left: PU 30%APP, right: PU 28%APP 2%nano MgO)

Systemic Approach of the Synergism in Flame Retarded Intumescent Polyurethanes

The purpose of this Ph.D work is to present and to understand the synergy observed in the fire performances of intumescent polyurethane (PU) formulations by the addition of nanoparticles (NP). Indeed, it was shown that the addition of ammonium polyphosphate (APP) in PU leads to interesting fire properties that can be enhanced substituting a small amount of APP by NPs (MgO, SiO_2, octamethyl polyhedral oligomeric silsesquioxanes (OMPOSS) and gold). The nature and content of the NPs play an important role on the fire retardant properties and mechanisms. First, a thermal stabilization was observed between APP and the different NPs except OMPOSS. The synergy mechanism was thus attributed to a condensed phase action where a range of chemical species, characterized by solid state NMR, are created upon heating the material in different conditions. The char properties, such as thermal conductivity, expansion and morphology, were then characterized using novel techniques (in particular tomography). It was shown that they are linked with the thermal barrier effect of the residual material explaining the good fire properties obtained when combining APP and NPs. The mechanical strength of chars developed in different conditions was also investigated but do not play a significant role on the synergy mechanism.

Keywords: **flame retardancy, polyurethane, intumescence, ammonium polyphosphate, synergy, nanoparticles**

Approche Systémique des Effets de Synergie dans les Procédés d'Ignifugation de Polyuréthanes Intumescents

L'objectif de ce travail de thèse est de mettre en évidence et de comprendre le mécanisme de synergie observé au niveau des propriétés retard au feu de polyuréthanes (PUs) intumescents par l'ajout de nanoparticules (NPs). En effet, l'addition de polyphosphate d'ammonium (APP) dans une matrice PU conduit à une amélioration de ses propriétés retard au feu. La substitution d'une petite quantité d'APP par des NPs (MgO, SiO_2, octamethyl polyhedral oligomeric silsesquioxanes (OMPOSS) et or) conduit de plus à un phénomène de synergie. Il a été montré que la nature et la quantité de NPs jouent un rôle important sur les propriétés retard au feu et sur le mécanisme de protection. L'étude de la stabilité thermique des différents systèmes a premièrement mis en évidence une stabilisation entre l'APP et les NPs à l'exception de l'OMPOSS. Il a donc été proposé que la synergie intervienne en phase condensée où diverses réactions chimiques, caractérisées par RMN du solide, ont lieu lors de la dégradation des matériaux entraînant la formation d'une barrière protectrice intumescente. Les propriétés de cette barrière, telles que sa conductivité thermique, son expansion et sa morphologie, ont été étudiées dans un second temps à l'aide de techniques spécifiques développées dans le cadre de cette étude (en particulier la tomographie). Ces propriétés ont été reliées à la meilleure protection observée pour le système contenant l'APP et les NPs. La résistance mécanique de barrières intumescentes développées dans différentes conditions a finalement été étudiée mais n'intervient pas dans le mécanisme de synergie.

Mots clés : **ignifugation, polyuréthane, intumescence, polyphosphate d'ammonium, synergie, nanoparticules**